Indubitably...

Promoters

Prof. dr. ir. Nico Boon
Department of Biochemical and Microbial Technology, Faculty of Bioscience Engineering, Ghent University, Ghent, Belgium.

Prof. dr. ir. Nele De Belie
Department of Structural Engineering, Faculty of Engineering and Architecture, Ghent University, Ghent, Belgium.

Members of the examination committee

Prof. dr. ir. Filip Tack (Chairman)
Department of Applied Analytical and Physical Chemistry, Faculty of Bioscience Engineering, Ghent University, Ghent, Belgium

Prof. dr. ir. Arne Verliefde (Secretary)
Department of Applied Analytical and Physical Chemistry, Faculty of Bioscience Engineering, Ghent University, Ghent, Belgium

Prof. em. dr. ir. Willy Verstraete
Department of Biochemical and Microbial Technology, Faculty of Bioscience Engineering, Ghent University, Ghent, Belgium

Prof. dr. ir. Robert J Lark
BRE Trust Centre for Sustainable Engineering, Energy and Environment, Cardiff University, Cardiff, Wales, UK.

Prof. dr. ir. Hubert Rahier
Department of Materials and Chemistry, Faculty of Engineering, Vrije Universiteit Brussel, Brussels, Belgium

Prof. dr. ir. Pascal Boeckx
Isotope Bioscience Laboratory, Department of Applied Analytical and Physical Chemistry, Faculty of Bioscience Engineering, Ghent University, Ghent, Belgium

Dean Faculty of Bioscience Engineering:
Prof. dr. ir. Marc Van Meirvenne

Rector Ghent University:
Prof. dr. Anne De Paepe

Microbial nitrate reduction induced autonomous self-healing in concrete

Yusuf Çağatay Erşan

Thesis submitted in fulfillment of the requirements for the degree of Doctor (PhD) in Applied Biological Sciences

Titel van het doctoraat in het Nederlands: Microbiële nitraat-reductie induceert autonome zelfheling in beton

Please refer to this work as:

Erşan, Y. Ç. (2016) Microbial nitrate reduction induced autonomous self-healing in concrete. PhD thesis, Ghent University, Belgium.

NOTATION INDEX

μCT	X-ray computed microtomography
ACDC	Activated compact denitrifying core
B	Bacteria
B1	*Diaphorobacter nitroreducens*
B2	*Pseudomonas aeruginosa*
CAPEX	Capital expenditure
CDW	Cell Dry Weight
COD	Chemical oxygen demand
C-S-H	Calcium silicate hydrate
DE	Diatomaceous earth
DP	Denitrifying pack
EC	Expanded clay particles
EDX	Energy dispersive X-ray spectroscopy
EPS	Extracellular polymeric substance
ESEM	Environmental scanning electron microscope
Eq	Equation
FTIR	Fourier transform infrared spectroscopy
GAC	Granular activated carbon particles
M9	Minimal nutrient media
MICP	Microbial induced carbonate precipitation
N	Nutrients
N/A	Not applicable
NM	Nutrient media
NOx	Total NO_3^- and NO_2^-
OPEX	Operational expenditure
OD	Optical density
PM	Protection material
R	Reference mortar specimen
RH	Relative humidity
rpm	Rotations per minute

Rxn	Reaction
SBR	Sequencing batch reactor
sem	standard error of the mean
SEM	Scanning electron microscopy
TN	Total nitrogen
TSS	Total suspended solids
VSS	Volatile suspended solids
w/c	Water to cement ratio

TABLE OF CONTENTS

CHAPTER

1

INTRODUCTION

CHAPTER

1

INTRODUCTION

1. Concrete

Concrete is a cementitious composite explored in Roman ages. A typical concrete has four main components; cement, water, coarse aggregates (typically 12 – 38 mm gravel) and fine aggregates (typically sand, size < 4.7 mm) [1,2]. Over the years, concrete became the most widely used construction material following the industrial production of Portland cement. On the one hand, by its high compressive strength, low cost, good fire resistance and practicality, concrete became the leading construction material with an annual demand of 11.5 billion ton/year. On the other hand, the high CO_2 footprint and low tensile strength are considered as the major drawbacks of concrete.

Concrete production is responsible for ~5 % of the global anthropogenic CO_2 emission [3–5] and around 80 % of its footprint is due to the cement production process [4]. Cement is produced by combining clinker with gypsum. To produce clinker it is necessary to heat limestone and claylike materials up to 1500 ^{o}C. This process is responsible from the direct CO_2 emission (50% of the total) since at mentioned temperatures $CaCO_3$ breaks down to CaO and CO_2 (calcination) [5]. The rest of the footprint is considered as indirect emission and comes from the energy production for heating and from transportation [5]. According to EPA, producing one ton of cement yields 900 to 1100 kg CO_2 [5]. The annual cement production was reported as 4.2 billion ton in 2014 [6,7] and it has an increasing trend (Figure 1.1).

According to given data in global carbon budget, cement production caused ~2 billion ton CO_2 emission in 2013 which corresponds to ~5 % of the global CO_2 production (39.5 Billion ton in 2013) [4]. The increasing environmental awareness prompted the attention to more optimized concrete mixes, alternative/supplementary binders and recycling options, to decrease the CO_2 emission caused during concrete production [8–11].
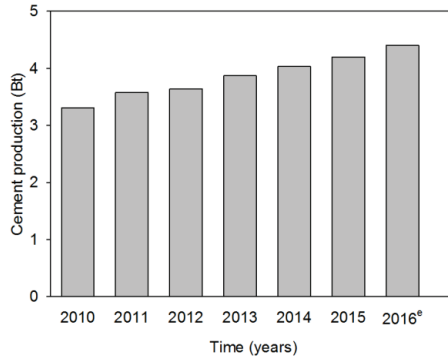
Figure 1.1 Global cement production in years (e: expected value based on the growth)(data acquired from Portland Cement Association report [7]))

Another disadvantage of the concrete is its heterogeneous matrix that causes the aforementioned weakness under tensile loads. This issue is being solved by using steel reinforcement bars or different types of fibers (steel, glass, plastic). So far, the most commonly used reinforcement tool is the steel rebars. The world steel association announced that 270 million ton steel was used for production of concrete reinforcing bars in 2014 [12]. Since the reinforcement tool is the main item carrying the tensile loads, the durability of the structure relies on its good condition. Although concrete provides passivation of the steel surface by its alkaline pH, concrete is not a very helpful partner for steel rebars to maintain their good state during service. The most common problem is the cracking of concrete which causes exposure of the steel reinforcement to ambient conditions by increasing permeability. This exposure eases the carbonation of concrete and related pH decrease. Therefore, the passivation of the rebar is hindered. Moreover the increased permeability enables chloride ingress, and eventually corrosion of the reinforcement and related durability problems occur.

1.1. Concrete cracks

Concrete exhibits a non-linear behavior under tensile load and its capacity for flexural deformation is around 10 % of its strain capacity under compression. Therefore, concrete is classified as a quasi-brittle material that has significant tendency to crack. Severe cracking occurs when concrete expose to tensile stresses that exceed its tensile strength. Tensile stresses may occur due to mechanical loading, some deleterious reactions and environmental attacks. However, it is hardly possible to determine a single reason for cracking. The most common reasons of concrete cracking are given in Table 1.1.

Among the given types, cracks occurring due to the drying shrinkage and due to the thermal stresses during the hydration process are considered as early age cracks. The early age cracks mainly form in the first couple of weeks and are considered as a durability issue since they jeopardize the good state of the steel rebar from the beginning.

Table 1.1 Reasons for cracking in concrete (after [13])

Types of cracks		
Cracking in plastic concrete	**Cracking in hardened concrete**	
	Pre-mature concrete (early age cracks)	Mature concrete
Formwork movement	Autogenous and drying shrinkage	Design load/accidental overload
Sub-grade movement	Thermal stresses during the hydration process	Fatigue
Plastic shrinkage		Drying shrinkage
Plastic settlement		External seasonal temperature variations
Autogenous shrinkage		Corrosion of reinforcement
Premature freezing		Freeze-thaw cycling
Scaling, crazing		Alkali-aggregate reactions
		Cement carbonation

Cracks occurring in pre-mature concrete can be observed in many forms. Klemczak and Knoppik-Wróbel [13] described their formation based on the structure type. Mostly random crack maps are observed in massive foundation slabs due to the hydration related temperature and moisture differences between the surface and the interior [13]. Differently, series of vertical cracks starting from the base are typical for medium thick structures such as walls since the limited deformation due to the shrinkage and thermal variations cause restraint stresses [13].

1.2. Influence of cracks on concrete durability

Structures expose to physical and chemical attacks throughout their life span and the permeability of the concrete plays an important role on the level of the damage created during

these attacks. The more permeable the concrete, the more susceptible the structure. Especially the presence of cracks substantially increases the concrete permeability and exacerbates the damage on steel reinforcement.

Cracking of concrete is a severe problem when the crack width exceeds a critical value arising aesthetics, durability and serviceability issues. The critical crack width highly depends on the intrinsic and extrinsic factors, thus there is no precise value as a restriction. However, in ACI 318-95 and earlier versions 0.41 mm is considered as a permissible crack width. Moreover, in ACI 224R-01 [14] and in EN 1992-1-1 [15], considering different exposure conditions and autogenous healing certain thresholds are recommended (Table 1.2). Apart from the recommended values, experimental values revealed that chloride ingress level in cracked and uncracked concrete was similar only if the crack width was less than 10 μm [16].

Table 1.2 Reasonable crack widths for reinforced concrete considering the autogenous healing

Exposure conditions	Crack width (μm)		
	ACI-224R [14]	EN-1992-1-1 [15]	
	Service load	Quasi-permanent load	Frequent load
Dry air or protective membrane	410	400	200
Humidity, moist air, soil	300	400	200
De-icing chemicals	180	300	200
Seawater and seawater spray, wetting and drying	150	300	200
Water retaining structures except non-pressure pipes	100	300	200

Concrete cracks are not stable and mostly develop with the effects of environmental factors. Freeze-thaw, external chemical attacks (Cl^-, SO_4^{2-}), intrinsic chemical reactions (e.g. corrosion, alkali silica reaction) can be mentioned as major mechanisms in crack development [14]. Therefore, repairing concrete cracks is of significance to maintain the healthy state of the structure and prevent durability issues. So far, most commonly used method for crack repair is injection of either epoxy resin or polyurethane foam through a core drilled next to the crack or from the surface. If the maintenance is not properly handled, the reinforcement starts to corrode and the failure of the structure becomes inevitable. The United States used 4.5

gigatons of cement in the years between 1901 – 2002 for infrastructure and it is reported in 2006 that the maintenance, repair and strengthening of the structures cost $18 to $21 billion/year [17]. The distribution of the maintenance costs is given in Table 1.3. Furthermore, the durability issues due to the reinforcement corrosion costs > $8.1 billion/year in US [18,19]. These values increase by a factor 10 if the traffic delays and lost productivity are also taken into account [18].

Table 1.3 Annual market segment costs of repair [17–19]

Structure	Maintenance cost (concrete) ($ Billion)	Corrosion related costs ($ Billion)
Bridges	8	7.8
Roadways	>4	N/A
Piers and wharfs	0.2	0.3
Buildings	2	N/A
Parking structures	0.5-1	N/A
Locks and dams	0.2	N/A
Residential areas	0.3	N/A
Industrial facilities	0.3	N/A
Water treatment	0.5	N/A
Pipelines	1	N/A
Miscellaneous structures	1	N/A

Considering the fact that currently China uses 60 % of the globally produced cement and only in between 2011 – 2013 they used 6.6 gigatons of cement, in the near future, the annual cost for repair and maintenance of the structures in global scale will be mentioned in $ trillion. Significant research is being done to find alternative ways to solve durability issues and decrease the maintenance costs. Development of self-healing concrete is one of the strategies.

2. Self-healing of concrete

2.1. Autogenous healing of the cracks

As previously mentioned, concrete is not the perfect partner for steel since cracking of concrete is unavoidable. Yet, concrete has intrinsic mechanisms that close the cracks to a certain extent which play an important role regarding protection of the steel reinforcement from a chemical attack. The phenomenon is called as "autogenous healing" and researchers put significant effort to explain the behavior. There are 4 main factors triggering the autogenous healing of a crack in concrete; (1) hydration of the unhydrated cement particles, (2) clogging of the crack by the transported impurities or sedimentation of fractured pieces, (3) swelling of the crack walls through calcium silicate hydrate (C-S-H) formation (4) formation of $CaCO_3$ minerals through the carbonation of portlandite (Figure 1.2) [20].
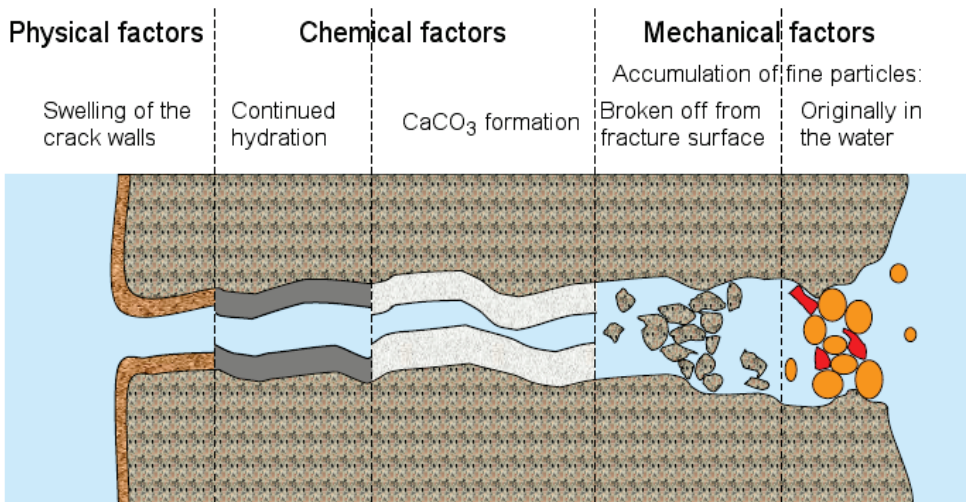
Figure 1.2 Factors triggering the autogenous healing of cracks in concrete [20]

Studies exploring the autogenous healing of concrete revealed that the healing capacity of concrete varies between crack widths of 10 μm and 300 μm [21–23]. As seen from the reported range, the performance is variable and hardly predictable. However, significant water tightness regain and partial strength regain were reported. Edvardsen [24] reported 80 to 99% decrease in the water permeability of cracked concrete due to autogenous healing of the cracks. Kenneth and Floyd [25] reported 25 % tensile strength regain following autogenous healing. These findings brought the idea that if autogenous healing could be either improved

to or replaced with a more stable and predictable phenomenon, manual repair of the concrete cracks would be history. Therefore, researchers embarked on development of strategies that offer improved, controllable and predictable healing of concrete cracks. These efforts can be considered as implementation of autonomous healing functionality into concrete.

2.2. Autonomous self-healing strategies

Strategies developed to achieve stable, controllable and predictable self-healing performances can be grouped in two; (1) use of fracture triggered additives, (2) stimulation of autogenous healing.

Capsule based and vascular based strategies are considered in the first group. In this type of approach, polymer based healing agents are introduced into the concrete either inside capsules during casting or through vascular systems from a reservoir after the crack occurred. By incorporating polyurethane containing glass tubes in mortar, 48 to 62 % strength regain could be achieved following autonomous healing of 400 μm crack width [26]. When microcapsules enclosing epoxy resin were incorporated in mortar, flexural strength regain was improved up to 1.3 times in comparison with the reference specimen [27]. The same method provided 1.8 times more compressive strength regain when compared to autogenously healed reference specimens [27]. An optimized system has not been achieved yet, thus development of a self-healing concrete by means of capsule based healing systems is in progress. Vascular systems were reported to be advantageous over capsule systems by enabling addition of healing agents on-site whenever necessary [21]. It was believed that this approach could extend the limits of healable crack width, yet it was found that healing agent starts to leak from the crack if the crack is too wide [21]. The largest healable crack width is reported as 0.3 mm by using vascular systems [28].

Stimulation and improvement of autogenous healing was another strategy for development of self-healing concrete. Researchers used superabsorbent polymers, shape memory alloys, micro fibers, natural fibers and bacteria to enhance the autogenous healing. The main idea of using fibers or shape memory alloys was to restrict the crack width to scales where autogenous healing is the most effective. Li et al. [29] introduced engineered cementitious composites (ECC) supplemented with fibers. The ECC cracks at several points and creates many small-scale micro cracks rather than one wider crack, thus the crack width could be kept < 50 μm. By this approach, the permeability of the concrete was also restricted to a certain scale during healing. Repeatable and predictable autogenous healing performances

could be achieved [30]. Moreover, healing of the cracks in natural environment without special water treatment could be achieved when ECC was used [31]. Another strategy to improve the crack healing was incorporating shape memory alloys which induce crack closure during the unloading of the structure [32,33]. Similarly, crack closure was reported when pre-stressed shrinkable polymer tendons were used [34,35]. In this case the triggering mechanism for crack closure was the externally applied heat.

One way to stimulate autogenous healing is to supply water inside the crack. In order to increase the available water for autogenous healing, superabsorbent polymers (SAP) were investigated and three mechanisms (1) primary sealing of the crack due to the swelling of the SAPs; (2) further cement hydration; (3) $CaCO_3$ precipitation inside the crack were observed [36–38]. Indeed the SAPs were trapping the water during wet periods and releasing the trapped water leading to further hydration of unhydrated cement particles and also stimulating the $CaCO_3$ precipitation. Water permeability of the cracked mortar specimens containing SAPs was substantially lower compared to the reference cracked mortar specimens.

Jonkers [39] described a strategy that bacterial spores were immobilized in concrete and thus upon crack formation microbial induced $CaCO_3$ precipitation (MICP) occurred in addition to the autogenously formed $CaCO_3$. The additional formation of $CaCO_3$ improved the self-sealing potential of the concrete [40].

3. Microbial induced $CaCO_3$ precipitation (MICP)

Microbial induced $CaCO_3$ precipitation was first reported in the late 19th century by Murray and Irvine (1889/1890) and Steinmann (1899/1901) in concurrence with urea decomposition by the marine microbiota [41]. The first extensive evidence for the interaction between $CaCO_3$ precipitation and bacteria was revealed by Nadson [41–43].

In aqueous solutions, chemical precipitation of compounds starts when the solution is saturated with their ions and further dissolution of the compounds is not possible. The solubility constant (K_{sp}) of $CaCO_3$ is 4.8×10^{-9} at 25 ^{o}C. Therefore, increasing CO_3^{2-} concentration in the presence of Ca^{2+} leads to $CaCO_3$ precipitation. The former change is where the bacteria play the major role in MICP. It was reported that most of the bacteria can induce $CaCO_3$ precipitation if the conditions allow. Simply, certain metabolic activities of bacteria lead to production of CO_2 and it partially turns into CO_3^{2-} in aqueous environment (Rxn (1.1)) followed by the $CaCO_3$ precipitation in the presence of Ca^{2+}. However, the effect of bacteria is not only limited to CO_2 production.

$$CO_{2(g)} \leftrightarrow CO_{2(aq)} + H_2O \leftrightarrow H_2CO_3 \leftrightarrow H^+ + HCO_3^- \leftrightarrow 2H^+ + CO_3^{2-} \qquad \text{(Rxn 1.1)}$$
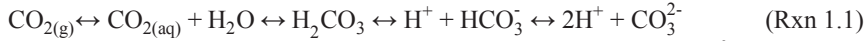
H_2CO_3 represents both the dissolved carbon dioxide and the carbonic acid. At 25 ^{o}C and 1 atm, the pK_H value of $CO_{2(aq)}$ is 1.46 and the pK_a values for carbonic acid and bicarbonate are 6.35 and 10.32, respectively.

The four key parameters driving MICP are listed as the presence of (1) Ca^{2+}, (2) dissolved inorganic carbon (DIC), (3) alkalinity, (4) nucleation sites. Bacteria play an active role in three of the mentioned parameters. In addition to CO_2 production, certain metabolic pathways lead to production of alkalinity which shifts the carbonate balance more towards the CO_3^{2-} (Rxn (1.1)) Moreover, during the precipitation process bacteria can serve as nucleation sites by concentrating Ca^{2+} ions around the negatively charged cell membrane. Aerobic or anaerobic oxidation of organic carbons (aerobic or anaerobic respiration), aerobic or anaerobic oxidation of organic nitrogen compounds, urea hydrolysis, sulfate reduction, photosynthesis can be mentioned as the major metabolic activities that can induce $CaCO_3$ precipitation in the presence of Ca^{2+}.

MICP has been investigated in different fields to obtain an improvement or provide a solution. Use of MICP is reported for soil consolidation, sandstone consolidation and sandstone production, surface treatment for cementitious materials and Ca^{2+} removal from waste streams [44–53]. Moreover, as previously mentioned, use of MICP is an effective strategy to induce autonomous self-healing of concrete. Although, the ureolysis pathway was the most prominent pathway in application oriented MICP studies, both aerobic respiration and ureolysis have been investigated for development of microbial self-healing concrete.

3.1. MICP for development of microbial self-healing concrete

The use of bacteria for autonomous crack repair in concrete was first mentioned in 2007 [39]. In following studies the concept was elaborated [54–56] and in 2011, first results on microbial self-healing concrete were available [40]. It was shown that bacteria can seal cracks up to 460μm in 100 days through aerobic oxidation of calcium lactate. Meanwhile, Van Tittelboom et al. [57] used the ureolytic strain *Bacillus sphaericus* for crack repair. The studies investigating ureolytic bacteria continued by combining the bacteria with different protective carriers [22,58–60] prior to concrete incorporation. Effective crack sealing up to 500 μm was reported for the combination of *Bacillus sphaericus* with hydrogels [59,60]. The studies on development of microbial self-healing concrete are summarized in Table 1.4

Table 1.4 Microbial self-healing concrete studies investigating intrinsic repair

Researchers	Bacterial strain - pathway	Protection	Treatment	Evaluation	Application scale
Jonkers and Schlangen [54], Wiktor and Jonkers [40]	*Bacillus cohnii*, *Bacillus pseudoformis* aerobic oxidation of organic carbon	N/A	Immersion; - glutamate and yeast extract medium	Bacterial survival Mechanical properties of the specimens through compressive strength tests Morphological investigation of precipitates through ESEM and EDX	Lab scale
	Bacillus alkalinitrilicus – aerobic oxidation of organic carbon	Light weight aggregates	Immersion; -fresh water	In situ bacterial activity through oxygen consumption Visual crack closure through optical microscope Characterization of the healing product through ESEM and FTIR	Lab scale
		Diatomaceous earth	Immersion; -fresh water -deposition media	Visual crack closure through optical microscope Water tightness through capillary water sorption Morphological investigation of healing product through SEM	Lab scale
		Microcapsules	(1) Relative humidity - > 95 % (2) Immersion; - fresh water - deposition media (3) wet/dry cycles: - fresh water - deposition media	Visual crack closure through optical microscope Water tightness through capillary water sorption and water permeability tests Mechanical properties of the specimens through compressive strength tests Characterization of the healing product through SEM/EDX	Lab scale
Wang et al. [22,58–60]	*Bacillus sphaericus* – urea hydrolysis	Hydrogels	(1) Relative humidity ->95 % ->60 % (2) wet/dry cycles: - fresh water	Visual crack closure through optical microscope X-ray μCT analysis for determination of healing products inside the crack Characterization of the healing product through SEM/EDX Water tightness through capillary water sorption and water permeability tests Bacterial activity through urea decomposition	Lab scale

Reference	Bacteria	Carrier	Healing condition	Characterization	Scale
Xu and Yao [61]	*Bacillus* sp.	N/A	Immersion; - distilled water	Mechanical properties through flexural and compressive strength tests Visual crack closure through optical microscope Mechanical properties of the precipitates through nano-indentation measurements Examination of the precipitates through SEM	Lab scale
Stuckrath et al. [62]	*Bacillus pseudofirmus* - aerobic oxidation of organic carbon	Light weight aggregates	Immersion; - tap water	Visual crack closure through optical microscope Characterization of the healing product through SEM and TGA	Lab scale
	Bacillus sphaericus – urea hydrolysis	Diatomaceous earth	Immersed in; - fresh water - urea solution	Mechanical properties through compressive strength tests Visual crack closure through optical microscope Bacterial survival through optical density measurements	Lab scale
Silva et al.[23,63]	*Bacillus cohnii* – aerobic oxidation of organic carbon	Diatomaceous earth	Immersed in; - fresh water - sodium lactate solution	Mechanical properties through compressive strength tests Visual crack closure through optical microscope Bacterial survival through optical density measurements	Lab scale
	Cyclic EnRiched Ureolytic Powder (CERUP)	Self-protected culture	Immersed in; - Demi water - Urea solution	Mechanical properties through compressive strength tests Visual crack closure through optical microscope	Lab scale
Luo et al. [64]	Spore forming alkali-resistant bacteria – aerobic oxidation of organic carbon	N/A	(1) Relative humidity - > 95% (2) Immersion; - tap water (3) wet/dry cycles: - fresh water	Visual crack closure through optical microscope Characterization of the healing product through SEM/EDX and XRD Water permeability	Lab scale

3.2. Disadvantages of currently investigated microbial self-healing processes

Microbial urea hydrolysis and aerobic oxidation of organic carbon have certain drawbacks regarding the application of microbial induced $CaCO_3$ precipitation (MICP) in concrete. First of all, both processes require O_2 as final electron acceptor to initiate and to keep the microbial activity. Yet, in concrete applications, O_2 availability inside the cracks can be limited, particularly in deeper parts of the cracks. Besides, solubility of O_2 in water (9.1 mg/L at 20 ^oC) is 10^2 to 10^5 times lower than the other types of electron acceptors (e.g. NO_3^- or SO_4^{2-}). Moreover, $CaCO_3$ precipitation itself entraps the bacterial cells and inhibits O_2 diffusion into cells [45]. Due to the O_2 limitation, inhibition of the microbial activity and the precipitation is possible during the self-healing process. From a performance point of view, aerobic oxidation has a disadvantage in terms of $CaCO_3$ precipitation yields. Unlike urea hydrolysis, aerobic oxidation only provides CO_2 and does not produce any alkalinity which means MICP yield of the process depends on external alkalinity [51]. Since concrete is an alkaline environment, aerobic oxidation is still applicable. However, it is prone to alkalinity limitations in long term microbial healing periods (around 14 weeks to complete 460 µm crack width [40]) due to the depletion of OH^- and autogenous carbonation at the crack mouth. Therefore, $CaCO_3$ precipitation yields and crack closure performances through aerobic oxidation highly depends on the concrete age and conditions which complicates the estimation of self-healing in-situ. From an environmental point of view, urea hydrolysis has the disadvantage of producing toxic by-products. Each mole of urea hydrolyzed leads to formation of 2 moles of ammonium [65]. In the alkaline concrete environment, ammonium turns into ammonia which is known for its toxicity for aquatic life [66]. Furthermore, this conversion process uses OH^- ions available in the matrix (Rxn (1.2)) and might cause degradation of concrete in the long term.

$$OH^- + NH_4^+ \leftrightarrow NH_3 + H_2O \qquad pK_a = 9.25 \qquad (Rxn\ 1.2)$$

Since transportation of produced ammonium and ammonia to water sources through the liquids and gases is inevitable, urea hydrolysis for concrete application is not an environment-friendly approach.

3.3. Denitrification as an alternative pathway

These issues already prompted the attention to alternative pathways in several MICP application areas and denitrification has been proposed for soil consolidation and Ca^{2+} removal from industrial wastewater [49,51,67].

Anoxic oxidation of organic carbon requires biological reduction of NO_3^- or NO_2^-. The process is called denitrification which does not produce any toxic by-products. Due to its highly negative standard Gibbs free energy (ΔG^o) (Rxn (1.3)), denitrification can be expected to dominate in the presence of nitrate (NO_3^-) and organic carbon under O_2 limited conditions.

$$5HCOO^- + 2NO_3^- \rightarrow N_2 + 3HCO_3^- + 2CO_3^{2-} + H_2O \qquad \Delta G^o = -1153 \text{ kJ/mole} \quad \text{(Rxn 1.3)}$$
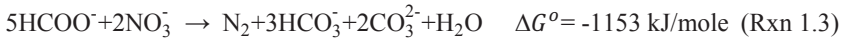
Biological reduction of NO_3^- generates CO_3^{2-} and HCO_3^- ions, which are necessary for $CaCO_3$ precipitation (Rxn (1.3)). Initial studies on MICP through denitrification were conducted to consolidate soil and sand [49–51]. Among the studies, the highest reported $CaCO_3$ precipitation yield, 10.6 g $CaCO_3$ /g NO_3-N in 3.5 days, was achieved through denitrifying activity of *Pseudomonas denitrificans* under nutrient rich conditions [49].

Through denitrification, maximum $CaCO_3$ precipitation rate of 180 g $CaCO_3$/h was reported for *Castellaniella denitrificans* after continuous feeding of a sand column for more than 70 days with nutrient rich media [51]. The average $CaCO_3$ precipitation rate of 100 days was reported as 125 g $CaCO_3$/h. In order to improve the precipitation rate, it was suggested to use more suitable strains in higher inoculum concentrations [51].

3.3.1. Advantages of the denitrification pathway in concrete application

It was concluded that $CaCO_3$ precipitation rates achieved through NO_3^- reduction were not enough for in situ application [51]. Indeed, under optimum conditions, MICP rates achieved through denitrification are 100 to 1000 times lower than those achieved through ureolysis [67]. However, in concrete applications the picture is different. Apart from its alkaline environment, in concrete cracks, oxygen and nutrients are also limited which are the main factors affecting germination rate and growth rate of the used microorganisms. $CaCO_3$ precipitation rate mainly depends on the initial bacteria concentration, their growth rate and specific metabolic activity of each bacterium in the relevant environment. Therefore, the condition in concrete cracks favors the denitrifying bacteria rather than the currently investigated cultures. Bacterial cultures that are able to grow on NO_3^- under nutrient limited conditions could supersede the MICP rate and self-healing performance of the aerobic

cultures that demand O_2 and nutrient rich environment to perform and ureolytic cultures that require O_2 to germinate and grow.

Denitrification can be advantageous over ureolysis and aerobic respiration when the necessary nutrients are considered. So far, for urea hydrolysis yeast extract and urea are being used. In aerobic respiration studies either calcium lactate or calcium glutamate was combined with yeast extract to promote bacterial activity. Organic substances are known to be incompatible with the cement matrix [20,55], therefore the incorporation of the mentioned nutrients should always be limited to certain extent. In the case of denitrification, commercial concrete admixtures calcium formate ($Ca(HCOO)_2$) and calcium nitrate ($Ca(NO_3)_2$) [68,69] can serve as nutrient source for NO_3^- reducing bacteria. Both compounds were reported to be used up to 4 % w/w cement without any problems [68,69]. The use of these concrete compatible chemicals can enable the use of higher amount of nutrients while avoiding any drastic changes in concrete properties.

Another advantage of denitrification over ureolysis and aerobic respiration is the production of NO_2^- during the NO_3^- reduction process (Rxn 1.4). Self-healing strategies using aerobic oxidation or ureolytic bacteria lack the preventive action to avoid exposure of the steel surface to corrosive substances during the healing period. However, it is possible to achieve simultaneous corrosion inhibition and crack healing by using NO_3^- reducing bacteria.

$$2HCOO^- + 2NO_3^- + 2H^+ \rightarrow 2CO_2 + 2NO_2^- + 2H_2O \qquad \text{(Rxn 1.4)}$$
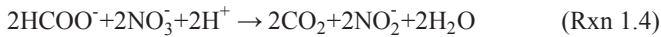
In alkaline conditions (pH ~ 9), microbial NO_2^- reduction is mostly suppressed by high rate NO_3^- reduction causing NO_2^- to accumulate, which is called partial/incomplete denitrification [70]. In an alkaline synthetic wastewater solution (pH 9), it was possible to achieve NO_2^- concentrations up to 0.065 M (3 g/L) in a few hours through partial denitrification [70]. Nitrite (NO_2^-) is commercially used in the form of $Ca(NO_2)_2$ in concrete industry to inhibit rebar corrosion [71]. It precedes Cl^- attack on ferrous oxides, the weakest points inside the passive ferric oxide layer, and rapidly oxidizes the ferrous ions to ferric oxide at the corrosion site which suppresses the corrosion [71]. The simplified chemistry of corrosion and corrosion inhibition in cracked concrete is shown in Figure 1.3. Studies on the formed oxide layer upon rapid oxidation of ferrous ions by NO_2^- revealed that the layer repairs the passive film and thus prevents dissolution of the rebar [71–73].

Plain concrete

Concrete containing Ca(NO$_2$)$_2$

Legend:
- Oxygen (O$_2$)
- Nitrite ion (NO$_2^-$)
- Rust (Fe$_2$O$_3$, Fe$_3$O$_4$, Fe(OH)$_3$, Fe(OH)$_3$,3H$_2$O)
- Ferric oxide layer (Fe$_2$O$_3$)
- Chloride ion (Cl$^-$)
- Ferrous ion (Fe^{2+})

Crack formation & exposure to ambient environment

Crack formation & exposure to ambient environment

Water ingress, Cl$^-$ attack on ferrous oxide film & dissolution of the rebar
Fe^0 = Fe^{2+} + 2e$^-$

Water ingress, NO$_2^-$ precedes Cl$^-$ to attack on ferrous oxide film

Continuous dissolution and transportation of ferrous ions towards surface, and their further oxidation by air.
xFe^{2+} + yO$_2$ + H$_2$O = Fe$_2$O$_3$, Fe$_3$O$_4$

Repair of the passive oxide film through rapid oxidation of Fe^{2+} by NO$_2^-$
2Fe^{2+} + 2OH$^-$ + 2NO$_2^-$ = 2NO + Fe$_2$O$_3$ + H$_2$O

Figure 1.3 Rebar corrosion and corrosion inhibition processes in cracked concrete

Studies on NO_2^- for corrosion inhibition have revealed that the optimum corrosion inhibition could be achieved when the $[NO_2^-]:[Cl^-]$ ratio was in the range of 0.34 – 1 [71,73,74]. Therefore, biological NO_3^- reduction has significant potential to inhibit corrosion in concrete environment. Despite its significant potential, biological NO_3^- reduction was not investigated for corrosion inhibition in concrete.

Denitrification can also be advantageous over currently investigated aerobic respiration and ureolysis pathways by the development of granular culture technology. Studies revealed that during the selective enrichment of granular bacteria, denitrifying bacteria dominate the core community of the granule [75,76]. The systematic placement of the cultures and the layered structure of the granular bacteria is attributed to the limitations in oxygen diffusion [75,76]. The depletion of the O_2 towards the core of the granule creates an anoxic zone and favors the enrichment of denitrifying bacteria [75]. In such organized cultures strong biofilm formation and enhanced extracellular polymeric substance (EPS) production was observed [77]. Formation of a mature biofilm, layered structure and excess amount of EPS around the core community make them less susceptible to toxicity and variations in the bulk environment. Therefore, using denitrification pathway for MICP in concrete environment also enables the employment of such granulated cultures and may avoid the need for protective carriers.

4. Up to date research needs

Considering the current state of the art, certain needs can be pointed out. First of all, an alternative MICP pathway for development of microbial self-healing concrete is necessary to enhance the self-healing performances and overcome the current drawbacks. Although biological NO_3^- reduction has potential for such exploitation, limited information is available about the NO_3^- reduction pathway for concrete application. Therefore, a comprehensive study investigating the use of the NO_3^- reduction pathway for concrete application is necessary. The investigation of bacteria for self-healing technology should be elaborated to a wider perspective to decrease the implementation cost of the technology and to make the technology even more sustainable. Although the self-healing performance of the microbial concrete is speculated to be similar regardless of its age, it is necessary to evaluate the performance of microbial concrete in different ages.

5. The goal and the scope of the thesis

The objective of the thesis is to investigate the NO_3^- reduction (denitrification) pathway for development of microbial self-healing concrete and fill the aforementioned research gaps. The study was divided in four main parts; (1) selection of the appropriate strains, (2) screening of the healing agents, (3) development of the microbial self-healing concrete, (4) evaluation of the achievements.

After this introductory chapter (**Chapter 1**), the thesis can be outlined as follows.

Part 1: Selection of the appropriate strains

Chapter 2

The need for the study: In order to develop microbial self-healing concrete, it was primarily necessary to define the type of the bacteria and their respective nutrients. Additionally, it was necessary to determine the $CaCO_3$ precipitation yields of their metabolic activity.

Main goal: Determination of the resilient axenic strains that can precipitate $CaCO_3$ by only using concrete admixtures and their further performance optimization.

Resilient NO_3^- reducing strains originated from soil were isolated by exposing them to harsh conditions, particularly to heat treatment, dehydration and starvation. Among the isolated cultures, further screening was done by varying inoculum concentration and supplementary PO_4-P concentration. The best performing strains were investigated for single and repetitive $CaCO_3$ precipitation.

Outcome: *Diaphorobacter nitroreducens* and *Pseudomonas aeruginosa* with precipitation yields of 14.1 and 18.9 g $CaCO_3$/g NO_3-N, respectively, were selected for further investigation in concrete (Part 2).

Part 2: Screening of healing agents

Chapter 3

The need for the study: Interactions between the admixtures (nutrients, bacteria, protective carriers), mortar and steel are significant for the durability and performance of the developed concrete. Therefore, it was necessary to investigate the individual and the combined effects of the selected admixtures on mortar and their stability after mortar incorporation is necessary.

Main goal: Investigation of the admixture combinations and their effect on mortar properties, bacterial activity and steel corrosion.

Commercial concrete admixtures $Ca(HCOO)_2$ and $Ca(NO_3)_2$ were used in fixed amounts as nutrient sources for bacteria. Previously selected strains were combined with the commercially available protective carriers and nutrients, and their combined influence on concrete properties was investigated. Biological granules were investigated as an alternative healing agent. The influence of bacterial activity on steel corrosion was also tested.

Outcome: Porous aggregates as well as bio-granules were found to be suitable for further investigation to develop microbial self-healing concrete (Part 3).

Part 3: Development of microbial self-healing concrete

Chapter 4:

The need for the study: MICP through NO_3^- reduction pathway had never been studied in concrete environment. Therefore, before carrying out any further research based on NO_3^- reduction pathway, it was necessary to prove the concept and its limits by using defined axenic NO_3^- reducing cultures.

Main goal: Proof of the concept that the NO_3^- reduction pathway can induce self-healing of concrete cracks through MICP when appropriate admixtures are used.

The selected healing agents (previously selected strains in combination with porous aggregates) were used to develop microbial self-healing concrete. The evolution of the different cracked specimens were investigated in time and the performance of microbial specimens was evaluated and further used to evidence the potential of the NO_3^- reduction pathway as a microbial self-healing strategy.

Outcome: Incorporation of NO_3^- reducing bacteria significantly improved the healing potential of mortar which proved the concept of using the denitrification pathway.

Chapter 5:

The need for the study: In order to decrease the additional cost coming with the self-healing properties it was necessary to investigate alternative cultures.

Main goal: The assessment of the self-healing performance of mortars containing self-protected bio-granules.

Self-protected non-axenic cultures were used to develop microbial self-healing concrete. Self-healing performances were evaluated in conjunction with spatial, characteristic and functional analysis of healing products.

Outcome: Addition of bio-granules significantly improved the healing potential, enhanced the crack closure performance and functionality regain.

<u>Part 4: Evaluation of the achievements</u>

Chapter 6:

Evaluation of the research outcomes and their key roles in the journey of microbial self-healing concrete technology from concept to market.

CHAPTER 1

PART I
SELECTION OF THE APPROPRIATE STRAINS

MICROBIAL INDUCED CACO₃ PRECIPITATION THROUGH NITRATE REDUCTION IN MINIMAL NUTRIENT ENVIRONMENT

MICROBIAL INDUCED CACO₃ PRECIPITATION THROUGH NITRATE REDUCTION IN MINIMAL NUTRIENT ENVIRONMENT

Abstract

So far, researchers investigated microbial induced $CaCO_3$ precipitation (MICP) for soil reinforcement, self-repairing concrete and Ca^{2+} removal from industrial waste streams. Reported MICP yields were mainly achieved under nutrient-rich conditions. However, creating the tested nutrient-rich conditions in intended applications is both an economical and a practical issue. Therefore, investigation of MICP in more realistic conditions is necessary. This study presents optimization of MICP through denitrification in minimal nutrient conditions. To optimize their MICP performances, we isolated two strains, *Pseudomonas aeruginosa* and *Diaphorobacter nitroreducens*, by following an application oriented selection procedure. Upon performance optimization, in 2 days *Diaphorobacter nitroreducens* and *Pseudomonas aeruginosa* precipitated 14.1 and 18.9 g $CaCO_3$/g NO_3-N, respectively. Repetitive $CaCO_3$ precipitation was also achieved from single inoculum in both 2 days and 3 weeks intervals. Selected strains and the process were further evaluated for crack repair in concrete. *Pseudomonas aeruginosa* and *Diaphorobacter nitroreducens* could be introduced as potential candidates for concrete applications due to their enhanced precipitation yields, resilience and performance under minimal nutrient conditions.

1. Introduction

The metabolic activities such as sulfate reduction, iron reduction [78], urea hydrolysis [65,79,80], denitrification [49,51], methane oxidation [52,81] and photosynthesis [41] are known to give rise to microbial induced calcium carbonate ($CaCO_3$) precipitation (MICP). Boquet et al. [82] stated that $CaCO_3$ precipitation is a common as well as a circumstantial behavior in the bacterial world where most of the bacteria are able to precipitate $CaCO_3$ under proper conditions. For MICP, bacteria create substantially alkaline pH conditions and produce dissolved inorganic carbon [41,83]. Furthermore, bacterial cells act as ideal nucleation sites for formation of $CaCO_3$ crystals [80,83].

Since urea hydrolysis yields significant amount of carbonate ions and pH increase which induce the $CaCO_3$ precipitation, it was extensively investigated for applications such as soil improvement [45,78], Ca^{2+} removal from paper mill wastewater [44,53] and microbial self-healing concrete [58,84]. *Bacillus pasteurii* and *Bacillus sphaericus* were the most prominent species in those studies [44,45,58,65,79,80]. MICP through ureolysis has certain drawbacks in application. For instance, one of the purposes in sand or soil improvement applications is to decrease permeability and protect groundwater sources from leakages. However, urea hydrolysis generates ammonium, which may easily pollute these sources [51]. Anaerobic/anoxic conditions which inhibit bacterial growth are also an issue in deeper parts of soil and concrete cracks. If the Ca^{2+} removal from industrial wastewater is considered, the cost of the treatment increases by addition of phosphoric acid and urea. More importantly, ammonia is produced, hence subsequent removal of ammonia is needed. These issues prompted the attention to alternative pathways.

Oxidation of organic carbon by reduction of NO_3^-, so called denitrification, does not produce toxic by-products. Due to its highly negative standard Gibbs free energy (ΔG^o) (Rxn 2.1), denitrification can be expected to dominate in the presence of nitrate (NO_3^-) and organic carbon under O_2 limited conditions.

$$CH_3COO^- + 2.6\ H^+ + 1.6\ NO_3^- \longrightarrow 2CO_2 + 0.8N_2 + 2.8H_2O \qquad \Delta G^o = -785 \text{ kJ/mole} \qquad \text{(Rxn 2.1)}$$
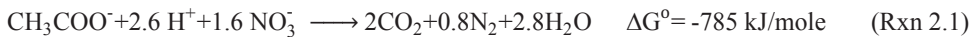
Biological reduction of NO_3^- generates CO_3^{2-} and HCO_3^- ions, which are necessary for $CaCO_3$ precipitation and the carbonate yield per mole of electron donor (per mole of acetate) is two times higher than that of ureolysis [49]. MICP through denitrification has been explored as an alternative pathway in soil reinforcement [49,51]. However, all the studies conducted so far were under nutrient-rich conditions and investigated for single use

performance. These favorable conditions are hard to provide in concrete applications. For instance one of the most important constituent for spore germination and bacterial activity is the yeast extract [84]. Yet, yeast extract is reported to cause severe retardation of concrete setting and also a decrease in compressive strength [20,55,85]. Moreover, the more the addition of extra nutrients the higher the cost of the self-healing concrete. Therefore, when considered for crack repair in concrete, MICP should take place under minimal nutrient conditions. Moreover, if the commercially available concrete admixtures can be used as nutrients, the outcomes will be more representative for applications in situ. Therefore, nitrate (NO$_3^-$) reduction can be advantageous since commercial concrete admixtures Ca-formate and Ca-nitrate can serve as electron donor and electron acceptor, respectively.

There are certain traits that the bacteria intended to use in concrete must have. For instance, bacterial agents ought to withstand temperatures around 70 ^{o}C during cement hydration [86]. Concrete has a dry matrix and adding the bacteria in the powder form is also more preferable since it is easy to transport and has longer shelf-life. Therefore, the bacteria should be resilient to dehydration. The formation of minerals around the bacteria during MICP affects the nutrient diffusion kinetics severely, hence the bacterial agent should be able to resist starvation [45]. Furthermore, single inoculum might need to perform repetitive precipitation in different intervals which is useful on repetitive healing of the same crack. Accordingly, this chapter presents the optimization of MICP through denitrification in minimal nutrient environment by using two newly isolated resilient strains, *Pseudomonas aeruginosa* and *Diaphorobacter nitroreducens*. The study was conducted in two consecutive steps; (1) isolation and selection of appropriate strains (2) performance optimization and repetitive CaCO$_3$ precipitation.

2. Material and methods

In all experiments, 125 ml PYREX$^®$ serum bottles (Corning, USA) with rubber stoppers and metal caps were used. Reactor headspaces were flushed with Argon (Ar) gas to provide anoxic conditions. Incubations were carried out at 28°C and on 120 rpm shaker. For all experiments, liquid and/or solid minimal media (modified M9 media) (Table 2.1), lacking of trace elements, yeast and vitamins, were used. Modified compositions of M9 media for different experimental set-ups are given in Table 2.1. Unless mentioned differently, for all CaCO$_3$ precipitation experiments non-buffered M9 media containing 2 mg/L PO$_4$-P (Table 2.1) (to minimize interference due to Ca$_3$(PO4)$_2$ formation, K_{sp},Ca$_3$(PO4)$_2$) << K_{sp},CaCO$_3$)

was used and pH measurements were conducted at the beginning and at the end of the experiments.

Table 2.1 Composition of the modified M9 media in different setups

Compounds		Isolation of strains & Kinetic growth	Dehydration, Re-activation	All CaCO₃ precipitation experiments
Buffer (g/L)	$Na_2HPO_4.7H_2O$	8.5	-	-
	KH_2PO_4	3	-	-
M9 salt solution (g/L)	NaCl	0.5	0.5	-
	$MgSO_4$	0.24	0.24	0.24
	$CaCl_2$	0.011	0.011	6.325
Carbon source (g/L)	Na-Formate	6	6	6
	Methanol	4	4	-
Nitrate source (g/L)	KNO_3	0.72	1.011	-
	$Ca(NO_3)_2.4H_2O$	-	-	1.18
Phosphorus source (g/L)	Na_3PO_4	-	0.105	0.0105

Initial biomass concentrations were set equally by using flow cytometer, and given as cells/mL throughout the study. Abiotic control experiments were simultaneously conducted to confirm precipitation due to bacterial activity.

2.1. Isolation and characterization of the bacterial strains

The denitrifiers were isolated from garden soil by inoculating two batch reactors containing sterile M9 media (Table 2.1) with a specific carbon source (either methanol or formate) and cyclic heat treatment. The reactors were incubated for 5 cycles with 90% volumetric exchange ratio. Each cycle was 3 days. At the end of each cycle, reactors were exposed to heat treatment (70°C for at least 20 minutes). Afterwards, reactor content was replaced with the sterile fresh medium based on the volumetric exchange ratio. The headspaces of the reactors were flushed with Argon (Ar) and the next cycle started. After the 5th cycle, streak plate method was used to separate the isolated strains. At the end of the isolation procedure, 10 strains were achieved in total. In order to characterize the isolated

strains, DNA extraction, dereplication (BOX-PCR) and 16S-PCR amplification experiments were carried out. Firstly, DNAs of the 10 isolates were extracted using the suggested FastPREP DNA extraction protocol [87]. The DNA concentrations were analyzed by using Nano-drop ND-100 spectrophotometer. DNA concentrations were diluted to 50 ng/µl for each sample for the further BOX-PCR and 16S-PCR amplification experiments. The BOX-PCR was carried out as described previously [88]. The amplified DNA fragments were separated by electrophoresis on 1.5% agarose gel. The amplified DNA bands after 4.5 h of electrophoresis at 100V were stained in ethidium bromide solution and visualized under UV light. Following DNA extraction and dereplication (BOX-PCR), the 16S-PCR amplification was carried out via universal primers 63F (5'-CAGGCCTAACACATGCAAGTC-3') and 1378R (5'-CGGTGTGTACAAGGCCCGGGAACG-3'). Afterwards, the closest BLAST hits were determined.

2.2. Selection of the most appropriate strains among the isolates

The isolated strains were further tested for their tolerance to dehydration and starvation stress. Upon 3 days growth in non-buffered M9 media (Table 2.1) at anoxic conditions, each strain (containing same amount of cells/mL) was plated on an M9 agar (containing formate/methanol specific to strains), and incubated at 28 ^{o}C for 3 days. Following bacterial growth, plates were kept at 37°C for 3 weeks until completely dried (Figure 2.1). Dried agars were immersed in 50 mL M9 media (Table 2.1) and NO$_3^-$ reduction was monitored under anoxic conditions. The isolates showing no or negligible activity were discarded.

Figure 2.1 Dehydrated agar

Secondly, growth rates of the strains in minimal media were compared. The buffered minimal media (M9 media) containing 1.65 g/L PO$_4$-P (Table 2.1) which was used during the isolation of the strains, was used for growth. The cultures were prepared in 96-well plates in

triplicates, sealed with PCR film (no headspace, no air contact) and incubated inside the microplate reader (Tecan Infinite® 200 Pro) at 28°C. Optical densities at 620nm (OD_{620}) were automatically measured each hour for 96 hours. Finally, to select the most appropriate strains for optimization experiments a preliminary test was conducted and strain tolerances to PO_4-P limitation and minimized inoculum concentration were determined (Test-1). Initial conditions of test-1 are given in Table 2.2.

2.3. Performance optimization and repetitive CaCO₃ precipitation

2.3.1. Optimization of CaCO₃ precipitation by using *D. nitroreducens* and *P. aeruginosa*

After the experiments in Section 2.1, 2 strains with an enhanced performance, namely *Pseudomonas aeruginosa* PAO1 (f2 in formate fed batch) and *Diaphorobacter nitroreducens* (m5 in methanol fed batch), were selected for optimization of CaCO₃ precipitation in minimal media. Initially, the effect of the carbon source on NO_3^- reduction performances of *P. aeruginosa* and *D. nitroreducens* was investigated. Each strain (initial concentration of 10^7 cells/mL) was incubated in both minimal mediums, containing 4g/L of formate or methanol as a carbon source, and their NO_3^- reduction and NO_2^- productions were monitored for 4 days. Since there was no difference between the performances, formate was chosen as a carbon source for the rest of the analyses.

Phosphorus may promote bacterial activity and denitrifiers can use $Ca_3(PO4)_2$ as PO_4-P source [89]. Therefore, in test-2, both strains were investigated at different PO_4-P concentrations ranging from 2 to 500 mg/L in the presence of Ca^{2+} (Table 2.2). PO_4-P concentrations in test bottles were set by using 1 g/L Na_3PO_4 stock solution. In all CaCO₃ precipitation experiments, dissolved Ca^{2+} concentrations were monitored to detect CaCO₃ precipitation. Therefore, to avoid possible interference on dissolved Ca^{2+} concentrations due to $Ca_3(PO4)_2$ precipitation, initial samples were taken after chemical $Ca_3(PO4)_2$ precipitation was completed (after 30 minutes). Completion of $Ca_3(PO4)_2$ precipitation was confirmed by comparing the theoretical Ca^{2+} losses due to $Ca_3(PO4)_2$ precipitation (1.5 moles Ca^{2+} per mole PO_4-P) with measured Ca^{2+} loss, which equals to theoretical initial Ca^{2+} concentration (2.5 g/L) subtracted by measured Ca^{2+} concentrations after 30 minutes. Optimization was continued by varying initial biomass concentrations (Test-3) to increase the CaCO3 precipitation rate (g CaCO3/L.d). Initial conditions for test-3 are given in Table 2.2.

Table 2.2. Initial biomass and initial PO$_4$-P concentrations were set differently in different experiments[a]

Tests	Strain conditions before inoculation	Theoretical[b] initial biomass (cells/mL)	Theoretical initial PO$_4$-P (mg/L)	Theoretical initial Ca^{2+} (g/L)
Test-1	**Strain tolerances to PO$_4$-P and initial biomass minimization**			
	Grown in NM for 4 days	10^5	2	2.5
	Grown in NM for 4 days	10^5	20	2.5
	Grown in NM for 4 days	10^7	2	2.5
Test-2	**Effect of initial PO$_4$-P concentration**			
C-1	Grown in NM for 4 days	10^8	2	2.5
C-2	Grown in NM for 4 days	10^8	20	2.5
C-3	Grown in NM for 4 days	10^8	50	2.5
C-4	Grown in NM for 4 days	10^8	100	2.5
C-5	Grown in NM for 4 days	10^8	200	2.5
C-6	Grown in NM for 4 days	10^8	500	2.5
Test-3	**Effect of initial biomass concentration**			
C-1	Grown in NM for 4 days	10^5	2	2.5
C-2	Grown in NM for 4 days	10^7	2	2.5
C-3	Grown in NM for 4 days	10^8	2	2.5
C-4[c]	Grown in NM for 4 days	10^9	2	2.5
Test-4	**Repetitive CaCO$_3$ precipitation**			
	Scenario-1 Repetitive CaCO$_3$ precipitation after 3 weeks from first precipitation			
C-1	"Test-3 C-4" were kept at 28°C for 3 weeks without feeding and shaking	NA	0	2.5
	Scenario-2 Repetitive CaCO$_3$ precipitation starting from optimized initial conditions			
C-1	Grown in NM for 4 days	10^9	2	2.5
C-2	Grown in NM for 4 days	10^9	20	2.5

[a]C: Condition, NM: Nutrient Media, NA: Not measured

[b]Theoretical values: Calculated initial concentrations from measured stock concentrations considering dilutions per test.

[c]C – 4: The batch used for Scenario-1 in test 4 after 3 weeks.

2.3.2. Repetitive CaCO$_3$ precipitation performances in minimal media

Following optimization, repetitive CaCO$_3$ precipitation performances starting from two different initial conditions were investigated (Test-4) to define the limits of the strains. In scenario-1, repetitive CaCO$_3$ precipitation performances of the strains were tested 3 weeks after their first precipitation period (by continuing 'Test-3 C-4' after 3 weeks, no fresh inoculation). In scenario-2 freshly grown cells were investigated for repetitive CaCO$_3$ precipitation. Initial conditions for both scenarios are given in Table 2.2. In order to promote repetitive precipitation, all bottles were fed with 8.2 g/L Ca(NO$_3$)$_2$ stock solution (equivalent NO$_3$-N concentration after feed – 140 mg/L) on the 2nd, 4th and 7th days. To avoid possible Ca^{2+} and carbon source limitation, on day 4, bottles were spiked from 126.5g/L CaCl$_2$ and 600 g/L NaHCOO stock solutions (equivalent concentrations of the compounds in tests bottles were 2.3 g/L and 4 g/L for dissolved Ca^{2+} and HCOO$^-$, respectively).

2.4. Analytical Methods

Samples were taken for NO$_3^-$, NO$_2^-$ and dissolved Ca^{2+} analyses. NO$_3^-$ and NO$_2^-$ concentrations were measured by using compact ion chromatography (IC) (Metrohm 761). Nitrogen gas (N$_2$) production was measured via a compact gas chromatographer (GC) (Global Analyser Solution, The Netherlands). Dissolved Ca^{2+} was measured by using Shimadzu AA-6300 atomic absorption spectroscopy (AAS) with ASC-6100 auto-sampler. Number of cells was measured by using the method described by van Nevel et al. [90] via Accuri C6 flow cytometer (BD Biosciences) equipped with a C sampler. Experiments were carried out in triplicates and the mean values with standard deviations were plotted. pH measurements were conducted by using Consort C532 pH meter with a SP10B electrode. Microphotographs of the precipitates were obtained by using FEI Quanta 200F scanning electron microscope at 10 kV and 15 kV accelerating voltages by using low-angle backscattered electrons. Statistical analyses were conducted using SigmaPlot v12.0 (Systat Software Inc, USA) to compare significant differences of values by means of one way ANOVA test (p=0.05).

3. Results and Discussion

3.1. Isolation and characterization of the bacterial strains

At the end of isolation, nine special strains (five from methanol fed batch, four from formate fed batch) were obtained (Figure 2.2).
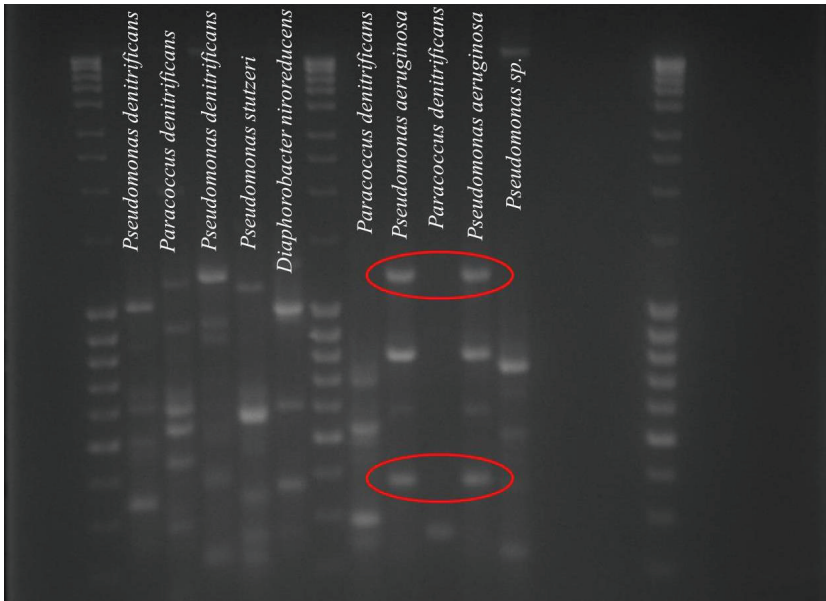
Figure 2.2 Dereplication-separation of DNA fragments via electrophoresis on 1.5% agarose gel (left to right the strains: first group m1-m5, second group f1-f5)

The isolates were Gram-negative, non-spore forming and mesophilic strains (Table 2.3). Sporulating strains are susceptible to deficiency of vitamins, trace elements and yeast extract especially during germination. Therefore, using M9 medium (Table 2.1) lacking of vitamins, trace elements and yeast extract, during the isolation procedure might have resulted in the elimination of sporulating strains. On the other hand, the existing information about the heat resistance of the isolated Gram-negative strains (Table 2.3) (*Paracoccus* sp., *Pseudomonas* sp., *Diaphorobacter* sp.) is limited. Bricha et al. [91] indicated viable cells of *P. aeruginosa* after exposure to 63°C for 30 minutes, and the resilience was attributed to the NaCl concentration and the pH of the solution. In this study, at pH 7, although the NaCl concentration was 0.05 % (w/v), which was 40 to 80 times lower than the values investigated by Bricha et al. [91], resistance to 70°C for more than 20 minutes was achieved. To our

knowledge, there is no reported evidence about the other isolated strains withstanding heat treatment which explains the majority (5 out of 9 specific isolates) of the *Pseudomonas* sp. in the isolates.

Table 2.3 Isolated strains and closest taxonomy identification[a]

Label	Species	Query Length (R – F)	Ident % (R – F)
m1	*Pseudomonas denitrificans* ATC 13867	1071 – 1115	99 – 98
m2	*Paracoccus denitrificans* PD1222	1091 – 801	97 – 96
m3	*Pseudomonas denitrificans* ATC 13867	398 – 1044	98 – 99
m4	*Pseudomonas stutzeri* A1501	734 – 1155	97 – 99
m5	*Diaphorobacter nitroreducens* TPSY	1096 – 1096	99 - 99
f1	*Paracoccus denitrificans* PD1222	1000 – 776	98 – 99
f2	*Pseudomonas aeruginosa* PAO1	1021 – 116	99 – 92
f3	*Paracoccus denitrificans* PD1222	1133 – NA	98 – NA
f4	*Pseudomonas aeruginosa* PAO1	1123 – 941	97 – 98
f5	*Pseudomonas* sp. UW4	151 – 160	100 – 98

[a]m: the species isolated by using methanol as carbon source

f: the species isolated by using formate as carbon source

R: results based on 1378r-reverse primer

F: results based on 63f-forward primer

3.2. Selection of the most appropriate strains among the isolates

Dehydration (osmotic stress, desiccation) and starvation are issues for a stable MICP applications in concrete environment. Therefore, the isolated strains were exposed to 3 weeks of dehydration and starvation. After resuscitation in minimal media (Table 2.1), all of the strains belonging to the MeOH batch were active, while only two of the strains (f2 and f5) belonging to the Formate batch were active in terms of NO_3^- reduction to NO_2^- and N_2 gas (Figure 2.3). It is known that Gram-positive bacteria are able to resist dehydration due to their thick peptidoglycan single-layer membrane and spore forming ability [92]. However, the results in this study indicated that Gram-negative bacteria, particularly *Pseudomonas* sp. and *Diaphorobacter nitroreducens*, are also capable to resist dehydration stress.

CHAPTER 2
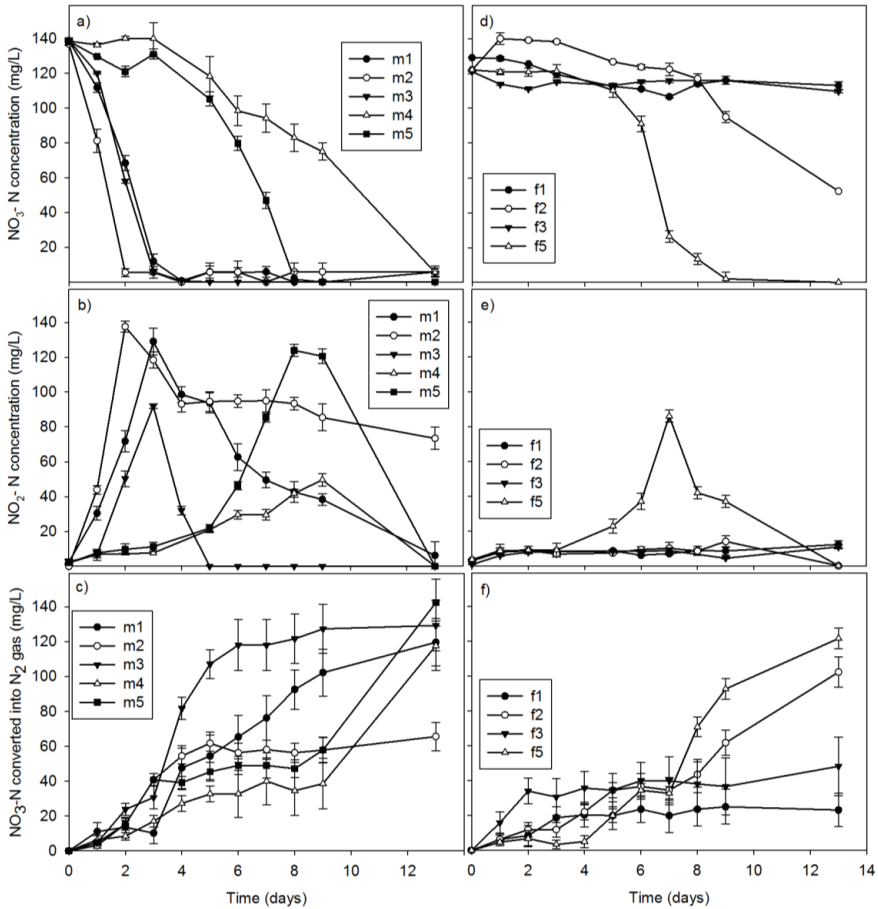
Figure 2.3 Resilient Gram-negative strains could reduce NO₃⁻ after 3 weeks exposure to dehydration and starvation stress (a, d) NO₃⁻ reduction; (b, e) NO₂-N production; (c, f) NO₃-N converted into N₂ gas; m: strains isolated from the batch fed with MeOH f: strains isolated from the batch fed with Formate

Only one strain (m2) from the *Paracoccus* isolates (m2, f1, f3) showed slight activity (Figure 2.3). *Pseudomonas aeruginosa* is reported to be isolated from air or contaminated dry surfaces and to be able to survive for months on dry surfaces [93]. Moreover, it has been shown that soil *Pseudomonas* sp. could change their microenvironment by producing extracellular polymeric substances (EPS), to enhance their survival in case of intracellular water loss [94]. Furthermore, *P. aeruginosa* PAO1 was also reported to resist high osmotic stress by producing compounds such as hydrophilins and osmoprotectans composed of *N*-acetylglutaminylglutamine amide (NAGGN), glutamate, alginate and trehalose [95,96].

Moreover, *Paracoccus denitrificans* was reported to utilize L- and D-Pro-B as well as tHyp-B as osmoprotectans to protect themselves under high osmotic stress [97]. Although there is limited information about osmotic stress resistance of *Diaphorobacter* sp, Kim et al. [98] recently isolated an outdoor air strain which could survive in the absence of water and has 97% similarity to *Diaphorobacter nitroreducens*. Since the strains in this study were isolated from soil which inherently exposes to certain harsh conditions such as drought, frost, high salt concentrations etc., the aforementioned protective mechanisms could have been further developed to resist unusual temperature and moisture conditions.

Growth rates of the strains (with positive results after dehydration test) in minimal medium were compared among each other. Results indicated that m5 had bi-phasic growth behavior while the other strains had monophasic growth pattern (Figure 2.4). This is because *D. nitroreducens* (m5) preferred to use NO_3^- prior to NO_2^- , which was also observed by Chakravarty et al. [99]. It was observed that most of the strains (m1, m2, m3, m4, f5) were linearly growing for the first 24 hours and afterwards continued with the exponential growth (Figure 2.4). However, lag phase of m5 and f2 lasted only for 6 hours. These results indicated that m5 and f2 are more responsive to the minimal nutrient environment.
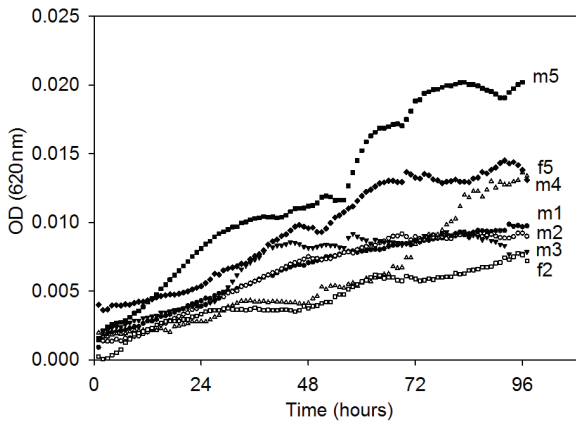
Figure 2.4 Growth kinetics of the strains for 96 hours in minimal medium

Diaphorobacter nitroreducens (m5) and *Pseudomonas aeruginosa* (f2) were determined as the fastest growing strains among the isolated strains, in minimal media conditions.

The first trial for $CaCO_3$ precipitation was conducted at cell concentration of 10^5 cells/mL and at PO_4-P concentration of 2 mg/L (Table 2.2). Yet, NO_3^- reduction activity could not be achieved from any of the strains at the end of 7 days (data not shown). There were two possibilities which may inhibit the bacterial activity. First possibility could be the P-

limitation. As previously mentioned, buffered media containing 1.65 g/L PO$_4$-P was used during the isolation (Table 2.1). When the PO$_4$-P concentration was decreased to 2 mg/L (modification to minimize Ca$_3$(PO4)$_2$ formation), decrease in denitrification performance of the strains was possible due to PO$_4$-P limitation. Second possibility was the poor inoculum concentration. Wang [84] indicated that initial bacteria concentration of less than 10^6 cell/mL caused inhibition of MICP. Both options were considered to determine the strains' susceptibility to minimization of PO$_4$-P and inoculum concentration.

3.2.1. Analyzing the possible PO$_4$-P limitation

PO$_4$-P is an essential microbial nutrient mainly contributing to the cell growth and being used in cellular polymer (nucleic acids, phospholipids, proteins) and adenosine triphosphate (ATP) synthesis. Recommended C:N:P ratios for effective nutrient removal from wastewater and for marine environment microorganisms are 100:5:1 and 106:16:1, respectively [100,101]. The only N source was NO$_3^-$ throughout the CaCO$_3$ precipitation experiments. The N:P ratio in the media was 70:1 (140 mg/L NO$_3$-N and 2 mg/L PO$_4$-P). Yet the available NO$_3^-$ was reduced during both energy and cell synthesis. Therefore, the actual N:P ratio should be calculated by only considering the NO$_3$-N used during cell synthesis. In order to estimate the portions of NO$_3$-N used for energy and cell synthesis, overall reaction of the formate oxidation through NO$_3^-$ reduction should be written. The overall reaction can be calculated from the half reactions as follows;

R_d: $0.5CO_2 + e^- + 0.5H^+ \rightarrow 0.5HCOO^-$ ΔG_d^o= 40.53 kJ/e$^-$ eq   (Rxn 2.2)

R_a: $0.2NO_3^- + 1.2H^+ + e^- \rightarrow 0.1N_2 + 0.6H_2O$ ΔG_a^o=-72.2 kJ/e$^-$ eq   (Rxn 2.3)
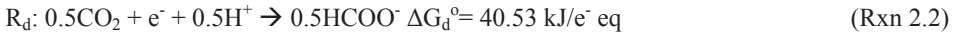
- When NO$_3^-$ is used for energy,

R_d – donor half reaction, R_a – acceptor half reaction, R_e – energy reaction

$$R_e= R_a-R_d \text{ (Equation 2.1)}$$

R_e: $0.5HCOO^- + 0.2NO_3^- + 0.7H^+ \rightarrow 0.1N_2 + 0.5CO_2 + 0.6 H_2O$ ΔG= -112.73 kJ/e$^-$ eq (Rxn 2.4)

- If NO$_3^-$ is also used for cell synthesis,

R_c: $0.036NO_3^- + 0.179CO_2 + 1.036H^+ + e^- \rightarrow 0.036 C_5H_7O_2N + 0.393H_2O$ (Rxn 2.5)

R_c – cell half reaction, R_s – synthesis reaction

$$R_s= R_c-R_d \text{ (Equation 2.2)}$$

R_s: $0.5HCOO^- + 0.036\ NO_3^- + 0.536H^+ \rightarrow 0.036\ C_5H_7O_2N + 0.321CO_2 + 0.393H_2O$ (Rxn 2.6)

- Assumption 1 – energy transfer efficiency, $\varepsilon = 0.55$ [102].
- Assumption 2 – cell synthesis happens through formate assimilation through Formate $\rightarrow$ pyruvate $\rightarrow$ cellular-C

$$\Delta G_p = 35.09\ \text{kJ/e}^-\ \text{eq} - \Delta G^0\ \text{(Equation 2.3)}$$

where

$\Delta G^0 = 40.53\ \text{kJ/e}^-$ eq for formate ($HCOO^-$), thus $\Delta G_p = -5.44\ \text{kJ/e}^-$ eq

R_s indicates that from 0.036 moles of NO_3, 4.07 g cells/e$^-$ can be produced. (cell MW: 113 g/mole).

Pyruvate $\rightarrow$ cellular-C requires 3.33 kJ/g cells [103].

$$\Delta G_{pc} = 3.33\ \text{kJ/g cell} \times 4.07\ \text{g cells/e}^-\ \text{eq (Equation 2.4)}$$

Total energy needed for synthesis $\Delta G_s = (\Delta G_p/\varepsilon^n) + (\Delta G_{pc}/\varepsilon)$ [102] (Equation 2.5)

where $n = +1$ if ΔGp is positive and -1 if ΔGp is negative

$\Delta G_s = 21.64\ \text{kJ/e}^-$ eq

$$\Delta G_r = \Delta G_a^0 - \Delta G_d^0 = -112.73\ \text{kJ e}^-\ \text{eq (Equation 2.6)}$$

The portion of the electron donor that needs to be oxidized to supply energy required for cell synthesis, A, can be calculated as;

$$A = -\Delta G_s/(\varepsilon \Delta G_r) = 0.35\ \text{(Equation 2.7)}$$

A, is also equal to the ratio of donor electrons used in energy reactions to those used in cell synthesis reactions (f_e^0/f_s^0):

$$f_e^0/f_s^0 = 0.35\ \text{(Equation 2.8)}$$

$$f_e^0 + f_s^0 = 1\ \text{(Equation 2.9)}$$

if these two equations are solved together;
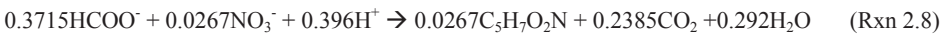
$f_e^0 = 0.26$ and $f_s^0 = 0.74$

Overall growth reaction $R = f_e^0 \times R_e + f_s^0 \times R_s$ (Equation 2.10)

$f_e^0 \times R_e$;

$0.1285HCOO^- + 0.0514NO_3^- + 0.182H^+ \rightarrow 0.0257N_2 + 0.1285CO_2 + 0.154H_2O$ (Rxn 2.7)

$f_s^0 \times R_s$:

$0.3715HCOO^- + 0.0267NO_3^- + 0.396H^+ \rightarrow 0.0267C_5H_7O_2N + 0.2385CO_2 + 0.292H_2O$ (Rxn 2.8)

Overall Reaction – R;

$0.5HCOO^- + 0.0781NO_3^- + 0.5781H^+ \rightarrow 0.0257N_2 + 0.0267C_5H_7O_2N + 0.367CO_2 + 0.446H_2O$ (Rxn 2.9)
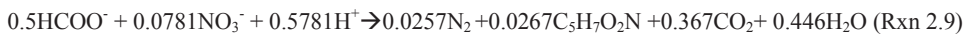
From the reactions (Rxn (2.7) and Rxn (2.8)) it can be found out that 26% and 74% of the NO$_3$-N is used for energy and cell synthesis, respectively. Since the initial NO$_3$-N concentration was 140 mg/L, the actual N:P ratio was 51. The N:P ratio of 51 was more than the values, C:N:P – 100:5:1, C:N:P – 106:16:1, suggested for efficient nutrient removal and cell synthesis, respectively [100,101]. Therefore, inhibition due to the PO$_4$-P limitation was highly possible.

3.2.2. Analyzing the effect of low initial bacteria concentration

The initial concentration of the bacteria plays an important role in MICP [84]. There was also the possible effect of PO$_4$-P limitation. Therefore, in order to understand the most significant effect, variables should be decreased to one. Accordingly, the biomass and PO$_4$-P concentrations were varied to determine if the strain susceptibility was due to PO$_4$-P limitation or the low initial cell concentrations. After comparison of the strains' performances in two batches at either higher PO$_4$-P (20 mg/L PO$_4$-P and 10^5 cells/mL) or higher biomass concentrations (2 mg/L PO$_4$-P and 10^7 cell/mL) (Table 2.2), it was found that 5 of the strains (m1, m2, m3, m4, f5) were more sensitive to PO$_4$-P deficiency (Figure 2.5) and were not active at 2 mg/L PO$_4$-P concentration even if the initial cell concentration was 10^7 cells/mL. On the other hand, two of the strains (m5 and f2) showed a moderate increase at higher PO$_4$-P concentration, while they showed remarkable activity with a higher initial biomass concentration at 2 mg/L PO$_4$-P concentration (Figure 2.5). Therefore, it can be said that all the strains were affected by the minimization of inoculum concentration while the strains f2 and m5 were tolerant to PO$_4$-P limitation. Hunter [89] indicated that under PO$_4$-P limitation, denitrification can be partially interrupted and NO$_2^-$ can accumulate; however, a N:P ratio of 100 or less is enough for complete denitrification. Yet, we revealed that P-limitation can severely inhibit denitrification activity of several strains especially in nutrient-poor environment.
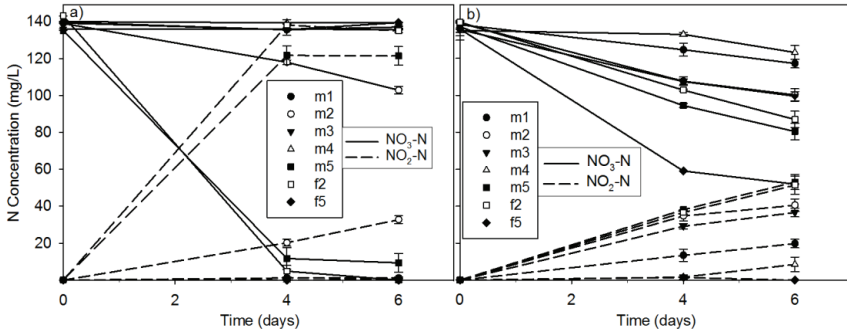
Figure 2.5 Response of the 7 dehydration-resilient strains' nitrate reduction performances to increase in either PO$_4$-P or biomass concentrations. (Initially negligible activity was achieved with initial cell concentration of 10^5 cells/mL at 2 mg/L PO$_4$-P) (a) Increasing initial biomass concentration to 10^7 cells/mL and keeping PO$_4$-P at 2 mg/L (N:P – 51:1); (b) Keeping initial biomass concentration at 10^5 cells/mL and increasing PO$_4$-P concentration to 20 mg/L (N:P – 5.1:1)

Considering the outcomes of the kinetic growth analysis and strain tolerances to PO$_4$-P limitation, isolates m5 (*Diaphorobacter nitroreducens*) and f2 (*Pseudomonas aeruginosa*) were selected for further investigation.

3.3. Performance optimization and repetitive CaCO$_3$ precipitation

3.3.1. Optimization of CaCO$_3$ precipitation by using *D. nitroreducens* and *P. aeruginosa*

No difference was observed in nitrate reduction activity of the both strains when either methanol or formate was used as a carbon source (Figure 2.6). Therefore, it was possible to use one of the commercial concrete admixture Ca/Na-Formate as a carbon source in further experiments regarding to optimization of CaCO$_3$ precipitation in minimal media.
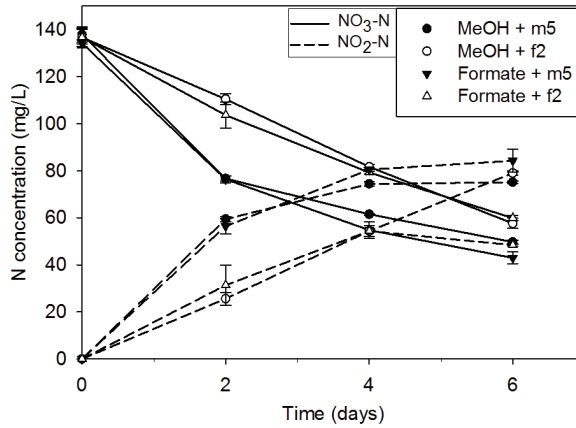
Figure 2.6 Denitrification activity of Diaphorobacter nitroreducens (m5) and

Pseudomonas aeruginosa (f2) in presence of either formate or methanol as carbon source

The rate limiting step in MICP through denitrification is the oxidation of carbon source by NO_3^- reducing bacteria (Rxn. (2.10)) since CaCO₃ crystals immediately form around the cells [83]. Therefore, either NO_3^- reduction rate or CaCO₃ precipitation rate (g CaCO₃/L.d) can be used for performance optimization. CaCO₃ precipitation rate and CaCO₃ precipitation yield (g CaCO₃/g NO₃-N) were optimized in this section.

$$5HCOO^- + 2NO_3^- + 7H^+ \rightarrow 5CO_2 + 6H_2O + N_2 \text{ (Rxn 2.10)}$$

The initial PO₄-P concentrations after the Ca(PO₄)₃ precipitation took place are given in Table 2.4. During test-2, no significant difference was observed between initial and final pH values as well as between initial pH values of the batches (Table 2.5).

Table 2.4 Measured initial dissolved Ca²⁺ concentrations in PO₄-P optimization

experiments

	Initial dissolved Ca²⁺ concentrations (g/L)					
Batches	P-2*	P-20	P-50	P-100	P-200	P-500
m5	2.45±0.04	2.47±0.10	2.40±0.04	2.25±0.00	2.09±0.03	1.49±0.04
f2	2.48±0.47	2.46±0.00	2.30±0.02	2.20±0.01	2.09±0.00	1.54±0.01

*P-X indicates the PO₄-P concentration (mg/L)

m5: batch inoculated with *Diaphorobacter nitroreducens*

f2: batch inoculated with *Pseudomonas aeruginosa*

Although the initial biomass concentrations were the same (10^8 cells/mL), the NO_3^- reduction performances were different. Among different PO_4-P concentrations, enhanced performances for both strains were achieved at 2 and 20 mg/L PO_4-P in 2 days (Figure 2.7). At the end of 4 days, *D. nitroreducens* reduced all the NO_3^- into NO_2^- and precipitated similar amounts of $CaCO_3$ (~0.72 g $CaCO_3$/L, ~12.8 g $CaCO_3$/g NO_3-N) at all the PO_4-P concentrations except at 500 mg/L PO_4-P which was ~50 % lower (Figure 2.7c). *P. aeruginosa* also reduced all the NO_3^- into NO_2^- and/or N_2 gas in 4 days. However, from 50 mg/L PO_4-P concentration onwards, NO_3^- and NO_2^- reduction rates, thus $CaCO_3$ precipitation rates decreased (5% at 50 mg/L PO_4-P and 29% at 500 mg/L PO_4-P).

Table 2.5 Initial and final pH values in PO$_4$-P optimization experiment (Test-2)

Day	P-2*	P-20	P-50	P-100	P-200	P-500
	Control					
Initial	7.3±0.0	7.4±0.1	7.3±0.1	7.3±0.1	7.2±0.1	7.3±0.1
Final	7.3±0.1	7.2±0.1	7.2±0.1	7.2±0.1	7.2±0.0	7.3±0.1
	m5 – *Diaphorobacter nitroreducens*					
Initial	7.4±0.1	7.4±0.1	7.4±0.1	7.3±0.1	7.3±0.1	7.3±0.1
Final	7.2±0.0	7.3±0.1	7.3±0.1	7.2±0.1	7.3±0.1	7.2±0.1
	f2 – *Pseudomonas aeruginosa*					
Initial	7.3±0.1	7.4±0.1	7.3±0.1	7.34±0.1	7.4±0.1	7.4±0.1
Final	7.2±0.0	7.3±0.1	7.2±0.0	7.3±0.0	7.3±0.1	7.5±0.1

*P-X indicates PO$_4$-P concentration (mg/L)

CHAPTER 2
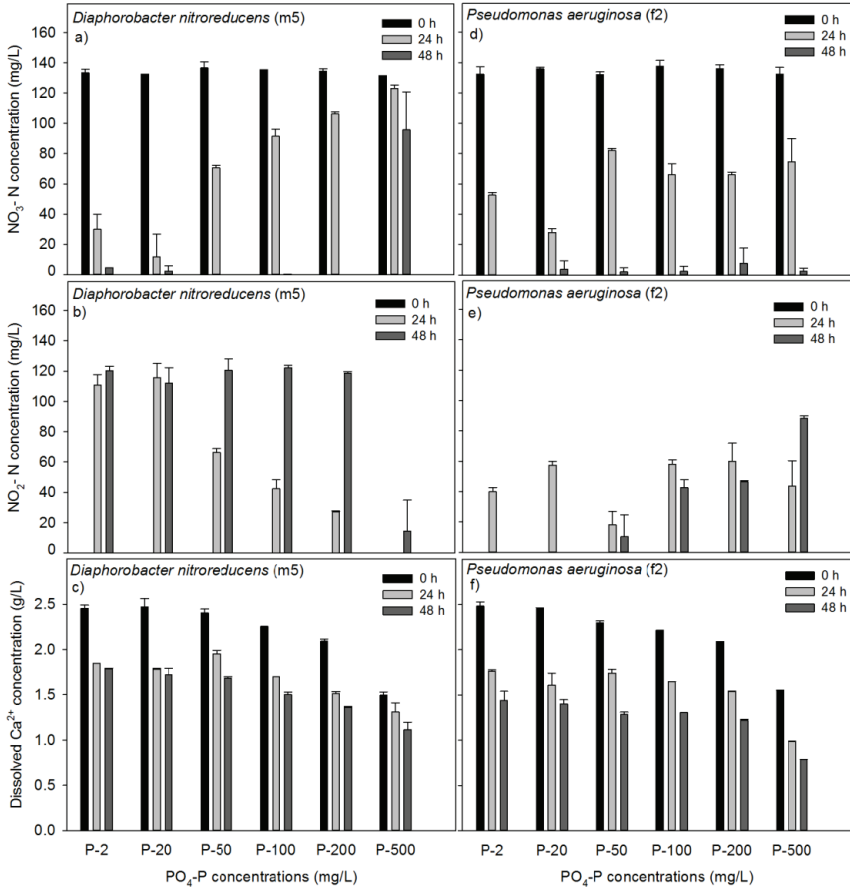
Figure 2.7 Increasing initial PO$_4$-P concentrations decreased the NO$_3^-$ reduction activity of strains in the presence of Ca^{2+} ions (initial Ca^{2+} concentration prior to PO$_4$-P addition: 2.5 g/L) (a, d) NO$_3$-N reduction activity; (b, e) NO$_2$-N production; (c, f) Dissolved Ca^{2+} loss due to CaCO$_3$ precipitation

The results of PO$_4$-P optimization revealed that in the presence of Ca^{2+}, PO$_4$-P has a negative effect on NO$_3^-$ reduction rate, thus CaCO$_3$ precipitation rate. Since the negative effect of PO$_4$-P on NO$_3^-$ reduction was observed only in the presence of Ca^{2+} ions (not during the previous experiments with buffered media containing 4 mg/L Ca^{2+} and 1.7 g/L PO$_4$-P), it was mostly related to triggered Ca$_3$(PO4)$_2$ precipitation. One of the governing parameters in CaCO$_3$ precipitation is the presence of nucleation sites. Bacteria, due to its negatively charged cell wall, attract positively charged ions and concentrate them around the cell wall [80,83]. Therefore, upon saturation either in the cell microenvironment due to metabolic by products

or in the bulk environment due to concentration increase, precipitation starts and primarily forms around the bacterial cells [83,104]. The importance of a nucleation site is not only specific for $CaCO_3$ precipitation but also crucial for all similar precipitates ($NH_4MgPO_4.6H_2O$, $Ca_3(PO_4)_2$, $CaSO_4.2H_2O$, etc.). Therefore, the negative effect of $Ca_3(PO_4)_2$ could be attributed to its rapid formation on the bacterial surface, which might occlude the bacteria from the bulk environment and hinder nutrient uptake rate. Furthermore, continuous occlusion of the cells might be detrimental and decrease the number of active cells (cells/mL). In this way, NO_3^- reduction, hence $CaCO_3$ precipitation could be delayed. The experimental procedure might also exacerbate the occlusion effect, since PO_4-P was added into the test solutions as a final ingredient to set initial PO_4-P concentrations while Ca^{2+} ions and bacteria were already in the test solutions. Hunter [89] indicated that denitrifiers can use the $Ca_3(PO_4)_2$ as PO_4-P source. Therefore, it can be said that $Ca_3(PO_4)_2$ itself was not inhibitory for the strains but, particularly, the rapid formation of the precipitate around the cell surface hindered the activity. As seen in Figure 2.7c and Figure 2.7f, the $CaCO_3$ precipitation rate decreased by half and at 500 mg/L PO_4-P even more. Moreover, up to 200 mg/L PO_4-P, as long as the nutrients were completely consumed, the amounts of $CaCO_3$ precipitations showed similarities, i.e. no negative effect on the $CaCO_3$ precipitation yields (g $CaCO_3$/g NO_3-N). Rivadeneyra et al. [105] also mentioned that in the presence of Ca^{2+}, PO_4-P has a negative effect on biological $CaCO_3$ precipitation. Our results and their observations, in particular to the significant inhibitory effect around and over 200 mg/L PO_4-P are in agreement. Coherently, due to $Ca_3(PO_4)_2$ formation around cell wall, 30% inhibition on ureolysis and $CaCO_3$ precipitation rates of *Bacillus pasteurii* was also reported [104].

Initial biomass concentration appeared to have an impact on $CaCO_3$ precipitation yield and rate. *D. nitroreducens* precipitated ~12.8 g $CaCO_3$/g NO_3-N at 10^8 cells/mL, while it increased to ~14.1 g $CaCO_3$/g NO_3-N at 10^9 cells/mL (Figure 2.8a-c). In addition to the increase in yield, the NO_3^- reduction and $CaCO_3$ precipitation rates increased with increasing biomass concentrations (Figure 2.8a,c). *D. nitroreducens* and *P. aeruginosa* precipitated ~1.68 g/L and ~2.6 g/L $CaCO_3$ in 4 days, respectively when the initial cell concentration was 10^8 cells/mL, while it took only 2 days to precipitate the same amount of $CaCO_3$ at 10^9 cells/mL (Figure 2.8).

CHAPTER 2
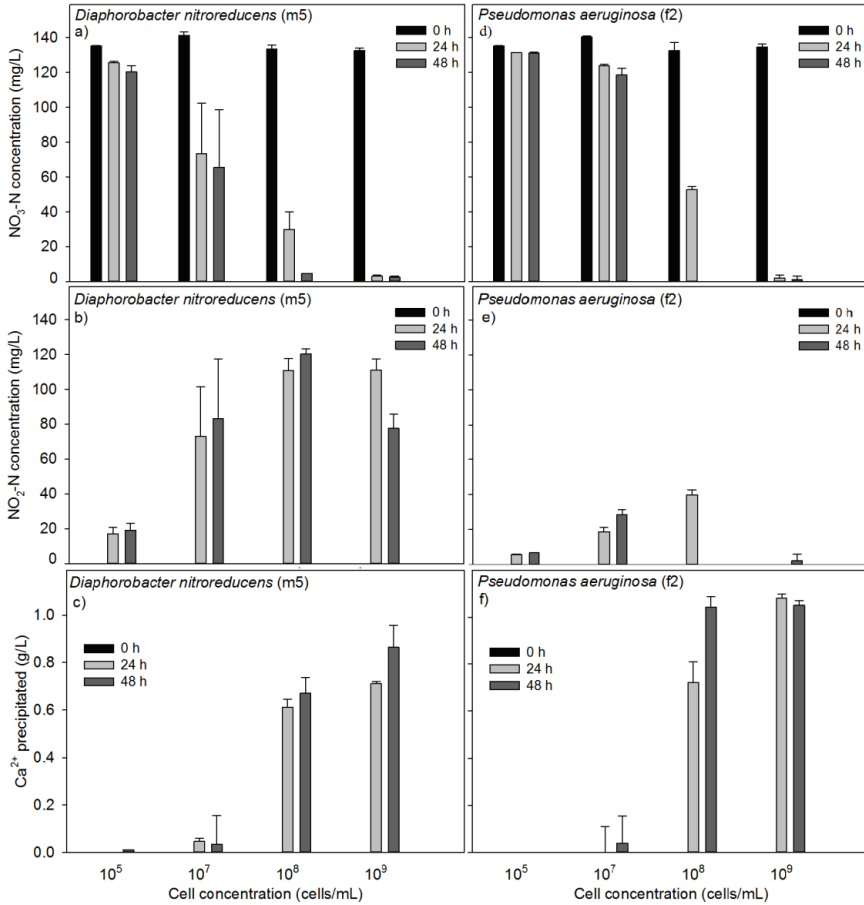
Figure 2.8 Increasing initial cell concentration increased the CaCO₃ precipitation rate (initial PO₄-P concentration: 2 mg/L, N:P–51, Ca²⁺ concentration 2.5 g/L). (a, d) NO₃-N reduction activity; (b, e) NO₂-N production; (c, f) The amount of Ca²⁺ precipitated

In test-2 and test-3 only 0.1 to 0.2 units of pH change was observed while considerable amount of precipitation was achieved. This was due to the formation of precipitates around the cells and low solubility of CaCO₃. Oxidation of $HCOO^-$ through denitrification consumes H^+ (produces alkalinity) and theoretically increases the pH up to 10.16 (Rxn. (2.10)). Therefore, one can expect observation of the same pH increase in CaCO₃ precipitation experiments. Yet, in the presence of Ca^{2+} ions, due to the low solubility of CaCO₃, precipitation starts in the microenvironment of the cells through (Rxn. (2.11)). Immediate

formation of $CaCO_3$ around the cells consumes the produced free OH^- ions and CO_2 which prevents the observation of pH increase in the bulk solution [83].

$$Ca^{2+}+CO_{2_{(aq)}}+2OH^-\rightarrow CaCO_{3_{(s)}}+2H_2O \qquad \text{(Rxn 2.11)}$$
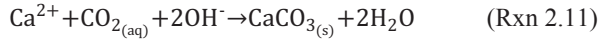
One of the objectives in this study was to optimize $CaCO_3$ precipitation in minimal medium environment. Therefore, it was necessary to compare the obtained values with theoretical maximum $CaCO_3$ precipitation yields that can be achieved from oxidation of formate through NO_3^- reduction. In order to calculate the theoretical values the limiting parameters should be defined. In all experiments the amount of Ca^{2+} was abundant and the Ca^{2+} concentration was not a limiting factor for the precipitation. There were three more parameters that can affect $CaCO_3$ precipitation; (1) the amount of alkalinity produced, (2) the amount of CO_2 produced, (3) the growth conditions. Maximum $CaCO_3$ precipitation can be achieved under optimal growth conditions during which the oxidation of formate happens according to Rxn (2.9). Therefore, when alkalinity is the limiting factor for $CaCO_3$ precipitation, maximum $CaCO_3$ precipitation yield can be calculated as;

(g $CaCO_3$/g NO_3^-) $= [\Delta H^+/\Delta NO_3^-] \times [\Delta CaCO_3/\Delta H^+] \times MW_{CaCO3}$ (Equation 2.11)

(g $CaCO_3$/g NO_3-$N_{reduced}$)=[(0.5781 mol H^+)/(0.0781 mol NO_3^-]×(50 g $CaCO_3$/ mol H^+)×(l mol NO_3^- / 14 g NO_3^--$N_{reduced}$) = 26.43 g $CaCO_3$/g NO_3-N reduced.

When the CO_2 available is limiting the $CaCO_3$ precipitation, the maximum $CaCO_3$ precipitation yield is;

(g $CaCO_3$/g NO_3^-) $= [\Delta CO_2/\Delta NO_3^-] \times [\Delta CaCO_3/\Delta CO_2] \times MW_{CaCO3}$ (Equation 2.12)

(g $CaCO_3$/g NO_3-$N_{reduced}$) = [(0.367 mol CO_2)/(0.0781 mol NO_3^-]×(100 g $CaCO_3$/ mol CO_2)x(l mol NO_3^- / 14 g NO_3^--$N_{reduced}$) = 33.56 g $CaCO_3$/g NO_3-N

Under limited growth conditions, all the NO_3^- provided is used for energy, thus the same calculations would be done for the Rxn (2.4);

When the produced alkalinity is controlling $CaCO_3$ precipitation, the yield is: 12.5 g $CaCO_3$/g NO_3-N

When the produced CO_2 is controlling $CaCO_3$ precipitation, the yield is: 17.85 g $CaCO_3$/g NO_3-N

Stoichiometric analysis of formate oxidation through complete denitrification (NO_3^- to N_2 gas) or partial denitrification (NO_3^- to NO_2^-) and the possible $CaCO_3$ yields were given in Table 2.6. Each case was considered for optimal growth and limited growth conditions for alkalinity limiting and for CO_2 limiting conditions. Regardless of the growth conditions, the

CaCO$_3$ precipitation yield is lower when alkalinity is controlling the precipitation. Therefore, maximum CaCO$_3$ precipitation yields that can be achieved under optimal and limited growth conditions are 26.43 g CaCO$_3$/g NO$_3$-N and 12.5 g CaCO$_3$/g NO$_3$-N, respectively.

The optimized values in this study were 14.1 g CaCO$_3$/g NO$_3$-N and 18.9 g CaCO$_3$/g NO$_3$-N for *D. nitroreducens* and *P. aeruginosa* in 2 days, respectively (Figure 2.8). Hence the CaCO$_3$ precipitation yields under optimized conditions were 53% and 72% of the values that can be achieved under optimal growth conditions (Figure 2.8c,f, Table 2.6). Although perfect optimization was not achieved, enhanced precipitation yields were obtained throughout the study compared to previously reported data. Karatas [49] reported 1.3 – 10.6 g CaCO$_3$/g NO$_3$-N precipitation yield in 3.5 to 40 days with *Pseudomonas denitrificans*. Van Paassen et al. [51] achieved a yield of 6 g CaCO$_3$/g NO$_3$-N by *Castellaniella denitrificans* in 7 days. In both studies nutrient-rich media was used. Despite of using minimal media in this study, enhanced performance could be achieved.

Table 2.6. Stoichiometric analysis of formate oxidation through denitrification and possible CaCO$_3$ yields

	Optimal growth conditions[a]		Limited growth conditions[b]	
	mole ΔH^+ per mole N_{red}	mole ΔCO_2 per mole N_{red}	mole ΔH^+ per mole N_{red}	mole ΔCO_2 per mole N_{red}
NO$_3^-$→NO$_2^-$	-2.8	2	-1	1
NO$_2^-$→N$_2$	-5.7	3.3	-2.4	1.5
NO$_3^-$→N$_2$	-7.4	4.7	-3.5	2.5
	g CaCO$_3$ per g NO$_x$-N$_{reduced}$			
	Alk. is limiting[c]	CO$_2$ is limiting[d]	Alk. is limiting	CO$_2$ is limiting
NO$_3^-$→NO$_2^-$	10	14.3	3.6	7.1
NO$_2^-$→N$_2$	20.3	23.5	8.6	10.7
NO$_3^-$→N$_2$	26.4	33.5	12.5	17.8

ε: energy transfer efficiency was taken as 0.55

ΔH^+: Acidity consumed/produced (-/+) during overall growth reaction

ΔCO_2: CO$_2$(g) consumed/produced (-/+) during overall growth reaction

[a] when NO$_3^-$ used for both energy and cell synthesis

[b] when NO$_3^-$ only used for energy, (no growth)

[c] when all of the produced alkalinity is consumed through CaCO$_3$ precipitation

[d] when all of the produced CO$_2$ is consumed through CaCO$_3$ precipitation

3.3.2. Repetitive CaCO₃ precipitation performances in minimal media

Both strains performed repetitive precipitation without additional cell inoculation. No significant differences were observed between the strains in terms of the total amount of $CaCO_3$ precipitated. There was no difference between performances at 2 and 20 mg/L initial PO_4-P concentrations. Therefore, the performances at 2 mg/L PO_4-P concentration was used to represent the performance of fresh inoculum (Figure 2.9). There were also no significant differences between old (Scenario – 1) and fresh strains (Scenario – 2) (Figure 2.9).
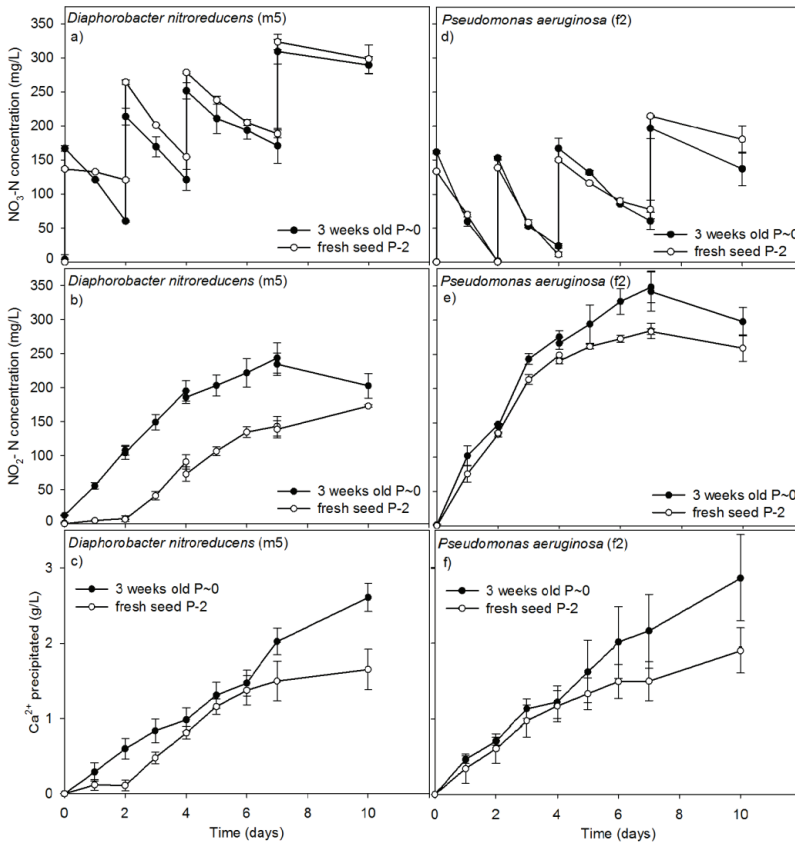
***Figure 2.9** Repetitive CaCO₃ precipitation and NO₃-N reduction performances of D. nitroreducens and P. aeruginosa under semi-continuous feeding of single inoculum (10⁹ cells/mL, P: PO₄-P) (a, d) NO₃-N reduction activity; (b, e) NO₂-N production; (c, f) The amount of Ca²⁺ precipitated based on dissolved Ca²⁺ measurements. Cultures of 3 weeks-old had been maintained in the solution since the earlier precipitation experiment. (Feeding: Ca(NO₃)₂ on days 2, 4, 7; NaCOOH and CaCl₂ on day 4)*

Throughout the experiment, in all batches, 0.1 and 0.2 units of pH change was observed (Table 2.7). *P. aeruginosa* reduced more NO$_3^-$ than *D. nitroreducens* during the entire test. Since *D. nitroreducens* preferred to use NO$_3^-$ primarily instead of NO$_2^-$ (Figure 2.4), NO$_2^-$ accumulated in the reactors as expected. Although *P. aeruginosa* had higher NO$_2^-$ reduction rate, it was not enough to prevent NO$_2^-$ accumulation. Nitrite (NO$_2^-$), in the form of free nitrous acid (FNA) can be inhibitory for bacterial growth and activity. The inhibitory effect of NO$_2^-$ is directly related to the pH of the environment which governs the free nitrous acid (FNA) (HNO$_2$) formation (Rxn (2.12). In this experiment, the highest NO$_2^-$ concentrations were observed on day 7 (798.4 mg/L in m5 reactor and 1143 mg/L in f2 reactor). Nevertheless, even higher values such as ~2.15 g/L NO$_2^-$ were reported to have no inhibitory effect on anoxic growth of *Pseudomonas denitrificans* [106].

$$NO_2^- + H^+ \longrightarrow HNO_2 \quad K_a=10^{-3.35} \ (T=28^oC) \qquad (Rxn \ 2.12)$$
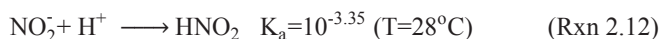
The calculated HNO$_2$ concentrations (based on Rxn. (2.12)) on day 7 (at pH 7.1) were 2.74μg/L and 3.93μg/L for m5 and f2, respectively. These values were also lower than the inhibitory FNA levels determined in other studies (10-25μg/L and >200 μg/L for 60% and complete inhibition of denitrifiers) [107,108]. Furthermore, the NO$_2^-$ reduction between day 7 and day 10 confirms that nitrite reductase enzymes, which are prone to the FNA inhibition, were still active.

Table 2.7 pH values during the repetitive CaCO$_3$ precipitation experiment (Test-4)

Day	Repetitive - old[1] cells			Repetitive – fresh inoculum at P-2[2]		
	Control	m5	f2	Control	m5	f2
0	7.1±0.1	7.3±0.1	7.3±0.1	7.2±0.0	7.4±0.1	7.5±0.1
1	7.1±0.0	7.9±0.1	7.3±0.1	7.2±0.1	7.1±0.1	7.2±0.1
2	7.1±0.0	8.3±0.0	7.6±0.1	7.0±0.0	7.1±0.0	7.3±0.1
3	7.2±0.1	7.6±0.0	7.4±0.1	7.0±0.0	7.2±0.1	7.1±0.1
4	6.9±0.1	7.3±0.1	7.3±0.0	6.9±0.0	7.2±0.1	7.1±0.1
5	6.9±0.1	7.1±0.1	7.2±0.0	7.0±0.0	7.3±0.1	7.2±0.0
6	7.0±0.1	7.2±0.1	7.2±0.1	6.9±0.1	7.1±0.0	7.2±0.1
7	6.9±0.1	7.3±0.1	7.3±0.1	6.9±0.1	7.2±0.1	7.1±0.0
10	6.9±0.1	7.3±0.0	7.3±0.1	6.9±0.1	7.1±0.1	7.2±0.1

[1] cells stayed in precipitation for 3 weeks

[2] P-X indicates PO$_4$-P concentration (mg/L)

The CaCO$_3$ precipitation of *D. nitroreducens* and *P. aeruginosa* (for fresh cultures only) stopped after day 5 and day 6, respectively. However, due to the ongoing NO$_3^-$ (60 mg/L NO$_3$-N) and NO$_2^-$ reduction until day 10, the old cells of both strains (Scenario-1) continued to precipitate CaCO$_3$ with a lower rate (Figure 2.9c,f). Further investigation of the precipitate under SEM revealed that the form of the CaCO$_3$ was aragonite and calcite which formed around the cells (Figure 2.10). Bacterial footprints were observed on the precipitates as gaps of 1-2μm in diameter. Formation of CaCO$_3$ around the cells can be detrimental or inhibitory by limiting nutrient uptake of the cells and diffusion kinetics [45,104], while it can also be beneficial for repetitive precipitation as it fixes cells in the matrix [45,51].

During test-4, the main inhibition was observed in NO$_3^-$ reduction after 1 g/L Ca^{2+} precipitated in the form of CaCO$_3$ (day 3 for f2 and day 5 for m5) (Figure 2.9). Similarly, during test-2, the same amount of Ca^{2+} in the form of Ca$_3$(PO4)$_2$ (at 500 mg/L PO$_4$-P concentration, about 1 g/L of Ca^{2+} was precipitated as Ca$_3$(PO4)$_2$) resulted in inhibition which was more evident for *D. nitroreducens* (Figure 2.7). The consistency between the inhibitory effects of two different form of precipitates, containing same amount of Ca^{2+} ions (~1 g/L Ca^{2+}), supported the idea that the decrease in bacterial activity was due to the accumulation of precipitates around the cells. Figure 2.10 confirms that CaCO$_3$ precipitates were mainly formed around the cells during test-4 which might decrease the number of active cells. It is also known from test-3 that the less the number of cells the less the NO$_3^-$ reduction and CaCO$_3$ precipitation activity.
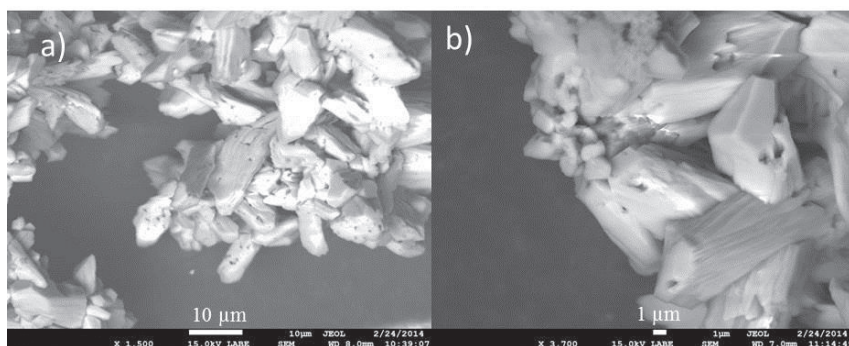

Figure 2.10 SEM photomicrographs of microbial footprints on aragonite and calcite crystals formed during repetitive CaCO$_3$ precipitation (a) precipitation formed by Diaphorobacter nitroreducens; (b) precipitation formed by Pseudomonas aeruginosa

Strains used in scenario-1, on the other hand, precipitated around 1 g/L Ca^{2+} during their first precipitation period in test-3 (Figure 2.8c,f), and after 3 weeks of idle period they could further precipitate during test-4 (Figure 2.9). Moreover, the inhibitory level of 1 g/L Ca^{2+} was not valid for the old cells (scenario-1) (Figure 2.9), since the solution was already containing precipitates (from 'test-3 C-4') on which crystals could further grow. Consistently, pH change in bulk solution was observed more (Table 2.7) since precipitates were also forming on other crystals besides their formation in cell microenvironment. It can be said that if the strains are provided with time to recover and grow (produce fresh cells) and the major nutrients are not limited in the bulk solution, they could precipitate CaCO$_3$ continuously. Optimization of the time required for recovery is necessary for improved repetitive performances.

All the optimization tests in this Chapter were conducted at 28 $^{\circ}$C. The studied temperature is considered in the optimum temperature range for the growth of mesophilic bacteria (25-40 $^{\circ}$C) while the actual temperature range for activity and growth of mesophiles is reported as 15-45 $^{\circ}$C [109]. Therefore, with a certain degree of variation in the performance, the reported bacteria can still be used in MICP applications where ambient temperature is between 15-45 $^{\circ}$C. Prior to application, the environmental conditions and their possible effect on CaCO$_3$ precipitation rate should be considered.

4. Conclusions

Enhanced CaCO$_3$ precipitation yields can be achieved in minimal nutrient environment if one of the specified resilient strains, *Pseudomonas aeruginosa* PAO1 or *Diaphorobacter nitroreducens*, is used.

Under optimized conditions in minimal nutrient environment, 72% and 53% of the maximum theoretical yield were achieved by *Pseudomonas aeruginosa* PAO1 and *Diaphorobacter nitroreducens*, respectively.

The amount of Ca^{2+} precipitated around the bacteria is of significance during repetitive CaCO$_3$ precipitation for decreasing the nutrient uptake rate and inhibiting the activity. In MICP applications, the intervals between two precipitation periods should be optimized based on recovery of active biomass concentration for stable repetitive performance.

The presented two strains have sufficient yield in minimal nutrient conditions and resilience to harsh environmental conditions, thus they can be considered to develop microbial self-healing concrete.

5. Acknowledgments

PART II
SCREENING OF HEALING AGENTS

CHAPTER

3

INTERACTION BETWEEN SELF-HEALING ADDITIVES, MORTAR AND STEEL

INTERACTION BETWEEN SELF-HEALING
ADDITIVES, MORTAR AND STEEL

Abstract

Protection methods/materials have been used to preserve the bacteria inside the concrete until the crack occurs. The compatibility of the protection materials with both bacteria and concrete is of significance to avoid problems regarding to bacteria-concrete interaction. A wide screening of commercially available materials is thus required to evaluate the alternatives. This chapter mainly covers the investigation of three commercially available protective carriers (diatomaceous earth, expanded clay particles and granular activated carbon particles) to understand the interaction between protective carriers, bacteria and mortar. In general survival of the bacteria with the aid of protective carriers and the influence of the self-healing additives (bacteria + nutrients + protective carriers) on mortar properties were investigated. Additionally, the effect of microbial NO_2^- production on steel corrosion was investigated. A novel self-protected culture was also produced and considered as an alternative to avoid protective carriers. Results indicated that protected bacteria as well as the self-protected culture could survive in mortar and became active 3 days after the pH dropped below 10. A week after the activation, 50-60 % of the initial NO_3^- was reduced to NO_2^-. Nitrite (NO_2^-) accumulation was observed at pH values around 9.5 and it led to a shift in E_{corr} values of the steel from -0.36 V to -0.14 V. Among the investigated protective carriers, granular activated carbon and expanded clay particles showed the best compatibility when combined with bacteria, nutrients and mortar.

1. Introduction

The interactions between concrete structures and living organisms is becoming more and more important in relation to the durability of concrete structures. Bacteria able to precipitate $CaCO_3$ through different pathways are being investigated to develop self-healing concrete structures [54,84]. It is known that to be used in concrete applications, bacteria should be able to withstand (1) high shear stress during mixing, (2) high temperatures during cement hydration, (3) starvation, (4) highly alkaline pH (pH~13 in concrete and pH~10 in cracks), (5) dehydration stress, (6) cement hydration related shrinkage and pore sizes <0.1 μm [58]. Previous studies revealed that regardless of their resilience, axenic cultures (spores or vegetative cells) require encapsulation or immobilization to withstand the harsh conditions, especially the high shear stress, the alkaline pH conditions and the crushing due to microstructure densification [40,110].

So far, in microbial self-healing concrete studies, several protective materials or encapsulation techniques have been tested [22,40,58,59,110]. Vegetative cells immobilized in silica gel and polyurethane revealed biological activity at considerable levels and they were able to heal concrete cracks up to 0.4 mm [110]. Moreover, it was shown that microencapsulated bacterial spores were able to induce $CaCO_3$ precipitation that was enough to close cracks up to 1 mm [22]. Hydrogels have also been used as encapsulation material to protect bacterial spores. The results showed that encapsulation with hydrogels allows bacteria to heal cracks varying between 0.2 and 0.5 mm [59]. However, all these encapsulation materials were reported to be expensive or inappropriate for concrete use [111]. In contrast, commercially available and less expensive materials such as diatomaceous earth and expanded clay were also examined as protection for the bacterial agents [40,58]. The immobilization of bacterial vegetative cells with diatomaceous earth proved to be effective regarding the maintenance of biological activity in cement paste [58]. The study showed that cracks up to 0.17 mm could be closed using diatomaceous earth immobilized bacteria. Bacterial spores encapsulated in expanded clay particles could also close cracks up to 0.46 mm [40].

Several other materials have already been described to protect bacteria from harsh environmental conditions. Among them, granular activated carbon can be pointed out as a bacteria and concrete compatible material [112,113]. Yet, to our knowledge, it has never been tested for bacterial protection in concrete environment. Besides, it is reported that bacteria are able to create self-organizing clusters, composed of compact self-immobilized cells to protect

CHAPTER 3

themselves from harsh conditions [114]. Such self-protection can avoid the need for additional protection material. It was also reported that the use of axenic cultures is 40 times more expensive than the use of non-axenic ones in concrete [111]. Not only the self-protection capabilities but also the economic feasibility is the advantage of these non-axenic cultures over the reported axenic cultures. Therefore, a clustered microbial culture could be an option for development of microbial self-healing concrete.

So far, reported protection methods are study-specific and their influence on concrete properties are not clearly defined. To develop a microbial self-healing concrete without losing the basic concrete functionalities, understanding of the interaction of the bacterial agents and the protective carriers with mortar is necessary.

Steel reinforcement also plays an important role for durability of concrete structures and microbial self-healing studies up to now have not described the effect of microbial activity on the steel rebars. The described microbial self-healing processes also lack the preventive action to avoid exposure of the steel surface to corrosive substances during the healing period. Therefore, the effect of the healing agents (nutrients+protective carriers+bacterial agent) and the microbial activity on steel reinforcement should also be investigated.

We previously reported two NO_3^- reducing axenic cultures namely, *Diaphorobacter nitroreducens* and *Pseudomonas aeruginosa* for their resilience to heat, dehydration and starvation [67]. Therefore, it is possible that with protective carriers these two axenic cultures could become functional in the context of self-healing of concrete. Since concrete admixtures $Ca(HCOO)_2$ and $Ca(NO_3)_2$ [68] can serve as nutrients for the reported denitrifying strains [67], the strategy is promising to develop a concrete compatible system. Moreover, NO_3^- reduction may also bring solution to aforementioned corrosion issues, since it leads to the production of NO_2^- which is known as corrosion inhibitor [70,115].

Accordingly, this chapter consists of four sections (1) key roles of protective carriers on activity and survival of the selected axenic cultures in different environments (pH 7, pH 9.5-10, pH~13 and after mortar incorporation) (2) self-encapsulation as a protection option (3) the influence of self-healing additives on mortar setting and strength (4) effect of microbial NO_3^- reduction on steel corrosion.

2. Material and methods

In this study, three different NO_3^- reducing cultures were tested. Two of them were axenic cultures, consisting of a single type of microorganisms. The third one was a non-axenic NO_3^- reducing culture named activated compact denitrifying core (ACDC). The axenic cultures were tested in combination with nutrients and different protective carriers. The non-axenic ACDC culture was also combined with the nutrients and tested without any additional protection than its own layered structure.

2.1. Axenic bacterial cultures

Two previously isolated axenic NO_3^- reducing cultures, (1) *Pseudomonas aeruginosa*, (2) *Diaphorobacter nitroreducens* were used. The axenic cultures were grown in 500 mL of nutrient media (NM) for 4 days and 10 L of NM was further inoculated with the grown culture. After 4 days of growth, bacterial cells were harvested (12.5 g cell dry weight) by centrifuging at 6300g for 7 minutes. Collected pellets were re-suspended in saline solution (8.5 g/L NaCl) prior to inoculation of the test bottles.

2.2. Protective carriers

During the two different sets of tests, the pH related activity of the cultures and the tests regarding to mortar incorporation; the axenic cultures were tested with and without protection. Performances were assessed by using three different protective carriers, namely diatomaceous earth, expanded clay and granular activated carbon. The diatomaceous earth powder used in the experiments was 5-200 μm in size, while expanded clay and granular activated carbon particles were 0.5-2 mm in size.

2.3. Incorporation of bacterial agents with protective carriers

A concentrated bacterial suspension containing either *Pseudomonas aeruginosa* or *Diaphorobacter nitroreducens* was incorporated in a protection material by using a vacuum saturation technique. Prior to tests, each protection material was autoclaved (at 1 bar, 120 °C for 20 min). Sterile materials were individually vacuumed (-0.85 bar) inside 100 mL bottles which were tightly closed with rubber stoppers and metal caps. Finally, a concentrated bacterial suspension was injected through the rubber stoppers and the bottles were further pressurized (+1 bar) with air to promote incorporation of bacteria in protective carriers.

Pressurized bottles were kept at room temperature for 48 h to enable migration of bacteria from solution to the surface or pores of the protection materials. The pressure was released just before the inoculation of the buffered media and addition to the mortar mix in pH dependent activity tests and tests regarding to mortar incorporation, respectively. The protective carrier:bacteria ratio was 50:1 and 10:1 w/w during the pH related activity and the tests regarding to mortar incorporation, respectively. The incorporated amounts of protective carriers and bacteria in different setups are given in Table 3.1.

Table 3.1 Tested combinations of bacterial cultures, nutrients and protection materials

Test batches	Bacteria[2] (g)	Protection material (g)			Media[3] (100 mL)	Ca(NO$_3$)$_2$ + Ca(HCOO)$_2$ (g)	Mortar[4]
		DE	EC	GAC			
pH dependent bacterial activity at pH 7, pH 9.5, pH 13							
Reference	0	0	0	0	+	N/A	N/A
PM control	0	12	0	0	+	N/A	N/A
	0	0	12	0	+	N/A	N/A
	0	0	0	12	+	N/A	N/A
UPB	B1 (0.25)	0	0	0	+	N/A	N/A
	B2 (0.25)	0	0	0	+	N/A	N/A
PB	B1 (0.25)	12	0	0	+	N/A	N/A
	B1 (0.25)	0	12	0	+	N/A	N/A
	B1 (0.25)	0	0	12	+	N/A	N/A
	B2 (0.25)	12	0	0	+	N/A	N/A
	B2 (0.25)	0	12	0	+	N/A	N/A
	B2 (0.25)	0	0	12	+	N/A	N/A
	ACDC (0.35)	0	0	0	+	N/A	N/A
Experiments regarding to mortar incorporation							
Survival of cultures in mortar environment upon 28 days curing							
Mortar control	0	0	0	0	N/A	0	+
PM control	0	22.5	0	0	N/A	13.5 + 9	+
	0	0	22.5	0	N/A	13.5 + 9	+
	0	0	0	22.5	N/A	13.5 + 9	+

UPB	B1 (2.25)	0	0	0	N/A	13.5 + 9	+
	B2 (2.25)	0	0	0	N/A	13.5 + 9	+
	B1 (2.25)	22.5	0	0	N/A	13.5 + 9	+
	B1 (2.25)	0	22.5	0	N/A	13.5 + 9	+
	B1 (2.25)	0	0	22.5	N/A	13.5 + 9	+
	B2 (2.25)	22.5	0	0	N/A	13.5 + 9	+
PB	B2 (2.25)	0	22.5	0	N/A	13.5 + 9	+
	B2 (2.25)	0	0	22.5	N/A	13.5 + 9	+
	ACDC (3.2)	0	0	0	N/A	13.5 + 9	+
	ACDC (6.4)	0	0	0	N/A	13.5 + 9	+
Mixtures for testing setting and strength properties							
Reference	0	0	0	0	N/A	0	+
R+Nutrients	0	0	0	0	N/A	13.5 + 9	+
	0	22.5	0	0	N/A	0	+
R+PM	0	0	22.5	0	N/A	0	+
	0	0	0	22.5	N/A	0	+
R+Bacteria	B1 (2.25)	0	0	0	N/A	0	+
	B2 (2.25)	0	0	0	N/A	0	+
R+PM+DP1	B1 (2.25)	22.5	0	0	N/A	13.5 + 9	+
	B1 (2.25)	0	22.5	0	N/A	13.5 + 9	+
	B1 (2.25)	0	0	22.5	N/A	13.5 + 9	+
R+PM+DP2	B2 (2.25)	22.5	0	0	N/A	13.5 + 9	+
	B2 (2.25)	0	22.5	0	N/A	13.5 + 9	+
	B2 (2.25)	0	0	22.5	N/A	13.5 + 9	+
R+ACDC	ACDC (3.2)	0	0	0	N/A	13.5 + 9	+
	ACDC (6.4)	0	0	0	N/A	13.5 + 9	+

[1]R: Reference; PM: protection material; B: Bacteria; UPB: unprotected bacteria; PB: protected bacteria; DE: diatomaceous earth; EC: expanded clay; GAC: granular activated carbon; Nutrients: $Ca(NO_3)_2$ + $Ca(HCOO)_2$; DP: Denitrifying pack = Bacteria + Nutrients
[2]B1: *Diaphorobacter nitroreducens*; B2: *Pseudomonas aeruginosa*; 70% of ACDC is bacteria thus 3.2 g = 2.25 g bacteria + 0.95g salt and 6.4 g = 4.5 g bacteria +1.9 g salt.
[3]Media compositions for different pH values are given in Table 3.2;
[4]Mortar (Sand:cement:water – 1350:450:225)

The amount of water in the bacterial suspension was deducted from the water content of the mortar specimens to keep the water/cement ratio (0.5 w/w) constant. The former was calculated by using the given equation (Eq. (3.1)).

$$m_{water}(g)= m_{final\ mixture}(g)-m_{dry\ materials}(g) \qquad \text{(Equation 3.1)}$$

where

m_{water}:the amount of water in the bacterial suspension

$m_{final\ mixture}$:total sum of protection material and bacterial suspension

$m_{dry\ materials}$:total sum of dry weight of bacterial cells and protection material

Only the axenic strains were encapsulated. The nutrients were not incorporated in protection materials and directly added to the mixture during mortar preparation.

Table 3.2 Solution compositions used in different experimental set-ups

| Compounds[1] | Experimental Set-ups | | | | | |
| | pH dependent activity | | | Survival after mortar incorporation[2] | Corrosion tests | |
	pH 7 (g/L)	pH 9.5 (g/L)	pH 13 (g/L)	9.5 < pH < 10 (g/L)	Test solution (g/L)	Inhibitory solution (g/L)
Na$_2$HPO$_4$	10.6	13.6	-	-	-	-
NaOH	-	0.1	-	-	-	-
HCl	0.9	-	-	-	-	-
Cement	-	-	20	-	-	-
NaCl	0.5	0.5	0.5	0.5	2.8	2.8
MgSO$_4$	0.2	0.2	0.2	0.2	0.2	0.2
CaCl$_2$	0.0	0.0	0.0	0.0	0.1	0.1
NaCOOH	6.0	6.0	6.0	6.0	10.0	10.0
NaNO$_3$	0.9	0.9	0.9	0.9	17	0.0
Na$_3$PO$_4$	-	-	0.1	-	0.1	0.1
NaNO$_2$				-	0.0	13.8

[1]Concentrations in bulk solution

[2]Final pH was adjusted by using 5 M HCl

2.4. Self-encapsulation as a protection option

2.4.1. Cultivation of self-protected granular culture

Activated compact denitrifying core (ACDC) granules were cultivated in a cylindrical sequencing batch reactor (SBR) (effective h=30 cm, Ø=12.5 cm and 50 % volume exchange ratio) by following a previously described procedure [76]. The setup is illustrated in Figure 3.1 and the operational conditions are given in Table 3.3. The SBR was operated with anoxic/aerobic period sequence (180 min anoxic and 155-168 min aerobic period). Different from the described procedure, minimal nutrient solution (COD:N – 5:1) was used as feed (4 times/day) and the solution composition is given in Table 3.3. Moreover, the initial pH of the feed solution was set between 9-9.5 by using concentrated NaOH solution (10 M). Granulation (94% of the volatile suspended solid (VSS) content) was achieved in 4 weeks and the reactor was operated for 7 months in total.
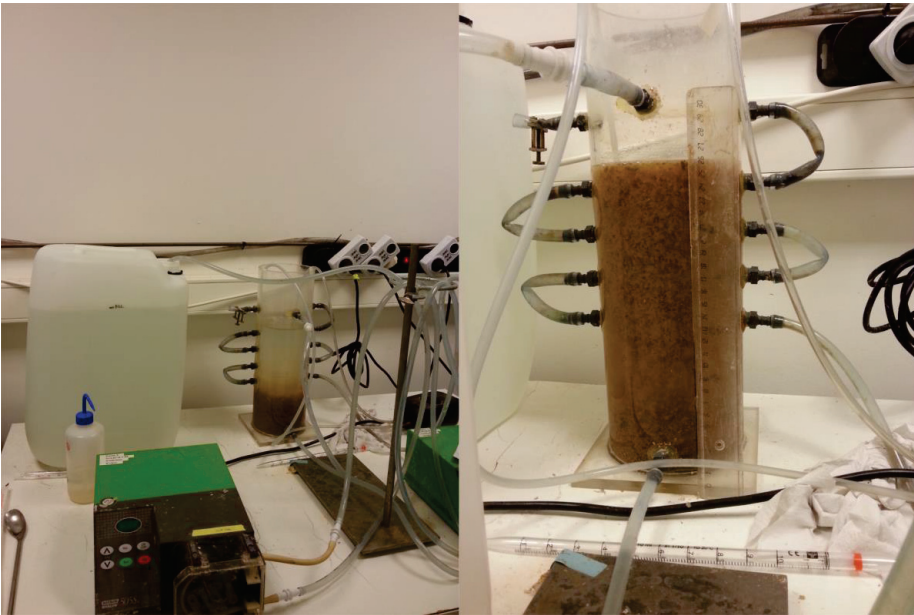
Figure 3.1 The sequencing batch reactor setup for ACDC production

ACDC granules were harvested from the reactor at the end of 2nd, 4th and 7th month. The harvested ACDC granules were dried for 48 hours in a drying tunnel at 60 ^{o}C with ventilation and stored at room temperature inside closed containers until the tests. The incorporated amounts of ACDC in different setups are given in Table 3.1. In order to have comparable

particle sizes with the protective carriers, dried ACDC granules of 0.5-2 mm in size were used. Sieving technique was used to collect the portion with the desired size range.

Table 3.3 The feed composition and operational conditionsfor cultivation of ACDC

Compounds	Concentrations (g/L)	Operational Parameters	Selection criteria
$NaNO_3$	1.70	Organic loading rate (g COD/L.d)	2.80
$NaHCOO$	5.35	Nitrogen loading rate (g N/L.d)	0.56
$Ca(HCOO)_2$	0.65	Cell yield (g VSS/g COD)	~ 0.17
Na_2HPO_4	0.05	Minimum settling velocity (m/h)	> 54
$MgSO_4.7H_2O$	0.18	N removal rate (%)	> 85
		Sludge retention time (d)	29
		Hydraulic retention time (h)	11

2.4.2. Quality assessment of the ACDC culture

During the steady operation of SBR, initial and effluent NOx-N (NO_3-N and NO_2-N) concentrations were monitored by sampling arbitrary cycles. The rough composition of the ACDC granules was also monitored through volatile (VSS) and total suspended solid (TSS) analysis after full granulation (> 90% granulation). The VSS:TSS ratio was used to determine the rough composition of the ACDC granules which appeared to be bacteria (0.7 w/w) and inorganic matter (0.3 w/w). Throughout the manuscript, ACDC amounts were given as cell dry weight (CDW) which represents 70% of the total ACDC amount used. The objective was to achieve granular culture containing an active denitrifying core. One of the indications of a denitrifying core is denitrification in aerobic periods [116] where the dissolved oxygen concentration in bulk environment is around 6 mg/L. Denitrification performance of the ACDC was monitored through kinetic NOx-N measurements with 15 minutes intervals during the aerobic period of a cycle.

2.5. Effect of pH on bacterial activity

Bacterial NO_3^- reduction activities were tested at pH 7 (neutral pH), pH 9.5 (expected pH in a concrete crack due to carbonation) and pH 13 (mortar mix pH) [117] with and without using protective carriers. Both protected and unprotected cultures were tested in 100 mL buffered minimal media by using a bacterial concentration of 2.5 g/L. Consistently, a non-

axenic culture, ACDC, was also tested by using a bacterial concentration of 2.5 g CDW /L (total ACDC concentration 3.6 g/L = 2.5 g/L bacteria + 0.9 g/L inorganic matter). Since ACDC is self-immobilized microbial culture, the culture as such – without further protection – was used. The minimal media compositions at different pH values are given in Table 3.2.

Upon 14 days exposure of bacterial cultures to pH 13, the pH was adjusted to pH <10 by using 5 M HCl. Therefore, the expected pH drop due to crack occurrence could be simulated and the changes in activity of cultures with and without protection could be monitored. Samples were taken for NO_3^- and NO_2^- analyses and the sampling intervals were decided based on the activity of the cultures. Tests were conducted in triplicates.

2.6. Tests regarding to mortar incorporation

2.6.1. Experimental planning

The objectives of the section was to evaluate the effect of protection materials/methods for so called microbial self-healing concrete. Thus, firstly, it was necessary to check if the bacterial agents can survive mortar incorporation with the aid of protective carriers. Secondly, it was necessary to evaluate the influence of (1) the bacterial agent (denitrifying bacteria) (2) the nutrients (3) the protection material, on mortar setting and strength properties.

Series of mortar specimens (40 × 40 × 160 mm) were prepared by using CEM I 52.5 N, tap water and standard sand (Table 3.1) according to the norm EN 196–1 and further cured at $20^{\circ}C$ and RH > 95% for 7 or 28 days prior to tests. During preparation of the samples with different combinations, aggregates were not replaced and thus sand:cement:water ratio was kept as 3:1:0.5.

The influence of the type of bacteria on compressive strength was investigated by incorporating plain bacteria (*Pseudomonas aeruginosa* or *Diaphorobacter nitroreducens*: 0.5% w/w cement) in mortar. It was assumed that physico-chemical properties of *Diaphorobacter nitroreducens* and *Pseudomonas aeruginosa* are similar to each other and representative for the vegetative cells. Therefore the effect on setting properties was only tested by using *Diaphorobacter nitroreducens* and considered as a representative for vegetative cells. The influences of the particular nutrients necessary to achieve microbial self-healing through denitrification were tested by incorporating plain nutrients (5% w/w cement: 13.5 g $Ca(NO_3)_2$ + 9 g $Ca(CHOO)_2$) in mortar. The influence of different protection materials was investigated by incorporating each protection material (5% w/w cement) in mortar.

Finally, batches containing all the necessary components (protected bacteria+nutrients) were investigated. Tested mortar specimens and their compositions are given in Table 3.1. Bacterial survival was tested following compressive strength tests.

2.6.2. Survival after mortar incorporation

Composition of the reference mortar mixture and the mixtures containing combination of nutrients (5 % w/w cement), bacteria (0.5 % w/w cement) and each one of the protection materials (5 % w/w cement) are given in Table 3.1.

Upon curing, compressive strength tests were conducted according to the standard NBN EN 196-1:2005 by using a test machine (Walter&Bai, 250/50, Switzerland). Immediately after the fracture of the specimens under compressive load, pieces of specimens were kept together without complete splitting (Figure 3.2) and stored in ethanol sterilized plastic containers. The containers were further opened in a sterile environment and the outer surfaces of specimens were sterilized by exposing to UV radiation for 30 minutes.

Figure 3.2 Specimens prior to splitting of the crack surface for bacteria extraction

Afterwards the specimens were split from the point of fracture and the incorporated bacteria were extracted from the inner crack surfaces. In order to extract the bacteria, crack surfaces were immersed in 60 mL of sterile minimal media and sonicated at low frequency at 120 W for 5 minutes. No PO_4-P was introduced into the media since it would react with the Ca^{2+} ions and form an insoluble compound ($K_{sp}(Ca_3(PO_4)_2)$=2.07 x 10^{-33}). After removal of the specimens the suspension was allowed to settle for 5 minutes and the supernatant was transferred into 50 mL of sterile minimal media. The pH of the final mixture was set between 9.5 and 10 by addition of 5 M HCl and the mixture was incubated at 28 ^{o}C on a 120 rpm

shaker. The same procedure was also applied for mortar mixtures without bacteria for control purposes. Overall, the tested batches were: reference, reference + protection material + nutrients, reference + protected bacteria + nutrients, reference + unprotected bacteria + nutrients. Since ACDC is a self-immobilized microbial culture, it was used without additional protective carrier.

Bacterial activity was followed through NO_3^- reduction activity. Samples were taken for NO_3^- and NO_2^- analyses and the sampling intervals were decided based on the activity of the cultures. Tests were conducted in triplicates.

2.7. Measurement of mortar properties

Initial and final setting times of different mortar mixtures, with similar consistency, were determined according to the standard ASTM C807–13 by using a Vicat needle. The initial setting time refers to the moment when the Vicat needle does not completely penetrate the test specimen. Final setting time refers to the moment when the Vicat needle does not penetrate at all the specimen. Measurements were conducted in a climate room (20 ^{o}C and 60% humidity). The 7 and 28 days compressive strength tests were conducted according to the standard NBN EN 196–1 (2005) by using a test machine (Walter&Bai, 250/50, Switzerland). Throughout the text, *D. nitroreducens* + $Ca(NO_3)_2$ + $Ca(HCOO)_2$ is termed as the denitrifying pack-1 and *P. aeruginosa* + $Ca(NO_3)_2$ + $Ca(HCOO)_2$ is termed as denitrifying pack-2. ACDC + $Ca(NO_3)_2$ + $Ca(HCOO)_2$ is termed as ACDC pack.

2.8. Effect of bacterial NO_3^- reduction on steel corrosion

The measurements were conducted in a closed electrochemical cell with a typical three-electrode setup; low carbon steel (Q Panel test substrates) with an exposed area of 452 mm² as working electrode, a saturated Ag/AgCl electrode as a reference electrode, and a platinum mesh as the counter electrode. The sample steel plates were degreased with acetone, rinsed with ethanol, and further air dried.

The compositions of inhibitory and corrosive electrolyte solutions are given in Table 3.2. The inhibitory solution was used as an indicative positive control. The positive control solution (inhibitory solution) was expected to inhibit steel corrosion since the $[NO_2^-]:[Cl^-]$ ratio of the solution was 4:1 (Table 3) which is more than the suggested ratio for effective corrosion inhibition [74]. The negative control solution (test solution) was used as corrosive reference (abiotic control). The negative control solution revealed the effect of the solution

content on steel corrosion. When the same solution was used with bacteria, the effect of biological NO_2^- production from NO_3^- could be determined. Fresh non-protected bacterial cultures (*Diaphorobacter nitroreducens*, *Pseudomonas aeruginosa*, ACDC) were used to inoculate corrosive electrolyte solution, and the differences in corrosive behavior were monitored. The initial bacteria concentration in the test bottles was 2.5 g CDW/L. All the test bottles were purged with N_2 gas for 5 minutes and further incubated at room conditions (20 °C without shaking). The polarization experiments were performed after 24 hours, and after 7 days of incubation.

The anodic and cathodic curves were recorded by polarizing the system from -10 mV to + 300 mV or from + 10 mV to - 300 mV, respectively, versus open circuit potential with a scan rate of 2 mV/s and a step potential of 1 mV. The anodic and cathodic curves were recorded separately and for each measurement an individual steel plate was used.

2.9. Data interpretation

According to the norms for evaluation of the setting time via Vicat needle (ASTM C191–04a and ASTM C807–13), samples with a difference of 12 minutes in the initial setting time are significantly different throughout the range of 49 to 202 minutes. Moreover, according to the same norms, samples with a difference of 20 minutes in the final setting time are significantly different throughout the range of 185 to 312 minutes.

The significance of variation between compressive strength values was analyzed by means of one way ANOVA test (p=0.05) using SigmaPlot v12.0 (Systat Software Inc., USA) software. Each sample was compared with the reference by using an LSD test (5%).

2.10. Analytical methods

The VSS and TSS analysis were done according to the standard methods [118]. Nitrate (NO_3^-) and nitrite (NO_2^-) concentrations were measured via compact ion chromatography (IC) (Metrohm, 761). pH measurements were conducted by using Consort C532 pH meter with a SP10B electrode. Microphotographs of the precipitates were obtained by using FEI Quanta 200F scanning electron microscope at 10 kV accelerating voltages and a working distance of 9 mm. Potentiometric measurements were carried out using an Autolab PGSTAT30 and PGSTAT100 potentiostat (Metrohm Autolab, B.V.), with Nova software for data acquisition. Corrosion current (i_{corr}) and corrosion potential (E_{corr}) were obtained from the Tafel slopes as described in [74].

3. Results

3.1. Self-encapsulation as a protection option

3.1.1. Quality of the self-protected ACDC culture

The appearance of the harvested ACDC granules are illustrated in Figure 3.3. After the drying process, the ACDC granules shrink and their color became darker (Figure 3.3). Based on the conducted solid analyses, the volatile suspended solid (VSS) concentration at steady-state operation was 5.5 ± 0.2 g/L and the total suspended solid concentration was 7.8 ± 0.4 g/L. At steady operation, ACDC:VSS ratio (the amount of granulated culture) in the system was more than 90 %.
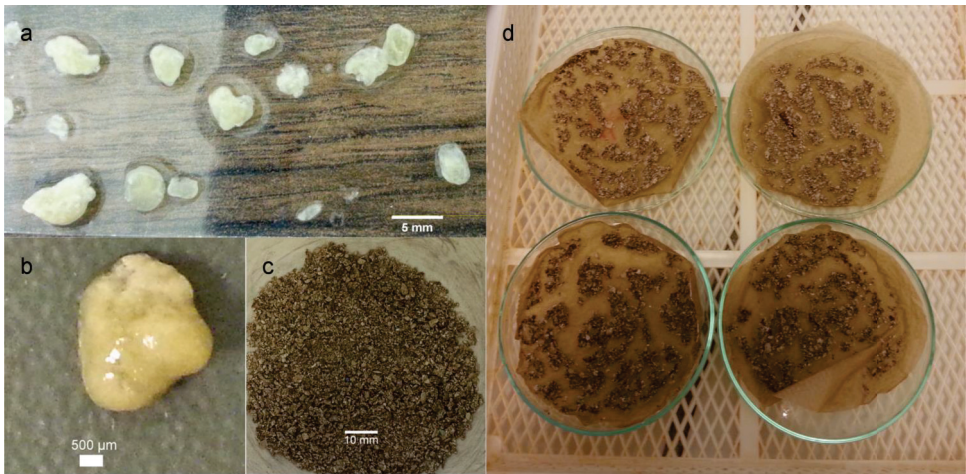
Figure 3.3 Appearance of the harvested ACDC granules (a,b) wet; (c,d) after drying

The only nitrogen (N) source fed to the system was NO_3-N. When the influent NO_3-N concentration (280 mg/L - Table 3.3), the volume exchange ratio (50%) and the residual NOx-N (~32 mg/L-Figure 3.4) concentration at the end of a cycle during steady operation were taken into consideration, one can calculate the denitrification performance of ACDC for both anoxic and aerobic periods. Regular NOx-N measurements revealed that at the end of anoxic period 69 % of the total nitrogen (TN) was consumed. Following kinetic NOx-N measurements in aerobic period (dissolved oxygen ~ 6mg/L), it appeared that there was simultaneous nitrification and denitrification. Results indicated that 34 % of the TN was consumed through simultaneous denitrification occurring in aerobic period (Figure 3.4).
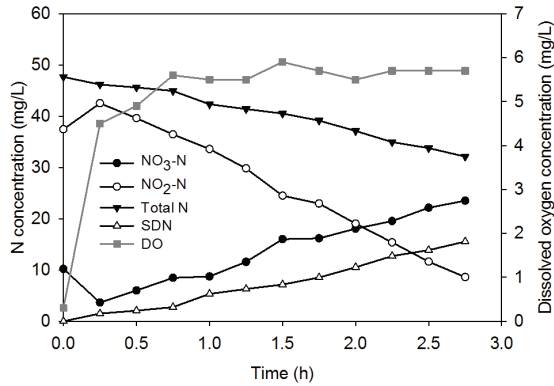
Figure 3.4 Kinetic NOx-N measurements during the aerobic period of an arbitrarily chosen SBR cycle (SDN: simultaneous denitrification, DO: dissolved oxygen concentration)

3.2. Performance of protected and unprotected bacteria at different pH environments

The NO_3^- reduction activities of unprotected axenic cultures at each pH condition (pH 7, pH 9.5 and pH 13) were used as a base to evaluate the effect of protection methods. The evolution of NOx-N (NO_3-N and NO_2-N) concentrations were used to compare the performances in each case. The NO_3^- reduction activities of *Diaphorobacter nitroreducens* with and without protection are given in Figure 3.5. Same type of illustration was used in Figure 3.6 to present NO_3^- reduction activities of *Pseudomonas aeruginosa* in each case. The activity of ACDC culture is given in Figure 3.7. Since the performance of axenic cultures were enhanced when they were incorporated in protective carriers (Figure 3.5 and Figure 3.6), the performance of ACDC was only compared with the activity of protected axenic cultures.

Results indicated that at every pH condition, ACDC, performed better than the axenic cultures regardless of their having protection or not (Figure 3.5 – Figure 3.7). A protective carrier was found to be indispensable to keep axenic vegetative cultures alive at pH values of 13. All carriers showed similar protective and performance boosting effect on axenic cultures. Unlike the cases with diatomaceous earth and expanded clay, NO_2^- accumulation was not observed when granular activated carbon was used as a protective carrier (Figure 3.5d and Figure 3.6d). Therefore, it can be said that the major improving effect of granular activated carbon was on NO_2^- reduction rather than on the whole process.

The axenic cultures were isolated by using buffered minimal media (pH ~7) and their denitrification performances were optimized at pH~7, in our previous work [119]. Therefore,

in this study, the obtained NO_3^- reduction activities of unprotected cells at pH 7 were representative for their actual performances and could be used as reference for further comparisons. Use of either diatomaceous earth or expanded clay improved the bacterial activity, and thus they completely reduced NO_3^- in 24 hours (Figure 3.5a,b,c and Figure 3.6a,b,c). Use of granular activated carbon as a carrier also enhanced the bacterial activity, particularly the NO_2^- reduction (Figure 3.5a,d and Figure 3.6a,d). ACDC revealed comparable results at pH 7 and it was also found that 78% of the NO_3^- was reduced in the first 3 hours (Figure 3.7a).

***Figure 3.5 NO_3^- reduction performances of Diaphorobacter nitroreducens at pH 7,
pH 9.5 and pH 13 with and without protection (a) unprotected; (b) diatomaceous earth
(DE) protected; (c) expanded clay (EC) protected (d) granular activated carbon (GAC)
protected; (error bars represent standard deviation, n=3)***

The positive effect of the protection materials and the natural protective layer of ACDC was more explicit at pH 9.5 (Figure 3.5 – Figure 3.7). The unprotected bacteria exhibited a slower reduction rate and the indicative NO_2^- peak was observed on day 4 instead of day 1 (Figure 3.5 and Figure 3.6). Complete denitrification was achieved in 7 days (Figure 3.5 and Figure 3.6). In contrast to that, for diatomaceous earth and expanded clay protected bacteria,

similar NO_2^- peaks due to NO_3^- reduction were observed after 24 hours (Figure 3.5b,c, and Figure 3.6b,c). Protection with granular activated carbon resulted in minor improvement of the NO_3^- reduction rate and significant improvement of the NO_2^- reduction rate. The latter was determined from the absence of expected NO_2^- peak throughout the experimental period (Figure 3.5d and Figure 3.6d).
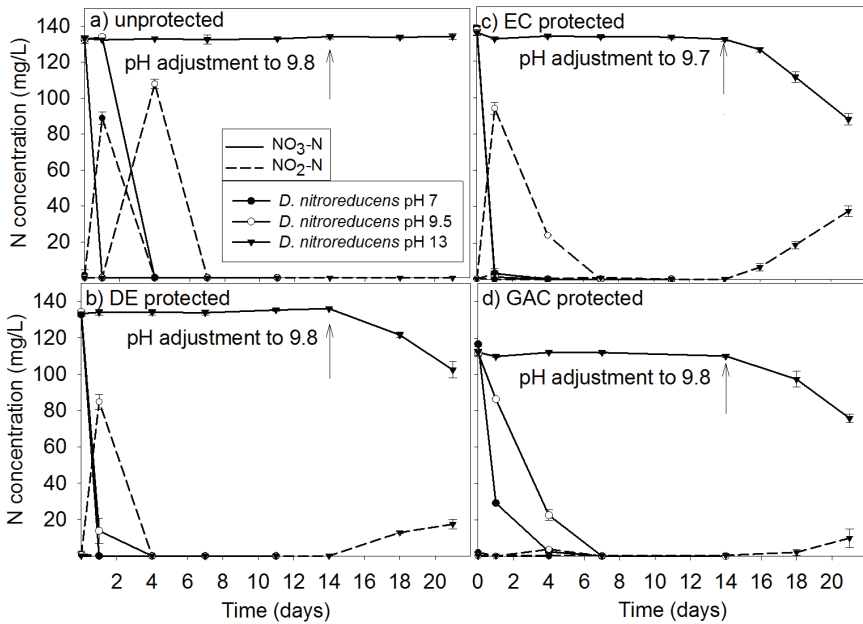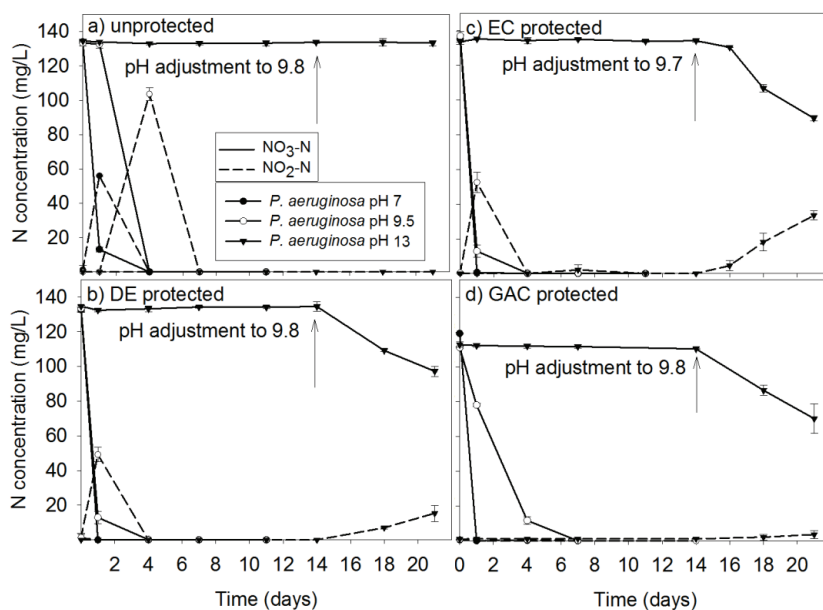

Figure 3.6 NO_3^- reduction performances of Pseudomonas aeruginosa at pH 7, pH 9.5 and pH 13 with and without protection (a) unprotected; (b) diatomaceous earth (DE) protected;(c) expanded clay (EC) protected; (d) granular activated carbon (GAC) protected; (error bars represent standard deviation, n=3)

At pH 9.5, ACDC was less affected than the protected axenic cultures when compared to their own performances at pH 7 (Figure 3.7a). The effect of alkaline pH was determined from the delay of NO_2^- reduction. At the end of 24 hours activity at pH 9.5, ACDC reduced 74 % (98 mg/L NOx-N reduced) of the initial total nitrogen (132 mg/L NO_3-N) while at the same pH the highest performance achieved with protected axenic cultures was recorded for EC protected *Pseudomonas aeruginosa* as 53 % (72 mg/L NOx-N reduced out of 137 mg/L NO_3-N) (Figure 3.6c and Figure 3.7a).

Both ACDC and axenic cultures were inhibited by alkaline pH around 13 (Figure 3.5 – Figure 3.7). No NO_3^- reduction was observed for 14 days, until the pH adjustment. The idea

behind the pH adjustment was to simulate an expected pH decrease after cracking of the concrete. Following pH adjustment, only the protected axenic cultures and self-immobilized ACDC showed significant activity. These results indicated that for intended application of *Pseudomonas aeruginosa* and *Diaphorobacter nitroreducens* in concrete, their encapsulation or immobilization is indispensable.
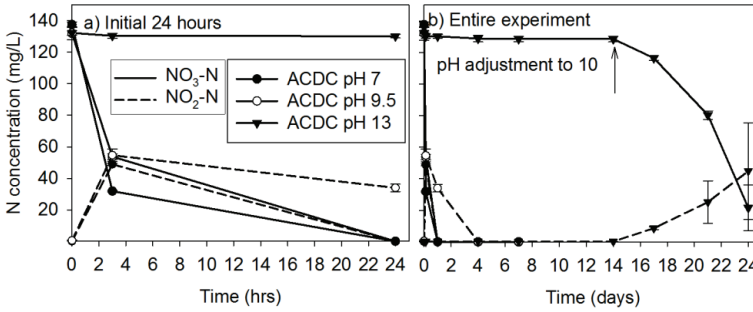
Figure 3.7 NO$_3^-$ reduction performances of ACDC at pH 7, pH 9.5 and pH 13
(a) first 24 hours; (b) entire experiment

3.3. Survival performances of the protected cultures after mortar incorporation

Encapsulated or immobilized vegetative axenic strains could survive mortar environment for 28 days. A lag phase of 3 days was observed before axenic bacterial cultures showed significant NO$_3^-$ reduction (Figure 3.8). Both axenic strains had similar NO$_3^-$ reduction rates, but *Diaphorobacter nitroreducens* accumulated more NO$_2^-$ which indicated that the axenic strains had differences in terms of electron acceptors (NO$_3^-$ and NO$_2^-$). *Diaphorobacter nitroreducens* primarily used NO$_3^-$, while *Pseudomonas aeruginosa* simultaneously used NO$_3^-$ and NO$_2^-$. The lag period of ACDC was longer than that of axenic cultures when an identical amount of biomass (0.5 % CDW w/w cement) were incorporated in mortar. Yet, significantly better performance was achieved in terms of NO$_3^-$ reduction rate (Figure 3.8d). Results indicated that, ACDC has higher specific NO$_3^-$ reduction rate compared to the axenic cultures after activation. Moreover, quicker activation and higher NO$_3^-$ reduction could be achieved by increasing the amount of ACDC incorporated from 0.5 to 1 % CDW (w/w cement) (Figure 3.8d).

The type of the protection material influenced the subsequent activity of the vegetative axenic cultures; the higher the NO$_3^-$ reduction rate the better the protection material. Bacteria immobilized on diatomaceous earth agglomerates, until the moment of extraction, showed

significantly less NO_3^- reduction than those encapsulated in porous protection materials (expanded clay and granular activated carbon) (Figure 3.8). If it is considered that during the extraction process applied to the inner crack surface, only the bacterial cells were collected, then the difference in NO_3^- reduction activities becomes indicative to evaluate the protective effect of each carrier until the moment of extraction. Better performances after resuscitation indicated that more bacteria could survive the mixing and curing period when protected with expanded clay or granular activated carbon rather than diatomaceous earth.

CHAPTER 3
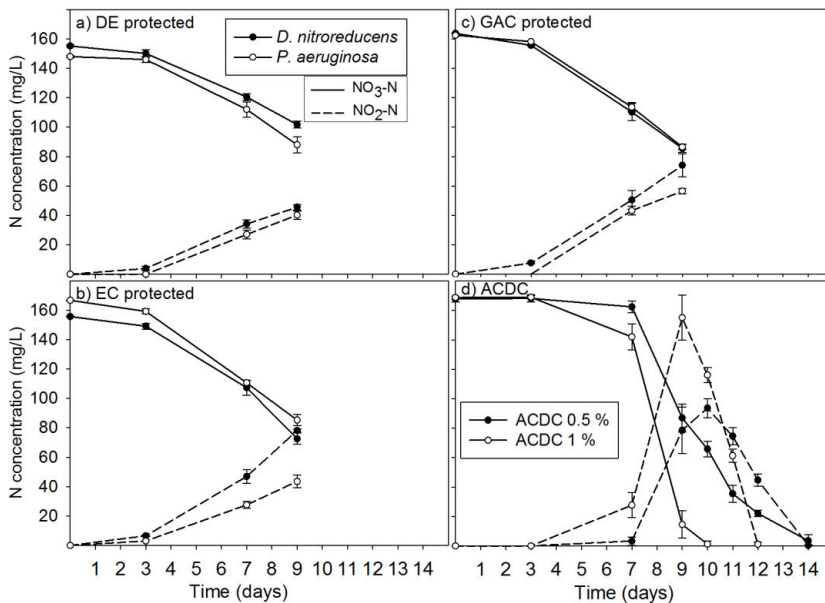
Figure 3.8 NO_3^- reduction activity of protected axenic cultures and self-immobilized non-axenic culture after 28 days in mortar; (a) diatomaceous earth (DE) protected; (b) expanded clay (EC) protected; (c) granular activated carbon (GAC) protected; (d) self-immobilized ACDC; (error bars represent standard deviation, n=3)

In the crack environment, NO_2^- accumulation is essential for corrosion inhibition. Therefore, the amount of NO_2^- produced due to the activity of surviving bacteria is of importance. After exposure to the mortar environment for 28 days, the peak NO_2^- concentrations produced by *Diaphorobacter nitroreducens*, *Pseudomonas aeruginosa* and ACDC were 257 ± 5 mg/L (5.6 ± 0.1 mM), 184 ± 5 mg/L (4.0 ± 0.1 mM), 308 ± 23 mg/L (6.7 ± 0.5 mM), respectively (Figure 3.8). The amount of NO_2-N accumulated from the reduction of NO_3-N in different cases are given in Table 3.4. *Pseudomonas aeruginosa* tended to reduce

NO_3^- and NO_2^- simultaneously, while *Diaphorobacter nitroreducens* preferred to use NO_3^- as a primary electron acceptor rather than NO_2^-. The difference in behavior was confirmed by the higher [NO_2-N accumulated]:[NO_3-N reduced] ratio of the latter (Table 3.4).

Table 3.4 The [NO$_2$-N accumulated]:[NO$_3$-N reduced] for different cases and times

Day[a]	NR[b] (mg/L)	NA[b] (mg/L)	[NA]:[NR] (%)	NR (mg/L)	NA (mg/L)	[NA]:[NR] (%)	NR (mg/L)	NA (mg/L)	[NA]:[NR] (%)
					D. nitroreducens				
		DE[b]			EC[b]			GAC[b]	
3	5	4	80	7	7	100	8	8	100
7	34	34	100	48	47	98	53	51	0.96
9	48	46	96	83	78	94	78	74	0.95
					P. aeruginosa				
		DE			EC			GAC	
3	2	0	0	8	3	38	4	0	0
7	34	27	79	49	28	57	45	43	96
9	60	40	67	82	44	54	72	57	79
					ACDC[b]				
		ACDC (0.5%)						ACDC (1%)	
7	5	3	60				27	27	100
9	81	79	98				155	155	100
10	102	94	92				168	116	69
11	132	75	57				169	61	36
12	146	45	31				169	1	1
14	164	0	0				0	0	0

[a]The ratios were calculated for the days the respective bacteria are significantly active.
[b]NR: NO_3-N reduced; NA: NO_2-N accumulated; DE: Diatomaceous earth; EC: Expanded clay; GAC: Granular activated carbon; ACDC: Activated compact denitrifying core (% w/w cement)

Besides, ACDC was a non-axenic culture containing different bacterial species, thus varying preferences on NO_3^- and NO_2^- could be observed throughout the experiment (Figure 3.8d, Table 3.4). The biomass concentration is of importance for NO_2^- accumulation. If the bacterial culture simultaneously uses NO_2^- and NO_3^- as electron acceptors (such as *Pseudomonas aeruginosa* and ACDC), at high biomass concentrations, some of the bacterial cells follow Reactions 1 – 4 while others follow Reactions 2 – 4. Therefore, for both ACDC and *Pseudomonas aeruginosa*, the higher the biomass concentration the lower the ratio of [NO_2^- accumulated]:[NO_3^- reduced]. For instance, on day 9, in the ACDC containing reactor 98-100% of the produced NO_2-N was accumulated and it gradually decreased with time (Table 3.4) due to the growth. Similarly for *Pseudomonas aeruginosa*, 96 % of the produced NO_2-N was accumulated on day 7 and decreased to 79 % on day 9 (Table 3.4). Contrarily, [NO_2-N accumulated]:[NO_3-N reduced] for *Diaphorobacter nitroreducens* was between 94-100 % despite the growth throughout the experimental period (Table 3.4) since NO_3^- reduction always preceded NO_2^- reduction due to the preferences of the culture. After 28 days in mortar, the amount of active bacteria that survived from the incorporation of 1 % ACDC

(w/w) led to production of higher NO_2^- concentrations than from the incorporation of 0.5 % ACDC (w/w) (Table 3.4, Figure 3.8d).

3.4. The influence of self-healing additives on setting and strength properties of mortar

3.4.1. Initial and final setting times of the mixtures

The initial and final setting times of the reference mortar mixture (sand:cement:water – 3:1:0.5) were of the order of 200 and 300 minutes, respectively (Figure 3.9). The setting times of different mixtures were evaluated by comparing them with the reference. Small but significant differences were observed in both initial and final setting times when either granular activated carbon or expanded clay (5% w/w cement) were incorporated in the mortar mixture. Relevant mixtures revealed a decrease up to 20 minutes in the initial setting time and an increase up to 30 minutes in the final setting time. The addition of diatomaceous earth (5% w/w cement) decreased the initial and final setting times to around 100 and 240 minutes, respectively (Figure 3.9).

The addition of unprotected *Diaphorobacter nitroreducens* (0.5 w/w cement) caused an increase of 40 minutes in both initial and final setting times (Figure 3.9). The addition of nutrients (2% $Ca(HCOO)_2$ + 3% $Ca(NO_3)_2$ w/w cement) did not change the initial setting time significantly while it caused a 40 minutes increase in the final setting time (Figure 3.9).
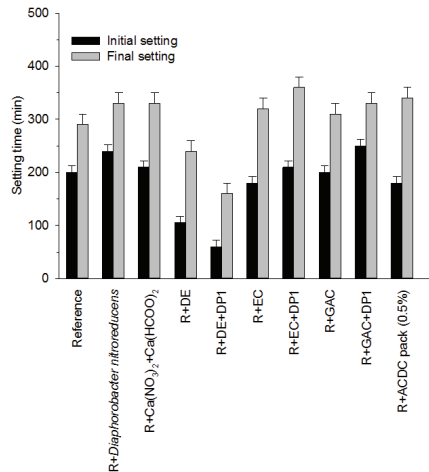

Figure 3.9 Initial and final setting times of the different mixtures tested. The bars represent standard deviation values of ±12 minutes for the initial setting time and ± 20 minutes for the final setting time according to ASTM C191–04a and ASTM C807–13.

The changes in setting properties were more noticeable for mixtures containing all the self-healing additives (denitrifying pack). The severe impact was observed when denitrifying pack was combined with diatomaceous earth. The initial setting time of the mixture was recorded as 60 minutes (Figure 3.9). Similar decrease was also observed in the final setting which was completed after 160 minutes. Contrarily, when denitrifying pack was combined with either expanded clay particles or granular activated carbon particles, the major effect was retardation. The initial setting time of the expanded clay+denitrifying pack mixture was similar to the reference, while the final setting was achieved with a 70 minutes delay compared to the reference and completed after 360 minutes (Figure 3.9). The mixture containing granular activated carbon showed a 50 minutes delay in initial setting while it was recorded as 40 minutes at the end of complete setting.

The use of self-protected non-axenic ACDC culture caused a decrease of 20 minutes on the initial setting time. However, it caused a 50 minutes increase in the final setting time (Figure 3.9).

3.4.2. Compressive strength of the mixtures

Compressive strengths of the reference samples were 50 ± 2 and 59 ± 2 MPa after 7 and 28 days, respectively. The compressive strengths, after 7 days, were not significantly different for the individual mixtures containing either nutrients ($Ca(NO_3)_2+Ca(CHOO)_2$), diatomaceous earth, diatomaceous earth+denitrifying pack (regardless of the bacteria type), expanded clay, granular activated carbon or ACDC pack (0.5%), when compared with the reference (Figure 3.10).

Moreover, after 28 days individual mixtures containing either nutrients ($Ca(NO_3)_2+Ca(CHOO)_2$), diatomaceous earth, diatomaceous earth+denitrifying pack, expanded clay, *Diaphorobacter nitroreducens*, *Pseudomonas aeruginosa* or ACDC pack (regardless of the ACDC dose) had similar compressive strengths when compared with the reference (Figure 3.10).

CHAPTER 3
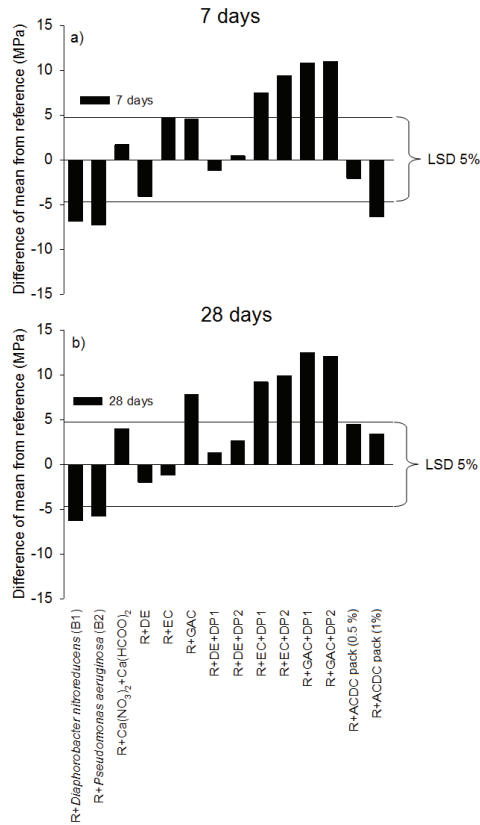
***Figure 3.10 Difference of the mean values for compressive strength results of the
tested samples after curing at 20 °C and RH>95% when compared with the reference using
one way ANOVA test, (a) after 7 days; b: after 28 days of curing.
LSD(7days,28days)=4.7 MPa***

Although the incorporation of axenic vegetative strains had no significant effect on 28
days compressive strength, they decreased the early age (7 days) compressive strength by
around 15 % when compared to the reference (Table 3.5). Improved compressive strengths
with respect to the reference one was achieved with mixtures containing either expanded
clay+denitrifying pack (regardless of the bacteria type) or granular activated
carbon+denitrifying pack (regardless of the bacteria type) after 7 days (Figure 3.10a). After
28 days curing, the mixtures containing either expanded clay+denitrifying pack (regardless of
the bacteria type), granular activated carbon or granular activated carbon+denitrifying pack
revealed greater compressive strength than the reference (Figure 3.10b).

Table 3.5 Compressive strength results for the tested samples after 7 and 28 days of curing at 20 ^{o}C and RH>95%

Mixture	Mean values±SD (MPa)	
	7 days	28 days
R	50.3±1.6	58.6±2.0
R+*Diaphorobacter nitroreducens*	43.4±0.7	52.3±1.5
R+*Pseudomonas aeruginosa*	43.0±0.7	52.8±2.4
R+Ca(NO$_3$)$_2$+Ca(HCOO)$_2$	52.0±2.1	62.6±1.8
R+DE	46.2±2.0	56.5±0.3
R+EC	55.0±2.3	57.4±9.3
R+GAC	54.9±1.7	66.4±1.3
R+DE+DP1	49.1±1.7	59.9±1.4
R+DE+DP2	50.7±1.3	61.2±0.6
R+EC+DP1	57.8±0.4	67.8±1.8
R+EC+DP2	59.7±1.2	68.5±5.7
R+GAC+DP1	61.1±1.4	71.0±2.3
R+GAC+DP2	61.3±0.8	70.7±2.3
R+ACDC pack (0.5%)	48.2±2.8	63.1±1.5
R+ACDC pack (1%)	43.8±2.4	60.7±2.0
5% LSD	4.7	4.7

[a]R: Reference, DE: Diatomaceous earth, EC: Expanded clay, GAC: Granular activated carbon, ACDC: Activated Compact Denitrifying Core, DP: Denitrifying pack (Axenic culture + Ca(NO$_3$)$_2$ + Ca(HCOO)$_2$), DP1: DP with *Diaphorobacter nitroreducens*; DP2: DP with *Pseudomonas aeruginosa*; SD: Standard deviation, LSD: Least significant difference (p=0.05, n=3)

3.5. Effect of microbial NO$_3^-$ reduction on steel corrosion

Results indicated that tested bacteria and their activity have no negative effects on steel. Instead, production of NO$_2^-$ can provide corrosion inhibition. The anodic and cathodic polarization curves (Tafel plots) of the carbon steel plates in different solutions containing different types of denitrifying bacteria are given in Figure 3.11. Corrosion current (I$_{corr}$) and corrosion potential (E$_{corr}$) values of the steel plates in the respective electrolyte solutions were determined from the Tafel slopes (Table 3.6).

Corrosion current of 36 mA/m^2 and a corrosion potential of -360 mV were obtained for the negative control (containing 2.9 g/L NaCl, 12.4 g/L NO$_3^-$) (Table 3.6). In the case of the positive control the corrosion was effectively inhibited in 24 hours and, E$_{corr}$ and I$_{corr}$ values were recorded as 0.1 mA/m^2 and -130 mV. Moreover, no pitting was observed (Figure 3.12b) which indicated that the amount of chemical NO$_2^-$ used was enough for surface passivation.
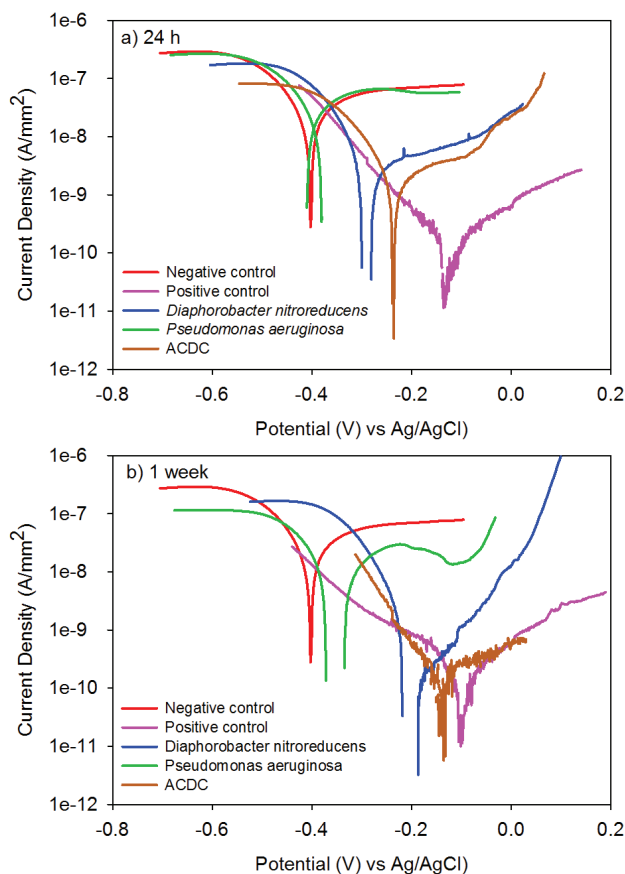
Figure 3.11 Polarization curves of steel plates immersed in control electrolytes and electrolytes incubated with different bacteria (a) 24 h incubation (b) 7 days incubation

After 24 h incubation of *Pseudomonas aeruginosa* in the electrolyte solution, the recorded polarization curves were similar to those of the negative control (Figure 3.11a). On the contrary, 24 h was enough for *Diaphorobacter nitroreducens* and ACDC to decrease I$_{corr}$ and shift E$_{corr}$ towards a more positive direction (Figure 3.11a), most likely due to the produced NO$_2^-$ through NO$_3^-$ reduction (Table 3.6). Although, two of the three tested cultures,

Diaphorobacter nitroreducens and ACDC, promoted passivation in 24 h by reducing NO_3^- to NO_2^-, the amount of NO_2^- was not enough for effective passivation. A passivity breakdown potential was observed around -90 mV which further caused pitting. Pitting could be confirmed visually, immediately after the polarization tests conducted (Figure 3.12d,f).

Table 3.6 I_{corr}, E_{corr} values obtained from Tafel plots and $[NO_2^-]:[Cl^-]$ ratio in different test batches[1]

Test	Time	pH	$[Cl^-]$ (mM)	$[NO_2^-]$ (mM)	$[Cl^-]:[OH^-]$	$[NO_2^-]:[Cl^-]$	I_{corr} (mA/m^2) (from Tafel)	E_{corr} (mV)
Negative control	24 h	9.1	48.9	-	3888	N/A	36	-360
	1 week	-	48.1	-	3817	N/A	-	
Positive control	24 h	9.3	47.4	190.4 ± 0.2	2376	4.01	0.1	-130
	1 week		48.8	190.1 ± 0.7	2452	3.89	0.1	-112
B1	24 h	9.2	47.7	11.2 ± 0.0	3010	0.24	2.8	-294
	1 week	9.0	48.6	26.8 ± 1.4	4860	0.55	0.3	-167
B2	24 h	9.3	47.7	3.4 ± 0.0	2382	0.07	43	-350
	1 week	9.2	48.1	4.1± 0.1	3034	0.09	7.2	-330
ACDC	24 h	9.1	47.8	19.8 ± 0.0	3797	0.41	1.8	-220
	1 week	8.8	47.8	57 ± 10.1	7576	1.19	0.2	-140

[1]B1: *Diaphorobacter nitroreducens*; B2: *Pseudomonas aeruginosa*; mM: concentration in electrolyte solution

All the tested cultures induced enhanced corrosion inhibition after 1 week of microbial activity when compared to performances achieved after 24 hours of microbial activity (Figure 3.11). All the polarization curves shifted more in the direction of the positive control compared to those recorded after 24 hours. The shift in polarization curves resulted in lower I_{corr} values and more noble E_{corr} values (Table 3.6). However, a passivity breakdown around -100 mV was determined as a steep increase of current density in the anodic curves recorded in the *Pseudomonas aeruginosa* and *Diaphorobacter nitroreducens* inoculated solutions (Figure 3.11b, Figure 3.12g,h). In one week, unlike the limited performance of the axenic cultures, ACDC showed distinctively better performance, and was even as effective as the direct addition of chemical NO_2^- (positive control) (Figure 3.11b). Furthermore, the amount of NO_2^- produced by ACDC was enough for stable passivation (Table 3.6), and thus no pitting was

observed (Figure 3.12i). The effect of produced NO_2^- was mainly determined in the anodic region from a current density drop of around two orders of magnitude compared to the negative control (Figure 3.11b).
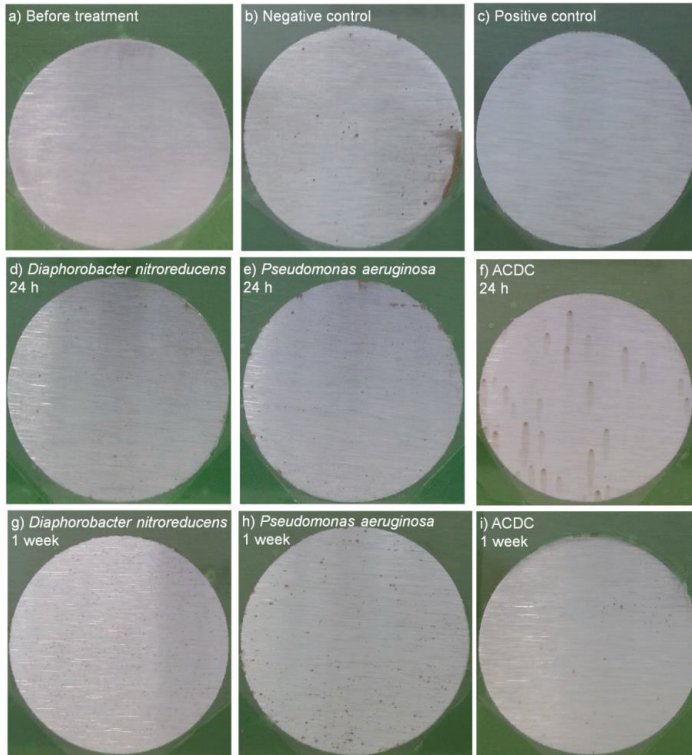
Figure 3.12 Appearance of the test plates immediately after anodic polarization in respective electrolyte solution

a) before immersion; b) in 2.9 g/L (0.05 M) Cl^- + 12.4 g/L (0.2 M) NO_3^-; c) in 2.9 g/L (0.05 M) Cl^- + 9.2 g/L (0.2 M) NO_2^-; d) in 2.9 g/L (0.05 M) Cl^- + 12.4 g/L (0.2 M) NO_3^- + Diaphorobacter nitroreducens after 24 h; e) in 2.9 g/L (0.05 M) Cl^- + 12.4 g/L (0.2 M) NO_3^- + Pseudomonas aeruginosa after 24 h; f) in 2.9 g/L (0.05 M) Cl^- + 12.4 g/L (0.2 M) NO_3^- + ACDC after 24 h; g) in 2.9 g/L (0.05 M) Cl^- + 12.4 g/L (0.2 M) NO_3^- + Diaphorobacter nitroreducens after 1 week; h) in 2.9 g/L (0.05 M) Cl^- + 12.4 g/L (0.2 M) NO_3^- + Pseudomonas aeruginosa after 1 week; i) in 2.9 g/L (0.05 M) Cl^- + 12.4 g/L (0.2 M) NO_3^- + ACDC after 1 week

4. Discussion

4.1. Quality of the self-protected ACDC culture

The denitrification performance achieved under aerobic conditions was an indication of a denitrifying core. The major reason of the denitrifying activity was the size of the granules that prevented oxygen diffusion creating an anoxic zone at the core [76]. The anoxic/aerobic operation enhanced the enrichment of nitrate reducing bacteria at the core of the granules which was consistent with the previous studies [76,120]. In addition to the denitrification, nitrification was also observed in aerobic period which indicated the presence of nitrite oxidizing bacteria near the surface of the granules. This type of placements was an indication for the aimed layered structure. The inorganic content of the ACDC was 30 % which was higher than the content of a typical granular biomass [76,120]. This was due to the feed composition that was enriched in terms of Ca^{2+} (0.10 g/L Ca^{2+}) compared to the synthetic feed composition used (contains 0.03 g/L Ca^{2+}) in the reference study [76]. The VSS/TSS ratio of 0.6 was reported for the anaerobic granules cultivated by using 0.15 g/L Ca^{2+} and increased to 0.7 when the influent Ca^{2+} concentration was 0.01 g/L [121]. Previous studies also showed that the Ca^{2+} related precipitates mainly form the inorganic content of the granular biomass [122]. Therefore, for ACDC, the major constituents of the inorganic content was expected to be $CaCO_3$ and $Ca(PO_4)_3$ which also act as a protective layer for the nitrate reducers at the core.

4.2. Performance of unprotected bacteria in different pH environments

Microbial activity at different pH values is of importance for the development of microbial self-healing concrete. To be appropriate for concrete application, bacteria should survive at pH 13 (pH in concrete) and be active at pH 9.5-10 (estimated pH in crack). In this study, NO_3^- reduction performances of the tested cultures varied depending on the pH conditions of the environment. Unprotected vegetative axenic cultures did not fulfill aforementioned requirements for concrete application. However, with the aid of protection materials promising performances were achieved.

It is known that several environmental factors control the microbial NO_3^- reduction. Presence of NO_3^- reducing bacteria, available nutrients and absence of oxygen are the main controlling parameters of the microbial NO_3^- reduction [123]. Besides, pH and temperature influence the activities and thus the denitrification rate [124]. Best denitrification activity for

Pseudomonas species were reported at pH 7.0-7.5 [123]. A wider pH range (pH 6.6 – 8.3) was determined by Simek et al. [125] for soil originated denitrifiers. Coherently, in this study, unprotected *Pseudomonas aeruginosa* showed the highest NO$_3^-$ reduction rate at pH 7 as well as *Diaphorobacter nitroreducens*.

Most of the denitrifying bacteria are sensitive to pH > 9.0 at which a significant decrease in their activity was reported [125,126]. A limited number of studies have reported high rate NO$_3^-$ reduction at pH values higher than 9.5 by acclimatizing the cultures [70,127]. If only the alkaliphilic denitrifying strains such as *Halomonas desiderata* were used significant biological NO$_3^-$ reduction could be achieved at highly alkaline conditions (pH values more than 10.5 or 11) [128]. The NO$_3^-$ reduction rate of the unprotected strains decreased 4 times at pH 9.5 when compared to their activity at pH 7. The decrease was attributed to the inhibition of NO$_3^-$ and NO$_2^-$ reduction due to the alkaline pH environment. Both unprotected axenic cultures did not show any activity at pH 13 and even after the pH adjustment. The pH of the environment can cause reversible or irreversible inhibition on bacterial activity [124]. The pH adjustment is one of the ways to regain inhibited activity [124]. Yet, results indicated that pH 13 caused irreversible inhibition and further death of the bacteria. Thus the unprotected vegetative axenic cultures are not suitable for concrete applications.

4.3. The role of protective carriers on bacterial activity at different pH environments

Incorporation of axenic bacteria with protective materials not only improved the performance of bacteria at pH 7 and at pH 9.5, but also protected the bacteria from detrimental effects of the alkaline pH environment (pH 13). Previous studies revealed that diatomaceous earth, expanded clay and granular activated carbon have a protective effect on vegetative bacterial strains under inhibitory conditions and thus resulted in higher bacterial activity than their plain activity [58,129,130].

Upon attaching to a surface, bacteria start to form a biofilm by producing extracellular polymeric substances (EPS) [131]. The biofilm and the surface properties of the carrier material play the major role on culture resilience to detrimental effects [131].

During the formation of a bacterial layer around the diatomaceous earth grains, bacteria produce extracellular polymeric substances [131] which induce agglomeration of the powder. This agglomeration results in a gummy paste [129] inside which the bacteria are trapped. Additionally, after mortar incorporation, the silica content of the diatomaceous earth starts to

react with the cement matrix and form calcium silicate hydrate gel around the agglomerates which also protects the bacteria from direct exposure to the alkali environment. The described biofilm formation also occurs on expanded clay and granular activated carbon particles [130] and could be visualized in this study (Figure 3.13a,b). The biofilm can form both on the outer surface and inside the pores if porous carriers are used. Following biofilm formation bacteria can create their own microenvironment in which the pH is less than the outer bulk solution [83]. The negative charges of diatomaceous earth [132], expanded clay [41] and granular activated carbon [133] could also be helpful to maintain the pH difference between the microenvironment and the bulk solution by repelling the OH$^-$ ions.
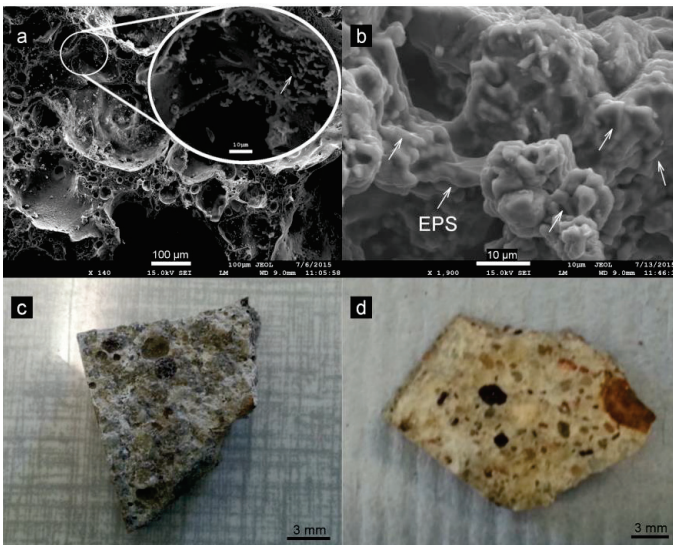
Figure 3.13 The distribution of bacteria and porous carries after mortar incorporation (a) bacteria in the pores of expanded clay particle; (b) bacteria on the porous surface of the granular activated carbon; (c,d) distribution of expanded clay and granular activated carbon particles on the part of the inner crack surface (EPS: Extracellular polymeric substance; except the EPS, ↗ shows the bacteria)

The mentioned local pH drops improved the bacterial survival and activity. Hence, at pH 9.5, the denitrification rate of axenic cultures protected with diatomaceous earth or expanded clay were as high as their denitrification rate at pH 7 without protection. Only NO$_2^-$ reduction activity was improved when either of the axenic cultures was incorporated in granular activated carbon at pH 7 and pH 9.5. Observed effect could be due to couple of

reasons directly or indirectly related to each other. First and the most likely reason is the higher surface area and higher micropore volume of granular activated carbon compared to expanded clay particles and agglomerated diatomaceous earth [130,134]. The surface area is important to determine the bacteria density on each particle which also affects the reduction rates. Comparing Figure 3.13a and Figure 3.13b, it can be said that the density of the biofilm was higher on activated carbon. The reduction rate would be much higher at sites where bacteria were more concentrated. Moreover, the amount of micropores is of significance for the diffusion of produced NO_2^- into the bulk solution. The higher the retention time for NO_2^- in the pore volume the higher the chance for its further reduction by the bacteria. Similarly the NO_3^- diffusion into the pores and through the biofilm might also be limited compared to its reduction rate which makes the produced NO_2^- more available for the bacterial consumption. Another reason might be the NO_3^- adsorption on the activated carbon surface. Adsorption studies revealed that NO_3^- adsorption on activated carbon is at least 1.5 times higher than NO_2^- adsorption [135–137] which means that in the presence of NO_3^- and NO_2^- together, NO_2^- would be more available for bacterial consumption. Although the adsorption of negatively charged molecules on the activated carbon surface increases at acidic pH values, it was shown that even at neutral pH values some degree of adsorption is possible [137,138]. Therefore, the higher NO_2^- reduction rate of axenic cultures when incorporated in granular activated carbon, may also be attributed to the relative abundance of NO_2^- compounds over NO_3^- and thus its higher availability for bacterial consumption inside the pores of granular activated carbon.

The self-immobilized non-axenic bacterial culture, ACDC, performed better than both unprotected and protected axenic strains. This might be due to the advantageous cooperative and coordinated activity of non-axenic cultures. Axenic cultures are normally more restricted in their metabolic potential than the so-called microbiomes, i.e. evolved microbial cultures [139,140]. The diversity of bacteria in non-axenic cultures provides a wider tolerance to changes in environmental factors, thus ACDC was expected to perform better than the axenic strains under certain extreme conditions. Furthermore, the production process of ACDC includes several stress parameters which promotes EPS production and biofilm formation [76]. Continuous EPS production promotes the agglomeration of different bacteria and formation of bacterial layers [75,76]. The layered structure of the ACDC protected the denitrifying core from the bulk environment and retarded the pH change in the core. Therefore, the core community could adapt its metabolism and survive in their microenvironment during the gradual pH increase.

4.4. Suitability of the protective carriers for bacteria incorporation in mortar

Apart from its alkaline pH, concrete has several other harsh conditions jeopardizing the survival of bacteria. Crushing of bacterial spores was reported due to the timewise decrease in pore size [55]. Dehydration and long-term starvation are other factors having influence on bacterial survival, particularly on the survival of vegetative cells. Both axenic cultures tested in this study were able to survive in mortar when protected by either diatomaceous earth, expanded clay or granular activated carbon. *Pseudomonas aeruginosa* and *Diaphorobacter nitroreducens* were already proven to be able to survive dehydration and starvation stress [67]. Therefore, the main roles of the protection materials in mortar incorporation were housing the bacteria and preventing the direct contact of the bacteria with the detrimental alkaline mortar matrix. Since we know from the obtained results that they are effectively protecting bacteria in alkaline solution, mortar incorporation was indicative for the robustness of the protection mechanism under shear and compression. Slightly better performance was achieved with the same bacteria, after 28 days exposure to mortar environment, when expanded clay or granular activated carbon was used as carriers rather than diatomaceous earth to protect the bacteria in mortar. The difference in performance indicated that more cells could survive the mortar incorporation when protected with aggregate like materials rather than a powder. Diatomaceous earth agglomerates can easily break during the mortar mixing due to the crashing between the aggregates while more robust expanded clay and granular activated carbon particles mostly dispersed with the aggregates (Figure 3.13c,d). Therefore, a portion of bacteria immobilized on/in diatomaceous earth expose to alkaline environment after the disintegration of diatomaceous earth agglomerates. The exposure continues until the calcium silicate hydrate formation around the cells due to the pozzolanic reaction. However, the pozzolanic reaction occurs stepwise and requires time to complete [141]. Therefore, following severe exposure to alkaline conditions lead to loss of some incorporated bacteria and a lower NO_3^- reduction activity.

The results indicated that the ACDC granules were robust enough to withstand mortar mixing and shrinkage during curing. The cultivation media was enriched by the addition of Ca^{2+} and Mg^{2+} during the production of ACDC (Table 3.3), thus robust ACDC granules could be achieved. Divalent atoms such as Ca^{2+} and Mg^{2+} have high impact on the stability of binding biopolymers (the EPS) between bacteria [122,142]. Moreover, hardly soluble $CaCO_3$ and $Ca_3(PO_4)_2$ ($K_{sp}(CaCO_3)= 4.8\times10^{-9}$ and $K_{sp}(Ca_3(PO_4)_2)=2.07 \times 10^{-33}$) formed inside and

around the granules increase the granule strength [122]. Since around 30% of the ACDC consists of these Ca^{2+} salts, the denitrifying core could be protected.

4.5. The influence of self-healing additives on setting and strength properties of mortar

4.5.1. Initial and final setting times of the mixtures

Both the initial and final setting times of the reference mortar were within the range of EN 197-1 2012. Granular activated carbon and expanded clay (5% w/w, 0.5-2 mm) are aggregate alike materials. Their incorporation with mortar resulted in minor changes in both initial and final setting times. Considerable decreases in both setting times were observed when diatomaceous earth (5% w/w, 5-200 µm) was added into the mortar mixture. The introduction of fine particles leads to the increase of the surface area in contact with water [143,144] and thus increases the reaction rate [145]. Previously reported results showed consistency with the ones obtained in this study [143].

Addition of unprotected *Diaphorobacter nitroreducens* (0.5 w/w) caused significant delay in mortar setting. It is known that organic impurities delay the chemical setting of mortar through complexation with free Ca^{2+} ions and/or adsorption on the surface of grown particles and hydration products [85]. Since bacterial cells are mostly composed of organic matter [146], their addition might cause a delay in setting time. Vegetative cells (*Diaphorobacter nitroreducens*) died within the first minutes due to the alkali pH (pH~13) [147] and thus their organic content was released into the mortar matrix, delaying the setting time about 40 minutes.

The nutrients for denitrifying bacteria, $Ca(HCOO)_2$ and $Ca(NO_3)_2$, are known to be accelerators [68,69]. However, in this study, combination of both admixtures was used which led to a slight increase in the final setting time. The retardation was still acceptable and in the range defined in EN 197-1 2012. Among the mixtures containing denitrifying pack, only the one with diatomaceous earth showed a distinctive decrease in both setting times. As described, the addition of diatomaceous earth increases the reactive surface area [143]. Moreover, the nutrients ($Ca(HCOO)_2$ and $Ca(NO_3)_2$), as known accelerators, were expected to decrease the setting time of the mortar mixtures [68,69]. Although plain incorporation of these nutrients had minor effect on the setting time, the combination of both diatomaceous earth and nutrients might cause the observed shortening in the setting time. In previous studies, diatomaceous earth could be successfully used with the ureolytic bacteria and their

respective nutrients (urea+yeast extract) [58]. The combination of yeast extract (organic matter) and diatomaceous earth most probably compensated their severe retardation and acceleration effects, respectively. Since the nutrients ($Ca(HCOO)_2$ and $Ca(NO_3)_2$) for denitrifying bacteria are also accelerators, use of diatomaceous earth in combination with denitrifying pack is not recommended.

The use of ACDC pack caused about an hour retardation in the final setting time. The delay in the final setting time could be attributed to the organic content of the non-axenic cultures since the specific contact area of ACDC granules consist of organic matter (70 %) and inorganic salts (30 %). As previously mentioned the salt content of the granules is mostly $CaCO_3$ [122] which should not affect the setting. Therefore, the possible reason for the delay is the presence of organic matter.

4.5.2. Compressive strengths of the mixtures

The compressive strength results obtained for the reference mortar samples after 7 and 28 days of curing were coherent with the type of cement used (CEM I 52.5N). It was found out that, there was no significant difference between mixtures containing denitrifying pack-1 (*Diaphorobacter nitroreducens*) and denitrifying pack-2 (*Pseudomonas aeruginosa*). Therefore, denitrifying pack results are discussed as one.

For the bacterial self-healing concrete application, it is of utmost importance to evaluate the effect of protection materials on the compressive strength. Previous results showed that the addition of diatomaceous earth (5% w/w) had minor to no influence on both 7 and 28 days compressive strength [20]. Consistent results were obtained in this study. A slight decrease on the compressive strength after 7 days was obtained while no differences between the mixture containing diatomaceous earth and the reference mixture were observed after 28 days.

It was found that the addition of granular activated carbon increased the compressive strength in the order of 13% after 28 days when compared to the reference samples. To our knowledge there is no information available about the effect of granular activated carbon on mortar properties. Therefore, the results obtained can be considered as a significant contribution to the knowledge about protective carriers. Based on the results, granular activated carbon appeared to be a concrete compatible protective carrier which can be an option to be considered in self-healing studies. The addition of expanded clay was found to have no effect on compressive strength after both 7 and 28 days. So far, the study of the use of expanded clay as protective carrier for microbial self-healing concrete was only conducted

by replacing the aggregate content by expanded clay particles (around 50%) which resulted in 50% decrease in compressive strength of the mortar [40,148]. In this study, expanded clay was incorporated in addition to the standard aggregate content. The amount added did not have a considerable effect on the mortar composition and thus on the density of the mixtures. Therefore, no differences in compressive strength were observed. Based on these finding, the expanded clay particles can still be an protective carrier option if used in limited amount without replacing the standard aggregate content of the mixtures.

The incorporation of either *Diaphorobacter nitroreducens* or *Pseudomonas aeruginosa* cells caused a decrease in compressive strength after 7 days. Both strains showed similar negative impact on the mortar strength at early age which indicated that the behavior of the mixtures containing identical amount of vegetative cells is similar. At the end of 28 days, the strength differences between the mixtures containing bacterial cells and the reference mixture were not significant. Based on these results, it can be said that the incorporation of 0.5% bacterial culture in mortar has no severe effect on cement hardening and it only delays the early age strength development.

Contrary to reported data [68], the addition of $Ca(NO_3)_2$ and $Ca(HCOO)_2$ caused no significant increase on both 7 and 28 days compressive strength. Although, plain incorporation of either expanded clay, granular activated carbon or nutrients for denitrifying bacteria showed a positive effect on the compressive strength, the results were not significantly different from the reference sample. However, a combination of the protective carriers and denitrifying pack (expanded clay+denitrifying pack and granular activated carbon+denitrifying pack) performed significantly better than the reference in terms of compressive strength. The improved effect was only observed with the porous carriers. This behavior could be an indication of a successful barrier between mortar matrix and the bacteria. The negative effect of organic matter on strength development is known [20,55]. Since the bacteria were absorbed into the pores of the porous carriers, the negative effect of the organic matter (bacteria) was not observed. The observed improvement can be attributed to the combined effect of both nutrients and encapsulation materials successfully filled with the bacterial agents.

In the case of mixtures containing diatomaceous earth+denitrifying pack, one would expect an increase in the compressive strength according to the reported data [68,84]. Instead, mixtures of diatomaceous earth+denitrifying pack mortar specimens showed no considerable difference compared to the reference. Complex chemical reactions and physical interactions might have caused this unexpected behavior and this requires further investigation.

Self-protected non-axenic ACDC culture showed different strength properties for different dosages at early age, yet the strength values obtained at the end of 28 days were not significantly different from each other. It was found that increasing the ACDC dose from 0.5 % to 1% (w/w cement) caused 13 % decrease of the early age strength. Yet, at the end of 28 days, both dosages had no considerable influence on the compressive strength of the mortar specimens when compared to reference. As previously mentioned, the addition of organic matter in mortar causes a decrease in compressive strength [20,55]. The structure of ACDC mostly prevents the contact of the biomass (organic matter) with the mortar matrix. Therefore, the observed behavior can be attributed to the minor contact between the biomass and the mortar matrix. As expected, when the dose is doubled the effect of organic matter is more pronounced especially the effect on early age strength.

4.6. Effect of microbial NO_3^- reduction on steel corrosion

Several studies reported use and investigation of $Ca(NO_2)_2$ as an anodic corrosion inhibitor in concrete [73,74]. Results of this study revealed that bacteria can also induce corrosion inhibition, particularly anodic corrosion inhibition, by producing NO_2^- from NO_3^-. The most stable passivation was achieved with the non-axenic ACDC culture. The NO_2^- production was due the microbial NO_3^- reduction during the metabolic oxidation of an organic carbon source. The inhibitory mechanism works by formation of a passive film layer on the steel surface when nitrite ions react with ferrous ions [71]. Both Cl^- and NO_2^- ions tend to react with Fe^{2+} and presence of NO_2^- increases the amount of Cl^- required for corrosion initiation [71]. Previous studies reported the importance of $[NO_2^-]:[Cl^-]$ ratio when NO_2^- was used for corrosion inhibition [73,74]. Insufficient NO_2^- concentrations may cause an unstable passivation, resulting in pitting corrosion [73]. Since ACDC could convert more NO_3^- into NO_2^- than the axenic cultures did in similar incubation periods, ACDC could induce a stable passivation. Different $[NO_2^-]:[Cl^-]$ ratios were recommended to achieve stable passive layer on the steel surface. In this study, through NO_2^- production of ACDC, stable passivation was obtained at $[NO_2^-]:[Cl^-]$ ratio of 1.19 (Table 3.6) which falls in the range described in the majority of the corrosion inhibition studies [73]. Since this is the first study describing microbial induced corrosion inhibition through NO_3 reduction, results could only be compared with the positive and negative controls conducted throughout the experiments. The E_{corr} values recorded for carbon steel plates in the negative control electrolyte were confirmed with the previously reported values with identical $[NO_2^-]:[Cl^-]$ ratio of 0 [115]. However,

similar comparison could not be made for E_{corr} values recorded in inhibitory electrolyte (positive control) since the electrolyte used in this study was more complex than the reported inhibitory electrolytes in terms of constituents. Yet, E_{corr} values achieved in positive control were significantly different from those achieved in the negative control. Therefore, the positive control could be used to determine effective corrosion inhibition by means of chemical NO_2^- and to further compare with microbial induced corrosion inhibition.

Although the results are promising to use denitrifying bacteria for corrosion inhibition, one can speculate that direct addition of NO_2^- is easier, more effective and more reliable, i.e. not dependent on bacterial activity. Nevertheless, it was reported that addition of high amounts of calcium nitrite to achieve effective corrosion inhibition may negatively affect the compressive strength in the long term [74]. Additionally, accelerated setting causes early age cracks. Moreover, added NO_2^- can diffuse from concrete structures to the water sources, which is not only toxic for aquatic life but also for plants and human beings. The amount of NO_2^- used for corrosion inhibition may vary from 0.25 % to 2 % w/w cement depending on the Cl^- content of the environment [73,74]. If bulk incorporation is taken into consideration, severe environmental impact is inevitable. Besides, for microbial induced corrosion inhibition, the necessary additive is $Ca(NO_3)_2$ which is relatively cheaper than $Ca(NO_2)_2$ [71]. Nitrate is also considerably less toxic than nitrite and has a beneficial effect on the concrete strength [68,149]. Moreover, $Ca(NO_3)_2$ can be used as an anti-freeze admixture or winter concreting admixture [69]. If coupled with relevant bacteria, $Ca(NO_3)_2$ can also be used as nutrient for bacteria to develop self-healing concrete, since the reduction of NO_3^- induces $CaCO_3$ precipitation and thus crack healing [119]. The latter is the most important advantage of the addition of bacteria over the addition of chemical NO_2^- for corrosion inhibition. Since microbial NO_3^- reduction leads to NO_2^- production as an intermediate product, simultaneous corrosion inhibition can be achieved during the microbial self-healing process. In this study, the tests were not conducted in mortar environment or in concrete pore solution. However, pH dependent activity and survival in mortar environment experiments revealed the fact that all the tested cultures could survive mortar incorporation with the aid of either additional protection or self-protection. Furthermore, they all tend to accumulate NO_2^- at crack similar pH environment (pH 9.5-10). Moreover, corrosion inhibition tests at pH 9 revealed that bacteria induce significant corrosion inhibition. Our previous work revealed that *Diaphorobacter nitroreducens*, ACDC and their corresponding nutrients do not significantly change the concrete properties [150]. Moreover, the tested protective carriers (diatomaceous earth, expanded clay and granular activated carbon) were found to be concrete compatible

CHAPTER 3

[150]. Therefore, combined with the previous results, these findings pave the way for use of the presented bacteria for simultaneous corrosion inhibition and crack healing in concrete.

5. Conclusions

Vegetative axenic NO_3^- reducing and $CaCO_3$ precipitating cultures, *Pseudomonas aeruginosa* and *Diaphorobacter nitroreducens*, could survive mortar environment if protected with either diatomaceous earth, expanded clay or granular activated carbon. Among the tested protective carriers, expanded clay and granular activated carbon are found to be more compatible with concrete and the necessary additives for development of self-healing concrete by means of NO_3^- reducing bacteria.

The tested cultures tend to accumulate NO_2^- at alkaline pH conditions. Microbial produced NO_2^- could inhibit steel corrosion up to a certain extent in corrosive electrolyte solution (0.05 M Cl^-, pH 9) and the controlling parameter was $[NO_2^-]:[Cl^-]$ ratio. Pitting corrosion occurred around -100 mV when $[NO_2^-]:[Cl^-]$ ratio was below 1. In one week, the non-axenic ACDC culture could accumulate 0.057 M (2.6 g/L) NO_2^- in electrolyte solution and induced stable passivation of the steel surface.

The self-protected non-axenic culture, ACDC, is to our best judgment, the most promising microbial based self-healing agent for concrete application. The culture did not require additional protection for mortar application and performed better than the protected axenic cultures in all the tested conditions. As a self-healing additive, ACDC did not cause any significant influence on mechanical properties of the mortar and could inhibit steel corrosion effectively.

6. Acknowledgements

Boon and Prof. Dr. Iris De Graeve regarding the improvement of the work in this chapter was significant. A sincere acknowledgement is then addressed to these people.

PART III
DEVELOPMENT OF
MICROBIAL SELF-HEALING
CONCRETE

CHAPTER

4

MICROBIAL SELF-HEALING MORTAR BY MEANS OF NITRATE REDUCING AXENIC CULTURES

MICROBIAL SELF-HEALING MORTAR BY MEANS OF NITRATE REDUCING AXENIC CULTURES

Abstract

Microbial self-healing appears a promising tool to avoid external maintenance requirements for early-age cracks in construction industry. The phenomenon has been widely investigated, yet the suggested microbial pathways are limited to ureolysis and the aerobic oxidation of carbon sources. Each of these pathways have certain drawbacks. Ureolysis leads to NH_4^+ production and thus NH_3 which is toxic for the aquatic environment. Aerobic oxidation is mostly efficient at the crack mouth due to the O_2 limitation inside the crack. Therefore, better alternatives are needed for application of self-healing concrete in situ. We present the NO_3^- reduction as an alternative microbial self-healing strategy. In the tests, we used previously described resilient vegetative NO_3^- reducing strains, and two different porous protective carriers. Nitrate (NO_3^-) reducing strains were loaded in protective carriers and investigated for their effect on self-healing performances of mortar. Healing performances up to 56 days were investigated. The highest crack width healed by the bacteria was 370 ± 20 μm in 28 days and 480 ± 16 μm in 56 days. Water tightness regain up to 85% was achieved at the end of 56 days for 465 ± 21 μm crack width. Healing products were identified as forms of $CaCO_3$ and were abundant in microbial specimens. Considerable amount of microbial induced $CaCO_3$ was found on the inner crack surface and no toxic by-products were produced at the end. These findings indicate that the NO_3^- reduction pathway is suitable for development of self-healing concrete having enhanced and environment-friendly properties.

1. Introduction

Autogenous healing can heal cracks up to 300 μm in cementitious materials [21]. To extend the existing autogenous healing capacity, microbial self-healing has been suggested. This approach, using bacteria as a healing additive for concrete, offers significant opportunity to avoid high-cost maintenance methods and long-term durability problems [55]. The major two additives of a microbial self-healing concrete are a suitable bacterial culture and the respective nutrients to support metabolic activity and trigger self-healing. Studies revealed that regardless of being vegetative cells or spores, bacteria can be useful for crack healing if only they are protected from the harsh concrete environment during the application [55,59]. Therefore, concrete and bacteria compatible protective carriers are needed. So far, two types of metabolic pathways were considered to enhance the self-healing potential of the concrete. The first pathway was the aerobic respiration of bacteria which leads to the production of dissolved inorganic carbon (DIC) (Eq.(4.1)) [40,55]. Simply by adding the protected bacterial spores and nutrients into mortar specimens, significant crack sealing performances up to 460 μm were achieved in 100 days [40]. Major drawbacks of the aerobic respiration pathway are the O_2 limited performance and poor $CaCO_3$ precipitation yield due to the lack of produced alkalinity and the CO_3^{2-} (Rxn. (4.1)) [51,67]. Indeed, the self-healing performance is dependent on OH^- ions leaching from the structure itself which are prone to wash out. Moreover, the O_2 concentrations are limited due to its low solubility in water (~9 mg/L at 20 ^{o}C) and restricted availability in deeper parts of the crack.

$$Ca(CH_3COO)_2 + 4O_2 \rightarrow CaCO_3 + 3CO_2 + 3H_2O \qquad (Rxn\ 4.1)$$
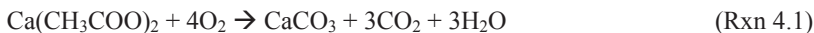
The second pathway, urea hydrolysis (Rxn. (4.2)), was already used in several microbial induced $CaCO_3$ precipitation studies prior to self-healing studies [45,48]. The process was known for its significant pH increase and for the high $CaCO_3$ precipitation rate [45,65]. Degradation of each mole of urea leads to production of two moles of NH_4^+ which increases the pH and induces a rapid $CaCO_3$ precipitation [65]. Microbial ureolysis induced crack closure up to 970 μm in 8 weeks of immersion under water [22]. Reported urea degrading bacteria are also known for their aerobic activity which means that their growth in-situ is still limited with the O_2 availability [151]. Moreover, occlusion of the bacteria due to the rapid precipitation of $CaCO_3$ around the cell membrane is detrimental for the cells [45,67]. These circumstances are disadvantageous for the continuous growth of the cells and stable $CaCO_3$ precipitation rate. The major drawback of urea hydrolysis pathway is related to NH_4^+ production. Ammonium ions are in balance with ammonia and under alkaline conditions

NH_4^+ turns into NH_3. This conversion jeopardizes the concrete microstructure since it may cause concrete degradation by consuming OH^- ions. Moreover, NH_3 is stated to be toxic for the environment, especially for the aquatic life [66].

$$CO(NH_2)_2 + 2H_2O + Ca(NO_3)_2 \rightarrow CaCO_3 + 2NH_4^+ + 2NO_3^- \qquad (Rxn\ 4.2)$$

Similar issues in other MICP applications such as soil consolidation and Ca^{2+} removal from the industrial waste streams prompted the attention to biological NO_3^- reduction as an alternative pathway [51,67]. Nitrate (NO_3^-) reduction mainly occurs under O_2 limited conditions and is performed by the bacteria that are able to respire on NO_3^- (Rxn. (4.3)).

$$Ca(HCOO)_2 + 0.4Ca(NO_3)_2 \rightarrow 1.4\ CaCO_3 + 0.4N_2 + 0.6\ CO_2 + H_2O\ (Rxn\ 4.3)$$

Similar to previously reported pathways, biological NO_3^- reduction also induces $CaCO_3$ precipitation. Unlike ureolysis no toxic by-products are formed during NO_3^- reduction. By producing significant amount of alkalinity the process yields $CaCO_3$ precipitation in the presence of Ca^{2+} ions regardless of the available OH^- ions. Nitrate (NO_3^-) reduction is not only advantageous by inducing enhanced $CaCO_3$ precipitation; it can also lead to the production of NO_2^- (Rxn.(4.4)) which is known as corrosion inhibitor [70,115].

$$2HCOO^- + 2NO_3^- + 2H^+ \rightarrow 2CO_2 + 2H_2O + 2NO_2^- \qquad (Rxn\ 4.4)$$
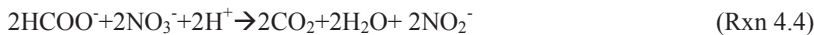
Although the NO_3^- reduction pathway was explored for different MICP applications, it has never been considered for concrete applications. Our previous work on the NO_3^- reduction pathway revealed that by using only the concrete admixtures (Ca-nitrate, Ca-formate), enhanced $CaCO_3$ precipitation performances could still be achieved which makes the process feasible for self-healing concrete [67]. Moreover, among possible healing additive combinations (nutrient+bacteria+protective carrier), use of porous protective carriers such as expanded clay particles, granular activated carbon or zeolite in combination with bacteria and nutrients was revealed to be harmless for physical properties of concrete [150]. Additionally, they appeared to be suitable for protecting bacteria in alkaline pH environments up to pH 13 [147]. Hereupon we present the assessment of self-healing performance of mortar containing NO_3^- reducing bacteria-based healing agents. The major objective of the study was to evidence the potential of NO_3^- reducing bacteria for development of microbial self-healing concrete. Within this scope, the chapter was composed of two main parts (1) preliminary assessment of NO_3^- reducing bacteria for microbial self-healing concrete (2) healing assessment and functionality regain under the defined conditions considering significant factors.

2. Material and methods

2.1. Bacterial cultures

As a self-healing additive, two soil originated axenic bacterial cultures, *Diaphorobacter nitroreducens* and *Pseudomonas aeruginosa*, were tested separately. These strains were isolated in a previous study [67] and kept for further testing. Cultures for mortar addition were grown in batch reactors by using nutrient media (NM). The grown bacterial cultures (each 1.25 g cell dry weight/L) were harvested by centrifuging at $6300 \times g$ for 7 minutes and re-suspended in saline solution (8.5 g/L NaCl). From each strain 2.25 g cell dry weight (CDW) was used as the bacterial agents.

2.2. Protective carriers and loading of the bacterial cells

As protective carriers either expanded clay particles (EC) or granular activated carbon (GAC) particles both 0.5 – 2 mm in size were used. Self-healing tests were conducted for two different crack ranges. For the crack width range from 100 – 500 μm expanded clay particles were used as a protective carrier and performance of specimens monitored only for 28 days. For the crack width range of 250 – 700 μm bacterial cultures were loaded in granular activated carbon particles and healing performance up to 56 days was investigated. Since longer treatment period may lead better healing, to clearly define the limits, an extended crack width range was tested.

Please consult **Chapter 3**, "Material and methods – Section 2.3" for detailed bacteria loading procedure to the protective carriers. The bottles containing the mixture were kept at room temperature (~20 ^{o}C) for 48 h before using as self-healing additive. Same loading procedure was applied for both protective carriers.

2.3. Preparation of the mortar specimens and formation of the cracks

Series of mortar specimens (30 × 30 × 360 mm), with an embedded steel reinforcement bar (Ø= 6 mm) positioned centrally, were prepared by using CEM I 52.5 N, tap water and standard sand according to the norm EN 196–1 and further cured at 20°C and RH > 95% for 28 days prior to cracking. The sand:cement:water ratio was 3:1:0.5. Pressure of the bottles was released and bacteria (0.5 % w/w cement) loaded protective carriers (5 % w/w cement) were added into the mortar mix during preparation without replacing any aggregates. The suspension not absorbed by the protective carriers was also added to the mortar mixture. The

amount of water in the bacterial suspension was deducted from the water content of the specimens to keep the water/cement ratio (0.5 w/w) constant as described previously in Chapter 3, Section 2.3, Equation 3.1[150]. The composition of each series is given in Table 4.1.

Table 4.1 Tested mortar series and their compositions

Series	PM[1] (g)	*P. aeruginosa* (g)	*D. nitroreducens* (g)	$Ca(NO_3)_2 + Ca(HCOO)_2$ (g)
Reference mortar[2]	0	0	0	0
Abiotic Control	EC (22.5)	0	0	13.5 + 9
	GAC (22.5)	0	0	13.5 + 9
Microbial specimen (R+N+PM+B)	EC (22.5)		2.25	13.5 + 9
	EC (22.5)	2.25	0	13.5 + 9
	GAC (22.5)		2.25	13.5 + 9
	GAC (22.5)	2.25		13.5 + 9

[1]R: Reference; N: Nutrients ($Ca(NO_3)_2$ + Ca(HCOO)); B: Bacteria; PM: Protection material; EC: Expanded clay particles; GAC: Granular activated carbon particles
[2]Reference mortar was prepared for each batch (Sand:Cement:Water (g): 1350:450:225).

Cured specimens (28 days at 20^oC and RH > 95 %) were subjected to a tensile stress by applying uniaxial tensile load at a speed of 0.01 mm/s on the embedded steel reinforcement bar under stroke control (Figure 4.1). Multiple cracks were achieved and the loading was kept until a desired average crack width was achieved. The average crack width was calculated via Eq. (4.1).

$$\delta = W_a * n + (\sigma/E) * L \qquad \text{(Equation 4.1)}$$

where;

δ is the elongation (the stroke in the loading program);

W_a is the average crack width (depends on the desired value)

n is the number of cracks observed on one surface;

σ is the average load in the plastic stage of the reinforcement, which equals to $560 N/mm^2$;

E is the E-modulus of the reinforcement, which equals to 210000 N/mm^2;

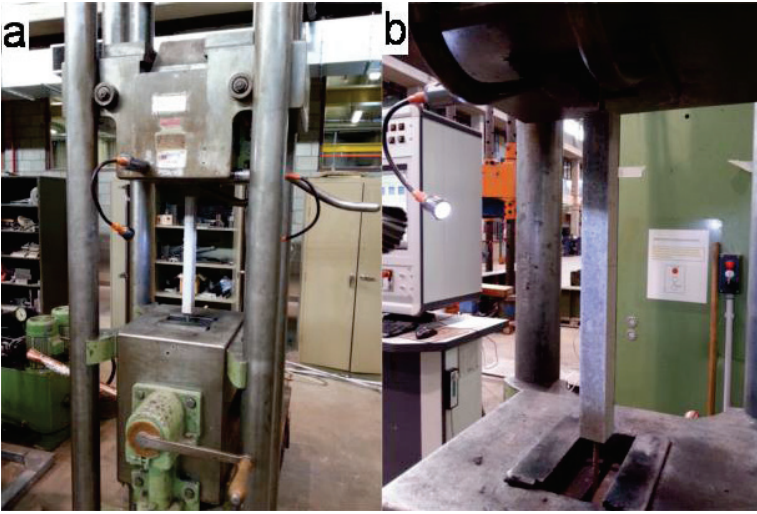L is the distance between two clamps (it was 360mm+50mm×2=460mm in this study).

Figure 4.1 Test setup for cracking of the reinforced mortar specimens (a) instrument used for tensile loading; (b)a closer view of the specimen and formation of cracks

The achieved crack width range, average crack width and batch specific protective carriers are summarized in Table 4.2. The mortar specimens containing bacteria + expanded clay + $Ca(NO_3)_2$ + $Ca(HCOO)_2$ were tested for 100 to 500 µm crack width with an average crack width of 300 µm. The mortar specimens containing bacteria+granular activated carbon+$Ca(NO_3)_2$+$Ca(HCOO)_2$ were tested for 250 to 700 µm crack width with an average crack width of 450 µm.

2.4. Self-healing treatment conditions

Following the cracking, specimens containing expanded clay particles were immersed in water for 28 days at ambient temperature of 20° C. Following the results of the first test, time was found to be the major factor to differentiate between autogenous healing and autonomous healing. Therefore, the specimens containing granular activated carbon were separated into two groups and each group was treated for different time periods under complete immersion. First group was tested for 28 days and the second group was tested for 56 days. Each group had its two series of control specimens (Table 4.1).

Table 4.2 Series and the tested particular crack conditions in each batch

Series	PM (g)	Crack width range (μm)	Average crack width (μm ± sem)	Incubation conditions
	EC	100 – 450	230 ± 9	28 days-water immersion
Reference	GAC	70 – 650	315 ± 12	28 days-water immersion
	GAC	200 – 550	330 ± 13	56 days-water immersion
	EC	75 – 550	260 ± 8	28 days-water immersion
Abiotic Control	GAC	230 – 680	420 ± 11	28 days-water immersion
	GAC	250 – 750	455 ± 20	56 days-water immersion
	EC + B1	75 – 550	280 ± 10	28 days-water immersion
	EC + B2	130 – 550	266 ± 8	28 days-water immersion
Microbial specimen (R+N+PM+B)	GAC + B1	180 – 690	420 ± 12	28 days-water immersion
	GAC + B1	190 – 640	380 ± 19	56 days-water immersion
	GAC + B2	175 – 730	450 ± 16	28 days-water immersion
	GAC + B2	220 – 740	490 ± 19	56 days-water immersion

[a]R: Reference (Sand:Cement:Water (g) – 1350:450:225); N: Nutrients ($Ca(NO_3)_2$ + $Ca(HCOO)_2$); PM: Protection materials; B: Bacteria; EC: Expanded clay, GAC: Granular activated carbon, B1: *Diaphorobacter nitroreducens*, B2: *Pseudomonas aeruginosa*, sem: Standard error of the mean

2.5. Quantification of self-healing properties

Crack closure was observed with respect to the treatment time through stereomicroscope with apochromatic optics (Leica S8 Apo). Obtained images were further analyzed by using image analysis software (The Leica Application Suite, LAS V3.7.0). The crack closure for the batch containing expanded clay particles was monitored weekly by taking the specimens out from their treatment conditions. During image taking, specimens exposed to ambient air conditions (~20 ^{o}C). Collected weekly data were further analyzed statistically to differentiate between autogenous healing and autonomous healing. The crack closure for the batches containing granular activated carbon was monitored on day 14, day 28 and day 56. At the end of 28 days, first batch was taken out for capillary sorption test and the rest were kept for another 28 days to complete 56 days of treatment time. Crack closure efficiency was calculated by using Eq. (4.2).

CHAPTER 4

$$\text{Crack closure \%} = (w_t / w_{initial}) \times 100 \qquad \text{(Equation 4.2)}$$

where

w_t = crack width measured at a certain day

$w_{initial}$ = initial crack width

In order to quantify the water tightness of the healed specimens capillary sorption tests were conducted. Prior to testing, the specimens were dried in a 40 ^{o}C oven until the mass changes in 24 hours were less than 0.1%. Similar crack widths were chosen for each specimen. Apart from the chosen crack the rest of the specimen was completely covered with aluminum tape to prevent evaporation. Therefore, only the area of 3 cm^2 (30 mm $\times$ 10 mm) surrounding the chosen crack contacted with water. The mass increase of specimens due to the absorbed water was monitored by regular time intervals. A wet towel was used to remove the remaining surface water droplets prior to weighing.

In order to analyze and identify the healing materials, specimens were cut into pieces by leaving 0.5 cm distance from the crack borders. The piece with the crack (10 $\times$ 30 $\times$ 30 mm) was further split through the crack into two pieces by using manual force. One of the surfaces was coated with carbon (~15–35 nm thickness) and analyzed under scanning electron microscopy coupled with energy dispersive X-ray spectroscopy (SEM/EDX). The second piece was used for Fourier transform infrared spectroscopy (FTIR) analysis. The composition at a certain depth was the main interest, thus on the crack surface, an area of 1 cm^2 (5 mm $\times$ 20 mm) was defined at a distance of 5 mm from the crack mouth and 2 mm from the reinforcement bar. The defined area was scraped by using a stainless steel spatula (5 mm width) and the pieces were collected (< 15 mg). Collected pieces were further ground into powder by using a mortar and pestle. A portion of the ground powder (< 5mg) was chemically characterized by using FTIR (Spectrum 100, Perkim Elmer Inc, USA). Presented spectra were the result of 32 scans with a resolution of 4 cm^{-1} in the range of 4000 – 600 cm^{-1}.

2.6. Statistical analysis

Differences between the healing of cracks in different series were compared using a repeated measures mixed model in SAS (version 9.4, SAS Institute, Cary, USA), accounting crack width and incubation time as fixed effects, and with the least square means (LS-means, $p < 0.05$) adjustment and Bonferroni correction for multiple comparisons. Similar approach was used to determine the effect of incubation time on crack closure efficiency by accounting the series type and crack width as fixed effects. Furthermore, the effect of protective carriers

was analyzed using non-repeated measures mixed model by accounting the bacteria type and crack width as fixed effects. Statistical analysis on capillary water absorption data were conducted using SigmaPlot 12.0 (Systat Software Inc USA) to compare significant differences by means of one way ANOVA test (p=0.05).

3. Results

3.1. Self-healing performance in the presence of NO_3^- reducing bacteria

The addition of both bacteria based additives and their respective nutrients had a similar positive influence on the self-healing potential of mortar specimens (Figure 4.2). Control specimens without bacteria showed self-healing of the cracks up to 300 μm crack width at the end of 28 days (Figure 4.2d). However, complete closure could not be achieved for crack widths more than 200 μm (Figure 4.2d and Figure 4.3). Among the control specimens, the ones containing expanded clay particles and nutrients showed significantly better healing performance than the reference mortar (Figure 4.2d).

Specimens containing bacteria loaded expanded clay particles could heal cracks up to 350-400 μm crack width (Figure 4.2d and Figure 4.3). The difference between the autogenous healing and the microbial healing became more noticeable in time. After 14 days of immersion in water, significant differences in the crack closure were observed between the reference specimen and the other specimens (Figure 4.2b). The bacteria containing specimens could be distinguished from the abiotic control, mortar containing empty expanded clay particles and nutrients, at different time periods. When *Diaphorobacter nitroreducens* was used as the bacterial agent, distinctive healing performances were achieved in 14 days (Figure 4.2b). Cracks up to 350 μm were closed more than 90% in 14 days. Following another 14 days of treatment, 100% crack closure for the cracks up to 350 μm and more than 90% crack closure for the crack widths between 350-400 μm were achieved (Figure 4.2d). When *Pseudomonas aeruginosa* was used as the healing agent, healing performances achieved in 21 days were still comparable to the performance of the abiotic control (Figure 4.2c). At the end of 28 days, specimens containing *Pseudomonas aeruginosa* revealed significantly better performance than the abiotic control (Figure 4.2d).
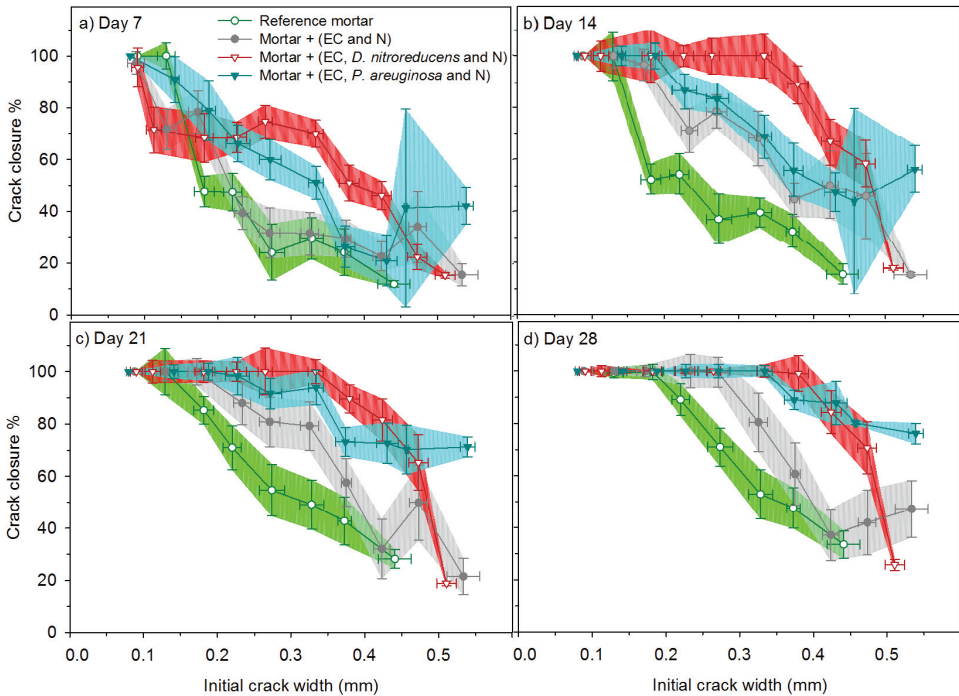
Figure 4.2 Autogenous and autonomous healing efficiencies at different crack width ranges after (a) 7 days; (b) 14 days; (c) 21 days; (d) 28 days immersion in fresh water; EC: Expanded clay particles; N: Nutrients – Ca(HCOO)₂ and Ca(NO₃)₂, (horizontal error bars represent the standard deviation, crack widths were grouped with 50 μm intervals, vertical error bars represent the standard error of the mean, n ≥5)

The observed difference was in the healing performance of cracks larger than 300 μm which appeared to be the limit for the healing potential of the abiotic control (Figure 4.2d and Figure 4.3b). Similar to the mortar containing *Diaphorobacter nitroreducens*, self-healing induced by *Pseudomonas aeruginosa* was also limited to the crack width range up to 350-400 μm (Figure 4.2d and Figure 4.3d).
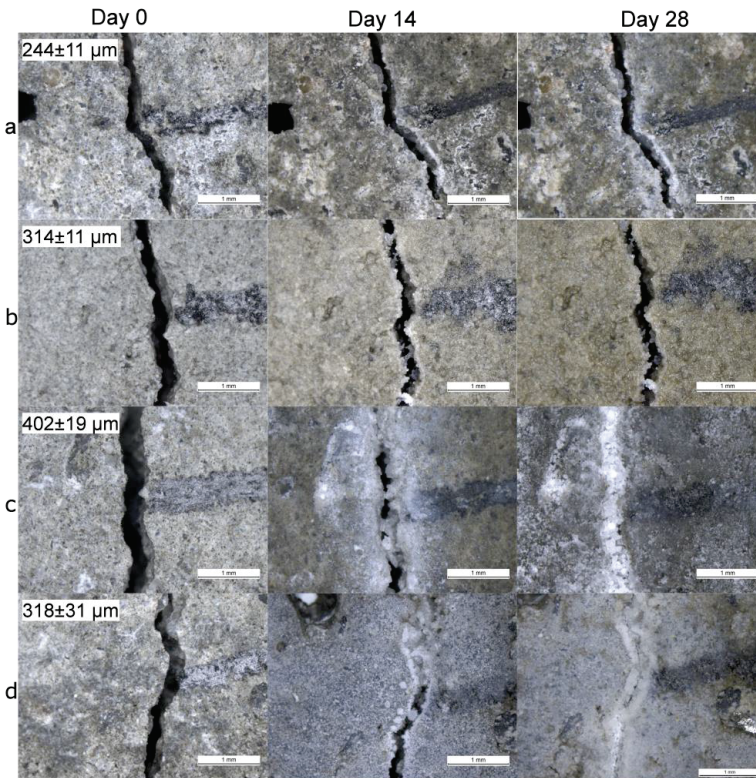
Figure 4.3 Photomicrographs showing biweekly evolution of cracks during 28 days of water immersion (a) reference mortar; (b) abiotic control; (c) mortar containing Diaphorobacter nitroreducens loaded expanded clay particles (d) mortar containing Pseudomonas aeruginosa loaded expanded clay particles (given values represent the average width of the shown crack ± standard deviation; scale bar is 1 mm)

Capillary sorption tests revealed that microbial induced healing could provide an improvement in water tightness compared to the autogenous healing (Figure 4.4). There was a substantial decrease in the amount of water absorbed by the specimens containing either of the bacterial agents compared to the control specimens. The specimens containing bacteria absorbed 50% and 40% less water than the reference mortar and abiotic control, respectively (Figure 4.4).

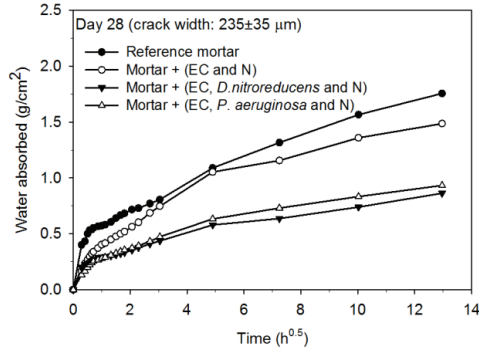*Figure 4.4 Water absorption of the control specimens and microbial specimens (containing expanded clay protected bacteria) after the healing period of 28 days (average crack width of the tested cracks prior to healing was 235 ± 35 μm); EC: Expanded clay particles; N: Nutrients – Ca(HCOO)$_2$ and Ca(NO$_3$)$_2$*

3.2. Granular activated carbon protected bacteria

The previously shown results revealed that the incorporation of NO_3^- reducing bacteria and their respective nutrients in mortar enhanced the healing potential of the mortar specimens. In this case, an alternative protective carrier, granular activated carbon, was used to incorporate bacterial agents Since the duration of the treatment was of importance (Figure 4.2 and Figure 4.3), evolution of the healing was also tested for 56 days. At the end of 28 days, for bacteria containing specimens, the limit for effective crack closure was recorded as 400 μm which was not significantly different than the obtained results where expanded clay particles were used as protective carrier (Figure 4.2d and Figure 4.5a). At the end of 56 days, two major outcomes appeared. First, the limit for microbial induced crack closure extended up to 500 μm crack width (Figure 4.5b and Figure 4.6). Second, a minor, but significant, improvement (~50 μm) on the maximum healed crack width was observed in abiotic control specimens (Figure 4.5b and Figure 4.6). Different from microbial specimens and abiotic control, there was no significant change in the healing limit of the reference series after increasing curing time from 28 days to 56 days (Figure 4.5).
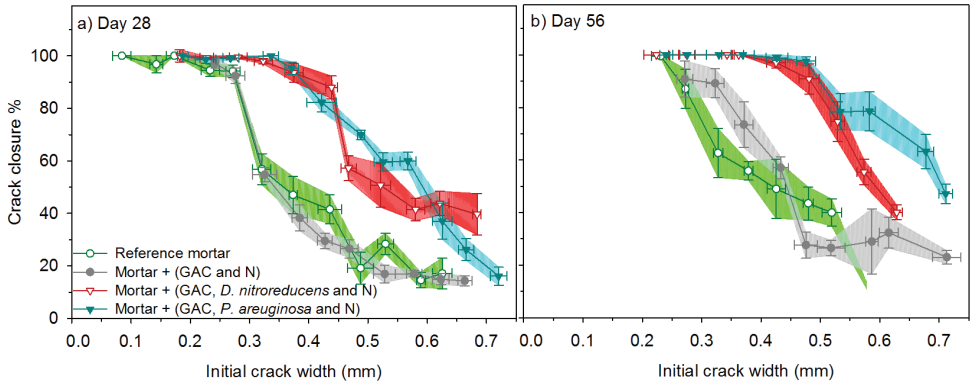
Figure 4.5 Autogenous and autonomous healing efficiencies at different crack width ranges after (a) 28 days; (b) 56 days immersion in fresh water; GAC: Granular activated carbon particles; N: Nutrients – Ca(HCOO)$_2$ and Ca(NO$_3$)$_2$, (horizontal error bars represent the standard deviation, crack widths were grouped with 50 μm intervals; vertical error bars represent the standard error of the mean, n ≥5)

The healing potential improvement in microbial samples from day 28 to day 56 indicated the continuous microbial activity which means that as long as there are nutrients available for the added bacteria (*Diaphorobacter nitroreducens* and *Pseudomonas aeruginosa*), CaCO$_3$ precipitation continues. These results are promising for healing of larger crack widths. However, there is one crucial point to be considered in microbial self-healing concrete. The presence of bacteria and nutrients inside the crack are of significance for achieving effective sealing or healing performance in time. The larger the crack width the higher the risk of healing agent (either bacteria, nutrients or CaCO$_3$ precipitates) wash out from the crack zone. During the experimental period, for the cracks larger than 500 μm, considerable amount of CaCO$_3$ precipitated through the crack and accumulated at the bottom of the container. Loss of the healing material most probably caused a decrease in the healing potential of the mortar specimens. However, it was not possible to quantify/include the effect whilst interpretation of results.

CHAPTER 4
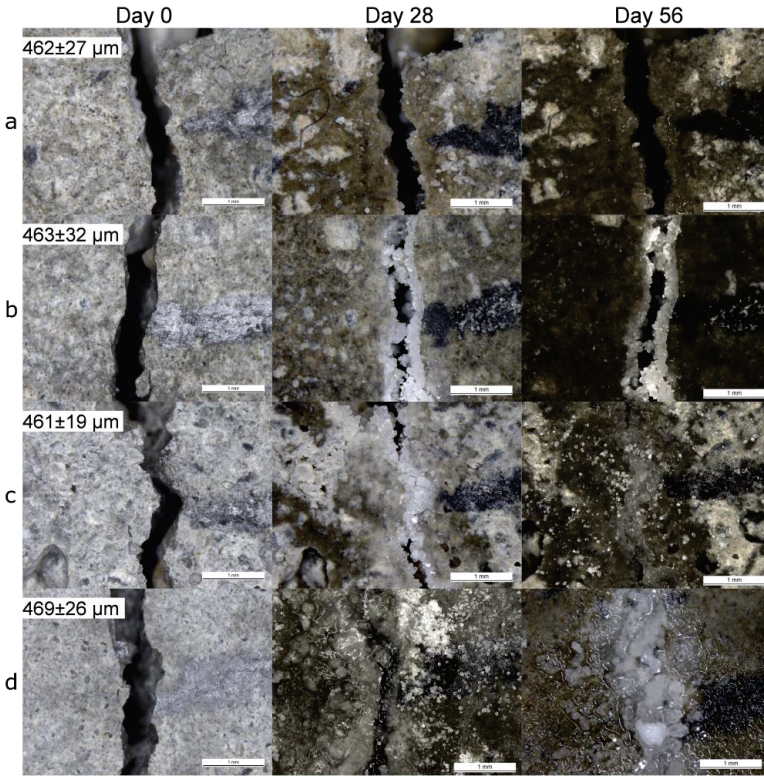
Figure 4.6 Photomicrographs showing the evolution of cracks after 28 days and 56 days of water immersion (a) reference mortar; (b) abiotic control; (c) mortar with Diaphorobacter nitroreducens loaded granular activated carbon particles (d) mortar with Pseudomonas aeruginosa loaded granular activated carbon particles (given values represent the average width of the shown crack ± standard deviation; scale bar is 1 mm)

Capillary sorption tests conducted on healed specimens at different healing periods (after 28 and 56 days) confirmed the positive effect of longer treatment period (Figure 4.7). After 28 days healing of 455±24 µm and 56 days healing of 465±21 µm crack widths, microbial specimens showed significantly better performance than the control specimens in terms of water tightness (Figure 4.7). However, in 28 days healing of 455±24 µm crack width, complete crack closure could not be achieved (Figure 4.6). Healing efficiency of the 450 µm crack width was recorded between 57-88 % (Figure 4.5a). Therefore, all of the specimens absorbed 8 – 12 times more water than the uncracked specimen (Figure 4.7a). After 28 days healing of an average crack width of 455±24 µm, microbial mortar specimens absorbed 30±4 % less water than the reference mortar specimens (Figure 4.7a). After increasing the healing

period from 28 days to 56 days, for an average crack width of 465±21 μm, enhanced crack closure was achieved, thus microbial mortar specimens absorbed 75±4 % less water than the reference mortar specimens (Figure 4.6 and Figure 4.7b). Furthermore, after 56 days healing, there was 6±4 % reduction in water absorption of abiotic control specimens compared to the values obtained after 28 days healing (Figure 4.7).
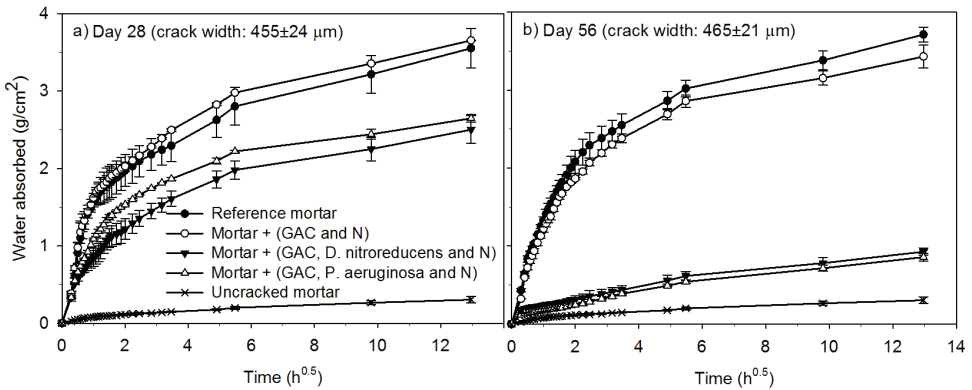
Figure 4.7 Water absorption of the uncracked, control and microbial specimens (containing granular activated carbon protected bacteria) after the healing period of (a) 28 days (b) 56 days; (average crack widths of the tested cracks prior to 28 days healing and 56 days healing were 455 ± 24 μm and 465 ± 21, respectively); GAC: Granular activated carbon particles; N: Nutrients – Ca(HCOO)$_2$ and Ca(NO$_3$)$_2$ (n=3, error bars represent the standard deviation)

3.3. Formation of healing material inside the crack

Biochemically formed CaCO$_3$ (in the form of calcite) precipitates were found during the visual inspection of the inner crack surface of bacteria containing specimens (Figure 4.8 and Figure 4.9). Traces and even remains of bacteria were found on the CaCO$_3$ precipitates formed. Moreover, some bacteria that were initially encapsulated in the pores of expanded clay particles could be visualized since the clay particles were broken during the crack propagation (Figure 4.8d). Unlike microbial specimens, on the inner crack surface of abiotic control, pores of the broken expanded clay particles were empty (Figure 4.8b). Additionally, on both control specimens (reference mortar and abiotic control), formation of C-S-H like compounds and ettringite like minerals were dominant inside the crack compared to CaCO$_3$ (mostly the product of partial carbonation) (Figure 4.8).

CHAPTER 4
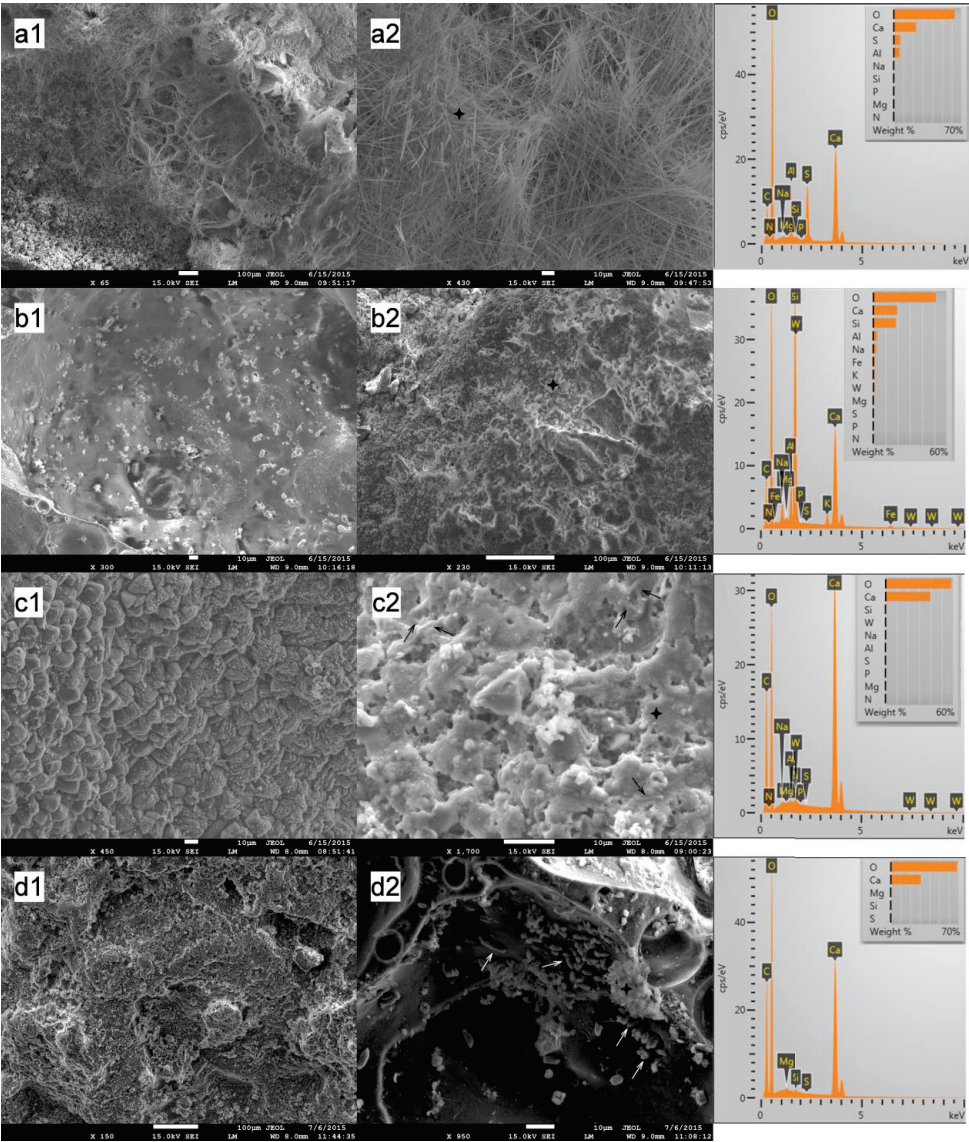
Figure 4.8 Representative SEM images and EDX analysis of the dominant healing material at the inner crack surface after 28 days healing period (a1,a2) reference mortar; (b1,b2) abiotic control; (c1,c2) mortar containing Diaphorobacter nitroreducens loaded expanded clay particles; (d1,d2) mortar containing Pseudomonas aeruginosa loaded expanded clay particles; '↗' shows bacteria, '+' shows the points analyzed via EDX.
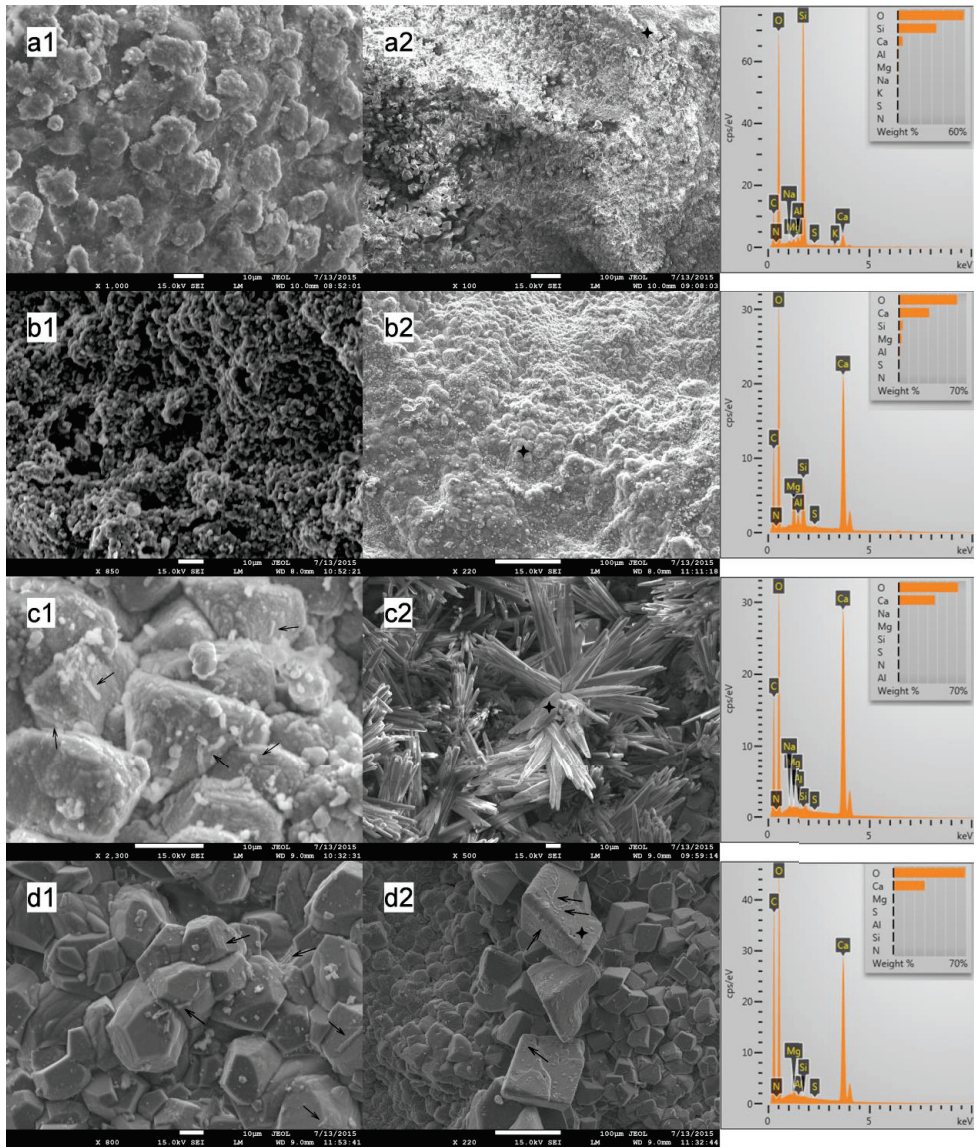
Figure 4.9 Representative SEM images and EDX analysis of the dominant healing material at the inner crack surface after 56 days healing period (a1,a2) reference mortar; (b1,b2) abiotic control; (c1,c2) mortar containing Diaphorobacter nitroreducens loaded granular activated carbon particles; (d1,d2) mortar containing Pseudomonas aeruginosa loaded granular activated carbon particles; '↗' shows bacteria, '+' shows the points analyzed via EDX.

3.4. Chemical characterization of healing material

During SEM imaging, the elemental composition of minerals were analyzed by using energy dispersive X-ray spectroscopy (EDX). Furthermore, collected powder samples were chemically characterized via FTIR analysis. The information collected from both analyses confirmed that the visualized minerals inside the crack of microbial specimens were $CaCO_3$ (Figure 4.8 – Figure 4.10). In addition to calcite (2509, 1793, 1414, 872 and 712 cm^{-1}), aragonite (696 cm^{-1}), ettringite (1162), bassanite (1085 cm^{-1}), C_2S (879 cm^{-1}), C-S-H (970, 1052, 1643, 1980, 2324 and 2163 cm^{-1}) and portlandite (3629 cm^{-1}) were found in the collected powder samples [152–155] (Figure 4.10). Similar to SEM observations, in the powders collected from control specimens, cement and its hydration products were as abundant as the calcite and aragonite. Contrarily, in the powder collected from the microbial specimens, different forms of $CaCO_3$ were the dominant compounds (Figure 4.10).

Figure 4.10 FTIR spectra of the healing materials collected from the inner crack surfaces of different specimens, EC: Expanded clay particles, GAC: Granular activated carbon particles, N: Nutrients – Ca(HCOO)$_2$ and Ca(NO$_3$)$_2$

4. Discussion

4.1. Autogenous self-healing versus microbial induced self-healing
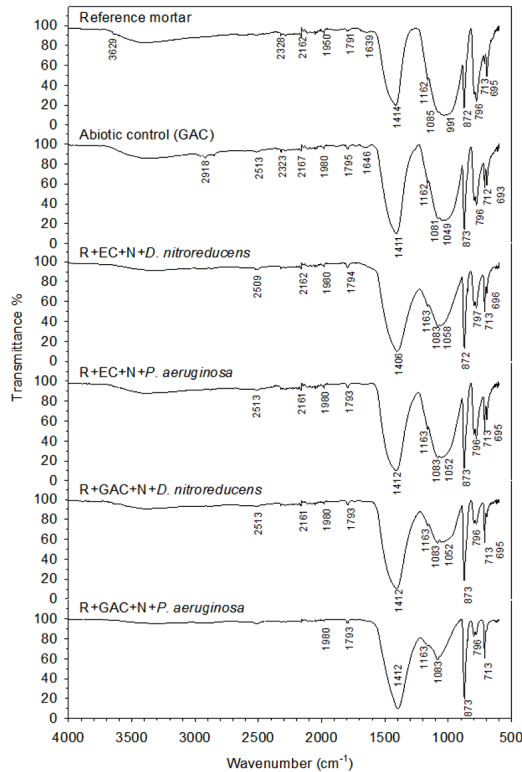
Expanded clay was used as a protective carrier in previous microbial self-healing studies and proven to be effective for bacterial activity [40]. Moreover, the expanded clay particles were reported to be compatible with *Diaphorobacter nitroreducens* and *Pseudomonas aeruginosa* as well as mortar [147,150]. Therefore, by using standard mortar composition (0.5 water/cement ratio) and a well-known bacterial carrier, possible variables that may affect autonomous self-healing were minimized. This approach was significant to understand the effect of bacterial agents on the self-healing performance of the mortar specimens and to evidence the potential of NO_3^- reducing bacteria for development of microbial self-healing concrete. Hence, the results presented in this study prove that NO_3^- reducing bacteria can be used as a self-healing additive in concrete.

Autogenous healing performance of the control specimens fell in the previously described crack width range (up to 300 μm) for fresh water immersion [21–23]. Major reasons of the autogenous healing were widely investigated already and listed as (i) further hydration of unhydrated cement paste, (ii) blockage due to the accumulation of broken pieces, (iii) formation of $CaCO_3$ at the crack mouth due to the carbonation of portlandite [21,24]. Among the control specimens, abiotic control containing everything ($Ca(HCOO)_2$, $Ca(NO_3)_2$ and expanded clay particles) except bacteria showed significantly better autogenous healing performance than the plain mortar, yet the performance was still worse than the bacteria containing specimens. The better healing of abiotic control specimens than the reference mortar might be due to two main reasons. First reason could be the positive effect of mineral admixtures on autogenous healing. It is known that the four main driving parameters for $CaCO_3$ precipitation are (i) the calcium concentration, (ii) the pH, (iii) the dissolved inorganic carbon concentration (iv) the presence of available nucleation sites [83]. Among these parameters, the calcium concentration and the presence of nucleation sites were different between the reference and the abiotic control specimens. Abiotic control had higher Ca^{2+} content due to the addition of $Ca(HCOO)_2$ and $Ca(NO_3)_2$. Therefore, it was possible to have more $CaCO_3$ precipitation during carbonation. Similar observations were reported in previous studies [22]. Another reason could be the growth of co-occurring microorganisms in the immersion water. The experiments were conducted under clean but not sterile conditions. Therefore, following leaching of nutrients from the mortar specimens into the immersion

CHAPTER 4

water, the solution became susceptible to contamination from air and even from the concrete itself. Their metabolic by-product CO_2 can contribute to the autogenous healing. Additionally, these bacteria could involve as an additional nucleation site during autogenous healing. Nonetheless, bacteria containing specimens extended the healing potential up to 400 μm in a 28 days treatment period and performed significantly better than both control specimens. Using granular activated carbon particles as a protective carrier instead of expanded clay led to similar results (p=0.05). The additional healing was due to the formation of $CaCO_3$ minerals upon metabolic activity of the microorganisms inside the crack. The process was mainly the biological oxidation of formate ($HCOO^-$), diffusing from the crack wall, through reduction of the leaching NO_3^- (Rxn. (4.3)) In addition to the inherent carbonation and related autogenous healing of mortar, bacterial activity inside the concrete led to production of additional CO_3^{2-} and enhanced the $CaCO_3$ precipitation, thus enabled healing of larger crack widths. Major indication of the bacterial activity was mineral formation in the deeper parts (5 <depth< 13 mm) of the crack and the bacteria found in/on the calcite and aragonite crystals.

There was significant improvement on the healing potential of microbial samples when the healing time extended from 28 days to 56 days. Different from the microbial samples, reference samples did not show any improvement in longer treatment period. However, in the crack range of 300 – 400 μm there was a significant increase in healing efficiency of the abiotic control samples compared to their performance in 28 days treatment. This time dependent increase in the autogenous healing performance could be attributed to the inevitable microbial contamination of the immersion water under non-sterile conditions. Nonetheless, microbial samples performed significantly better healing performance than the abiotic control for the cracks larger than 300 μm. These results indicated that the addition of well-defined bacteria promoted the self-healing compared to randomly growing bacteria in the presence of nutrients as in the case of abiotic control.

Microbial healing efficiencies achieved using either expanded clay protected bacteria or granular activated carbon protected bacteria in a 28 days treatment period were comparable with the previously reported microbial self-healing results [22,23,40,59]. Most crack closure results through the ureolysis pathway reported healable crack widths in between 300 to 500 μm [23,59]. By incorporating hydrogel protected ureolytic bacterial spores in mortar, more than 80% healing in mortar specimens was achieved for cracks up to 485 μm in 28 days [59]. Non-axenic ureolytic spores, so called CERUP, could provide self-healing of cracks up to 350-400 μm crack width range in 28 days [23]. So far, different from ureolysis, aerobic oxidation of organic carbon is also considered for microbial self-healing. Wiktor and Jonkers

[40] reported complete crack healing up to 460 μm in 100 days by using expanded clay particles loaded with aerobic-bacterial spores as self-healing additive. In our work it appeared that similar healing efficiency could be achieved in 56 days by using NO_3^- reducing bacteria and similar protective carriers. Moreover, healing performances achieved with NO_3^- reducing bacteria in 28 days were comparable with the healing performance achieved with aerobic bacteria between 40 – 70 days. There might be several reasons for the observed enhanced performance. First of all, the initial curing time reported in the study was 56 days while in our study it was 28 days. The difference in curing time might affect the portion of unhydrated cement and thus the healing properties [21,22]. Indeed, the considerable difference between the autogenous healing potential of the reference specimens in two studies confirms such effect. The reported autogenous healing was up to 180 μm [40] while in this study up to 250 μm could be achieved in reference specimens. Another reason might be the effect of microbial pathways which were different. During aerobic oxidation of organic carbon, O_2 is the vital element to keep the microbial activity. The only O_2 source during the reported incubation conditions was the air-water interface which depends on the water surface area and the depth of the water, thus might be limited by the diffusion rate. Therefore, the healing rate might be influenced by the O_2 dissolution rate and delayed in the reported microbial self-healing results. In this study, the organic carbon ($HCOO^-$) was oxidized through NO_3^- reduction process which dominates under O_2 limited conditions. Another crucial point influencing $CaCO_3$ precipitation rate is the initial amount of bacterial agents used. The amount of bacteria used in the reported study [40] was ambiguous and might be less than the amount of bacterial agents used (0.5 % w/w cement) in this study. Therefore, it might be the reason that the $CaCO_3$ precipitation rate in our study was considerably higher and led to earlier healing of similar crack widths when compared to the reported results.

4.2. Water tightness

In all cases investigated, microbial samples showed substantial decrease in the amount of water absorbed compared to control samples. The chosen average crack width was 235 ± 35 μm which falls in the autogenous healing range, specific to the setup where expanded clay particles were used as protective carrier. The crack width was representing the zone where abiotic control showed >90 % crack closure efficiency. Yet, still the microbial healed specimens showed considerably better water tightness than the reference specimens. These results revealed the major influence of the thickness of the sealing. Apparently, the

CHAPTER 4

autogenous healing was only efficient in terms of the sealing of the cracks at the crack mouth. Therefore, water passing through the filling material could easily penetrate towards the reinforcement bar. Contrarily, microbial specimens also provided sealing in the deeper parts of the cracks and prevented the capillary water transport by several layers or by a thicker $CaCO_3$ barrier. Major reason of the difference was the CO_2 concentration inside the crack which is one of the driving parameters for $CaCO_3$ precipitation [83]. $CaCO_3$ precipitation in autogenous healing mostly occurs at the crack mouth due to the limits in CO_2 dissolution and penetration through the crack [156]. In microbial healing, NO_3^- reducing bacteria produces CO_2 inside the crack as a result of their microbial activity, thus increase the CO_2 concentration. Indeed, chemical and physical characterization of the filling material inside the cracks (5 mm <depth< 13 mm) of control and microbial samples showed considerable difference. In microbial samples calcite and aragonite was abundant over the hydration products. In control samples mostly partially carbonated portlandite, ettringite and C-S-H were found. Eventually, the $CaCO_3$ precipitation occurs in the deeper parts of the crack played the major role in substantial decrease of water absorption observed in microbial samples.

In the second setup where granular activated carbon particles were used as protective carrier, the tested average crack width was almost doubled. Although it is not perfectly correlated, crack width has an influence on the amount of water absorbed through the crack. The wider the crack width the higher the amount of water inside the crack (until the range that capillary suction is not possible) leading to higher water absorption. Therefore, capillary water absorption could be used effectively for quantification of functionality regain of the partially healed cracks.

Previously reported water absorption values for an uncracked reference specimen were similar to the value we obtained in this study [22]. The water absorption of an uncracked specimen is representative for flawless healing and thus 100 % water tightness regain. The capillary sorption test was not conducted for cracked specimens prior to healing, therefore the sorption following autogenous healing can be considered as the zero point for microbial healing while the sorption for uncracked specimens can be considered as maximum regain of water tightness. Therefore by using the information obtained from the capillary sorption tests, one can calculate the water tightness regain by Eq. (4.3);

$$\text{Water tightness regain} = (1 - \frac{m_{\text{healed}} - m_{\text{uncracked}}}{m_{\text{autogenously healed}} - m_{\text{uncracked}}}) \times 100 \quad \text{(Equation 4.3)}$$

where;

$m_{\text{autogenously healed}}$= water absorbed after autogenous healing

m_{healed}= water absorbed after any type of healing

$m_{\text{uncracked}}$= water absorbed by uncracked specimen

After 28 days healing of 455±24 µm cracks by bacteria, the crack closure efficiency was between 57 – 88 % (Figure 4.5a) and the water tightness regain was 28 – 33 %. Substantial water tightness regain (82 – 85 %, Figure 4.5b) was achieved only after 56 days when the healing efficiency of 465±21 µm crack width was more than 90% with less variation.

5. Conclusions

Resilient vegetative cells incorporated in porous protective carriers can be an alternative to spores for development of microbial self-healing concrete.

Granular activated carbon particles can serve as effective as expanded clay particles to protect bacteria in mortar environment until the crack propagation.

Anoxic oxidation of organic carbon through nitrate reduction pathway is a promising, effective and environmentally friendly process improving the self-healing of the mortar cracks up to 480 ± 16 µm crack width in 56 days.

Concrete admixtures $Ca(HCOO)_2$ and $Ca(NO_3)_2$ can also serve as nutrient sources for microbial self-healing.

As long as nutrients are present in the crack environment, microbial activity continues and induces closure of larger cracks, thus the amount of nutrients to be used in concrete should be optimized.

Microbial samples and microbial induced healing can be distinguished from the autogenous healing by the formation and abundance of $CaCO_3$ precipitates rather than hydration products on the inner crack surface in the case of continuous immersion.

6. Acknowledgments

CHAPTER 4

CHAPTER 4

CHAPTER

5

NON-AXENIC SELF-PROTECTED CULTURE AS A SELF-HEALING ADDITIVE FOR MORTAR

NON-AXENIC SELF-PROTECTED CULTURE AS A SELF-HEALING ADDITIVE FOR MORTAR

Abstract

Exploiting microbial induced $CaCO_3$ precipitation using (protected) axenic cultures is one of the proposed methods for development of microbial self-healing concrete. Yet, only a few of the suggested healing agents were economically feasible for in situ application. This study presents a NO_3- reducing self-protected enrichment culture as a self-healing additive for concrete. Concrete admixtures $Ca(NO_3)_2$ and $Ca(HCOO)_2$ were used as nutrients. The enrichment culture, grown as granules (0.5 – 2 mm) consisting of 70 % biomass and 30 % inorganic salts were added into mortar without any additional protection. Upon 28 days curing, mortar specimens were subjected to direct tensile load and multiple cracks (0.1 – 0.6 mm) were achieved. Cracked specimens were immersed in water for 28 days and effective crack closure up to 0.5 mm crack width was achieved through calcite precipitation. Microbial activity during crack healing was monitored through weekly NOx analysis which revealed that 92±2 % of the available NO_3- was consumed. Another set of specimens were cracked after 6 months curing, thus the effect of curing time on healing efficiency was investigated, and mineral formation at the inner crack surfaces was observed, resulting in 70 % less capillary water absorption compared to healed control specimens. In conclusion, enriched mixed denitrifying cultures structured in self-protecting granules are very promising strategies to enhance microbial self-healing.

1. Introduction

Cracking of concrete is inevitable due to its heterogeneous matrix and brittle nature. Early age cracks in concrete mostly occur a few days after casting and facilitate the migration of aggressive substances towards the steel reinforcement. Microbial induced $CaCO_3$ precipitation (MICP) became a popular research topic and an effective strategy for autonomous healing of concrete cracks. As described so far, typical components of a healing agent in microbial self-healing concrete are the bacterial agent, a protective carrier and the necessary nutrients for stimulation of bacterial activity [40,59,60,157]. Recent advances in bacteria-based self-healing concrete brought the technology closer to application. For instance, in 2014, a large scale application of self-healing concrete took place in Ecuador [158], yet the performance is unknown. Axenic cultures having specific traits are the main interest as bacterial agents by now [40,59,60,157]. On the one hand, using an axenic culture is important to evidence the potential of proposed microbial pathways for their use in microbial self-healing concrete. Moreover, the use of axenic cultures eases the control of the process and minimizes unexpected results. On the other hand, using either of the currently proposed axenic strains as bacterial agents results in a considerable increase in the cost of the product [111]. Several options can be considered to decrease the cost of the healing agent (protected bacteria+nutrients) such as using commercially available protective carriers instead of microcapsules, or decreasing the amount of bacterial agent used depending on the expectations of the manufacturer. Differently, replacing axenic cultures by non-axenic cultures that are derived from side-streams can be a feasible alternative. In a recent study, Silva et al. [23] revealed that non-axenic cultures can also be produced to follow a single pathway by applying selective processes and thus the production cost can be decreased 40 times. Furthermore, in terms of the provided self-healing performance up to 400 μm crack width, the non-axenic ureolytic powder appeared to be as effective as *Bacillus sphaericus* which is one of the most popular axenic strains used in self-healing concrete studies [23,60]. Moreover, the culture is reported to be a self-protected culture avoiding use of protective carriers for concrete application [23,150]. Since the concrete industry demands inexpensive solutions for durability issues, use of self-protected non-axenic cultures can pave the way for application of microbial self-healing concrete.

Apart from ureolysis, aerobic respiration and anoxic oxidation of organic carbon through NO_3^- reduction are the other two pathways that are proven to be useful for development of microbial self-healing concrete [40,147]. Wiktor and Jonkers [40] reported

crack closure up to 460 μm in 100 days for mortar specimens containing bacteria loaded light-weight aggregates. It is also known that the NO_3^- reduction pathway leads to $CaCO_3$ precipitation and in our previous work $CaCO_3$ yields up to 18.9 g $CaCO_3$/g NO_3-N were achieved by only using the concrete admixtures $Ca(HCOO)_2$ and $Ca(NO_3)_2$ as nutrients [67]. Moreover, we reported that NO_3^- reducing axenic strains could induce closure of concrete cracks up to 400 μm in 28 days [159]. However, studies investigating these pathways are limited to use of axenic cultures. Therefore, it is necessary to produce and test self-protected non-axenic cultures that are able to follow the NO_3^- reduction pathway for development of microbial self-healing concrete.

Granular bacterial cultures can be an option for use of non-axenic cultures in concrete. One of the main advantages of granulated cultures is the systematic placement of cultures in a compact form [75]. For instance granules can consist of aerobic heterotrophs, denitrifiers, poly-phosphate accumulating bacteria and nitrifiers at the same time [75]. Depending on the cultivation process, selective enrichment of the certain type of species in a granulated culture is possible. Moreover, the compact form and the layered structure of granular biomass is advantageous for protection of the bacteria at the core [116]. Studies revealed that granulated bacteria can be dried, stored and re-activated in case of necessity [160]. Therefore, it is possible to achieve a self-protected nitrate reducing community for concrete application by using the granulation phenomenon.

For such need, special granules called "activated compact denitrifying core" (ACDC) were cultivated in this study. Previous investigations revealed that ACDC can survive mortar incorporation, inhibits steel corrosion and is compatible with concrete [150,161]. Yet, the self-healing performances of mortar specimens containing ACDC granules have not been tested. Therefore, it is necessary to investigate ACDC for development of microbial self-healing concrete. Furthermore, to our knowledge, microbial self-healing concrete studies are mostly limited to curing periods up to 56 days [22,40,60] which is far from the concrete ages in situ. Thus, the self-healing performance of bacteria-based concrete at the long term is still a question. Accordingly the study was conducted in two consecutive steps (1) assessing the self-healing performance of mortar specimens containing ACDC, (2) assessing the self-healing performance of concrete cracks occurring after 6 months curing.

CHAPTER 5

2. Materials and methods

2.1. The self-protected non-axenic culture

Please consult **Chapter 3** "Materials methods – Section 2.4.1" for detailed description of the production procedure. In this study, dried ACDC granules (0.5 – 2 mm) were used as bacterial agent for development of microbial self-healing concrete. Regarding the experiments conducted with CEM I 52.5N, two different cell dry weight (CDW) doses (0.5 % w/w and 1 % w/w cement) were investigated. Only one dose (0.5 w/w cement) was tested during the experiments done on mortars prepared with CEM I 42.5N. The ACDC granules composed of 70 % bacteria and 30 % inorganic salts. Throughout the text doses are given by considering cell dry weight amounts which represents the 70 % of the total amount of ACDC used.

2.2. Preparation of the mortar specimens and formation of the cracks

Different type of mortars were prepared to conduct different experiments. Prismatic specimens with reinforcement were prepared to analyze different crack widths and to determine the effect of ACDC culture doses on self-healing performance and water tightness regain of the mortars. Cylindrical specimens were prepared for water permeability and μCT analysis.

2.2.1. Prismatic series prepared with CEM I 52.5N

Series of mortar specimens (30 × 30 × 360 mm) with an embedded steel reinforcement bar (Ø= 6 mm) were prepared by using CEM I 52.5 N, tap water and standard sand according to the norm EN 196–1 and further cured at 20°C and RH > 95% for 28 days and 6 months prior to cracking. The sand:cement:water ratio was 3:1:0.5. Self-healing additives consisted of nutrients and self-protected bacterial agent. Commercial concrete admixtures calcium formate $(Ca(HCOO)_2 – 2\%$ w/w cement) and calcium nitrate $(Ca(NO_3)_2 – 3\%$ w/w cement) were used as nutrients. Dry ACDC granules (0.5 – 2 mm in size) were used as bacterial agent and added into the mix during the mortar preparation.

Cured specimens (at 20°C and RH > 95%) were subjected to a tensile stress by applying uniaxial tensile load at a speed of 0.01 mm/s on the embedded steel reinforcement bar under stroke control. Multiple cracks were achieved and the load was increased until a desired average crack width was achieved. The average crack width was calculated as described in **Chapter 4**, "Materials methods – Section 2.3 – Eq. (4.1).

The mortar specimens cured for 28 days were tested for 100 to 600 μm crack width range. The mortar specimens cured for 6 months were tested for 100 to 500 μm crack width. Average crack widths of each series are given in Table 5.1. Following the cracking, specimens were immersed in water for 28 days at 20° C in a temperature controlled room.

Table 5.1 Detailed information about the tested prismatic specimen series

Series	Bacteria dose (% w/w cement)	Crack width range (μm)	Average crack width (μm ± sem)	Age (curing time)
Reference	N/A	65 – 490	250 ± 9	28 days
	N/A	100 – 500	280 ± 5	6 months
Abiotic Control (R+N)	N/A	65 – 530	270 ± 10	28 days
	N/A	120 – 500	260 ± 5	6 months
Microbial Specimen (R+N+ACDC)[1]	0.5	100 – 640	400 ± 10	28 days
	1	90 – 640	350 ± 10	28 days
	0.5	130 – 550	320 ± 7	6 months
	1	120 – 500	310 ± 5	6 months

[1]R: Reference mortar (sand:cement:water (g)- 1350:450:225); sem: standard error of the mean; ACDC: Activated Compact Denitrifying Core; N:Nutrients 2 % $Ca(HCOO)_2$ + 3% $Ca(NO_3)_2$; N/A: Not applicable

2.2.2. Cylindrical series prepared with CEM I 42.5N

Cylinders (60 mm long and with a diameter of 33.5 mm) were cast by using CEM I 42.5N, tap water and sand according to EN 1015-11. The molds were designed to have two diametrically opposite notches (2 mm wide and 3 mm deep) on the specimens all the way running down their side. Specimens were cured for 28 days, in tightly sealed plastic bags at room temperature. At the end of the curing period specimens were wrapped with polyethylene film and split under compressive load. Steel rods were used to support the notches during loading. Compressive loading was applied on the steel rods at 0.01 m.s^{-1} until the specimens diametrically split along the notches (Figure 5.1).

CHAPTER 5
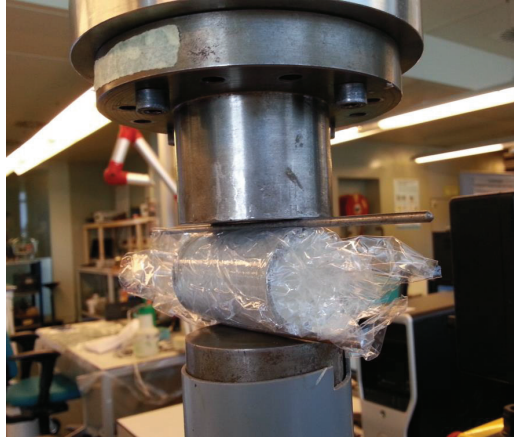
Figure 5.1 Splitting of the cylindrical specimens under compressive loading

The fine particles created on the inner surface of the specimens during the cracking were gently swept out by completely splitting and blowing the inner surface of the specimens. Metal spacers of 2.4 mm wide were placed between the notches and the split halves were glued to achieve defined cracks of 400 μm wide. A mixture of Plex 7742 and liquid Pleximon 801 (Evonik Röhm GmbH, Darmstadt, Germany) was used to glue the halves of the specimens along the notches. In total two reference series, one abiotic control series and one ACDC series were prepared. Each series had 10 specimens and they were used for crack closure monitoring, μCT analysis and water permeability tests (Table 5.2).

Table 5.2 The number of specimens and their respective average crack widths regarding to each test set-up

Series	Tests			
	Permeability[2]		μCT	
	Number of tested specimens	Initial average crack width[1] (μm)	Number of tested specimens	Initial average crack width[1] (μm)
Reference 1	10	404 ± 41	3	400 ± 11
Reference 2	10	408 ± 31	N/A[3]	N/A
Abiotic control	10	409 ± 28	3	397 ± 5
ACDC	10	399 ± 27	3	398 ± 4

[1]Average crack widths were calculated based on the measurements via optical microscope before healing
[2]Permeability of "Reference 2" was only tested before and the others were tested only after the healing period
[3]N/A: Not applicable

One of the reference series (R1) was used to determine the autogenous healing potential and exposed to identical conditions as the abiotic control and ACDC series. The second reference series (R2) was used only during water permeability analysis to quantify the water flow through the 400 µm crack before healing. The type of the series, the amount of specimens used in different tests and the average crack widths are given in Table 5.2.

After cracking and the initial µCT analysis, reference 1, abiotic control and ACDC series were immersed in fresh tap water for 28 days. During the immersion, the water depth inside the buckets was ~100 mm.

2.3. Quantification of self-healing properties

2.3.1. Crack closure

Crack closure was observed biweekly through stereomicroscope with apochromatic optics (Leica S8 Apo). Obtained images were further analyzed for the decrease in crack width by using image analysis software (The Leica Application Suite, LAS 2.8). During microscopic analysis, specimens were exposed to ambient air conditions (~20 $^{\circ}$C). Crack closure efficiency was calculated by using Eq.(5.1).

$$\text{Crack closure \%} = [1- (w_t / w_{initial})] \times 100 \qquad \text{(Equation 5.1)}$$

where

w_t = crack width measured at a certain time t(d)

$w_{initial}$ = initial crack width

2.3.2. Water tightness regain

In order to quantify the water tightness of the healed specimens capillary sorption tests were conducted. Prior to testing, the specimens were dried in an oven at 40 $^{\circ}$C until the mass changes in 24 hours were less than 0.1%. Similar crack widths were chosen for each specimen. Apart from the chosen crack the rest of the specimen was completely covered with aluminum tape to prevent water ingress and evaporation. Therefore, only the area of 3 cm^2 (30 mm × 10 mm) surrounding the chosen crack contacted with water. The mass increase of specimens due to the absorbed water was monitored in regular time intervals. A wet towel was used to remove the remaining surface water droplets prior to weighing. Water tightness regain was calculated by considering the water tightness of the uncracked specimen as a goal

CHAPTER 5

of 100% regain and the water tightness of the autogenously healed specimen as a reference. The calculations were done by following Eq. (5.2).

$$\text{Water tightness regain (\%)} = \left(1 - \frac{m_{healed} - m_{uncracked}}{m_{autogenously\ healed} - m_{uncracked}}\right) \times 100 \qquad \text{(Equation 5.2)}$$

where;

$m_{autogenously\ healed}$ = water absorbed after autogenous healing

m_{healed} = water absorbed after any type of healing

$m_{uncracked}$ = water absorbed by uncracked specimen

2.3.3. Water permeability

The rapid water permeability test described by Palin et al. [162] was used for quantification. In total five permeability columns were set up to run in parallel Figure 5.2a. The water level in each column was 1 to 1.05 m resulting in 0.1 bar water head (Figure 5.2b). The water head was kept as steady as possible throughout the experiment. From each series, eight cracked specimens were tested. Fresh tap water was poured into containers connected to the upper side of each column. The cracked specimens were placed at the bottom end of the column by using holders and gaskets (Figure 5.2). Container outlets were controlled with screwed caps and water was released at the same time for each column initiating the water permeability test. A digital stopwatch was used to track the time elapsed during the permeability test. Separate catchment buckets were used to collect the water flowing through each crack. The weight of the collected water was recorded at the end of 5 min, 10 min and 30 min. The procedure was repeated until all the specimens from each series were tested.

The water flowing through the crack washes out compounds for healing (fine particles, healing agent, OH⁻ ions, etc.) and influences the pH. Therefore, an initial permeability test was not conducted for the specimens prior to healing. Instead, a batch of 10 cracked reference specimens (400 µm crack width), named R2, were prepared and they were used to check the initial flow prior to healing. Other batches (reference, abiotic control and ACDC) were tested only after healing. The permeability of healed batches were compared among each other and with the initial permeability achieved from the R2 batch.
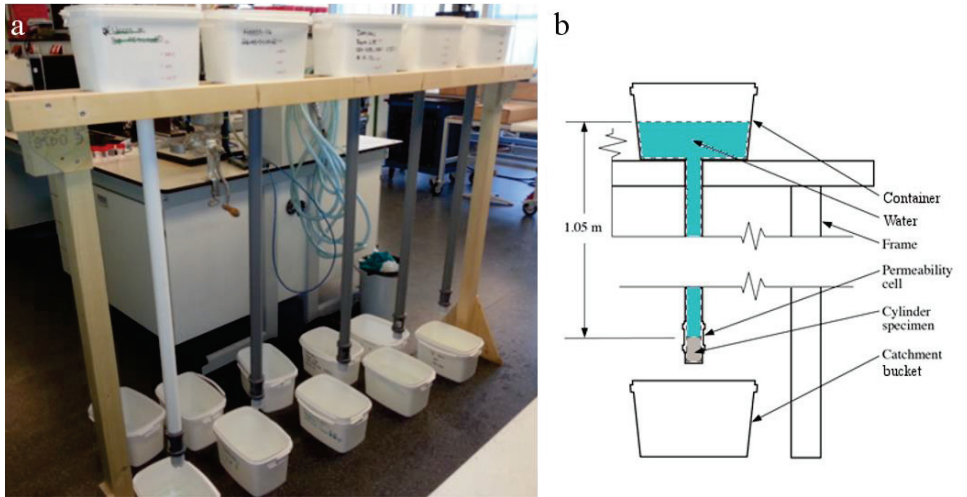
Figure 5.2 Illustration of water permeability test, (a) the five column set-up used during experiments; (b) the schematic representation of the set-up (redrafted after [162]*)*

2.4. X-ray computed tomography (3D analysis of the crack sealing)

X-ray computed tomography (CT) was used to monitor crack healing along the crack depth. From each series three specimens were selected for crack analysis through CT (phoenix|X-ray, GE, Wunstorf, Germany). Selected specimens were scanned after cracking and following the 28 days of healing period. During the X-ray tomography to keep the resolution as high as possible only 37 mm of a 60 mm specimen could be visualized and the voxel size of 16.6 µm was achieved. In order to easily differentiate the microbial induced $CaCO_3$ from autogenously formed $CaCO_3$, the bottom halves of the specimens were investigated. The scan rate was an image per 0.25^{o} axial rotation, resulting in 1440 tomographic images over a complete 360° rotation. The interference of the beam hardening was minimized by using a 200 µm thick copper filter. Taken raw images were further reconstructed by using VG Studio Max 2.0 (Volume Graphics GmbH, Heidelberg, Germany) to visualize the effective through crack width, the sealing materials and their spatial distribution.

2.5. Mechanical and chemical characteristics of the healing material

A representative mortar slice was carefully sawn from each mortar bar by leaving ~5 mm distance from the crack borders and prepared for further testing. The samples (~10 mm x

25 mm x 25 mm) were embedded in Wood's alloy at their side surfaces and in epoxy resin at their top surface. The epoxy could not penetrate into the pores of the mortar specimen, only into the crack, and thus did not interfere with the mechanical properties of the calcite and C-S-H whilst indentation measurements. Surface quality is of importance for accurate determination of elastic moduli and hardness by indentation. Therefore, the specimens were gently ground using diamond grinding discs (grade 80, 220, 600 and 1200) and polished using diamond suspensions (6, 3 and 1 µm) in order to obtain a smooth surface. Finally, a carbon coating was applied and the specimens were vacuum-dried before investigation.

A Hitachi S-4300SE/N SEM, equipped with a special stage to combine the indentation technique with SEM/EDX, was used during the investigation of mechanical properties. Such a combined system was beneficial to have certainty about the test location and the mineral phase for which the mechanical properties were measured and calculated. Moreover, the chemical composition of the products formed in the crack could be verified by energy dispersive X-ray analyses (EDX). During the indentation tests, the samples were visualized in the SEM with an accelerating voltage of 10 kV and a working distance of 35 mm. Furthermore, images with higher resolution were obtained at an acceleration voltage of 15 kV and a working distance of 8-10 mm. The micrographs shown for the 28 days old specimens were obtained with the latter settings.

The indentation tests were performed using the micro-hardness tester of the company Kammrath & Weiss. The load and displacement of the diamond Berkovich indenter were monitored with an accuracy of 0.5 mN and 1 nm, respectively. The displacement of the indenter was determined by means of a laser, which reflects on the Wood's alloy and allows to measure very accurately the penetration of the indenter in the matrix. Moreover, the displacement values were corrected to take into account the compliance of the test frame. Tests on cement-based materials showed that the value for the compliance C_f of the used test frame is 0.000561 µm/mN. The load cycle used for the indentation tests is given in Figure 5.3. The load was increased to 25 mN at a speed of 0.8 mN/s and held constant for 15 seconds to avoid plastic effects. Thereafter, the load was decreased at the same speed (Figure 5.3). Based on the curve presenting the load in function of the penetration depth of the indenter (Figure 5.4), the hardness could be determined without visualization of the indentation.
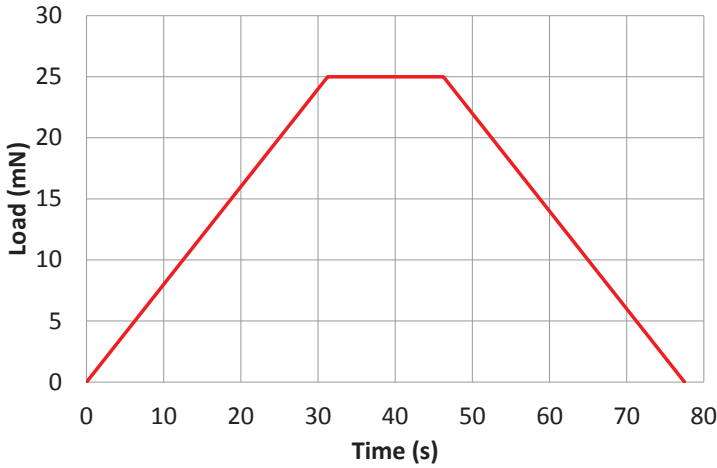
Figure 5.3 Load cycle for the indentation test
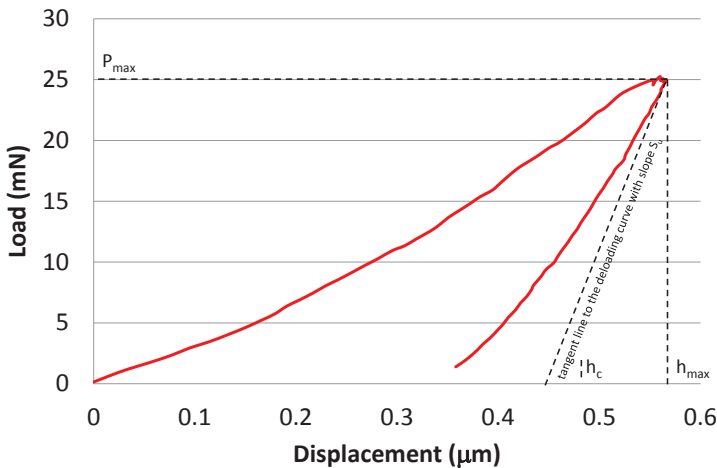
Figure 5.4 Typical load-displacement curve, measured during the indentation test
(example for indentation on calcite)

As the maximum penetration was always more than 400 nm, the measurements were situated at the micro-hardness level [163] and the Martens hardness H_M [GPa] had to be calculated as the ratio of the maximum load P_{max} [mN] to the contact surface area A_c [µm²] (Eq. (5.3)). For a Berkovich indenter, A_c can be calculated in function of h_c (Eq.(5.4)). Eq.(5.4) is based on the fact that the behavior of the Berkovich indenter can be modelled by a conical indenter with a half-included angle of 70.3°, giving the same depth-to-area

relationship [164]. h_c [µm] is the contact depth as used in the calculation of the hardness by Oliver and Pharr [165] and is calculated based on the maximum penetration depth h_{max} [µm] (Figure 5.4).

$$H_M = \frac{P_{max}}{A_C} \qquad \text{(Equation 5.3)}$$

$$A_C = 26.43 \cdot h_c^2 \qquad \text{(Equation 5.4)}$$

$$h_c = h_{max} - \varepsilon \cdot \frac{P_{max}}{S_u} \text{ with } S_u = \left(\frac{dP}{dh}\right)_{h=h_{max}} \qquad \text{(Equation 5.5)}$$

where

P_{max} = the maximum load (mN)

S_u = the slope at the deloading curve in $h = h_{max}$ (mN/µm)

ε = the geometrical constant equals to 0.75 according to Oliver and Pharr [164]

An approximate estimation of the E-modulus could be made based on the results obtained in this study. Therefore, the reduced modulus of elasticity (E_R) [GPa] was first calculated with Eq.(5.6), taking into account Eq.(5.7).

$$\frac{1}{S_u} = \left(\frac{dh}{dP}\right)_{h=hmax} = C_f + \frac{\sqrt{\pi}}{2} \cdot \frac{1}{\beta \cdot \lambda \cdot E_R} \cdot \frac{1}{\sqrt{A_{CP}}} \qquad \text{(Equation 5.6)}$$

$$A_{CP} = 24.5 \cdot h_c^2 \qquad \text{(Equation 5.7)}$$

where

C_f = compliance value for the used test frame which equals to 0.000561 µm/mN

E_R = modulus of elasticity

β and λ = correction factors which equal to 1.05 [164] and 1.1 [166], respectively

A_{cP} = the projected contact area (µm²) as described in Oliver and Pharr [165]

h_c = the depth (µm) as described in Oliver and Pharr [165]

The E-modulus of the tested material (E_m) is then calculated with Eq. (5.8).

$$\frac{1}{E_r} = \frac{1-v_m^2}{E_m} + \frac{1-v_i^2}{E_i} \qquad \text{(Equation 5.8)}$$

where

v_m = estimated value for the Poisson coefficient of the tested cement based material which equals to 0.3

v_i = the Poisson coefficient of the diamond indenter which equals to 0.07

E_i = the E-modulus of the diamond indenter which equals to 1140 GPa

The mechanical characteristics of the original cement paste and the $CaCO_3$ precipitated in the crack were determined by indentation tests. 10 – 15 indentations were performed per test sample and per phase.

The inner crack surface of the mature specimens (6 months cured) was also analyzed, yet indentation tests were not conducted for these samples. During the visual inspection and EDX analysis of mature specimens FEI Quanta 200F SEM/EDX was used. In order to analyze and identify the healing materials inside the crack, a sawn sample with the crack (10 × 30 × 30 mm) was further split through the crack into two pieces by using manual force. One of the surfaces was coated with carbon (~15 – 35 nm thickness) and analyzed under SEM/EDX. The micrographs showing the inner crack surface of the mature specimens were taken at accelerating voltage of 15 kV and a working distance of 8-9 mm. The second piece was used for Fourier transform infrared spectroscopy (FTIR) analysis. The composition at a certain depth was the main interest, thus on the crack surface, an area of 1 cm^2 (5 mm × 20 mm) was defined at a distance of 5 mm from the crack mouth and 2 mm from the reinforcement bar. The defined area was scraped by using a stainless steel spatula (5 mm width) and the pieces were collected (< 15 mg). Collected pieces were further ground into powder by using a mortar and pestle. A portion of the ground powder (<5 mg) was chemically characterized by using FTIR (Spectrum 100, Perkim Elmer Inc, USA). Presented spectra were the result of 32 scans with a resolution of 4 cm^{-1} in the range of 4000 – 600 cm^{-1}.

2.6. Analytical methods

The VSS and TSS analysis were done according to the standard methods [118]. Nitrate (NO_3^-) and nitrite (NO_2^-) concentrations were measured via compact ion chromatography (IC) (Metrohm, 761).

Differences between the healing of cracks in different series were compared using a repeated measures mixed model in SAS (version 9.4, SAS Institute, Cary, USA), accounting crack width and incubation time as fixed effects, and with the least square means (LS-means, $p<0.05$) adjustment and Bonferroni correction for multiple comparisons. Similar approach was used to determine the effect of cracking age on crack closure efficiency by accounting the series type and crack width as fixed effects. Statistical analysis on capillary water absorption and water permeability data were conducted using SigmaPlot 12.0 (Systat Software Inc USA) to compare significant differences by means of one way ANOVA test ($p=0.05$).

CHAPTER 5

3. Results

3.1. Self-healing performance of microbial mortars containing ACDC culture

The addition of ACDC and nutrients (concrete admixtures $Ca(HCOO)_2$ and $Ca(NO_3)_2$) significantly improved the self-healing potential of mortar specimens (Figure 5.5a and Figure 5.6). At the end of 28 days immersion in water, self-healing performances of the mortars containing 0.5 % ACDC were similar to the ones containing 1% ACDC. Cracks up to 500 μm crack width were closed more than 90% (Figure 5.5a). The limit for the autogenous healing was recorded as 200 μm and 250 μm for reference specimen and abiotic control specimen, respectively (Figure 5.5a). Crack closure performances of the reference specimens sharply decreased when the initial crack widths were more than 200 μm. Among the control specimens, the ones containing nutrients (abiotic control) showed significantly better healing performance and could close cracks up to 250 μm (Figure 5.5a).
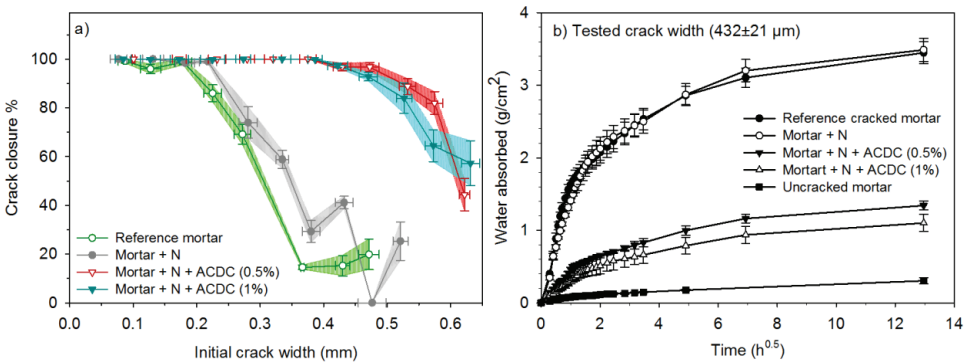
Figure 5.5 The enhanced self-healing performance of the 28 days old microbial specimens over the control specimens, (a) the crack closure performance (horizontal error bars represent the standard deviation, crack widths were grouped with 50 μm intervals, vertical error bars represent the standard error of the mean, n ≥5) (b) capillary sorption around the crack zone of the healed specimens (N: Nutrients – 2 % $Ca(HCOO)_2$ + 3 % $Ca(NO_3)_2$; the error bars represent the standard deviation, n=3).

Capillary sorption tests revealed that microbial specimens could have a better water tightness than the control specimens (Figure 5.5b). The capillary sorption tests were conducted around the cracks with 432±21 μm crack width for the specimens cracked at 28 days and healed for 28 days. Reference and abiotic control specimens were found to be

similar in terms of water tightness. After the 28 days healing period, the microbial specimens containing 1% and 0.5 % ACDC (w/w cement) absorbed 68±5 % and 61±4 % less water around the crack (~432±21 µm initial crack width) than the reference specimens, respectively (Figure 5.5b). Different from the crack closure performances, in terms of water tightness, there was a slight but significant difference between the microbial specimens containing two different amounts of ACDC. Mortar specimens containing 1 % ACDC absorbed 18±8 % less water than the mortar specimens containing 0.5 % ACDC (Figure 5.5b).
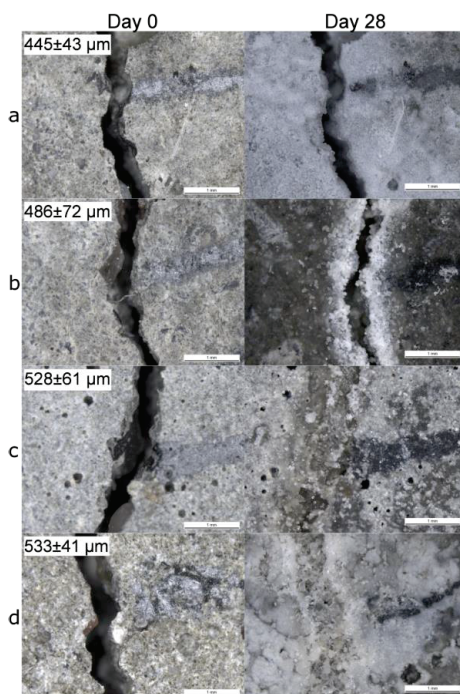
Figure 5.6 The micrographs showing the initial (before incubation) and the final (after 28 days incubation) appearance of the cracks of the 28 days old specimens (a) reference specimen (b) abiotic control (reference + 5 % nutrients) (c) specimen with 0.5 % ACDC and 5% nutrients (d) specimen with 1 % ACDC and 5 % nutrients (N: Nutrients – 2 % Ca(HCOO)$_2$ + 3 % Ca(NO$_3$)$_2$; amounts are in terms of w/w cement; scale bar is 1 mm)

3.2. Water permeability results

The water permeability test was conducted to quantify the decrease in water flow rate through a crack after autogenous and autonomous healing. For the purpose, initial flow rate was measured on the created crack width (~400 µm) prior to healing. The effect of healing

regardless of being autogenous or autonomous, was compared according to the initial flow rate and further compared among each other. The average flow rates measured after 5, 10 and 30 minutes were not significantly different between each other. The average flow rate obtained through a crack of 408 ± 31 μm in 30 minutes was 253 ± 40 cm^3/min (Figure 5.7). After autogenous healing of 404 ± 41 μm cracks for 28 days, the average flow rate (at the end of 30 minutes permeability test) through the crack was significantly different than that obtained for the unhealed crack and recorded as 196 ± 28 cm^3/min (Figure 5.7). There was no significant difference between the flow rates obtained from cracks of autogenously healed reference specimens and the abiotic control specimens. The average flow rate through the 409 ± 28 μm cracks at the end of 30 minutes was 190 ± 33 cm^3/min (Figure 5.7). Substantial decrease in water permeability was achieved following 28 days of microbial induced healing. The average flow rate through the autonomously healed 399 ± 27 μm cracks was recorded as 37 ± 19 cm^3/min at the end of 30 minutes permeability test (Figure 5.7).
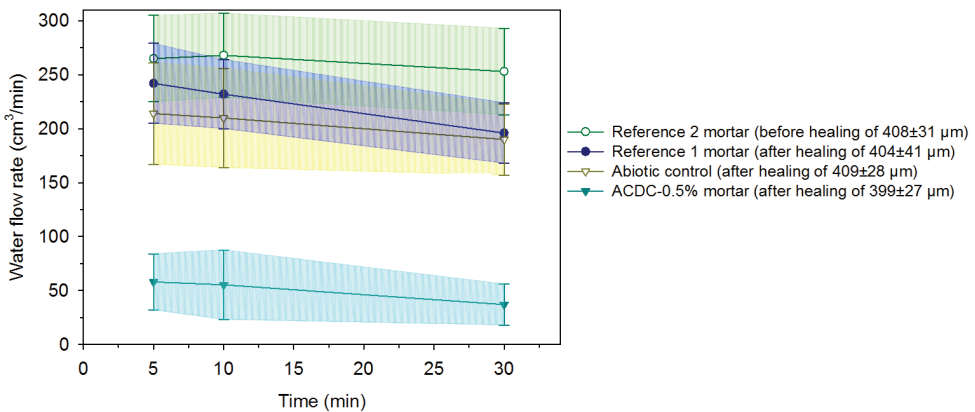
Figure 5.7 Evolution of the water flow rates during the 30 minutes water permeability test and the differences between water flow rates through the unhealed cracks, autogenously healed cracks and autonomously healed cracks

The findings indicated that autogenous healing of ~400 μm cracks leads to a ~25 % decrease in water permeability when compared to the unhealed cracks. By incorporating ACDC in mortar specimens, around 80% decrease in water permeability could be achieved upon 28 days healing period. Compared to plain mortar specimens, microbial specimens perform considerably better to protect the steel reinforcement when a crack of around 400 μm occurs.

3.3. Nutrient availability and the microbial activity during incubation

One of the components of microbial self-healing concrete is the nutrients that initiate and maintain the bacterial activity. Therefore, availability of the nutrients for the bacteria is important. The results of the abiotic control are representative for the NOx-N passed from mortar to the solution, thus indicates the nutrient availability (Figure 5.8a). Based on the results, it is possible to calculate the percentage of the available nutrients compared to the added amount of nutrients as follows;

- Approximate volume of a batch of a mortar mixture = 1000 cm^3
- Amount of $Ca(NO_3)_2$ in a batch of mortar = 3 % w/w cement = 13.5 g
- Amount of NO_3-N in a batch of mortar = 2.3 g
- Dimensions of a specimen 3 cm × 3 cm × 36 cm – reinforcement bar Ø= 6 mm

Therefore; the approximate volume of mortar in one specimen could be calculated by using Eq. (5.9).

$$V = (h \times W \times L) - (\Pi \times r^2 \times h) \qquad \text{(Equation 5.9)}$$

$$V = (3 \times 3 \times 36)\ cm^3 - (\Pi \times 0.3^2 \times 36)\ cm^3 = 314\ cm^3$$

where;

V= volume of the mortar

W, L and h = width, length and the height respectively

- Assumption 1: Homogenous distribution

Amount of NO_3-N in one specimen = 2.3 g × 314 cm^3/1000 cm^3 = 0.722 g NO_3-N

Percentage passed from mortar to the solution = (0.103 g/0.722 g) × 100 = 14 %

The calculations revealed that around 14 % of the NO_3-N in a mortar specimen became available for microbial use. Weekly measurements of the NOx-N revealed that 92±2 % of the available NO_3-N was consumed by the ACDC culture during the crack closure process which confirms the bacterial activity (Figure 5.8a). The observed activity (NO_3^- reduction rate) significantly improved after pH decreased below 10 (Figure 5.8a,b).

CHAPTER 5
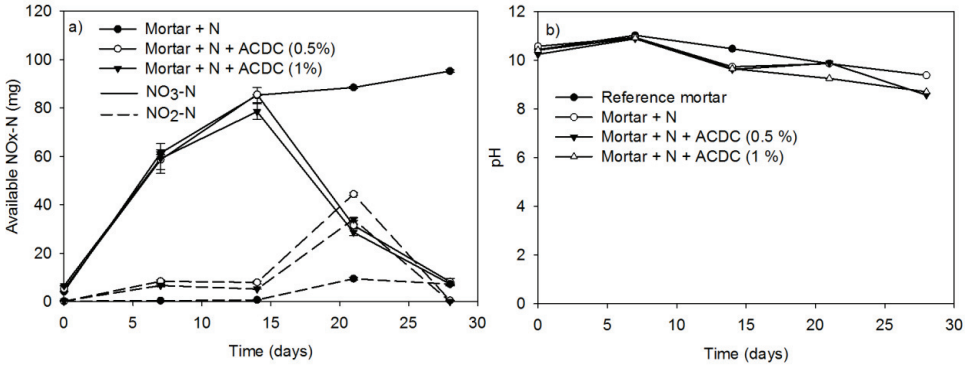
Figure 5.8 Evolution of the available NOx-N in the bulk solutions during the 28 days incubation of the 28 days old specimens and the pH of the solution (a) mass of the available NOx-N (b) the pH change (N: Nutrients – 2 % Ca(HCOO)$_2$ + 3 % Ca(NO$_3$)$_2$; n=3, error bars represent the standard deviation)

3.4. X-ray computed tomography results

The images obtained via X-ray tomography enabled determination of the effective sealing depth. Since only half of the specimens were investigated, complete spatial distribution of the healing materials could not be achieved. However, the image analysis at the bottom half of the specimens was enough to differentiate between autogenously healed specimens and microbial healed specimens. The images before healing showed that a crack with a consistent crack width and without any impurities could be achieved for all tested series. After the healing period, regardless of the cross section direction, no visible precipitation was detected in the 2D images of the reference and the abiotic control specimens (Figure 5.9and Figure 5.10). Contrarily, following the 28 days healing period considerable amount of precipitation could be visualized in the images of microbial specimen in the Y direction (Figure 5.11). The precipitation depth was recorded as 5 to 8 mm from the surface. 2D images obtained in Z direction at the same depth revealed that the precipitation was formed along the crack (Figure 5.11).

Initial crack - Y direction

After healing - Y direction

Initial crack - Z direction

After healing - Z direction
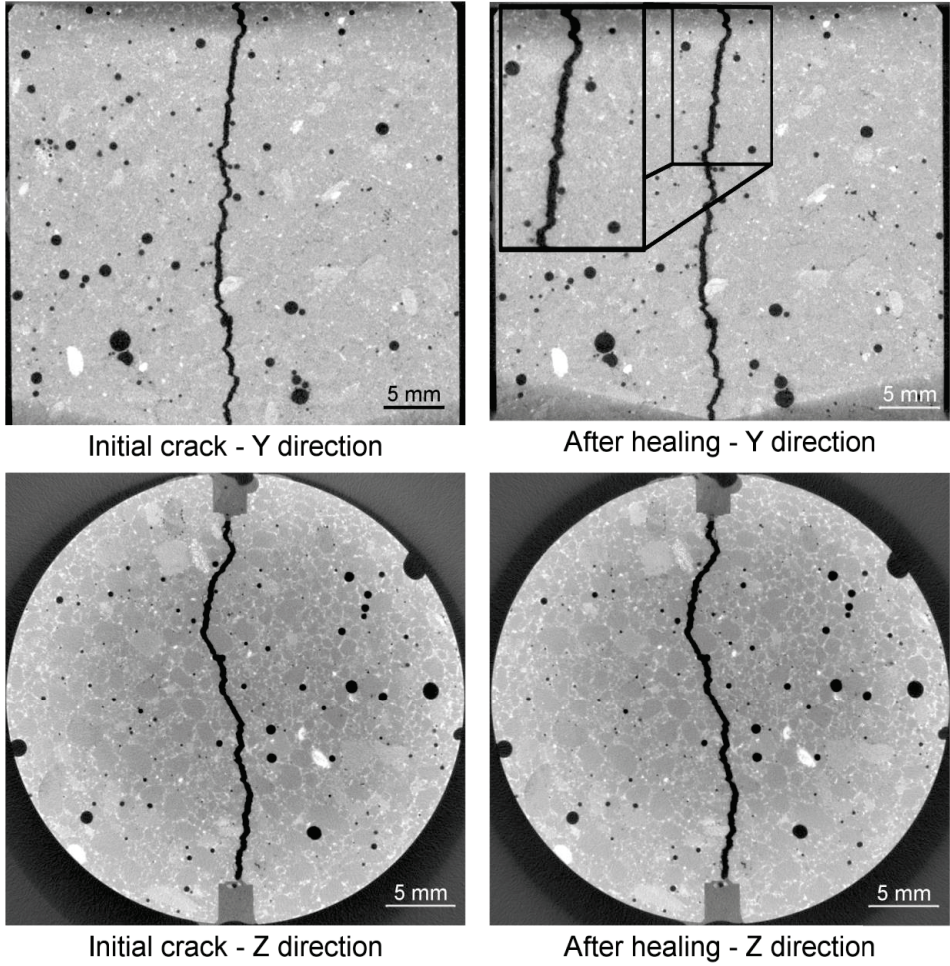
Figure 5.9 Cross sectional views of the same location in a reference specimen before and after the 28 days healing period
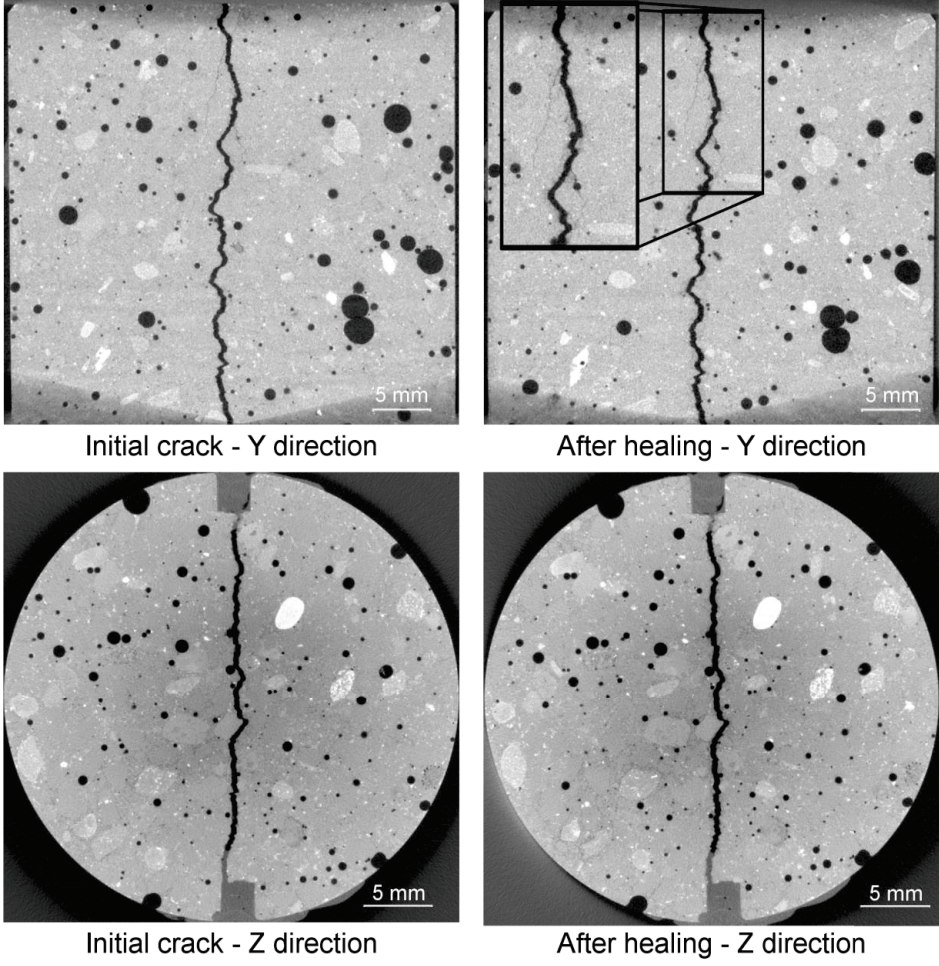
Figure 5.10 Cross sectional views of the same location in an abiotic control specimen
before and after the 28 days healing period

Initial crack - Y direction   After healing - Y direction

Initial crack - Z direction   After healing - Z direction
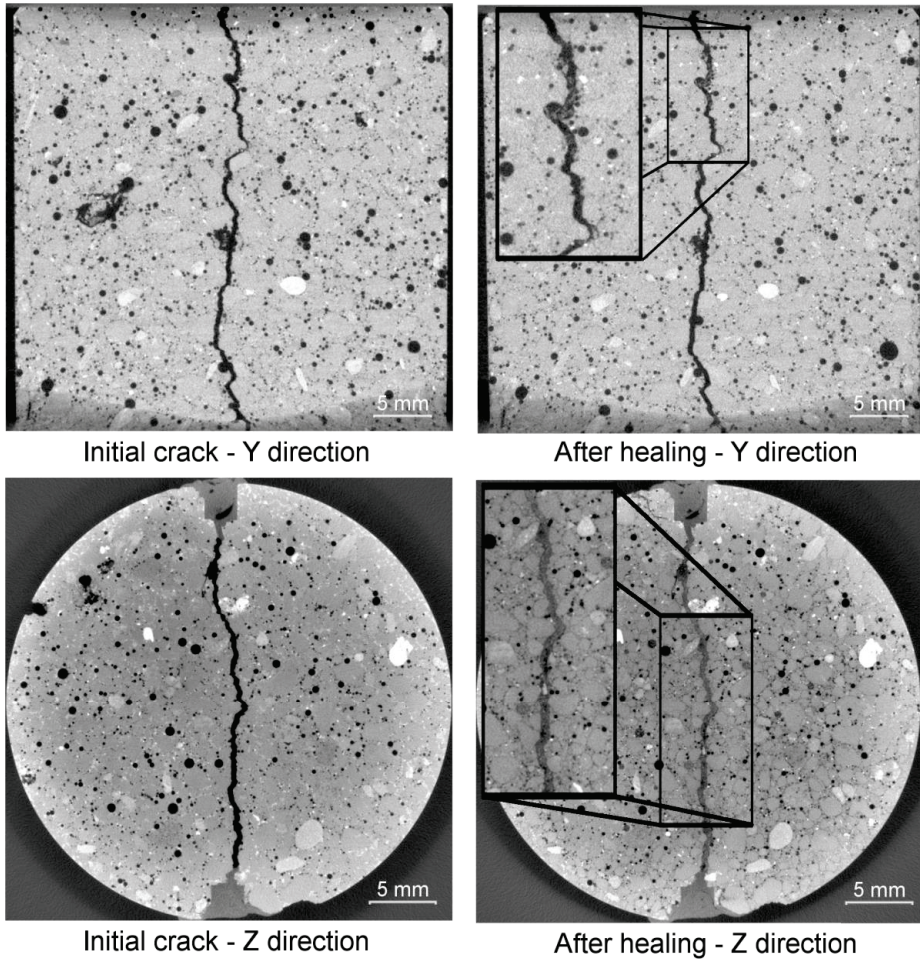
Figure 5.11 Cross sectional views of the same location in an ACDC specimen before and after the 28 days of healing period

3.5. Mechanical properties of the healing material inside the crack

The abundant formation on the inner crack surface of the microbial specimen was a white colored precipitate (Figure 5.12a). Visual inspection revealed that observed white precipitates were biochemically formed $CaCO_3$ (in the form of calcite) (Figure 5.12c,d). Moreover, a portion of the ACDC granule (~ 40 µm wide) and the $CaCO_3$ formation around the cluster could be visualized during the SEM analysis (Figure 5.12d). Additionally, individual bacterial remains were also found on precipitates (Figure 5.12c).
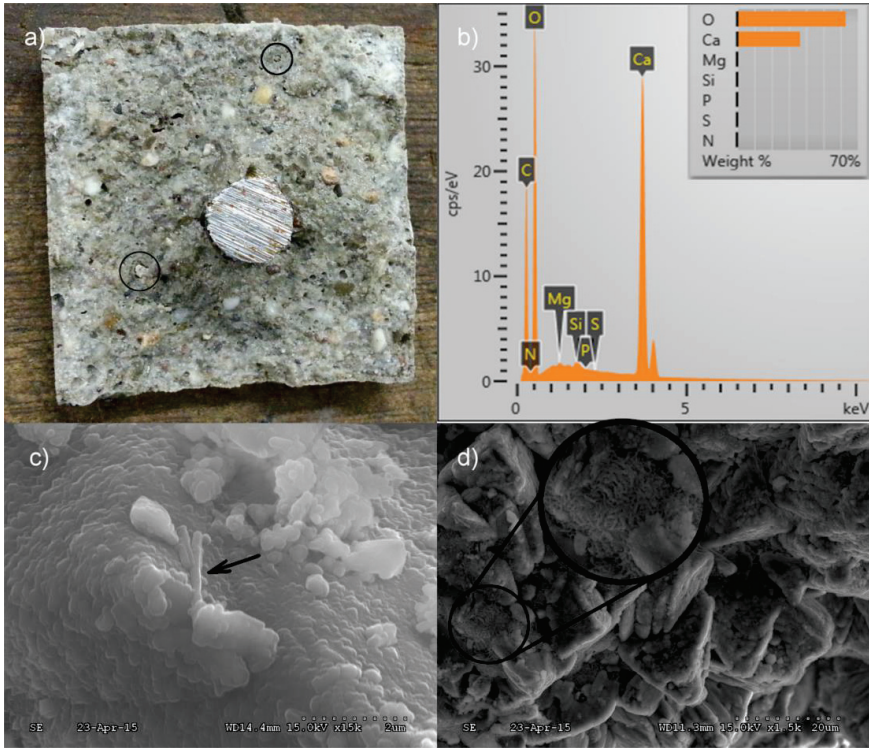
Figure 5.12 Micrographs showing the inner crack surface of the 28 days old microbial specimen and the EDX results (a) inner crack surface appearance of microbial specimen after splitting; (b) chemical composition of the minerals around the bacteria; (c,d) SEM micrographs of the inner crack surface ('↗' indicates the individual bacterial remains, '○' indicates the calcified ACDC cluster)

In addition to visual analysis, mechanical properties of the calcite crystals were quantified through indentation tests (Figure 5.13). Martens hardness was measured and based on the available data approximate E-modulus values were calculated. The Martens hardness values of 2.1 ± 0.2 GPa and 2.1 ± 0.7 GPa were achieved from the tested $CaCO_3$ minerals in reference and microbial specimens, respectively (Figure 5.14a).
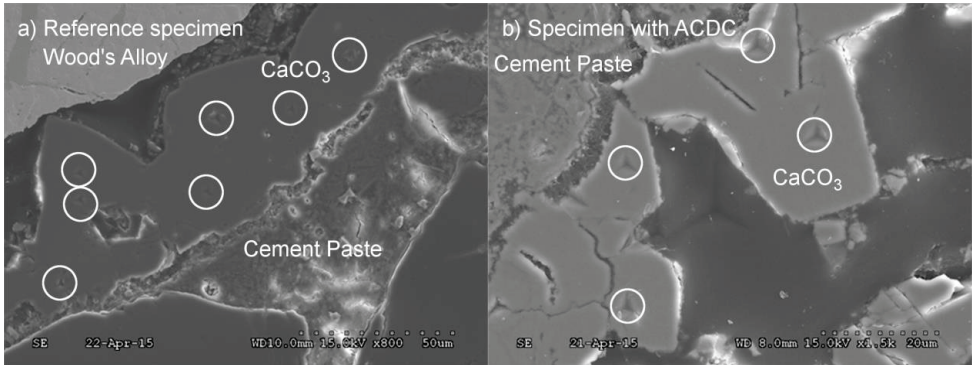
Figure 5.13 SEM micrographs showing the indentation points whilst mechanical testing of the calcite (a) calcite formed in reference specimen (b) calcite formed in microbial specimen (0.5 % ACDC)
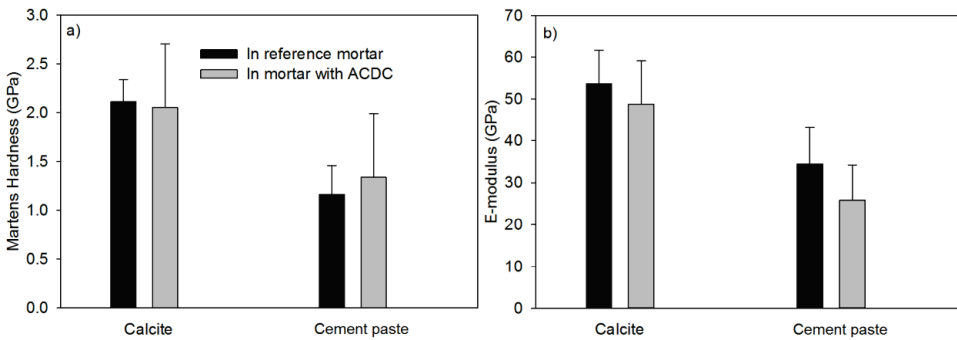
Figure 5.14 Mechanical properties of the calcite and the cement paste found in autogenously and microbial healed specimens (a) Martens hardness values; (b) calculated modulus of elasticity (n ≥10, error bars represent the standard deviation)

The variation of hardness values for $CaCO_3$ minerals were higher in microbial specimens than the reference specimens, yet they did not significantly differ among the specimens (Figure 5.14a). Further visual inspection of the indentation points revealed that on some of the minerals nano-cracks occurred under indentation load (Figure 5.15).

These observed cracks were not particular for a certain type of specimen and observed in both cases. Following indentation tests, sampling points and the different layers were visualized. Indentation measurements were also conducted on hydrated cement paste. Martens hardness values of 1.2±0.3 GPa and 1.3±0.7 were obtained for the hydrated cement paste in reference and microbial samples, respectively (Figure 5.14a).
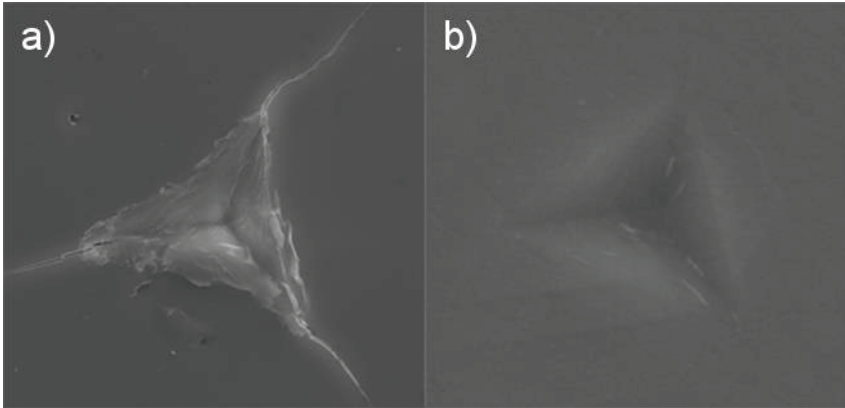
Figure 5.15 Indentation on calcite causing (a) cracks; (b) no cracks

E-modulus values for the tested $CaCO_3$ minerals were calculated as 54±10 GPa and 49±8 GPa from the data obtained whilst testing reference and microbial samples, respectively (Figure 5.14b). The E-modulus values for the hydrated cement paste were 35±9 GPa and 26±8 GPa for reference and microbial specimens (Figure 5.14b).

3.6. Chemical characterization of the healing material

In addition to the SEM imaging, the elemental composition of minerals was analyzed by using energy dispersive X-ray spectroscopy (EDX). Visualized minerals were composed of Ca, C and O elements which indicated that the minerals were most probably $CaCO_3$. In order to confirm the EDX results, powders were collected from the counter face of the crack surface and chemically characterized via FTIR analysis. The information collected from both analyses revealed that the visualized and tested minerals inside the crack of microbial specimens were $CaCO_3$ (Figure 5.12b and Figure 5.16). In addition to calcite (2513, 1793, 1412, 873 and 713 cm^{-1}), aragonite (696 cm^{-1}), ettringite (1163 cm^{-1}), bassanite (1083 cm^{-1}), C_2S (873 cm^{-1}), C-S-H (1052, 1980 and 2163 cm^{-1}) and portlandite (3649 cm^{-1}) were found in the collected powder samples [152–155] (Figure 5.16). In the powders collected from control specimens, cement and its hydration products were as abundant as the forms of $CaCO_3$ (Figure 5.16) Contrarily, in the powder collected from the microbial specimens, different forms of $CaCO_3$ were the dominant compounds (Figure 5.16).
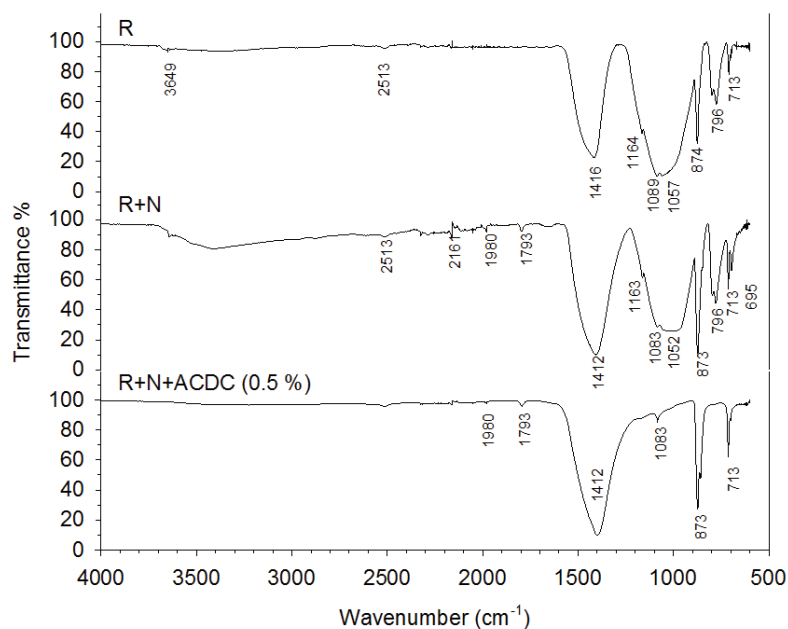
Figure 5.16 FTIR spectra of the healing materials collected from the inner crack surfaces of 28 days old specimens (R: Reference; N: Nutrients – 2% Ca(HCOO)$_2$ + 3 % Ca(NO$_3$)$_2$; 5 mm< sampling depth <13 mm)

3.7. Effect of age on microbial crack healing

Autogenous healing performance of the control specimens significantly decreased when the cracks formed after 6 months curing instead of 28 days curing (Figure 5.17a and Figure 11). Based on the data obtained for the investigated crack width range (100 – 500 µm), autogenous healing performance after 6 months was recorded as 86±8 % for 135 µm crack width and gradually decreased with an increasing initial crack width (Figure 5.17a). Although, a noticeable decrease also appeared in microbial samples, ~90% crack closure was achieved for the cracks up to 400 µm crack width (Figure 5.17a). The closure performance of the cracks larger than 400 µm was still more than 70% (Figure 5.17a and Figure 5.18).
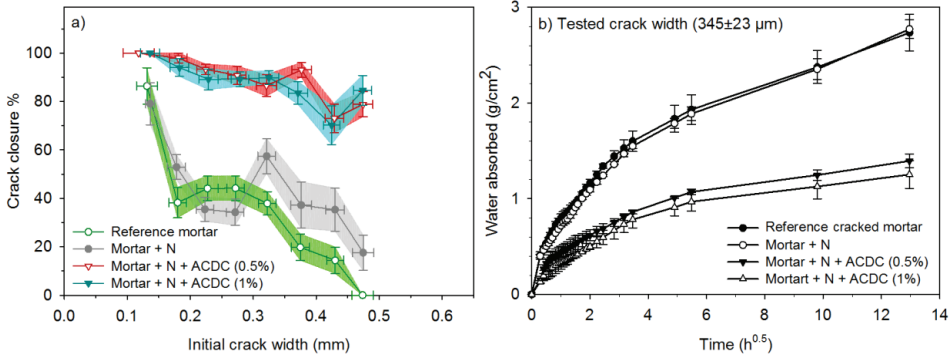
Figure 5.17 The enhanced self-healing performance of the 6 months old microbial specimens over the control specimens (a) the crack closure performance (horizontal error bars represent the standard deviation, crack widths were grouped with 50 μm intervals, vertical error bars represent the standard error of the mean, n ≥5) (b) capillary sorption around the crack zone of the healed specimens (N: Nutrients – 2 % Ca(HCOO)$_2$ + 3 % Ca(NO$_3$)$_2$; the error bars represent the standard deviation, n=3).

Capillary sorption tests revealed that microbial specimens could have a better water tightness than the control specimens (Figure 5.17b). The capillary sorption tests were conducted around the cracks with 345±23 µm crack width for 6 month old specimens. Reference and abiotic control specimens were found to be similar in terms of water tightness (Figure 5.17b). After the 28 days healing period, the microbial specimens containing 1% and 0.5 % ACDC (w/w cement) absorbed 54±8 % and 49±6 less water around the crack (~345±23 µm initial crack width) than the reference specimens, respectively (Figure 5.17b). Among the microbial specimens, no significant differences were observed in terms of water tightness.
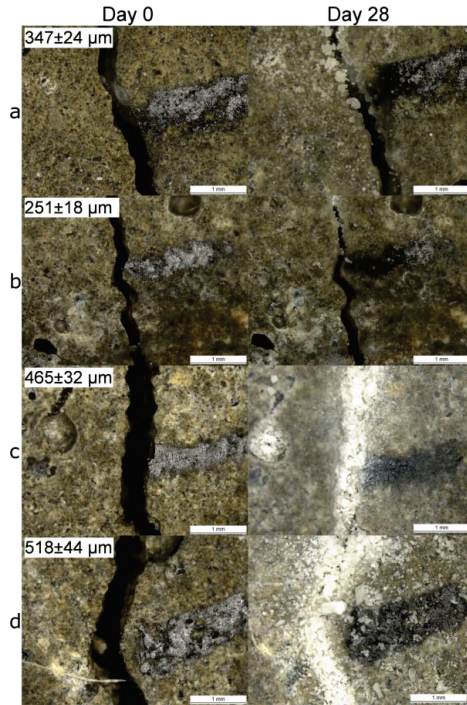
Figure 5.18 The micrographs showing the initial and the final (after 28 days incubation) appearance of the cracks of the 6 months old specimens (a) reference specimen; (b) abiotic control (reference + 5 % nutrients); (c) specimen with 0.5 % ACDC and 5 % nutrients; (d) specimen with 1 % ACDC and 5 % nutrients (Nutrients – 2 % Ca(HCOO)$_2$ + 3 % Ca(NO$_3$)$_2$; weight percentages are in terms of cement weight; scale bar is 1 mm)

The inner crack surface was visually explored in both control and microbial specimens. During the visual inspection of microbial specimens, a significant amount of biochemically formed CaCO$_3$ minerals and calcified bacteria were found (Figure 5.19c,d). In EDX spectrums obtained on the inner crack surface of the control specimens, Si peaks were significant which was indicating the abundance of C-S-H (Figure 5.19a,b). Differently, the C and O peaks were remarkable in microbial specimens indicating the abundance of CaCO$_3$ (Figure 5.19c,d). Moreover, some ettringite shaped formations were found (Figure 5.19b).
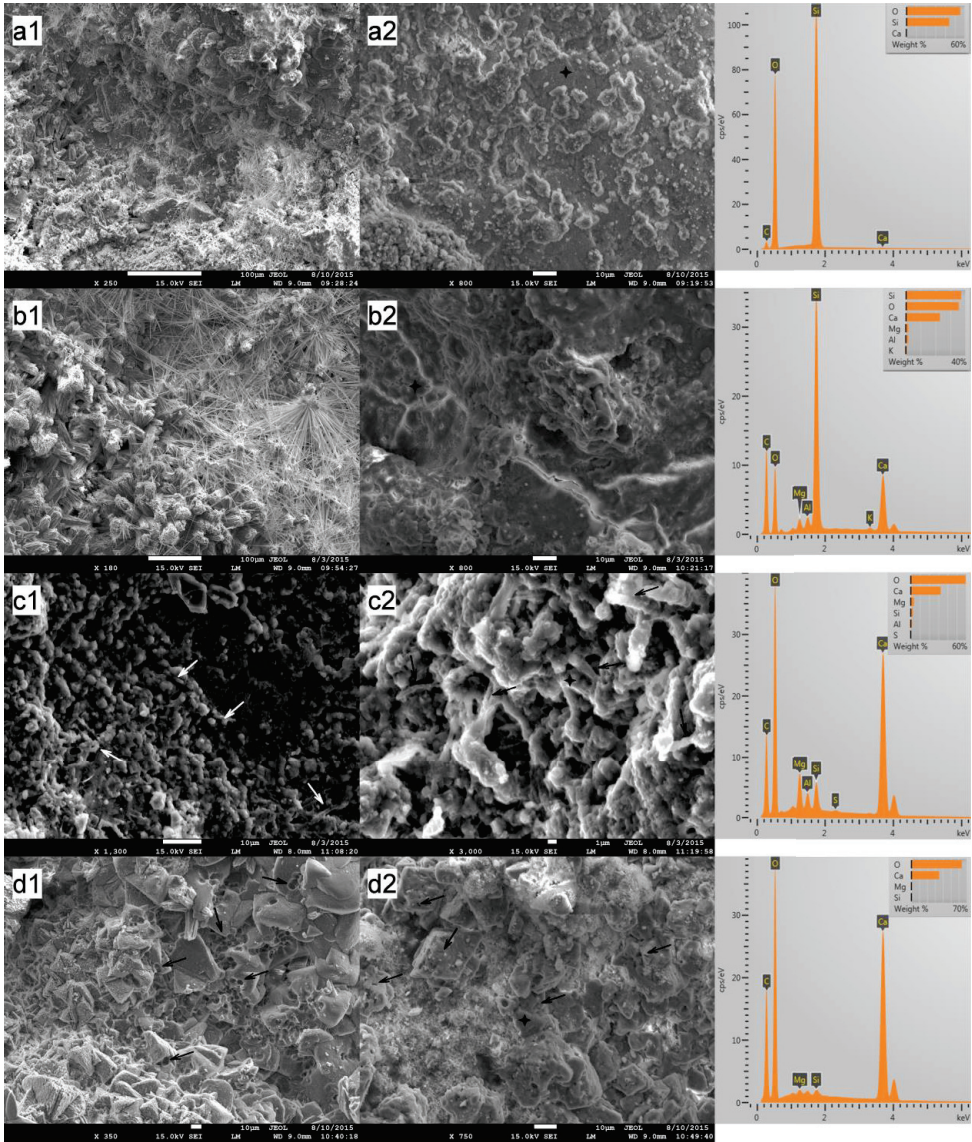
Figure 5.19 Representative SEM micrographs and EDX analysis of the dominant healing material on the inner crack surface of 6 months old specimens after 28 days of healing (a1,a2) reference mortar; (b1,b2) abiotic control (reference + 5 % nutrients); (c1,c2) mortar containing 0.5 % ACDC and 5 % nutrients; (d1,d2) mortar containing 1% ACDC and 5 % nutrient (Nutrients – 2 % Ca(HCOO)$_2$ + 3 % Ca(NO$_3$)$_2$; weight percentages are in terms of cement weight; '↗' indicates the calcified bacterial remains; '+' indicates the points analyzed via EDX)

4. Discussion

4.1. Crack closure and functionality regain

Autogenous healing limits of the 28 days old mortar specimens were recorded as 200 and 250 μm for reference and abiotic control, respectively. Previous studies reported comparable results under similar incubation conditions (immersion in tap water) [21–23]. The better crack closure performance of the abiotic control specimens than the reference specimens could be due to the positive effect of admixtures on $CaCO_3$ precipitation. The pH, the Ca^{2+} concentration, the dissolved inorganic carbon concentration and the presence of nucleation sites are four main parameters stimulating the $CaCO_3$ precipitation. The abiotic control had higher Ca^{2+} concentration due to the addition of $Ca(HCOO)_2$ and $Ca(NO_3)_2$ which might improve the $CaCO_3$ precipitation and thus the crack closure performance of the abiotic control. Similar behavior was reported in previous studies [22,58]. The autogenous healing performance significantly decreased when the cracks formed in mature specimens (6 months old). It was not possible to effectively close the 150 μm crack width through autogenous healing. Yang et al. [30], also suggested that the crack widths on mature specimens should be kept less than 150 μm which is consistent with our observation. These results indicated that the hydration of the unhydrated cement in pre-mature samples has significant influence on autogenous healing potential. Unlike the abiotic control, microbial specimens considerably improved the self-healing potential for both early age and mature cracks. Although it is known that the spores can survive in extreme environments for a long time [167], the self-healing performance of a mature microbial concrete was always a concern. In this study, the crack closure performance of a mature microbial mortar was more than 90 % up to a crack width of 400 μm. The limit was three to four times higher than the autogenous healing limit of a mature mortar specimen. Therefore, it can be said that microbial mortars offer self-healing not only for early age cracks but also for the mature cracks. During the incubation period of 28 days old mortar specimens, available NOx-N concentrations were measured. The consumption of the available NO_3-N confirmed that the enhanced crack closure performance observed in microbial specimens was due to the microbial activity. Bacterial remains on calcite minerals and mineral formation around the ACDC agglomerates also evidence the self-healing through microbial induced $CaCO_3$ precipitation.

Crack closure achieved through MICP after 28 days treatment period were comparable with the previously reported microbial self-healing results [22,23,40,59]. Microbial self-

CHAPTER 5

healing studies where ureolytic spores were used as bacterial healing agent reported closure of cracks up to 350 – 400 µm crack in 28 days [23,60]. By incorporating hydrogel protected ureolytic bacterial spores in mortar, more than 80% crack closure up to 485 µm crack width was achieved in 28 days [59]. Wiktor and Jonkers [40] reported complete crack healing up to 460 µm in 100 days by using expanded clay particles loaded with aerobic-bacterial spores as self-healing additive. The mentioned studies were conducted by using axenic bacterial spores. Incorporation of ACDC appears to give slightly better performance in terms of the healable crack width range and the healing rate. To our knowledge, the only reported trial of non-axenic culture as bacterial agent for microbial self-healing concrete was done with the Cyclic EnRiched Ureolytic Powder (CERUP) [23]. Similar to ACDC, CERUP was reported as a self-protected non-axenic culture [23,150]. By incorporating 1 % CERUP (cell dry weight/weight cement), the self-healing limit of the mortar specimens could be extended to 450 µm crack width [23]. In this study by incorporating 1 % ACDC (cell dry weight/weight cement) crack closure up to 500 µm was achieved in the same healing period which is comparable with the reported performance of microbial mortar containing CERUP.

Visual crack closure should always be coupled with other quantification methods to further assess the self-healing performance of mortar specimens [156]. For example, functionality regain is one of the major interests in self-healing studies [26,58,110,168,169]. So far, strength and water tightness are the common properties being investigated to quantify self-healing efficiency in many studies [26,169–171]. Considering the initial average crack widths in this study (between 200 – 400 µm), it can be said that significant strength regain is unlikely. The major reason is; the amount of $CaCO_3$ produced from the available nutrients was not enough to fill such large cracks and provide strength regain. Since the microbial activity could be followed in this study, one can roughly calculate how much of the crack volume could be completely filled. As results indicated, 14 % (102.7 mg) of the NO_3-N in a mortar specimen (722 mg) became available for microbial consumption and 91 % (93.5 mg) of it was reduced by the bacteria at the end of 28 days. In a previous study, the $CaCO_3$ precipitation yields of non-axenic cultures were reported as 12.7 g $CaCO_3$/g NO_3-N when $Ca(NO_3)_2$ and $NaHCOO$ were used as nutrients [67]. Based on the reported precipitation yield, the NO_3^- reduction occurred leads to precipitation of ~1.2 g $CaCO_3$. Major form of the $CaCO_3$ sealing the cracks was calcite and the density of calcite is 2.7 g/cm^3. Therefore, the amount of $CaCO_3$ produced in this study was enough to fill approximately 440 mm^3 crack volume. The dimensions of the specimen were $30 \times 30 \times 360$ mm. The initial average crack width of the 28 days old microbial specimen (containing 0.5 % ACDC) was 400±10 µm and it

had 4 cracks on the surface. Therefore, one can roughly calculate the total crack volume in the specimen as 1440 ± 36 mm^3. These values reveal that the microbial produced $CaCO_3$ could only fill 30 % of the total crack volume created. The μCT analysis also showed that the cracks (398 ± 4 μm) in the microbial specimens were generally sealed with around a 5 to 8 mm thick $CaCO_3$ layer at either end of the crack and locally at the inner parts of the crack but that most of the crack volume was empty. Hence for such large crack widths strength regain through microbial induced $CaCO_3$ precipitation is unlikely.

We believe that for concrete durability, protection of the steel reinforcement against corrosion is of significance. In order to protect the steel reinforcement from the aggressive substances, water tightness should be regained to a certain extent following the self-healing of the cracks. A capillary sorption test is one of the ways to quantify the water tightness of the mortar and concrete specimens. In capillary sorption tests conducted, the reference specimen represents the autogenous regain that occurs in regular cracked mortar. The uncracked mortar on the other hand represents the 100 % water tightness regain. Therefore, these two values can be considered for evaluation of the water tightness regain through microbial self-healing. Based on the results, microbial self-healing provided 66 % (0.5 % ACDC) to 74 % (1% ACDC) water tightness regain for a tested average crack width of 432 ± 21 μm. Similar to capillary sorption, a water permeability test also gives significant information about the state of the concrete. According to permeability results, microbial specimens containing 0.5 % ACDC could decrease the water flow rate through a ~400 μm crack by 80 % in 28 days. The permeability technique used in this study was a novel approach described in [162]. Therefore, it was not possible to compare the obtained improvement in microbial specimens with the improvements reported in other self-healing studies.

Since no capillary sorption experiments were conducted for mature uncracked concrete, water tightness regain could not be calculated for mature specimens. Nevertheless, it is still known that mature microbial specimens absorbed 49 to 54 % less water than the mature control specimens after the healing period. Mentioned major difference between autogenous healing and microbial healing is indicative for a better water tightness regain.

4.2. The healing material and its mechanical properties

In addition to the crack closure ratio, the amount of the healing material and the thickness of the sealing might influence the capillary water absorption. It is reported that autogenous healing mostly occurs at the crack mouth due to the limits in CO_2 dissolution and

related low concentrations inside the crack [156]. One of the major advantages of microbial healing over autogenous healing is the production of CO_2 inside the crack. In this process, the activity of the bacteria in the deeper parts of the crack plays a major role. Since O_2 has dissolution and penetration limits similar to CO_2, bacterial activity that requires aerobic conditions would be inhibited inside the crack. Contrarily, nitrate (NO_3^-) reducing bacteria only rely on presence of NO_3^- and organic carbon [67] which could be provided in mortar. Therefore, it was highly possible to observe $CaCO_3$ formation inside the crack. Indeed, chemical and physical characterization of the filling material inside the cracks (5 mm <depth< 13 mm) revealed that the control and microbial samples have different compounds. The major compound found inside the crack was $CaCO_3$ in microbial samples regardless of their curing age. The found minerals were mostly together with bacterial footprints and bacterial remains which indicated that MICP took place. Visual analysis was further confirmed through EDX and FTIR analysis. Results indicated that inside the cracks of premature control specimens, ettringite and C-S-H were as dominant as $CaCO_3$. Contrarily in the powder collected from microbial specimen, forms of $CaCO_3$ were the major compounds. In mature control specimens (reference mortar and abiotic control), C-S-H was dominant inside the crack compared to $CaCO_3$ (mostly as a result of partial carbonation).

The mechanical properties of the healing materials inside the crack were also tested to elucidate if the microbial induced $CaCO_3$ has weaknesses compared to autogenously formed $CaCO_3$. It is well known that microbial induced $CaCO_3$ has pores/holes due to the growth of the minerals around the bacteria. One of the concerns is a possible decrease in mechanical properties of the microbial calcite due to the porous structure. Weaknesses in mechanical properties may cause detachment or deterioration of the $CaCO_3$ minerals which jeopardize the maintenance of functionality regain after self-healing. According to our findings, there is no significant difference between autogenously formed $CaCO_3$ and microbial induced $CaCO_3$. However, the variation in Martens hardness was higher for microbial induced $CaCO_3$ compared to the autogenously formed $CaCO_3$. The difference in variation could be attributed to the influence of bacteria related pores. Nevertheless, they did not significantly change the mechanical properties.

To our knowledge, the information about hardness of calcite deposits in cracks is very scarce. Reported hardness values for microbial calcite deposits (between 2.5 to 3 GPa) are comparable with our findings [61]. Regardless of being autogenously formed or microbial induced, the E-modulus values of calcite minerals were between 40-50 GPa which were consistent with the reported values for microbial $CaCO_3$ deposits (40 – 50 GPa) [61].

4.3. The cost evaluation for the implementation of the ACDC culture in concrete

Calculations were done based on the production of ACDC (kg) in a 1 m^3 reactor. Under steady operational conditions, the suspended solid concentrations in SBR are 7.8 ± 0.4 g/L TSS and 5.5 ± 0.2 g/L VSS and SVI 45 mL/g (Chapter 3 – Section 3.1.1). It was assumed that the VSS concentration is equal to the cell dry weight (CDW). For steady production and prevention of nutrient accumulation inside the reactor VSS concentration should always be higher than 3 g/L. The ACDC production yield is 2.5 g CDW/L.week, which enables ACDC harvesting once a week. Therefore, in a 1 m^3 SBR reactor, the production yield is 2.5 kg ACDC per week (~100 L of wet ACDC can be collected after the settling period, concentration of the collected wet ACDC is 25 g CDW/L).

4.3.1. Operational expenditure (OPEX)

A week of operation requires 28 cycles (4 cycles/day). The volumetric exchange ratio in each cycle is 50 % (500 L/cycle). Therefore, the total feed volume required to produce 1 kg CDW ACDC is 5.6 m^3 (0.5 m^3/cycle × 28 cycles/week × 1 week/2.5 kg CDW ACDC). The loading rate of the sequencing batch reactor (SBR) can be decreased by half while keeping the COD:N ratio constant (5:1), since there is no need for high loading rate acclimation prior to concrete application. According to the new loading rate, the amount of nutrients required to produce 1 kg of ACDC cost 8.0 € (Table 5.3).

Table 5.3 Minimal medium cost calculation for production of ACDC in an SBR

Compounds	Concentrations (g/L)	Amount required (kg/kg ACDC)	Cost[1] (€/ 100 kg)	Cost (€/kg ACDC)
NaNO$_3$	0.85	4.76	42.5	2.02
NaHCOO	2.67	14.95	38.2	5.71
Ca(HCOO)$_2$	0.33	1.85	5.1	0.09
Na$_2$HPO$_4$.2H$_2$O	0.03	0.17	45	0.08
MgSO$_4$.7H$_2$O	0.09	0.5	26.4	0.13
Total	-	-	-	**8.03**

[1]Unit prices are based on the quotation (23/07/2015) from BRENNTAG N.V., Belgium, See Appendix 1

The influent pump providing the feed into the reactor works 4 times/day and 1 h each time. The Grundfos COMFORT (PM**)** pump with 2.5 W energy consumption can serve for

CHAPTER 5

such an application. The electricity price for industrial consumption is 0.1 €/kWh [172]. Therefore the operation of the influent pump costs 0.0028 €/kg ACDC (0.0025 kW × 1 hour/cycle × 28 cycles/week × 1 week/2.5 kg ACDC × 0.1 €/kWh). Effluent collection and ACDC collection can be done by using valves instead of pumps. Therefore, they are not considered under operational costs.

During the aeration period, an air blower works 3 hours/cycle to supply oxygen and provide mixing to the reactor [76]. The Vpuk-TSC 40 air blower can be used to aerate the system. For a capacity of 40 m^3/h energy consumption is 0.2 kW [173]. Therefore the cost of aeration is 0.67 €/kg ACDC (0.2 kW × 3 hour/cycle × 28 cycles/week × 1 week/2.5 kg ACDC × 0.1 €/kWh).

Following a simple settling process the water content of the collected ACDC is around 96 %. Therefore, the water content of the 100 L of wet ACDC (25 g CDW/L) is 96 L. A drying process costs 30 €/m^3 water evaporated [63]. Therefore the drying cost can be calculated as 1.15 €/kg CDW ACDC (30 €/m^3 × 0.096 m^3 water/2.5 kg CDW ACDC)

Analyses required to monitor the production process require 1.5 h/week. A worker earns 50 €/h [63]. Therefore, the labor work during the production of ACDC can be calculated as 30 €/kg CDW ACDC (50 €/h × 1.5 h/week × 1 week/2.5kg CDW ACDC). If the monitoring is done through automatic measurements, this cost can be decreased by a factor 4. Therefore, it becomes 7.5 €/kg CDW ACDC.

The considered parameters are the most relevant parameters during the production of ACDC culture. When the OPEX costs are considered, the production cost of ACDC is about 40 €/kg. In order to reach a total cost of a product CAPEX should also be considered. One of the typical ways to include CAPEX in cost analysis is considering the CAPEX equal to the OPEX [63]. Therefore, the total cost of the ACDC becomes 80 €/kg most of which is the labor work (Table 5.4). If the reactor and the ACDC quality can be monitored automatically, then the labor work can be decreased by a factor 4 which makes the new OPEX range as 17.4 €/kg ACDC but still the CAPEX should be kept around 40 €/kg to be able to compensate a cost increase due to the automation which makes the total cost as 57.4 €/kg. The values calculated for production of a kg of ACDC granules in 1 m^3 SBR are summarized in Table 5.4.

Table 5.4 OPEX costs for production of ACDC for mortar application

Parameter	Cost (€/kg ACDC)	
	Manual monitoring	Automated monitoring
Nutrient solution	8.0	8.0
Aeration	0.7	0.7
Pumping	~0.0	~0.0
Drying	1.2	1.2
Labor work	30	7.5
Sub-total	**40**	**17.4**
CAPEX	40	40
Total	**80**	**57.4**

4.4. The advantages of self-protected non-axenic ACDC culture

The recorded microbial induced self-healing performances by means of a self-protected non-axenic culture appeared to be similar to the previously reported microbial self-healing results where axenic cultures and protective carriers were used. It is reported that the production of the axenic spores becomes expensive for an industrial scale application [111]. ACDC is advantageous over reported axenic cultures in many aspects. First of all, the cultivation was done in minimal media which contains concrete admixtures as main nutrients and does not contain trace elements, vitamins and yeast extract. Therefore, the cost for nutrients could be decreased when compared to the previously reported nutrient solutions for the growth of axenic cultures [22,111]. Secondly, the ACDC is a self-protected culture by its layered structure that avoids the need for a protective carrier. Therefore, direct incorporation of the dried ACDC in mortar or concrete is possible. The third advantage is the easy separation of the ACDC from the cultivation media which avoids the centrifugation process. Since ACDC is a type of granular culture with a compact structure, the sludge volume index (SVI) values of the mixture are between 35-45 mL/g. Therefore, a simple settling period of 2-5 minutes enables to separate ACDC from the liquor. The separated ACDC is ready for drying without further treatment. Eventually, the mentioned advantages play a crucial role to decrease the cost of the healing agent (Table 5.5) compared to reported cost for implementation of protected axenic cultures (1095 to 2401 €/m^3 concrete) [63]. In this study, 0.5 % ACDC in terms of CDW/weight cement (0.71 % ACDC/w cement) was found to be

CHAPTER 5

enough to achieve a significant microbial induced crack closure in concrete when combined with 3% $Ca(NO_3)_2$ and 2% $Ca(HCOO)_2$. Therefore, for an additional cost of ~135.6 €/m^3 of concrete, self-healing properties of the concrete can be improved significantly (Table 5.5).

Table 5.5 The additives and the additional cost for production of 1 m^3 microbial self-healing concrete by means of ACDC

Parameter	Material cost (€/100 kg)	Amount in self-healing concrete[1] (kg)	Cost (€/m^3 concrete)
$Ca(HCOO)_2$	5.1	9	0.5
$Ca(NO_3)_2.4H_2O$	30.5	19.5	5.9
ACDC[1]	~5740	2.25	129.2
Total			**135.6**

[1]The amount of ACDC is in terms of cell dry weight content. Addition of 2.25 g bacteria in the form of ACDC requires addition of 3.21 g ACDC since only 70% of the ACDC is bacteria.

Yet, these are approximate values based on the findings from 3.2 L scale reactors and tests on lab scale mortar specimens. In order to have a better and brighter picture, further research on optimization and up-scaling of the process is required. The amount of nutrients and the bacterial agent required for a significantly improved self-healing performance should also be optimized to avoid over/under estimations in economic analysis.

5. Conclusions

Combination of ACDC and certain concrete admixtures improved the self-healing capability of the mortar specimens.

Microbial self-healing by means of the ACDC culture is not only effective for early age cracks but also closes the cracks occurring in mature specimens.

Incorporation of ACDC (0.5 w/w cement) provided water tightness regain up to 74 % and water permeability decrease of 80% upon 28 days healing of ~430 µm and ~400 µm crack width, respectively.

Microbial induced $CaCO_3$ minerals have similar mechanical properties as the autogenously formed $CaCO_3$ minerals when compared through micro-indentation.

Microbial self-healing with ACDC can be distinguished from the autogenous healing by formation of $CaCO_3$ minerals all over the inner crack surface rather than only near the crack mouth.

Self-protected non-axenic cultures are an economically feasible alternative for development of microbial self-healing concrete.

6. Acknowledgments

CHAPTER 5

CHAPTER

6

GENERAL DISCUSSION AND
FUTURE RECOMMENDATIONS

1. General discussion

1.1. Revisiting the research needs

As stated in **Chapter 1**, self-healing materials are being designed to construct the future in a more sustainable way with less external maintenance. Self-healing concrete is one of the smart materials being investigated in the context. In order to improve the self-healing capability of concrete, exploitation of microbial induced $CaCO_3$ precipitation (MICP) was considered as one of the options and so far, two microbial pathways, i.e. aerobic respiration and urea hydrolysis, have been proposed to achieve the microbial self-healing concrete goal [40,84]. The drawbacks of the aerobic respiration were pointed out as the O_2 limitation and the dependency to external alkalinity since the process itself does not produce any alkalinity. The disadvantages of urea hydrolysis were listed as production of toxic by-products, O_2 requirement for bacterial growth and possible degradation of concrete in long term due to the $NH_4^+ \leftrightarrow NH_3$ balance. Due to the drawbacks of the current microbial pathways, a need for an alternative pathway for development of microbial self-healing concrete arises. Although NO_3^- reduction was explored for MICP in different fields, the phenomenon has not been investigated for concrete application. Therefore the main intention in this thesis work was to explore the potential of the NO_3^- reduction pathway for concrete application regarding to improvement of self-healing properties. The second detected need in the current state of the art was to decrease the implementation cost of the technology. Previous studies emphasized the implementation cost and ease of application [63,84]. Therefore, in the context of this thesis work, the combination of two different approaches was used. The first approach was

leading towards more proof of the concept by using the NO_3^- reducing axenic strains to evidence the applicability of the strategy and determining its limits. The second approach was more application oriented by modifying the explored strategy to improve the practicality and decrease the implementation cost.

1.2. Research outcomes

1.2.1. The use of axenic cultures

The major focus in **Chapter 2** was to select the appropriate strains that can be used to prove the concept of microbial self-healing concrete through biological nitrate reduction. Resistance to nutrient limitation, starvation, dehydration, thermal stress and inoculum minimization were the main desired resilience characteristics of the bacteria during the selection procedure. The isolated strains were Gram-negative non-sporulating bacteria instead of the more resilient spore forming bacteria. The elimination of the spore forming bacteria was attributed to the absence of yeast extract and trace elements during the selection procedure. These findings revealed the importance of yeast extract for the germination, growth and activity of spore forming bacteria, which have been investigated in the microbial self-healing concrete studies so far. The results were in line with the previous studies reporting the need of at least 2 g/L yeast extract for a significant outgrowth of spore forming bacteria [84]. Therefore, by choosing resilient vegetative strains such as *Diaphorobacter nitroreducens* and *Pseudomonas aeruginosa*, it is possible to avoid dependence on the yeast extract which is an expensive and incompatible constituent for concrete application.

Since the main phenomenon used in bacteria based self-healing concrete is MICP, experiments were designed to optimize the $CaCO_3$ precipitation yield of the selected bacteria. Therefore, the MICP potential of the selected bacteria could be determined as 18.9 g $CaCO_3$/g NO_3-N and 14.1 g $CaCO_3$/g NO_3-N for *Pseudomonas aeruginosa* and *Diaphorobacter nitroreducens*, respectively. Different from the previous studies, the optimization was done under minimal nutrient conditions. Since concrete is a nutrient poor environment, investigated conditions were more representative for the in situ availability of the nutrients. Moreover, the electron donor (formate) and the electron acceptor (nitrate) used during optimization could easily be incorporated in concrete in the form of commercial concrete admixtures $Ca(HCOO)_2$ and $Ca(NO_3)_2$ [68,69]. Therefore, the implementation becomes easier and more economically feasible compared to previously described strategies. The optimized precipitation yields by

means of *Pseudomonas aeruginosa* and *Diaphorobacter nitroreducens* were 72 and 53 % of the maximum theoretical yield, respectively. Although the optimized values seem relatively far from the maximum theoretical yield, they are less susceptible to variation depending on the nutrient availability. Successful repetitive $CaCO_3$ precipitation with a rate of 30 - 50 g $CaCO_3$/h could be achieved with both strains which can be beneficial for repetitive healing of the same crack in case of necessity. It was also revealed that regardless of the type of the mineral, precipitate formation around the bacteria significantly decreased the bacterial activity and may lead to complete loss of active cells. These observations were in line with the observations in previous MICP studies. However, it was found out that a recovery time even without any nutrient or inoculum supplement enables bacteria to save themselves and reach their initial activity state.

Although several harsh conditions such as heat, starvation, nutrient limitation and dehydration were applied during the selection of the bacteria, alkaline pH was not one of them. Alkalinity was investigated separately in **Chapter 3** since not only alkaliphilic strains but also alkali-tolerant strains can be used in concrete applications. It has been reported that regardless of their resilience bacteria should be incorporated with protective carriers before adding into concrete [55]. Therefore, selecting only for alkaliphilic bacteria would eliminate some options that can still be useful with the aid of protective carriers. Investigation of the selected bacterial strains at different pH environments (pH 7, pH 9.5 and pH 13) with and without protective carriers was necessary to understand their tolerance to alkalinity. By keeping the ease of implementation and cost in mind, commercially available protective carriers namely, expanded clay particles, granular activated carbon particles and diatomaceous earth powder were chosen for investigation. The results revealed that both bacterial strains were compatible with all the protective carriers which were in consistency with the results of previous studies investigating interaction of bacteria with diatomaceous earth, expanded clay particles and granular activated carbon [40,58,130]. Incorporation in protective carriers also improved strain performances up to 4 times at pH 9.5 when compared to their plain performances. This improvement was attributed to the biofilm formation on the particles which creates favorable conditions for bacteria [83,174]. Moreover, the biofilm formation provided resilience to the bacteria under alkaline conditions. The obtained results were useful to decide on the composition of different healing agents. In microbial self-healing concrete, healing agents are composed of a combination of bacteria, protective carriers and nutrients. Combination of different components may cause different effects in mortar environment. Therefore, it would not be safe to rely on previous results during the selection of

healing agents. In that sense, Chapter 3 was also important to evaluate the compatibility of different healing agents with mortar. Obtained results were completely different than the previous results. Previously in combination with ureolytic bacteria and thus with nutrients necessary for urea hydrolysis (urea + yeast extract), diatomaceous earth was reported to be useful [58,63]. However, significant acceleration in mortar setting (from 290 minutes to 160 minutes) was achieved in this study when diatomaceous earth was incorporated with $Ca(HCOO)_2$ and $Ca(NO_3)_2$. Another determined disadvantage of the diatomaceous earth was its protection mechanism which was not very efficient to protect vegetative strains during mortar mixing when compared to aggregate like materials (expanded clay particles and granular activated carbon particles). When protected with aggregate like materials during mortar incorporation, the subsequent activity of the investigated bacterial strains *Pseudomonas aeruginosa* and *Diaphorobacter nitroreducens* were up to 20 % higher than the ones protected with diatomaceous earth. The difference in the survival rate was due to the robustness of the material during the mixing. Diatomaceous earth agglomerates were disintegrated during mixing and caused exposure of a portion of the bacteria to detrimental alkaline environment. Contrarily, aggregate like materials were more stable and provided better protection during the mixing process. Previously, Wang et al.[58] revealed that diatomaceous earth provided good protection for bacteria. However, in their case, bacterial endospores were used which are resistant under alkaline conditions. Therefore, the major protective role of the diatomaceous earth was starting with the pozzolanic activity inside the matrix and following gel formation around the bacterial seeds. These results revealed that powder carriers are not the perfect options if vegetative bacterial strains are used for concrete application. Moreover, the use of pozzolanic carriers in combination with the accelerating concrete admixtures that can serve as nutrient for bacteria should be avoided to prevent workability problems.

The major purpose of self-healing concrete is to protect the steel reinforcement and solve the related durability issues. In that perspective the results obtained in corrosion inhibition tests and further crack closure experiments in Chapter 4 were important. First of all, the results evidenced that the NO_3^- reducing pathway is useful for development of microbial self-healing concrete. Moreover, it was shown that biologically produced NO_2^-, the intermediate product of biological NO_3^- reduction, could inhibit corrosion of the steel if the conditions promote NO_2^- accumulation leading to $[NO_2^-]:[Cl^-]$ ratio of more than 1. This can be an advantage to achieve simultaneous corrosion inhibition during self-healing of the concrete cracks. However, it seems unlikely to achieve such corrosion inhibition under certain

environmental conditions such as marine environment. Since $[NO_2^-]:[Cl^-]$ ratio is the major parameter for effective corrosion inhibition, the exposed Cl^- concentration has utmost importance. The typical Cl^- concentration for seawater is reported as 0.54 M (19 g/L) [175]. Therefore, to achieve a simultaneous corrosion inhibition during self-healing of a marine exposed concrete, at least 0.54 M biological NO_2^- (7.56 g/L NO_2-N) production is necessary. The highest NO_2^- concentration achieved in Chapter 3 was 0.057 M (0.798 g/L NO_2-N) which revealed that for cracked concrete exposed to seawater, corrosion inhibition through biological NO_2^- production is hardly possible. Yet, cracked concrete structures being exposed to either ground water, surface water or surface runoff can still benefit from the microbial induced corrosion inhibition and self-healing simultaneously, since the average Cl^- concentrations for these water types are stated to be between 0.29 to 8.5 mM (10 – 300 mg/L) [176,177].

As stated in Chapter 1, one of the ideas behind the development of autonomous self-healing strategies is to improve autogenous healing to more predictable, controllable and repeatable healing. Considering this framework, the results of **Chapter 4** reveal a successful improvement of healing potential in a more predictable and repeatable way. Although, a variation is observed in autogenous healing potential in two different setups with two different carriers, the microbial induced healing did not significantly change in different cases. The healing potential achieved in 28 days healing period, could be enhanced from 250 – 300 μm to 350 – 400 μm. These results were obtained following full immersion of the specimens and it was observed that the time plays the most crucial role in autonomous healing. Tests were also conducted by changing the incubation conditions to 1 week immersion and 1 week humidity (> 95 % RH) curing (data not shown) and it was concluded that effective time period should be considered as the immersion/water contact time rather than the total time. When the immersion time was doubled (from 28 days to 56 days) only the autonomous healing was improved and the healing potential was recorded as ~500 μm. Considering these performances which are similar to the performances of previously described microbial mortars, biological NO_3^- reduction can be proposed as a new and environment friendly alternative for development of microbial self-healing concrete. As the reasonable crack widths for water retaining structures and the structures exposed to humidity are ~100 μm and ~300 μm [14], respectively, the performance of the developed microbial mortars can be considered as enough to minimize durability issues. Moreover, after 28 days healing microbial specimens resulted in ~50 % more water tightness than the autogenously healed specimens for an initial crack width of ~240 μm. The water tightness regain of

CHAPTER 6

microbial specimens was ~80 % for an initial crack width of ~450 µm after 56 days of healing period. Since the water and the moisture are the main carriers of aggressive substances towards the reinforcing bar through the concrete cracks, the regain in water tightness is important. Achieved water tightness performances were promising to prevent corrosion related durability issues.

1.2.2. Regarding the use of self-protected non-axenic cultures

Although the self-healing performances obtained by employing axenic cultures in mortar environment are promising, the application procedure of these strains does not perfectly fit into the aforementioned application oriented approach. The use of protective carriers, the unpredictable shelf life of the bacteria in vegetative state and the application costs are the main issues making selected axenic cultures not very suitable for application. Moreover among the investigated axenic cultures, *Pseudomonas aeruginosa* is classified as a bio-safety level-2 (BSL-2) microorganism which means it is a pathogenic strain. The most pronounced drawback of using axenic cultures is the cost of the implementation. It was described by Silva [63] that implementation of the axenic cultures into mortar in similar quantities to ones investigated in this thesis work, costs of the order of 1000 to 2500 €/m^3 of concrete for development of microbial self-healing concrete. Therefore, after having followed the proof of principle approach by using well-defined bacterial communities such as axenic cultures, it was necessary to approach the concept in an industrial way. In that perspective, partially in **Chapter 3** and more in detail in **Chapter 5**, self-protected non-axenic culture was investigated for self-healing purposes. Bio-granules formed through systematic self-immobilization of bacteria were considered as an alternative to protected axenic cultures. Results revealed that bio-granules could indeed be an alternative. First of all, compared to protected axenic cultures the NO_3^- reduction rate of ACDC was at least 20 % higher at pH 9.5. Moreover, ACDC was found to be concrete compatible up to addition of 1 % w/w cement. Additionally, when incorporated in mortar ACDC could increase the crack closure potential up to 500 µm crack width for 28 days healing period. A similar performance could only be achieved after 56 days when axenic cultures were used, which makes ACDC granules even a better option rather than an alternative. ACDC was also providing improved water tightness regain at the end of 28 days when compared to axenic cultures. After 28 days healing of a comparable crack width (~450 µm) the difference in water tightness regain was ~40 % between the microbial specimens containing ACDC and the ones containing granular

activated carbon protected axenic culture. In addition to the water tightness regain, the water permeability under pressure could be decreased. Under 0.1 bar water pressure, the permeability of the healed specimens was 80 % less than their initial permeability before healing. Detailed analysis revealed that significant precipitation could be observed up to a depth of 8 mm, but the remaining crack volume was empty. One of the major concerns about microbial concrete is the stability of the bacteria inside the concrete matrix in long term. In Chapter 5, it was revealed that when cracks were formed after 6 months curing period (at 20 ^{o}C and >95 % RH) a slight decrease in bacterial performance occurred. Yet, the crack closure efficiency was still stable up to 400 μm. The shift in healing potential was attributed to the decrease in autogenous healing which occurs more or less to the same extent in all the specimens regardless of being microbial or not. The lower the amount of $CaCO_3$ produced through autogenous healing the higher the need for microbial induced $CaCO_3$. Therefore a shift in autogenous healing potential might also affect the healing potential of the microbial specimens. These findings revealed that in the long term, the performance of incorporated ACDC is stable but there is a decrease in healing potential of the mature cracks due to the decrease in autogenous healing potential.

Most importantly, the major aim, bringing the technology closer to application, was achieved by decreasing the cost of the implementation around 10 times. Overall, predictable, controllable and repeatable healing functionality could be added to concrete by almost doubling its production price.

1.3. Challenges and future perspectives

The approach used in this thesis work provided some knowledge to progress further in development of microbial self-healing concrete, yet also created some new challenges and related research lines. Therefore, some further points in shade to discover and challenges to overcome can be presented.

1.3.1. Recommendations for exploiting described NO_3^- reducing axenic cultures for MICP and self-healing concrete

The strategy followed and the results achieved in Chapter 2 helped to elucidate the potential of biological nitrate reduction for MICP applications. The outcomes of Chapter 2 are not only significant for concrete applications but also for other MICP applications such as soil consolidation and Ca^{2+} removal from wastewater.

The use of presented axenic cultures for development of self-healing concrete has certain drawbacks. First of all, the strains are vegetative and regardless of their resilience vegetative strains cannot stay stable for a long time (i.e. concrete life-time) under desiccated state. This brings the problem that if presented strains are used in concrete, after a while the concrete will lose significant portion of its autonomous healing potential. Therefore, they may only be useful for early age cracks and the cost for achieving such limited functionality may become unfeasible. Nevertheless, the use of axenic cultures is always essential to evidence the potential of the microbial pathways investigated for development of self-healing concrete and should be the initial step in research.

Since the use of described axenic cultures for microbial self-healing concrete applications is not economically feasible, alternative applications should be considered for the presented strains. The described strains *Pseudomonas aeruginosa* and *Diaphorobacter nitroreducens* can be used as reference strains to explore and evaluate the performance of alternative cultures intended for MICP applications. For instance one of the challenges is the Ca^{2+} removal from industrial waste streams such as paper mill wastewater. In particular to the closed system pulp and paper facilities that are reusing the wastewater after treatment, Ca^{2+} concentrations are relatively high and cause problems in the pipelines. Ureolysis has been used as one of the methods for removal of Ca^{2+} form these streams. However, to achieve ureolysis, addition of urea and phosphoric acid is required. This process leads production of ammonia in the system and hence subsequent removal of ammonia is needed. Contrarily, the denitrification process has higher $CaCO_3$ precipitation yield and does not produce additional pollutants. The $CaCO_3$ precipitation yield of ureolysis can be calculated as ~4.5 g $CaCO_3$/g Urea-N from the reported data for Ca^{2+} removal from wastewater streams [44,53,178]. The yield obtained in Chapter 2 was between 14.1 to 18.9 g $CaCO_3$/g NO_3-N. Urea hydrolysis occurs under aerobic conditions which promotes bacterial growth and increases biomass yield. In contrast to that, anoxic oxidation of organic matter (through NO_3^- reduction) has lower biomass yield, thus higher inorganic carbon (CO_2) production and $CaCO_3$ yield. Therefore, the denitrification process becomes less expensive than ureolysis for Ca^{2+} removal from wastewater. The Ca^{2+} concentration in wastewater of a typical closed system paper mill industry is ~0.5 g /L and the sCOD is around 1.3 g/L [44,67,178]. If the minimum obtained yield in Chapter 2 is taken as reference, instead of adding 0.6 g Urea/L, by only adding ~0.1 g NO_3-N /L the same Ca^{2+} removal can be achieved. Removal of 0.1 g NO_3-N/L consumes ~0.3 g/L of the sCOD which means that a simple A/O (anoxic–aerobic) system can easily remove Ca^{2+}, NO_3^- and sCOD from the system. Therefore, investigation of continuous Ca^{2+}

removal from the Ca^{2+} rich waste streams could be a possible research line. In such study, the described axenic strains *Pseudomonas aeruginosa* and *Diaphorobacter nitroreducens* can be used as inoculum or a base for the removal potential of the reactor.

Another possible application area for the presented strains is soil reinforcement. The mechanical properties of the base soil is important for stability of structures and problems occur due to insufficient quality such as road and railway settlements. Moreover, concrete sinking and related damages happen if the base soil is poorly compacted. Therefore, to avoid these problems, it is important to improve the base soil and sand quality if necessary. One of the ways to improve mechanical properties of soil is MICP. So far, soil reinforcement studies by means of MICP included two main biological processes, either ureolysis or denitrification [45,46,49,51,78]. To our knowledge, among the studies, the highest reported $CaCO_3$ precipitation yield, 10.6 g $CaCO_3$/g NO_3-N in 3.5 days, was achieved through denitrifying activity of *Pseudomonas denitrificans* under nutrient rich conditions [49]. The $CaCO_3$ precipitation yields of the cultures described in Chapter 2 (14.1–18.9 g $CaCO_3$/g NO_3-N) can be considered as an improvement. The main disadvantage of denitrification compared to ureolysis was reported as its lower $CaCO_3$ precipitation rate [51,78]. $CaCO_3$ precipitation rate mainly depends on the initial bacteria concentration, their growth rate and specific metabolic activity of each bacterium in the relevant environment. As previously mentioned, anoxic oxidation of organic matter decreases the growth rate and causes slower $CaCO_3$ precipitation rate. Through ureolysis, $CaCO_3$ precipitation rates from 10 to 120 g $CaCO_3$/h were reported [45]. However, it was also reported that ureolytic bacteria could not grow in situ [45,51] which brings several practical issues in addition to its aforementioned environmental impact. First of all, prior to the remediation, the field should be inoculated with certain bacteria grown under completely aerobic and nutrient rich conditions [45]. Since the inoculum cannot grow on site, upon inoculation, the time for remediation was limited with the life-time of the inoculated bacteria until the decay period [45,46]. Secondly, it was shown that specific activity of the bacteria decreased with time and depth due to several reasons which caused variation in precipitation rates and thus the amount of precipitate [45]. Different from ureolytic bacteria, denitrifying bacteria can grow and perform under oxygen limited conditions on site [49,51]. Therefore, despite its lower $CaCO_3$ precipitation rate, the denitrification process enables long term remediation on site by using a single inoculum that can further grow onsite. Through denitrification, a maximum $CaCO_3$ precipitation rate of 180 mg $CaCO_3$/h was reported for *Castellaniella denitrificans* after continuous feeding of a sand column for more than 70 days with nutrient rich media [51]. The average $CaCO_3$ precipitation

CHAPTER 6

rate of 100 days was reported as 125 mg $CaCO_3$/h. On the one hand, continuous supplementation of nutrient rich media for 100 days to maintain $CaCO_3$ precipitation and growth of *Castellaniella denitrificans* can be considered as an economical and practical drawback. On the other hand, if the minimal nutrient were used for feeding, lacking of trace elements and vitamins would cause a decrease in growth rate and thus the $CaCO_3$ precipitation rate. In order to improve the precipitation rate, it was suggested to use more suitable strains in higher inoculum concentrations [51]. Strains presented in Chapter 2, *Pseudomonas aeruginosa* and *Diaphorobacter nitroreducens*, could be the potential candidates for more feasible application. The reported $CaCO_3$ precipitation yield of *Castellaniella denitrificans*, in nutrient rich environment, was 2–3 times lower than $CaCO_3$ precipitation yields achieved Chapter 2 under minimal nutrient conditions. Moreover, both *Pseudomonas aeruginosa* and *Diaphorobacter nitroreducens* were found to be the fastest growing strains in minimal nutrient conditions among different isolated strains. In addition to that, they are able to precipitate $CaCO_3$ in semi-continuous feeding. Therefore, use of either *Pseudomonas aeruginosa* or *Diaphorobacter nitroreducens* could decrease the cost of the application and provide repetitive $CaCO_3$ precipitation in soil environment via semi-continuous operation. For a single inoculum of 10^9 cells/mL, the $CaCO_3$ precipitation rates were recorded as 30 – 50 mg $CaCO_3$/h in 2 days and 3 weeks precipitation intervals in Chapter 2, respectively. Since precipitation rate may vary due to the intervals in semi-continuous operation, further optimization of the operation is necessary to achieve more stable precipitation rate. Furthermore, on site soil reinforcement performances of both strains should be investigated under optimized semi-continuous operation.

1.3.2. Recommendations for development of microbial self-healing concrete

At the final stage of this thesis work, bio-granules were investigated as bacterial agent for development of microbial self-healing concrete. Although successful results were achieved, there is still significant margin for improvement. First of all, it was found that only ~14 % of the nutrients became available during the healing period. Nutrient availability is of significance to achieve an effective microbial $CaCO_3$ precipitation. It was observed in Chapter 4 that if the nutrients are available the healing potential increases in time. Therefore, optimization of the amount of nutrients is necessary considering the needs of the structure and the allowable crack widths.

It was also observed that the ACDC culture could only start significant nutrient consumption when the pH decreased below 10 around 2 weeks after the crack occurrence. So far, all the studies are using static immersion conditions which enable keeping the nutrients available until the bacterial consumption starts. Unfortunately, such stability of leached nutrients is most probably not possible in situ due to the wash-out. Hence, the healing potential of the microbial concrete becomes highly susceptible to immersion conditions. On the one hand, since presence of water is a prerequisite in bacteria based self-healing, application in immersed structures becomes the best option. On the other hand, keeping nutrients available until the bacterial consumption starts is a major challenge. Therefore, it is necessary to be investigated. Some suggestions can be made for such research. Since the challenge is the water mobility around the structure, water should be trapped. For horizontal structures such as tunnels under water, the problem is minor and water can be trapped inside the crack due to gravitational and capillary forces. However, for vertical structures such as bridge piers or dock piers, it is necessary to surround the immersed part of the structure with another layer of material. The additional layer should provide stability to the water between two layers. Another possible solution to keep the nutrients available for bacterial consumption is the use of controlled-release nutrients. The concept is being used for fertilizers which increase the duration for the release of nutrients from granulated fertilizer to soil. Inspired by this concept, such nutrient granules with low solubility can be added into concrete to avoid the nutrient wash-out with the water. Of course, comprehensive research is necessary to characterize different complexes, to investigate their compatibility with mortar and to optimize their nutrient release rate based on the bacterial activity under conditions similar to the concrete crack environment.

The healing duration is also an important factor which should be carefully defined for different structures depending on their purpose and the environments they are exposed to. In this study, healing of the cracks up to 500 μm could be achieved in 28 days. However, these results were obtained when the specimens were completely immersed in water. Considering the availability of water, temperature variations, amount of bacterial agent used and nutrient availability (due to diffusion from mortar) the healing duration can significantly change. Apart from that, self-healing also initiates with the occurrence of micro-cracks that are hardly possible to be detected with bare eyes. Hence it may avoid further development of the cracks if the healing rate is higher than the development rate. The idea of self-healing is to increase durability of the structures rather than competing for the healing of the largest crack width at

the shortest time period. Therefore, it is necessary to optimize and modify the mix designs according to the contractors expectations and the relevant environmental conditions.

Another challenge in the application of microbial self-healing concrete is the cost of the technology. The average price for plain concrete is reported as 85 €/m^3 in 2013 for US [179]. An economic evaluation on small scale production of ACDC revealed that the switch from axenic cultures to non-axenic cultures can decrease the cost by factor 10, yet the total cost of implementation still brings ~100 % additional cost in the total structure. The acceptable cost increase in construction industry for such implementation is around 20 % [172] which means the cost of the bacterial agent should still be decreased by 5 times. One simple way of decreasing the cost of bacterial agent is to decrease the amount of bacteria used. However, such approach may have a considerable decrease in the self-healing potential and the healing rate. As previously mentioned, such modification should only be made based on the contractors expectations from a microbial self-healing concrete. In Chapter 5 of this thesis work, two different doses of ACDC were investigated and there were no significant difference in performances. Therefore, one can start from ACDC dose of 0.5 % w/w cement and decrease the threshold to optimize the amount of ACDC necessary. Another approach could be the modification of the production process of ACDC. As stated in "Chapter 5 – Discussion Section 4.3", at least 3 g/L of ACDC concentration should be kept inside the reactor to maintain the production stability. If bio-granules can be obtained from a full scale granular biomass reactor and further processed to achieve ACDC granules, the production rate can be increased and the cost can be decreased. In such operation, the processing time will be approximately two weeks (56 cycles) and the full batch can be harvested at the end. A batch capacity of an SBR reactor having granular biomass can be up to 8.5 g/L VSS. Therefore, the ACDC production yield can be increased to ~4 kg CDW/week in a m^3 reactor by modifying the process as a post-modification of a waste biomass. This would decrease the production cost by a factor ~2. Yet, the cell yield of granulating cultures is relatively low (0.17 g VSS/g COD for ACDC) which makes the production of granules a slow process. Hence it is highly possible that the granules from a waste sludge line of a full scale granular biomass plant will not be enough to supply the demand from the concrete industry. Use of non-axenic cultures as bacterial agent has one major challenge that the content of the culture is not easily predictable. Although selective conditions are applied during the ACDC production, it was not certain that the content is pathogen free. As presented in Chapter 2, a pathogenic strain *Pseudomonas aeruginosa* could survive the intense selection procedure. Therefore, comprehensive characterization of ACDC culture is always necessary prior to application in order to fulfill

the safety requirements. Since the production process of ACDC has quite stable parameters, the culture community in ACDC is not expected to change significantly. Therefore, denaturing gradient gel electrophoresis (DGGE) analysis in regular intervals should be included in quality control of ACDC batches. Another challenge related to the culture content is the denitrifying core content. The co-cultures placed in outer layers of ACDC have significance for protection of the core during concrete incorporation and the portion of the denitrifying core is responsible for the subsequent activity during crack closure. Therefore, it is necessary to determine the relative distribution of the communities. Following determination, an optimization study should be conducted to maximize the denitrifying core content and optimize the necessary protective layer thickness for effective incorporation. By this approach the amount of ACDC incorporation necessary to achieve similar healing potentials can be decreased which will decrease the cost as well.

In Chapter 3, it was revealed that corrosion inhibition is possible through biological NO_3^- reduction to NO_2^-. The chemical consumption of NO_2^- by Fe^{2+} ions will have effect on the $CaCO_3$ yield of the bacterial agent since the chemical consumption will precede the biological reduction. Therefore, it may cause inconsistencies between bench scale results and on site performances. In order to achieve a corrosion resistant microbial self-healing concrete, it is necessary to optimize $CaCO_3$ precipitation yield of the cultures in the presence of Fe^{2+} ions.

In Chapter 5, during the μCT analysis it was realized that the microstructure of microbial specimens is more porous than the control specimens. This was attributed to the swelling and shrinkage of ACDC granules during mixing and curing, respectively. It is known that the porous structure is helpful to resist freeze-thaw damage. Considering that perspective, incorporation of ACDC can improve the freeze-thaw resistance of the concrete. Further investigation is necessary to evidence this possibility.

Additional functionalities such as corrosion inhibition and freeze-thaw resistance coming with the addition of ACDC can positively affect the industrial perception of microbial self-healing concrete and expedite the transition from concept to market. As Edward Teller stated "The science of today is the technology of tomorrow", hence the quicker the better.

CHAPTER 6

ABSTRACT

ABSTRACT

A portion of CO_2 produced as a result of metabolic activity can be converted into insoluble carbonates and thus substantial amount of the sedimentary carbonate deposits formed at the Earth's surface is attributed to intra- or extracellular microbial activity. The phenomenon is called microbial induced carbonate precipitation (MICP). The metabolic activities, namely aerobic respiration, sulfate reduction, iron reduction, urea hydrolysis, nitrate reduction, methane oxidation and photosynthesis are known to give rise to MICP. Calcium carbonate ($CaCO_3$) precipitation is a common as well as a circumstantial behavior in the bacterial world, which implies that most of the bacteria are able to precipitate calcite crystals if the environmental conditions favor them. By the growing interest in the interaction between microorganisms and construction materials, MICP came into consideration as a repair strategy for concrete cracks. Due to its heterogeneous matrix, cracking of concrete is almost inevitable and the cracks may cause significant durability problems. Therefore, regular external maintenance of the structures is required to prevent cracking related durability issues. Placing micro-laborers, the bacteria, inside the concrete structures and exploiting their ability to precipitate filling materials such as $CaCO_3$ may avoid the need for extrinsic maintenance and make the structures self-healing.

Significant research has been conducted to develop a microbial self-healing concrete. In the current state of the art two separate metabolic pathways, aerobic respiration and urea hydrolysis, and the respective bacteria are described for such utilization. However, each of these pathways has certain drawbacks that require improvement. Ureolysis leads to NH_3 production which is toxic for the environment and harmful for the concrete matrix. Aerobic respiration is mostly efficient at the crack mouth due to the O_2 limitations inside the crack. Therefore, a need for an alternative arises. This thesis work presents the investigation of biological nitrate (NO_3^-) reduction for intrinsic repair of concrete cracks. The major objectives were to explore the potential of biological nitrate (NO_3^-) reduction as an alternative metabolic pathway for development of microbial self-healing concrete and to bring the developed technology closer to market by modifying parameters.

In order to purely investigate the potential of NO_3^- reduction pathway, axenic cultures

containing single type of bacteria were used at initial stage. The axenic cultures were combined with commercial protective carriers and tested in mortar to evaluate their influence on self-healing properties of mortar.

The bacteria for axenic cultures were isolated from soil by applying stress conditions that are similar to the ones the bacteria would face in concrete environment such as dehydration, temperature shock, starvation and limitation in supplementary nutrients and vitamins. Qualifying strains *Diaphorobacter nitroreducens* and *Pseudomonas aeruginosa* were further investigated for optimization of their MICP performance under concrete similar nutrient environment which contains only the carbon source ($HCOO^-$), electron acceptor (NO_3^-) and precipitation initiator (Ca^{2+}). Repetitive precipitation capability of a single inoculum was investigated in case repetitive crack closure would be required on site. As a result $CaCO_3$ precipitation yields of 14.1 g $CaCO_3$/g NO_3-N and 18.7 g $CaCO_3$/g NO_3-N were achieved for *Diaphorobacter nitroreducens* and *Pseudomonas aeruginosa*, respectively. The $CaCO_3$ precipitation rates were between 30-50 mg/h and the strain resilience was found high enough to proceed further.

Regardless of their resilience axenic cultures should be immobilized on protective carriers prior to concrete incorporation to prevent their being crushed inside the concrete due to the shrinkage of the matrix in time. Therefore, commercial protective carriers like diatomaceous earth powder, expanded clay particles and granular activated carbon particles were tested for their compatibility with the selected strains *Diaphorobacter nitroreducens* and *Pseudomonas aeruginosa* and for their protection efficiency in different pH environments (pH 7, pH 9.5 and pH 13). Furthermore, the suitability of protective carriers for mortar incorporation was investigated. The most important parameter was their effectiveness in terms of protecting bacteria during mortar mixing and the subsequent period inside the mortar until cracking. Secondly, their compatibility with mortar and with the nutrients that would be necessary for bacterial activity during crack repair, were tested. Finally, it was necessary to test the influence of bacterial activity on steel reinforcement. Results indicated that all the protective carriers were compatible with the bacteria and enabled their survival in mortar environment for 28 days. Significant bacterial activity could be achieved from the bacteria collected from crack surfaces. Among the investigated protective carriers diatomaceous earth was 20 % less efficient than the aggregate like carriers in terms of bacteria protection during mortar incorporation. Additionally, diatomaceous earth was not compatible with the nutrients that bacteria require for crack repair, thus caused about 130 minutes decrease in mortar setting time. Expanded clay particles and granular activated carbon particles showed great

compatibility with both mortar and the nutrients, hence did not influence the mortar properties significantly. Regarding the bacteria-steel interaction, positive results indicating corrosion inhibition due to the microbial produced NO_2^-, were obtained. Therefore, it was safe and beneficial to use the bacteria for further investigation and either expanded clay particles or granular activated carbon particles could be used as carrier in such tests.

In order to evidence the potential of biological NO_3^- reduction for development of self-healing concrete, it was necessary to investigate the improvement in crack healing potential of mortar. Selected axenic bacterial strains *Diaphorobacter nitroreducens* and *Pseudomonas aeruginosa* were incorporated in mortar (0.5 % w/w cement) by using either expanded clay particles or granular activated carbon particles (5 % w/w cement) and tested for intrinsic crack repair. Healing of cracks with crack widths varying from 100 to 750 μm were tested. When the cracked specimens were fully immersed in water for 28 days, the healing potential for the ones containing bacteria was ~400 μm. No significant difference was achieved when either the bacteria or the protective carrier was interchanged. When the immersion time was extended to 56 days, the healing potential of the specimens were recorded as ~500 µm. At the end of 56 days healing of ~450 µm crack, the water tightness regain was ~85 %. Eventually, the results evidenced the potential of biological NO_3^- reduction and thus created more freedom for modifications of healing agents to bring the technology closer to application.

Microbial self-healing concrete can cost around 1300 to 2800 €/m^3 concrete if axenic cultures typically used to prove the concept are implemented at the same amount investigated in this thesis work. Since one of the main objectives was to bring the developed technology closer to the market, it was necessary to extend the research on possible bacterial agents. Therefore, use of non-axenic cultures was considered. An innovative approach was followed and special bio-granules consisting of many different bacteria (70 % of the granule content) were produced at lab scale and further investigated as a self-protected bacterial agent. Their performance at different pH conditions (pH 7, pH 9.5 and pH 13) and subsequent activity after mortar incorporation were tested. Furthermore, their compatibility with mortar was investigated by evaluating changes in compressive strength and setting of mortar. Without any external protection or a carrier, bio-granules showed comparable performances with those achieved with the protected axenic cultures under similar environmental conditions. Furthermore, the granules were highly compatible with the mortar at the investigated doses (0.7 % w/w cement and 1.4 % w/w cement) which made them promising alternatives to axenic cultures.

The possible variation in the performance of microbial self-healing concrete due to the

replacement of protected axenic cultures with self-protected non-axenic cultures should be tested. Therefore, mortar specimens containing bacteria in the granular form (at a dose 0.5 and 1 % bacteria w/w cement) were prepared and subjected to tensile load after 28 days to create multiple cracks with the crack widths ranging between 90 – 640 μm. Identical specimens were prepared to test the self-healing performance of mature cracks that were created after 6 months curing. Effectively self-healing crack widths in the microbial specimens were recorded as ~500 μm and ~400 μm for early age cracks and mature cracks. After 28 days healing of a ~450 μm crack width the water tightness regain was up to 74 %. Moreover, after 28 days healing, the water permeability through a ~400 μm crack width decreased by 80 % due to the microbial induced $CaCO_3$ precipitation inside the crack. Stable performance from bacteria could be achieved for healing of the early age cracks and mature cracks while the autogenous self-healing and thus the total healing potential significantly decreased in time.

In conclusion, in this thesis work, the significant potential of biological NO_3^- reduction for development of microbial self-healing concrete was successfully demonstrated and by the efforts on modification of bacterial agents, the cost of microbial self-healing concrete was reduced to ~240 €/m^3 concrete. In future studies, it is recommended to use axenic cultures for determining the constrains of the technology and the rooms for improvement, while non-axenic cultures, particularly the self-protected non-axenic cultures, for application purposes.

ABSTRACT

Een gedeelte van de biologisch geproduceerde koolstofdioxide kan worden neergeslagen in onoplosbare carbonaten en een aanzienlijke hoeveelheid van de huidige sedimentaire carbonaatafzettingen kan dan ook worden toegeschreven aan microbiële activiteit. Dit fenomeen wordt microbieel geïnduceerde carbonaatprecipitatie (MICP) genoemd. Van veel metabolische processen, zoals aerobe respiratie, sulfaatreductie, ijzerreductie, hydrolyse van ureum, nitraatreductie, methaanoxidatie en fotosynthese is gekend dat ze carbonaat precipiteren, onder andere onder de vorm van calcietkristallen. Er is een toenemende belangstelling om micro-organismen te combineren met bouwmaterialen, en MICP kan in aanmerking komen als een reparatiestrategie om scheuren in beton te herstellen. Door zijn heterogene matrix zijn scheuren in beton quasi onvermijdelijk en deze scheuren veroorzaken aanzienlijke duurzaamheidsproblemen. Daarom zijn regelmatige inspectie en onderhoud van constructies onontbeerlijk. Door micro-werkmannen, de bacteriën, in het beton te brengen en gebruik te maken van hun capaciteit om $CaCO_3$ te precipiteren, wordt het beton zelfhelend en verdwijnt de nood aan manueel onderhoud.

Er is reeds een aanzienlijke hoeveelheid onderzoek uitgevoerd rond het microbieel zelfherstellend beton. De focus ligt vooral op twee metabole processen: aerobe respiratie en de hydrolyse van ureum. Echter, elk van deze processen heeft bepaalde nadelen. Ureolyse leidt tot NH_3 productie, die toxisch is voor het milieu en schadelijk is voor de betonmatrix. Aerobe ademhaling is vooral efficiënt aan het oppervlak van de scheur, aangezien dieper in de barst O_2 tekorten kunnen ontstaan. In dit proefschrift werd een alternatief metabolisch proces onderzocht om MICP te induceren, namelijk biologische nitraat (NO_3^-) reductie voor intrinsieke reparatie van scheuren in beton. De belangrijkste doelstellingen waren om het potentieel van biologisch nitraat (NO_3^-) te verkennen als alternatieve technologie voor microbieel zelfhelend beton en om de technologie dichter bij de markt te brengen door aanpassing van de parameters.

Om het potentieel van de denitrificatie te onderzoeken werden in de beginfase reinculturen geïsoleerd. Deze reinculturen werden met commerciële beschermende dragers

getest in mortel. Tijdens het isolatieproces werden stress-omstandigheden opgelegd die lijken op de betonomgeving (uitdroging, temperatuurschok, uithongering). Twee isolaten, namelijk *Diaphorobacter nitroreducens* en *Pseudomonas aeruginosa*, werden verder onderzocht voor de optimalisatie van hun MICP proces. Ze werden getest onder omstandigheden die vergelijkbaar zijn met de betonomgeving en de groeimedia bevatten enkel een koolstofbron ($HCOO^-$), een elektronacceptor (NO_3^-) en neerslaginitiator (Ca^{2+}). Het vermogen om herhaaldelijk $CaCO_3$ te precipiteren werd onderzocht voor het geval dat er op dezelfde plaats meerdere herstellingen dienen te gebeuren. $CaCO_3$-precipitatie opbrengsten van 14,1 g $CaCO_3$ / g NO_3-N en 18,7 g $CaCO_3$ / g NO_3-N werden bereikt voor *Diaphorobacter nitroreducens* en *Pseudomonas aeruginosa*, respectievelijk. De $CaCO_3$ precipitatiesnelheden waren tussen 30-50 mg / h en de stammen werden voldoende resistent bevonden om deze verder te testen.

Ongeacht hun weerstand, dienen axenische culturen geïmmobiliseerd te worden op beschermende dragers vooraleer ze aan beton toegevoegd worden om te voorkomen dat ze verpletterd worden als gevolg van de optredende krimp van de matrix. Daarom werden commerciële beschermende dragers zoals diatomeeënaarde, geëxpandeerde kleikorrels en granulaire actieve kooldeeltjes getest op hun verenigbaarheid met de geselecteerde kolonies *Diaphorobacter nitroreducens* en *Pseudomonas aeruginosa* en op hun beschermend effect bij verschillende pH-waarden (pH 7, pH 9,5 en pH 13). Bovendien werd de geschiktheid van de beschermende dragers voor gebruik in mortel onderzocht. De belangrijkste parameter was de effectiviteit op vlak van bescherming van bacteriën tijdens het mortelmengen en tot het moment van scheurvorming. Ten tweede werd de verenigbaarheid met de mortel en voedingsstoffen, die tijdens bacterieel scheurherstel noodzakelijk zijn, getest. Tenslotte was het noodzakelijk om de invloed van de bacteriële activiteit op de stalen wapening te testen. Resultaten toonden aan dat alle beschermende dragers verenigbaar waren met de bacteriën en de bacteriën voor 28 dagen overleefden in mortel. Significante bacteriële activiteit werd gevonden bij de bacteriën verzameld van het scheuroppervlak. Van de onderzochte beschermende dragers was diatomeeënaarde 20 % minder efficiënt op het gebied van de bescherming van bacteriën tijdens mortelinmenging dan de granulaattypes. Bovendien bleek diatomeeënaarde niet verenigbaar met de voedingsstoffen die bacteriën nodig hebben voor het herstellen van barsten, waardoor de bindingstijd van de mortel met ongeveer 130 minuten afnam. Geëxpandeerde kleideeltjes en granulaire actieve kooldeeltjes toonden goede compatibiliteit met zowel de mortel als de voedingsstoffen, waardoor de morteleigenschappen niet significant beïnvloed werden. Wat de interactie tussen bacteriën en stalen wapening betreft, wezen de positieve resultaten op corrosie-inhibitie door de microbiële geproduceerde

NO_2^-. Daarom was het veilig en gunstig de bacteriën verder te onderzoeken en geëxpandeerde kleideeltjes of granulaire actieve koolstofdeeltjes te gebruiken als drager in dergelijke testen.

Om te bewijzen dat biologische NO_3^--reductie potentieel heeft in zelfhelend beton, was het noodzakelijk het verbeterde scheurherstel van deze mortels aan te tonen. De geselecteerde bacteriële kolonies *Diaphorobacter nitroreducens* en *Pseudomonas aeruginosa* (0.5 gewichtspercent t.o.v. cement), ingekapseld in geëxpandeerde klei of granulaire actieve kooldeeltjes (5 gewichtspercent t.o.v. cement), werden aan de mortel toegevoegd en getest voor intrinsiek scheurherstel. De heling van scheuren met wijdtes tussen 100 en 750 mm werd getest. Wanneer de gescheurde bacteriële proefstukken volledig ondergedompeld werden in water voor 28 dagen, konden scheuren tot ~400 mm geheeld worden. Er werd geen significant verschil vastgesteld bij het gebruik van de verschillende types bacteriën en verschillende dragers. Wanneer de onderdompelingstijd verlengd werd tot 56 dagen, konden scheuren tot ~500 mm hersteld worden. De herwinning in waterdichtheid bedroeg ~85% voor scheuren met een wijdte van ~450 mm na 56 dagen heling. Deze resultaten toonden aan dat biologische NO_3^--reductie potentieel heeft en dat er ruimte is om wijzigingen aan te brengen aan de helende agentia om zo de technologie dichter bij de markt te brengen.

Microbieel zelfhelend beton kost ~1300 tot 2800 €/m³ bij het gebruik van axenische culturen in dezelfde hoeveelheid als aangewend in dit doctoraat. Deze axenische culturen worden meestal gebruikt in experimentele studies om het concept aan te tonen. Aangezien één van de belangrijkste doelen van dit onderzoek was om de ontwikkelde technologie dichter bij de markt te brengen, was het noodzakelijk het onderzoek naar mogelijke bacteriële agentia uit te breiden. Het gebruik van niet-axenische culturen werd daarom beschouwd. Een innovatieve benadering werd gevolgd, waarbij speciale bio-granulaten, bestaande uit verschillende types bacteriën (70% van het granulaatgehalte) geproduceerd werden op laboschaal en onderzocht werden als zelfbeschermd helend agens. Hun gedrag bij verschillende pH-waarden (pH 7, pH 9,5 en pH 13) en hun activiteit na inbreng in mortels werd getest. Verder werd hun compatibiliteit met mortel onderzocht door de verandering in druksterkte en bindingstijd te evalueren.

Zonder enige bescherming of drager vertoonden biogranulaten dezelfde prestatie als de beschermde axenische culturen onder dezelfde omstandigheden. Verder waren de granulaten compatibel met de mortel bij de onderzochte dosissen (0,7 gewichtspercent t.o.v. cement en 1,4 gewichtspercent t.o.v. cement) wat hen een veelbelovend alternatief maakt voor de axenische culturen.

De mogelijke wijziging in de performantie van microbieel zelfhelend beton, wanneer

beschermde axenische culturen vervangen worden door zelfbeschermde niet-axenische culturen, moet onderzocht worden. Hiertoe werden mortelproefstukken met gegranuleerde bacteriën vervaardigd (in een dosis van 0.5 en 1 gewichts-% bacteriën versus cement) en onderworpen aan een trekkracht na 28 dagen nabehandeling om meerdere scheuren te creëren met scheurwijdte tussen 90 en 640 µm. Identieke proefstukken werden gemaakt om de zelfhelende performantie te onderzoeken van scheuren gevormd na 6 maand nabehandeling. Scheuren in microbiële monsters werden effectief geheeld voor scheurwijdtes tot ~500 µm en ~400 µm, voor scheuren gevormd op jonge respectievelijk oudere leeftijd.

Na 28 dagen heling van een scheur met een wijdte van ~450 µm, werd 74% van de waterdichtheid herwonnen. Bovendien verminderde de waterdoorlatendheid na 28 dagen heling van een scheur van ~400 µm met 80% door de microbieel geïnduceerde $CaCO_3$ precipitatie in de scheur. Een stabiele werking van de bacteriën werd bekomen voor de heling van jonge scheuren en scheuren gevormd op latere leeftijd, terwijl de autogene heling en dus ook de totale heling significant daalden met de ouderdom van het beton.

Samenvattend kan gesteld worden dat in deze doctoraatsthesis het potentieel van biologische NO_3^--reductie voor de ontwikkeling van microbieel zelfhelend beton succesvol gedemonstreerd werd. Bovendien werd door de inspanningen om de microbiële agentia te modificeren, de kost van het microbieel zelfhelend beton gereduceerd tot ~240 €/m^3.

In toekomstige studies is het aan te raden om axenische culturen te gebruiken om de grenzen van de technologie en de ruimte voor verbetering af te tasten, terwijl de niet-axenische culturen, meer bepaald de zelfbeschermde niet-axenische culturen kunnen aangewend worden voor praktische toepassingen.

REFERENCES

[1] E. Pe, A.N. Re, ERMCO Guide to EN206:2013 1, 2014.

[2] T. Hirschi, H. Knauber, M. Lanz, J. Schrabback, C. Spirig, U. Waeber, Construction Sika ® Concrete Handbook, 2005.

[3] J.M. Crow, The concrete conundrum, Chem World. March (2008) 62–66.

[4] C. Le Quéré, R. Moriarty, R.M. Andrew, G.P. Peters, P. Ciais, P. Friedlingstein, et al., Global carbon budget 2014, Earth Syst Sci Data. 7 (2015) 47–85. doi:10.5194/essd-7-47-2015.

[5] NRMCA, Concrete CO_2 Fact Sheet, 2012.

[6] H.G. van Oss, U.S Geological Survey, Mineral commodity summaries, 2015.

[7] Portland Cement Association, World Cement Consumption, 2014.

[8] P. Van Den Heede, N. De Belie, A service life based global warming potential for high-volume fly ash concrete exposed to carbonation, Constr Build Mater. 55 (2014) 183–193. doi:10.1016/j.conbuildmat.2014.01.033.

[9] M. De Schepper, P. Verlé, I. Van Driessche, N. De Belie, Use of Secondary Slags in Completely Recyclable Concrete, J Mater Civ Eng. 27 (2012) 1–9. doi:10.1061/(ASCE)MT.1943-5533.0001133.

[10] M. De Schepper, P. Van den Heede, I. Van Driessche, N. De Belie, Life Cycle Assessment of Completely Recyclable Concrete, Materials (Basel). 7 (2014) 6010–6027. doi:10.3390/ma7086010.

[11] P. Van den Heede, M. Maes, N. De Belie, Influence of active crack width control on the chloride penetration resistance and global warming potential of slabs made with fly ash + silica fume concrete, Constr Build Mater. 67 (2013) 74–80. doi:10.1016/j.conbuildmat.2013.10.032.

[12] World Steel Association, Steel Statistical Yearbook, 2014.

[13] B. Klemczak, A. Knoppik-Wróbel, Early age thermal and shrinkage cracks in concrete structures - description of the problem, Archit Civ Eng Environ. (2011).

[14] ACI Committee 224, ACI 224 - Control of Cracking in Concrete Structures, 2008.

[15] EN 1992, EN 1992-1-1 General rules and rules for buildings, 2004.

[16] M. Maes, Combined effects of chlorides and sulphates on cracked and self-healing concrete in marine environments, PhD Thesis, Ghent University, Belgium, 2014. doi:10.1073/pnas.0703993104.

[17] Strategy Development Council, Vision 2020-A Vision for the Concrete Repair , Protection and Strengthening Industry, 2006.

[18] M. Yunovich, N.G. Thompson, T.B. Vanyos, L. Lave, Highway bridges-Appendix D,

2002.

[19]   M. Yunovich, A.J. Mierzwa, Waterways and Ports-Appendix F, 2002.

[20]   M. de Rooij, K. Van Tittelboom, N. De Belie, E. Schlangen, Self-healing phenomena in cement-based materials, 2011.

[21]   K. Van Tittelboom, N. De Belie, Self-Healing in Cementitious Materials—A Review, Materials (Basel). 6 (2013) 2182–2217. doi:10.3390/ma6062182.

[22]   J. Wang, H. Soens, W. Verstraete, N. De Belie, Self-healing concrete by use of microencapsulated bacterial spores, Cem Concr Res. 56 (2014) 139–152. doi:10.1016/j.cemconres.2013.11.009.

[23]   F. Silva, N. De Belie, N. Boon, W. Verstraete, Production of non-axenic ureolytic spores for self-healing concrete applications, Constr Build Mater. (2015). doi:10.1016/j.conbuildmat.2015.05.049.

[24]   C. Edvardsen, Water permeability and autogenous healing of cracks in concrete, ACI Mater J. 96 (1999) 448–454.

[25]   R. Kenneth, O. Floyd, Autogenous healing of cement paste, ACI Mater J. 52 (1956) 1083–1098.

[26]   K. Van Tittelboom, N. De Belie, D. Van Loo, P. Jacobs, Self-healing efficiency of cementitious materials containing tubular capsules filled with healing agent, Cem Concr Compos. 33 (2011) 497–505. doi:10.1016/j.cemconcomp.2011.01.004.

[27]   W. Li, Z. Jiang, Z. Yang, N. Zhao, W. Yuan, Self-healing efficiency of cementitious materials containing microcapsules filled with healing adhesive: mechanical restoration and healing process monitored by water absorption., PLoS One. 8 (2013) e81616. doi:10.1371/journal.pone.0081616.

[28]   L. Sun, W.Y. Yu, Q. Ge, Experimental research on the self-healing performance of micro-cracks in concrete bridge, Adv Mater Res. 250-253 (2011) 28–32.

[29]   V.C. Li, Y. Mook, Y. Chan, Feasibility study of a passive smart self-healing cementitious composite, Compos Part B. 29 (1998) 819–827.

[30]   Y. Yang, M.D. Lepech, E.-H. Yang, V.C. Li, Autogenous healing of engineered cementitious composites under wet–dry cycles, Cem Concr Res. 39 (2009) 382–390. doi:10.1016/j.cemconres.2009.01.013.

[31]   E. Herbert, V. Li, Self-healing of microcracks in engineered cementitious composites (ECC) under a natural environment, Materials (Basel). 6 (2013) 2831–2845. doi:10.3390/ma6072831.

[32]   Y. Kuang, J. Ou, Self-repairing performance of concrete beams strengthened using superelastic SMA wires in combination with adhesives released from hollow fibers, Smart Mater Struct. 17 (2008) 025020. doi:10.1088/0964-1726/17/2/025020.

[33]   Y. Kuang, J. Ou, Passive self-repairing concrete beams, J Cent South Univ Technol. 15 (2008) 411–417.

[34]   B. Isaacs, R. Lark, T. Jefferson, Crack healing of cementitious materials using shrinkable polymer tendons, Struct Concr. 14 (2013) 138–147.

[35]   A. Jefferson, C. Joseph, R. Lark, B. Isaacs, S. Dunn, B. Weager, A new system for crack closure of cementitious materials using shrinkable polymers, Cem Concr Res. 40 (2010) 795–801. doi:10.1016/j.cemconres.2010.01.004.

[36]   D. Snoeck, S. Steuperaert, K. Van Tittelboom, P. Dubruel, N. De Belie, Visualization

of water penetration in cementitious materials with superabsorbent polymers by means of neutron radiography, Cem Concr Res. 42 (2012) 1113–1121. doi:10.1016/j.cemconres.2012.05.005.

[37]   H.X.D. Lee, H.S. Wong, N.R. Buenfeld, The potential of superabsorbent polymer for self-sealing cracks in concrete, Adv Appl Ceram. 109 (2010) 296–302.

[38]   A. Mignon, D. Snoeck, D. Schaubroeck, N. Luickx, P. Dubruel, S. Van Vlierberghe, et al., pH-responsive superabsorbent polymers: A pathway to self-healing of mortar, React Funct Polym. 93 (2015) 68–76. doi:10.1016/j.reactfunctpolym.2015.06.003.

[39]   H.M. Jonkers, Self Healing Concrete : A Biological Approach, in: S. van der Zwaag (Ed.), Self Heal Mater Altern Approach to 20 Centuries Mater Sci, 2007: pp. 195–204.

[40]   V. Wiktor, H.M. Jonkers, Quantification of crack-healing in novel bacteria-based self-healing concrete, Cem Concr Compos. 33 (2011) 763–770. doi:10.1016/j.cemconcomp.2011.03.012.

[41]   H.L. Ehrlich, D. Newman, Geomicrobiology, 5th Ed, CRC Press, New York, 2008.

[42]   G. Nadson, Microorganisms as Geologic Agents. I. Tr Komisii Isslect Min Vodg, St. Petersburg: Slavyanska, 1903., in: I Tr Komisii Isslect Min Vodg, St. Petersburg: Slavyanska, 1903.

[43]   G. Nadson, Beitrag zur Kenntnis der bakteriogenen Kalkablagerung, Arch Fur Hydrobiol. 19 (1928) 154–164.

[44]   F. Hammes, A. Seka, K. Van Hege, T. Van de Wiele, J. Vanderdeelen, S.D. Siciliano, et al., Calcium removal from industrial wastewater by bio-catalytic $CaCO_3$ precipitation, J Chem Technol Biotechnol. 78 (2003) 670–677. doi:10.1002/jctb.840.

[45]   V.S. Whiffin, L. van Paassen, M.P. Harkes, Microbial Carbonate Precipitation as a Soil Improvement Technique, Geomicrobiol J. 24 (2007) 417–423. doi:10.1080/01490450701436505.

[46]   M.P. Harkes, L. a. van Paassen, J.L. Booster, V.S. Whiffin, M.C.M. van Loosdrecht, Fixation and distribution of bacterial activity in sand to induce carbonate precipitation for ground reinforcement, Ecol Eng. 36 (2010) 112–117. doi:10.1016/j.ecoleng.2009.01.004.

[47]   W. De Muynck, D. Debrouwer, N. De Belie, W. Verstraete, Bacterial carbonate precipitation improves the durability of cementitious materials, Cem Concr Res. 38 (2008) 1005–1014. doi:10.1016/j.cemconres.2008.03.005.

[48]   W. De Muynck, K. Cox, N. De Belie, W. Verstraete, Bacterial carbonate precipitation as an alternative surface treatment for concrete, Constr Build Mater. 22 (2008) 875–885. doi:10.1016/j.conbuildmat.2006.12.011.

[49]   I. Karatas, Microbiological improvement of the physical properties of soils, PhD Thesis, Arizona State University, US, 2008.

[50]   W.R.L. Van Der Star, E. Taher, M.P. Harkes, M. Blauw, M.C.M. Van Loosdrecht, L. a. Van Paassen, Use of waste streams and microbes for in situ transformation of sand into sandstone, in: Proc Int Symp Gr Improv Technol Case Hist, Research Publishing Services, Singapore, 2009: pp. 177–182. doi:10.3850/GI126.

[51]   L. van Paassen, C.M. Daza, M. Staal, D.Y. Sorokin, W. van der Zon, M.C.M. van Loosdrecht, Potential soil reinforcement by biological denitrification, Ecol Eng. 36 (2010) 168–175. doi:10.1016/j.ecoleng.2009.03.026.

[52]   G. Ganendra, W. De Muynck, A. Ho, E.C. Arvaniti, B. Hosseinkhani, J.A. Ramos, et al., Formate oxidation-driven calcium carbonate precipitation by *Methylocystis parvus* OBBP., Appl Environ Microbiol. 80 (2014) 4659–67. doi:10.1128/AEM.01349-14.

[53]   F. Hammes, A. Seka, S. De Knijf, W. Verstraete, A novel approach to calcium removal from calcium-rich industrial wastewater, Water Res. 37 (2003) 699–704.

[54]   H.M. Jonkers, E. Schlangen, A two component bacteria-based self-healing concrete, Concr Repair, Rehabil Retrofit II. (2009) 215–220.

[55]   H.M. Jonkers, A. Thijssen, G. Muyzer, O. Copuroglu, E. Schlangen, Application of bacteria as self-healing agent for the development of sustainable concrete, Ecol Eng. 36 (2010) 230–235. doi:10.1016/j.ecoleng.2008.12.036.

[56]   H.M. Jonkers, Bacteria-based self-healing concrete, HERON. 56 (2011) 1–12.

[57]   K. Van Tittelboom, N. De Belie, W. De Muynck, W. Verstraete, Use of bacteria to repair cracks in concrete, Cem Concr Res. 40 (2010) 157–166. doi:10.1016/j.cemconres.2009.08.025.

[58]   J. Wang, N. De Belie, W. Verstraete, Diatomaceous earth as a protective vehicle for bacteria applied for self-healing concrete., J Ind Microbiol Biotechnol. 39 (2012) 567–77. doi:10.1007/s10295-011-1037-1.

[59]   J. Wang, D. Snoeck, S. Van Vlierberghe, W. Verstraete, N. De Belie, Application of hydrogel encapsulated carbonate precipitating bacteria for approaching a realistic self-healing in concrete, Constr Build Mater. 68 (2014) 110–119. doi:10.1016/j.conbuildmat.2014.06.018.

[60]   J. Wang, J. Dewanckele, V. Cnudde, S. Van Vlierberghe, W. Verstraete, N. De Belie, X-ray computed tomography proof of bacterial-based self-healing in concrete, Cem Concr Compos. 53 (2014) 289–304. doi:10.1016/j.cemconcomp.2014.07.014.

[61]   J. Xu, W. Yao, Multiscale mechanical quantification of self-healing concrete incorporating non-ureolytic bacteria-based healing agent, Cem Concr Res. 64 (2014) 1–10. doi:10.1016/j.cemconres.2014.06.003.

[62]   C. Stuckrath, R. Serpell, L.M. Valenzuela, M. Lopez, Quantification of chemical and biological calcium carbonate precipitation: Performance of self-healing in reinforced mortar containing chemical admixtures, Cem Concr Compos. 50 (2014) 10–15. doi:10.1016/j.cemconcomp.2014.02.005.

[63]   F.B. Silva, Up-scaling the production of bacteria for self-healing concrete application, PhD Thesis, Ghent University, 2015.

[64]   M. Luo, C. Qian, R. Li, Factors affecting crack repairing capacity of bacteria-based self-healing concrete, Constr Build Mater. 87 (2015) 1–7. doi:10.1016/j.conbuildmat.2015.03.117.

[65]   F. Hammes, N. Boon, J. De Villiers, W. Verstraete, S.D. Siciliano, Strain-specific ureolytic microbial calcium carbonate precipitation, Appl Environ Microbiol. 69 (2003) 4901–4909. doi:10.1128/AEM.69.8.4901.

[66]   D.J. Randall, T.K.N. Tsui, Ammonia toxicity in fish, Mar Pollut Bull. 45 (2002) 17–23.

[67]   Y.Ç. Erşan, N. De Belie, N. Boon, Microbially induced $CaCO_3$ precipitation through denitrification : An optimization study in minimal nutrient environment, Biochem Eng J. 101 (2015) 108–118. doi:10.1016/j.bej.2015.05.006.

[68]   V.S. Ramachandran, Concrete Admixtures Handbook, 2nd ed., Elsevier, 1996.

[69]   H. Justnes, E.C. Nygaard, Calcium nitrate as a multifunctional concrete admixture, in: Proc Int RILEM Conf Role Admixtures High Perform Concr, México, 1999: pp. 199–212.

[70]   C. Glass, J. Silverstein, Denitrification kinetics of high nitrate concentration water: pH effect on inhibition and nitrite accumulation, Water Res. 32 (1998) 831–839. doi:10.1016/S0043-1354(97)00260-1.

[71]   J.M. Gaidis, Chemistry of corrosion inhibitors, Cem Concr Compos. 26 (2004) 181–189. doi:10.1016/S0958-9465(03)00037-4.

[72]   P. Garcés, P. Saura, a. Méndez, E. Zornoza, C. Andrade, Effect of nitrite in corrosion of reinforcing steel in neutral and acid solutions simulating the electrolytic environments of micropores of concrete in the propagation period, Corros Sci. 50 (2008) 498–509. doi:10.1016/j.corsci.2007.08.016.

[73]   T.A. Söylev, M.G. Richardson, Corrosion inhibitors for steel in concrete: State-of-the-art report, Constr Build Mater. 22 (2008) 609–622. doi:10.1016/j.conbuildmat.2006.10.013.

[74]   K.Y. Ann, H.S. Jung, H.S. Kim, S.S. Kim, H.Y. Moon, Effect of calcium nitrite-based corrosion inhibitor in preventing corrosion of embedded steel in concrete, Cem Concr Res. 36 (2006) 530–535. doi:10.1016/j.cemconres.2005.09.003.

[75]   D. Gao, L. Liu, H. Liang, W.-M. Wu, Aerobic granular sludge: characterization, mechanism of granulation and application to wastewater treatment, Crit Rev Biotechnol. 31 (2011) 137–52. doi:10.3109/07388551.2010.497961.

[76]   Y.Ç. Erşan, T.H. Erguder, The effects of aerobic/anoxic period sequence on aerobic granulation and COD/N treatment efficiency., Bioresour Technol. 148 (2013) 149–56. doi:10.1016/j.biortech.2013.08.096.

[77]   C. Caudan, A. Filali, M. Spérandio, E. Girbal-Neuhauser, Multiple EPS interactions involved in the cohesion and structure of aerobic granules., Chemosphere. 117 (2014) 262–70. doi:10.1016/j.chemosphere.2014.07.020.

[78]   J.T. DeJong, B.M. Mortensen, B.C. Martinez, D.C. Nelson, Bio-mediated soil improvement, Ecol Eng. 36 (2010) 197–210. doi:10.1016/j.ecoleng.2008.12.029.

[79]   J. Dick, W. De Windt, B. De Graef, H. Saveyn, P. Van der Meeren, N. De Belie, et al., Bio-deposition of a calcium carbonate layer on degraded limestone by Bacillus species., Biodegradation. 17 (2006) 357–67. doi:10.1007/s10532-005-9006-x.

[80]   W. De Muynck, N. De Belie, W. Verstraete, Microbial carbonate precipitation in construction materials: A review, Ecol Eng. 36 (2010) 118–136. doi:10.1016/j.ecoleng.2009.02.006.

[81]   L. Maignien, D. Depreiter, a. Foubert, J. Reveillaud, L. De Mol, P. Boeckx, et al., Anaerobic oxidation of methane in a cold-water coral carbonate mound from the Gulf of Cadiz, Int J Earth Sci. 100 (2010) 1413–1422. doi:10.1007/s00531-010-0528-z.

[82]   E. Boquet, A. Boronat, A. Ramos-Cormenzana, Production of calcite (calcium carbonate) crystals by soil bacteria is a general phenomenon, Nature. 246 (1973) 527–529.

[83]   F. Hammes, W. Verstraete, Key roles of pH and calcium metabolism in microbial carbonate precipitation, Rev Environ Sci Biotechnol. 1 (2002) 3–7. http://www.springerlink.com/index/X9A9BU4P3XVRCPPJ.pdf.

[84]   J. Wang, Self-healing concrete by means of immobilized carbonate precipitating

bacteria, PhD Thesis, Ghent University, Belgium, 2013.

[85] B. Khan, B. Baradan, The effect of sugar on setting-time of various types of cements, Sci Vis. 8 (2002) 71–78.

[86] V. Tydlitát, T. Matas, C. Robert, Effect of w/c and temperature on the early-stage hydration heat development in Portland-limestone cement, Constr Build Mater. 50 (2014) 140–147. doi:10.1016/j.conbuildmat.2013.09.020.

[87] R. Vilchez, C. Pozo, M.A. Gomez, B. Rodelas, J. Gonzalez-Lopez, Dominance of sphingomonads in a copper-exposed biofilm community for groundwater treatment, Microbiology. 153 (2007) 325–337. doi:10.1099/mic.0.2006/002139-0.

[88] B.R. Mohapatra, A. Mazumder, Comparative efficacy of five different rep-PCR methods to discriminate *Escherichia coli* populations in aquatic environments., Water Sci Technol. 58 (2008) 537–547. doi:10.2166/wst.2008.424.

[89] W.J. Hunter, Accumulation of nitrite in denitrifying barriers when phosphate is limiting., J Contam Hydrol. 66 (2003) 79–91. doi:10.1016/S0169-7722(03)00008-1.

[90] S. Van Nevel, S. Koetzsch, H.-U. Weilenmann, N. Boon, F. Hammes, Routine bacterial analysis with automated flow cytometry., J Microbiol Methods. 94 (2013) 73–6. doi:10.1016/j.mimet.2013.05.007.

[91] S. Bricha, K. Ounine, S. Oulkheir, N. El Haloui, B. Attarassi, Heat resistance of *Pseudomonas aeruginosa* in preparations at the base of cucumber, tomato and lettuce as affected by pH and sodium chloride, World J Biol Res. 3 (2010) 1–8.

[92] T. Paustian, G. Roberts, Through the microscope: Adventures in Microbiology, Textbook Consortia, 4th Edition, 2014. 60 (n.d.). http://www.microbiologytext.com/index.php?module=Book&func=displayarticle&art_id=60.

[93] A. Kramer, I. Schwebke, G. Kampf, How long do nosocomial pathogens persist on inanimate surfaces? A systematic review., BMC Infect Dis. 6 (2006) 130–137. doi:10.1186/1471-2334-6-130.

[94] E.B. Roberson, M.K. Firestone, Relationship between desiccation and exopolysaccharide production in a soil *Pseudomonas* sp ., Appl Environ Microbiol. 58 (1992) 1284–1291.

[95] M.R.D. Souza-Ault, L.T. Smith, G.M. Smith, Roles of N-Acetylglutaminylglutamine Amide and glycine betaine in adaptation of *Pseudomonas aeruginosa* to osmotic stress, Appl Environ Microbiol. 59 (1993) 473–478.

[96] S.J. Wenner, Hydrating the *Pseudomonas aeruginosa* periplasm under desiccating conditions, Iowa State University, 2014.

[97] R. Kumar, S. Zhao, M.W. Vetting, Prediction and biochemical demonstration of a catabolic pathway for the osmoprotectant proline betaine, MBio. e00933-13 (2014). doi:10.1128/mBio.00933-13.Updated.

[98] S.-J. Kim, J.-Y. Moon, J.-H. Ahn, H.-Y. Weon, S.-B. Hong, S.-J. Seok, et al., *Diaphorobacter aerolatus* sp. nov., isolated from air, and emended description of the genus *Diaphorobacter*., Int J Syst Evol Microbiol. 64 (2014) 513–517. doi:10.1099/ijs.0.051060-0.

[99] S.S. Chakravarthy, S. Pande, A. Kapoor, A.S. Nerurkar, Comparison of denitrification between *Paracoccus* sp. and *Diaphorobacter* sp., Appl Biochem Biotechnol. 165 (2011) 260–9. doi:10.1007/s12010-011-9248-5.

[100] A. Redfield, The biological control of chemical factors in the environment, Am Sci. September (1958) 205–230.

[101] G. Tchobanoglous, F. Burton, H. Stensel, Wastewater Engineering, Treatment, Disposal, and Reuse, 4th Ed, McGraw-Hill, Inc, New York, 2004.

[102] B.E. Rittmann, P. McCarty, Environmental Biotechnology: Principles and Applications, McGraw-Hill, Inc, 2001.

[103] P. McCarty, Energetics and bacterial growth, in: S.D. Fraust, V.J. Hunter (Eds.), Org Compd Aquat Environ, Marcel Dekker, New York, 1971.

[104] S. Dupraz, M. Parmentier, B. Ménez, F. Guyot, Experimental and numerical modeling of bacterially induced pH increase and calcite precipitation in saline aquifers, Chem Geol. 265 (2009) 44–53. doi:10.1016/j.chemgeo.2009.05.003.

[105] M.A. Rivadeneyra, I. Perez-Garcia, V. Salmeron, A. Ramos-Cormenzana, Bacterial precipitation of calcium carbonate in presence of phosphate, Soil Biol Biochem. 17 (1985) 171–172. doi:10.1016/0038-0717(85)90111-7.

[106] B. Radcliffe, D. Nicholas, Some properties of a nitrite reductase from *Pseudomonas denitrificans*, Biochim Biophys Acta. 153 (1968) 545–554.

[107] J. Ma, Q. Yang, S. Wang, L. Wang, A. Takigawa, Y. Peng, Effect of free nitrous acid as inhibitors on nitrate reduction by a biological nutrient removal sludge., J Hazard Mater. 175 (2010) 518–523. doi:10.1016/j.jhazmat.2009.10.036.

[108] Y. Zhou, L. Ganda, M. Lim, Z. Yuan, S. Kjelleberg, W.J. Ng, Free nitrous acid (FNA) inhibition on denitrifying poly-phosphate accumulating organisms (DPAOs)., Appl Microbiol Biotechnol. 88 (2010) 359–369. doi:10.1007/s00253-010-2780-3.

[109] G.J. Tortora, B.R. Funke, C.L. Case, Microbiology - An Introduction, 11th Ed, Pearson, New York, 2013.

[110] J. Wang, K. Van Tittelboom, N. De Belie, W. Verstraete, Use of silica gel or polyurethane immobilized bacteria for self-healing concrete, Constr Build Mater. 26 (2012) 532–540. doi:10.1016/j.conbuildmat.2011.06.054.

[111] F.B. Silva, N. Boon, N. De Belie, W. Verstraete, Industrial Application of Biological Self-healing Concrete: Challenges and Economical Feasibility, J Commer Biotechnol. 21 (2015) 31–38. doi:10.5912/jcb662.

[112] C. Valverde-Sarmiento, D. Espinosa-Iglesias, M.I. Bautista-Toledo, M. a. Álvarez-Merino, F.J. Maldonado-Hódar, F. Carrasco-Marín, et al., Bacteria supported on carbon films for water denitrification, Chem Eng J. 259 (2015) 424–429. doi:10.1016/j.cej.2014.08.034.

[113] M. Horgnies, F. Serre, I. Dubois-brugger, E. Gartner, NOx De - pollution Using Activated Charcoal Concrete - From Laboratory Experiments to Tests with Prototype Garages, Cem Concr Res. 42 (2014) 1348–1355.

[114] E. Ben-Jacob, I. Cohen, H. Levine, Cooperative self-organization of microorganisms, Adv Phys. 49 (2000) 395–554. doi:10.1080/000187300405228.

[115] A. Królikowski, J. Kuziak, Impedance study on calcium nitrite as a penetrating corrosion inhibitor for steel in concrete, Electrochim Acta. 56 (2011) 7845–7853. doi:10.1016/j.electacta.2011.01.069.

[116] Y.Ç. Erşan, T.H. Erguder, The effect of seed sludge type on aerobic granulation via anoxic-aerobic operation., Environ Technol. 35 (2014) 2928–39.

doi:10.1080/09593330.2014.925513.

[117] Y. Ji, M. Wu, B. Ding, F. Liu, F. Gao, The experimental investigation of width of semi-carbonation zone in carbonated concrete, Constr Build Mater. 65 (2014) 67–75. doi:10.1016/j.conbuildmat.2014.04.095.

[118] APHA, AWWA, WEF, Standard Methods for Examination of water and wastewater, 22nd Editi, 2012.

[119] Y.Ç. Erşan, J. Wang, N. Boon, N. De Belie, Ureolysis and denitrification based microbial strategies for self-healing concrete, in: Concr Solut Proc, 2014: pp. 59–64. doi:10.1201/b17394-10.

[120] J. Wan, Y. Bessière, M. Spérandio, Alternating anoxic feast/aerobic famine condition for improving granular sludge formation in sequencing batch airlift reactor at reduced aeration rate., Water Res. 43 (2009) 5097–108. doi:10.1016/j.watres.2009.08.045.

[121] H.Q.M. Yu, J.H. Tay, H.H.P. Fang, The roles of calcium in sludge granulation during uasb reactor start-up, Water Res. 35 (2001) 1052–1060.

[122] T.T. Ren, L. Liu, G.P. Sheng, X.W. Liu, H.Q. Yu, M.C. Zhang, et al., Calcium spatial distribution in aerobic granules and its effects on granule structure, strength and bioactivity., Water Res. 42 (2008) 3343–52. doi:10.1016/j.watres.2008.04.015.

[123] K.L. Thomas, D. Lloyd, L. Boddy, Effects of oxygen, pH and nitrate concentration on denitrification by *Pseudomonas* species. FEMS Microbiol. Lett. 118: 181 – 186., FEMS Microbiol Lett. 118 (1994) 181–186.

[124] W.T. Frankenberbger, J.B. Johanson, Effect of pH on enzyme stability in soils, Soil Biol Biochem. 14 (1982) 433–437.

[125] M. Simek, L. Jisova, D.W. Hopkins, What is the so-called optimum pH for denitrification in soil?, Soil Biol Biochem. 34 (2002) 1227–1234.

[126] J.K. Thomsen, T. Geest, R.P. Cox, Mass spectrometric studies of the effect of pH on the accumulation of intermediates in denitrification by *Paracoccus denitrificans*, Appl Environ Microbiol. 60 (1994) 536–541.

[127] P.B. Dhamole, R.R. Nair, S.F. D'Souza, S.S. Lele, Denitrification of highly alkaline nitrate waste using adapted sludge., Appl Biochem Biotechnol. 151 (2008) 433–40. doi:10.1007/s12010-008-8211-6.

[128] Y. Rafrafi, H. Ranaivomanana, A. Bertron, A. Albrecht, B. Erable, Surface and bacterial reduction of nitrate at alkaline pH: Conditions comparable to a nuclear waste repository, Int Biodeterior Biodegradation. 101 (2015) 12–22. doi:10.1016/j.ibiod.2015.03.013.

[129] K.D. Feng, J.-M. Racke, Y.F. Bollag, Use of immobilized bacteria to treat industrial wastewater containing a chlorinated pyridinol, Appl Microbiol Biotechnol. 47 (1997) 73–77.

[130] F.X. Simon, Y. Penru, M.M. Micó, J. Llorens, S. Esplugas, S. Baig, Biological activity in expanded clay (EC) and granulated activated carbon (GAC) seawater filters, Desalination. 328 (2013) 67–73. doi:10.1016/j.desal.2013.08.018.

[131] G. O'Toole, H.B. Kaplan, R. Kolter, Biofilm formation as microbial development, Annu Rev Microbiol. 54 (2000) 49–79.

[132] S.R. Farrah, D.R. Preston, G.A. Toranzos, M. Girard, G.A. Erdos, V. Vasuhdivan, Use of Modified Diatomaceous Earth for Removal and Recovery of Viruses in Watert,

Appl Environ Microbiol. 57 (1991) 2502–2506.

[133] J. Rivera-Utrilla, I. Bautista-Toledo, M.A. Ferro-Garcia, C. Moreno-Castilla, Activated carbon surface modifications by adsorption of bacteria and their effect on aqueous lead adsorption, J Chem Technol Biotechnol. 76 (2001) 1209–1215. doi:10.1002/jctb.506.

[134] C.-C. Ho, P.-H. Wang, Efficiency of a Multi-Soil-Layering System on Wastewater Treatment Using Environment-Friendly Filter Materials, Int J Environ Res Public Health. 12 (2015) 3362–3380. doi:10.3390/ijerph120303362.

[135] N. Öztürk, E.T. Köse, A kinetic study of nitrite adsorption onto sepiolite and powdered activated carbon, Desalination. 223 (2008) 174–179. doi:10.1016/j.desal.2007.01.209.

[136] S.A. Mir, Effect of electrolytes on the adsorption of nitrite and nitrate from aqueous solutions by activated carbon, J Appl Sci Environ Manag. 14 (2010) 5–11.

[137] N. Öztürk, E. Bektaş, Nitrate removal from aqueous solution by adsorption onto various materials, J Hazard Mater. 112 (2004) 155–162. doi:10.1016/j.jhazmat.2004.05.001.

[138] H. Demiral, G. Gündüzoğlu, Removal of nitrate from aqueous solutions by activated carbon prepared from sugar beet bagasse., Bioresour Technol. 101 (2010) 1675–1680. doi:10.1016/j.biortech.2009.09.087.

[139] G. Hamer, Microbial consortia for multiple pollutant biodegradation, Pure Appl Chem. 69 (1997) 2343–2356.

[140] C. Qian, L. Chen, H. Rong, X. Yuan, Hydrogen production by mixed culture of several facultative bacteria and anaerobic bacteria, Prog Nat Sci Mater Int. 21 (2011) 506–511. doi:10.1016/S1002-0071(12)60090-2.

[141] C. Poon, L. Lam, S.C. Kou, Y. Wong, R. Wong, Rate of pozzolanic reaction of metakaolin in high-performance cement pastes, Cem Concr Res. 31 (2001) 1301–1306.

[142] S.N. Liss, I.G. Droppo, G.G. Leppard, T.G. Milligan, Flocculation in Natural and Engineered Environmental Systems, 1st ed, CRC Press, Florida, US, 2004.

[143] L. Senff, D. Hotza, J. a Labrincha, Effect of diatomite addition on fresh and hardened properties of mortars investigated through mixture experiments, Adv Appl Ceram. 110 (2011) 142–150. doi:10.1179/1743676110Y.0000000009.

[144] J.M. Justice, K.E. Kurtis, Influence of Metakaolin Surface Area on Properties of Cement-Based Materials, (2007) 762–771.

[145] B.B. Sabir, S. Wild, J. Bai, Metakaolin and calcined clays as pozzolans for concrete : a review, 23 (2001).

[146] A. Nasseri, S. Rasoul-Amini, M. Morowvat, Y. Ghasemi, Single Cell Protein: Production and Process, Am J Food Technol. 6 (2011) 103–116.

[147] Y.Ç. Erşan, N. De Belie, N. Boon, Resilient Denitrifiers Wink at Microbial Self-Healing Concrete, Int J Environ Eng. 2 (2015) 28–32.

[148] H.M. Jonkers, Bacteria-based self-healing concrete, in: HERON Vol 56, 2011: pp. 1–12.

[149] U.S. Environmental Protection Agency, Nitrates and Nitrites - TEACH Chemical summary, 2007.

[150] Y.Ç. Erşan, F.B. Silva, N. Boon, W. Verstraete, N. De Belie, Screening of bacteria and concrete compatible protection materials, Constr Build Mater. 88 (2015) 196–203. doi:10.1016/j.conbuildmat.2015.04.027.

[151] F.G. Priest, Biological control of mosquitoes and other biting flies by *Bacillus sphaericus* and *Bacillus thuringiensis*, J Appl Bacteriol. 72 (1992) 357–369.

[152] M.Y.A. Mollah, W. Yu, R. Schennach, D.L. Cocke, A Fourier transform infrared spectroscopic investigation of the early hydration of Portland cement and the influence of sodium lignosulfonate, Cem Concr Res. 30 (2000) 267–273.

[153] T.L. Hughes, C.M. Methven, T.G. Jones, S.H. Pelham, P. Fletcher, C. Hall, Determining Cement Composition by Fourier Transform Infrared Spectroscopy, Adv Cem Based Mater. 2 (1995) 91–104.

[154] P. Yu, R.J. Kirkpatrick, B. Poe, P.F. McMillan, X. Cong, Structure of Calcium Silicate Hydrate (C-S-H): Near-, Mid-, and Far-Infrared Spectroscopy, J Am Ceram Soc. 82 (2004) 742–748. doi:10.1111/j.1151-2916.1999.tb01826.x.

[155] M.A. Trezza, A. Valle, O.B. Aires, Hydration Study of Ordinary Portland Cement in the Presence of Zinc Ions, Mater Res. 10 (2007) 331–334.

[156] D. Palin, V. Wiktor, H.M. Jonkers, Autogenous healing of marine exposed concrete: Characterization and quantification through visual crack closure, Cem Concr Res. 73 (2015) 17–24. doi:10.1016/j.cemconres.2015.02.021.

[157] V. Achal, A. Mukerjee, M. Sudhakara Reddy, Biogenic treatment improves the durability and remediates the cracks of concrete structures, Constr Build Mater. 48 (2013) 1–5. doi:10.1016/j.conbuildmat.2013.06.061.

[158] M.G. Sierra-Beltran, H.M. Jonkers, M. Ortiz, Field application of self--healing concrete with natural fibres as linings for irrigation canals in Ecuador, in: Fifth Int Conf Self-Healing Mater, Durham, NC, 2015: p. 32.

[159] Y.Ç. Erşan, E. Hernandez-Sanabria, N. De Belie, N. Boon, Enhanced crack healing performance of microbial concrete through nitrate reduction, Cem Concr Compos. (submitted).

[160] Y. Lv, C. Wan, X. Liu, Y. Zhang, D.-J. Lee, J.-H. Tay, Drying and re-cultivation of aerobic granules., Bioresour Technol. 129 (2013) 700–3. doi:10.1016/j.biortech.2012.12.178.

[161] Y.Ç. Erşan, H. Verbruggen, I. De Graeve, W. Verstraete, N. De Belie, N. Boon, Nitrate reducing CaCO3 precipitating bacteria survive in mortar and inhibit steel corrosion, Cem Concr Res. (2016).

[162] D. Palin, Y.C. Ersan, V. Wiktor, N. De Belie, H.M. Jonkers, A rapid and repeatable method for establishing the water permeability of cracked mortar specimens, in: FIB Symp 2015 - Concr Innov Des, Copenhagen, Denmark, 2015: pp. 333–334.

[163] D. Chicot, Hardness length-scale factor to model nano- and micro-indentation size effects, Mater Sci Eng A. 499 (2009) 454–461. doi:10.1016/j.msea.2008.09.040.

[164] W.C. Oliver, G.M. Pharr, Measurement of hardness and elastic modulus by instrumented indentation : Advances in understanding and refinements to methodology, J Mater Res. 19 (2004) 3–20.

[165] W.C. Oliver, G.M. Pharr, An improved technique for determining hardness and elastic modulus using load and displacement sensing indentation experiments, J Mater Res. 7 (1992) 1564–1583.

[166] J.C. Hay, A. Bolshakov, G.M. Pharr, A critical examination of the fundamental relations used in the analysis of nanoindentation data, J Mater. 14 (2008) 2296–2305.

[167] C. Harwood, S. Cutting, Molecular biological methods for *Bacillus*, John Wiley & Sons, 1990.

[168] H.-W. Reinhardt, M. Jooss, Permeability and self-healing of cracked concrete as a function of temperature and crack width, Cem Concr Res. 33 (2003) 981–985. doi:10.1016/S0008-8846(02)01099-2.

[169] V.C. Li, E. Herbert, Robust Self-Healing Concrete for Sustainable Infrastructure, J Adv Concr Technol. 10 (2012) 207–218. doi:10.3151/jact.10.207.

[170] S.K. Ramachandran, V. Ramakrishnan, S.S. Bang, Remediation of Concrete Using Micro-Organisms, ACI Mater J. 98 (2001) 3–9.

[171] S.S. Bang, J.K. Galinat, V. Ramakrishnan, Calcite precipitation induced by polyurethane-immobilized *Bacillus pasteurii*, Enzyme Microb Technol. 28 (2001) 404–409.

[172] F. Silva, N. Boon, N. De Belie, W. Verstraete, Industrial application of biological self-healing concrete: Challenges and economical feasibility, Commer Biotechnol. 21 (2015) 31–38. doi:10.5912/jcb662.

[173] Vpuk-Vacuum pumps UK, Side chanel blowers- Model TSC.pdf, (2015) 19.

[174] R.C. Hunter, T.J. Beveridge, Application of a pH-sensitive fluoroprobe (C-SNARF-4) for pH microenvironment analysis in *Pseudomonas aeruginosa* biofilms, Appl Environ Microbiol. 71 (2005) 2501–2510. doi:10.1128/AEM.71.5.2501.

[175] Composition of seawater, Water Cond Purif Mag. (2005). http://www.lenntech.com/composition-seawater.htm (accessed December 30, 2015).

[176] J.R. Mullaney, D.L. Lorenz, A.D. Arnston, Chloride in Groundwater and Surface Water in Areas Underlain by the Glacial Aquifer System Northern United States, 2009.

[177] K.M. Gardner, T. V Royer, Effect of Road Salt Application on Seasonal Chloride Concentrations and Toxicity in South-Central Indiana Streams, J Environ Qual. 39 (2010) 1036. doi:10.2134/jeq2009.0402.

[178] L.H.A. Habets, A. Deschildre, H. Knelissen, J. Arrieta, Zero effluent by application of biological treatment at high temperature, in: Proc. Intl. Environ. Conf. Exhib, Denver, US, 2000: pp. 833–839.

[179] M.J. Olivarri, Highlights of the 2014 National Ready Mixed Concrete Association Industry Data Survey (Analysis of 2013 Data), Concr Focus. (2014) oc1–oc5.

REFERENCES

CURRICULUM VITAE

CURRICULUM VITAE

Yusuf Çağatay Erşan holds a master degree in Environmental Engineering obtained in 2013 from Middle East Technical University, Ankara, Turkey. In February 2013 he started his PhD work at Ghent University as a research fellow in European Union Seventh Framework Programme [FP7/2007-2013]-(Marie Curie action SHeMat "Training Network for Self-Healing Materials: from Concepts to Market"). During his PhD he worked in both the Laboratory of Microbial Ecology and Technology (LabMET) and Magnel Laboratory for Concrete Research to investigate the biological nitrate reduction as an alternative pathway for development of microbial self-healing concrete. In the context of his research he worked with both axenic and non-axenic cultures. He was the first researcher investigating the biological nitrate reduction for corrosion inhibition of steel and the use of bio-granules for development of self-healing concrete. His research led to several journal publications and was presented in many international conferences. During his PhD, he guided one master student investigating bio-deposition for surface treatment of degraded stones. He also has 4 years of experience in teaching classes for Bachelor and Master students in the field.

PERSONAL INFORMATION

Yusuf Çağatay Erşan   yusufcagatay.ersan@ugent.be
Sint-Amandstraat 30, Bus 6   Edinburgh – January 23, 1989
9000 Gent   not married
+32 470924995   Turkish

EDUCATION

2013 – 2016	PhD Applied Biological Sciences, Faculty of Bioscience Engineering, Ghent University
2011 – 2013	MSc Environmental Engineering, Middle East Technical University (3.86/4.00).
2011 –	Bachelor in English Language and Literature, Hacettepe University
2006 – 2011	Bachelor in Environmental Engineering, Middle East Technical University (2.72/4.00).

PROFESSIONAL EXPERIENCE

2011-2012   MSc student / Teaching Assistant at Environmental Engineering Department, Middle East Technical University
               Promoter: Assoc. Prof. dr. ir. Tuba H. Erguder

TEACHING EXPERIENCE

Bachelor's degree courses in Environmental Engineering Department at Middle East Technical University

2011-2012	Spring	ENVE304 Unit Operations and Processes of Wastewater Treatment
		ENVE330 Principles of Environmental Engineering
2012-2013	Fall	ENVE201 Fundamentals of Environmental Engineering
		ENVE208 Environmental Chemistry Laboratory

Master's degree courses in Bioscience Engineering at Ghent University

2013-2014	Fall	Practical exercises of Microbial Ecology and Environmental Sanitation course
2014-2015	Fall	Practical exercises of Microbial Ecology and Environmental Sanitation course
2015-2016	Fall	Practical exercises of Microbial Ecology and Environmental Sanitation course

PROFESSIONAL TRAINING

2014	Effective scientific communication, Principae, Belgium
2014	Leadership foundation by Dan Steer.
2014	Concrete Microscopy, TU Delft
2014	Stand and deliver: Giving presentations, VOX coaching, UK.
2011	ISO 14001: Environmental Management Systems, Union of Environmental Engineers, Turkey.

2011   OHSAS 18001: Worker Health and Safety, SASTEK, Turkey
2011   ISO 17025: Laboratory Accreditation Standards (from Strengthening Quality Infrastructure in Turkey Project - TR0702.12.01/001, EU financed)

EXTRA-CURRICULAR ACTIVITIES

2011-2013 Active member of the Turkish Red Crescent Youth.

SCIENTIFIC CONTRIBUTIONS

Articles available in the international peer reviewed journals covered by SCI core list (A1)

Erşan, Y.Ç., Palin, D., Jonkers H.M., De Belie, N., Boon, N. Quantification of microbial self-healing through a rapid permeability test and X-ray computed tomography. Manuscript in preparation.

Erşan, Y.Ç., Hernandez-Sanabria, E., De Belie, N., Boon, N. Enhanced crack healing performance of microbial concrete through nitrate reduction. Submitted to Cement and Concrete Composites.

Erşan, Y.Ç., Gruyaert, E., Louis, G., Lors, C., Boon, N. De Belie, N. (2015) Self-protected nitrate reducing culture for intrinsic repair of concrete cracks. Frontiers in Microbiology, 6:1228.

Erşan, Y.Ç., Verbruggen H., De Graeve, I., Verstraete, W., De Belie, N., Boon, N. Nitrate reducing $CaCO_3$ precipitating bacteria survive in mortar and inhibit steel corrosion. Cement and Concrete Research (Accepted with minor revisions).

Erşan, Y.Ç., Silva, F.B., Boon, N., Verstraete, W., De Belie, N. (2015) Screening of bacteria and concrete compatible protection materials. Construction and Building Materials, 88, 196-203.

Erşan, Y.Ç., De Belie, N., Boon, N. (2015). Microbially induced $CaCO_3$ precipitation through denitrification: An optimization study in minimal nutrient environment. Biochemical Engineering Journal, 101, 108-118.

Erşan, Y.Ç., Erguder T.H. (2014). The effect of seed sludge type on aerobic granulation via anoxic-aerobic operation. Environmental Technology, 35, 2928-2939.

Erşan, Y.Ç., Erguder T.H. (2013). The effects of aerobic/anoxic period sequence on aerobic granulation and COD/N treatment efficiency. Bioresource Technology, 148, 149-156.

Articles available in an international peer reviewed journal (A2)

Erşan, Y.Ç., De Belie, N., Boon, N. (2015). Resilient denitrifiers wink at microbial self-healing concrete. International Journal of Environmental Engineering, 2, 28-32.

Chapters in books (B2)

Tziviloglou, E., Van Tittelboom, K., Palin, D., Wang, J., Sierra-Beltran, M.G., **Erşan, Y.Ç.**, Mors, R., Wiktor, V., Jonkers, H.M., Schlangen, E., De Belie, N. Bio-based self-healing concrete: From research to field application. In: Hager, M.D., Schubert, U.S., van der Zwaag, S. (eds.) Advances in Polymer Sciences, Volume on Self-healing Materials, Springer. In press.

International conference proceedings (C1)

Erşan, Y.Ç., Wang, J., Boon, N., De Belie, N. (2014). Ureolysis and denitrification based microbial strategies for self-healing concrete. Concrete Solutions Proceedings, 1-3 September Belfast, UK, 59-64.

Ersan, Y.Ç., Kocaturk, I, Erguder, T.H. "Effect of seed sludge type on aerobic granulation and treatment efficiency of granules". The 6th International Conference on Environmental Science and Technology, June 25-29 Houston, USA.

International conference abstracts (C4)

Erşan, Y.Ç., De Belie, N., Boon, N. Non-axenic nitrate reducing culture supersedes axenic cultures in development of microbial self-healing concrete. Abstracts of the E-MRS Fall Meeting Symposium on Self-healing materials from concepts to market. 15-18 September, 2015, Warsaw, Poland

Erşan, Y.Ç., Boon, N., De Belie, N. Microbial self-healing concrete: Denitrification as an enhanced and environment-friendly approach. Abstracts of the 5th International Conference on Self-Healing Materials, 22-24 June, 2015 Durham, USA.

Palin, D., **Erşan, Y.Ç.**, Wiktor, V., De Belie, N., Jonkers, H.M. Rapid and repeatable method for establishing the permeability of cracked mortar specimens. Abstracts of fib Symposium of Concrete-Innovation and Design, 18-20 May, 2015, Copenhagen. Denmark.

APPENDIX

APPENDIX I

Brenntag price offer for ACDC feed solution compounds (July 23rd, 2015)

ConnectingChemistry

BRENNTAG

E-Mail

To:	Avecom NV		From:	Tom Plets
	Filipe Silva			
Email:	filipe.silva@avecom.be		Subject:	10148
Date:	23/07/2015		Direct dial:	+32 (0)56 78 82 62
			Email:	yamina.bourennani@brenntag.be

Dear Mr. Silva,

Referring to your request we are pleased to offer the following, based on our general sales conditions:

Product Name	SAP Code	Packaging	Quantity	Price
Calcium Nitrate Tetrahydrate	13477344	Big bags	25 mT	€ 30,5/100 kg
Disodium Phosphate Dihydrate	10028247	Big bags	25 mT	€ 45,0/100 kg
Magnesium Suphate Heptahydrate	10034998	Big bags	25 mT	€ 26,4/100 kg
Sodium Formate	141537XX	Big bags	25 mT	€ 38,2/100 kg
Calcium Formate Perstorp	544172XX	Big bags	25 mT	€ 5,1/100 kg
Sodium Nitrate	7632000X	Big bags	25 mT	€ 42,5/100 kg

VAT	: not included.
Terms of delivery	: CPT Belgium.
Time of delivery	: to discuss.
Terms of payment	: 30 days end of month.
Validity offer	: current prices.
Administration cost	: € 10, if the value of the goods is less than € 100

We hope to have made a competitive offer and are looking forward to your positive reply. In the meantime, we remain at your disposal for any further information.

Kind regards

Yamina Bourennani

Internal Account Manager

Industrial Sales & Services

ACKNOWLEDGMENTS

ACKNOWLEDGMENTS

One cannot simply achieve a PhD degree on his own. Behind this work there is a prodigious network built on friendship, collaboration, devotion and sacrifice. I might have thanked you several times during my PhD, yet I still want to specify it once more.

First and foremost, I would like to express my profound gratitude to my supervisors Prof. Dr. Nico Boon and Prof. Dr. Nele De Belie for believing in me and my ideals and giving me the chance to be the part of their working groups. I have learnt a lot from you; not only scientific knowledge but also planning, management, guidance skills. Thanks for helping and guiding me whenever I needed despite the fact that you had a very busy schedule.

I want to thank to my examination committee members Prof. Dr. Willy Verstraete, Prof. Dr. Robert Lark, Prof. Dr. Huber Rahier, Prof. Dr. Pascal Boeckx and Prof. Dr. Arne Verliefde for their valuable comments and remarks which improved the quality of this PhD thesis significantly. I am grateful to Prof. Verstraete, in particular, since he also guided and gave me suggestions throughout my whole PhD period, as if he was my supervisor.

Dr. Jianyun Wang deserves special gratitude for teaching me all the basics about concrete, and the way of working to achieve the most reliable results. Apart from that, I would like to thank all the colleagues in Prof. De Belie's group, especially the ones working on self-healing concrete; Willem De Muynck, Kim Van Tittelboom, Elke Gruyaert, Didier Snoeck, Arn Mignon, Mathias Maes and Bjorn van Belleghem for the fruitful discussions we had on my experimental results.

The technical and administrative assistance received from the staff members in both Magnel Laboratory and LabMET were greatly appreciated. I would like to specify some people for their considerable contribution to my PhD work and related activities; Christine Graveel, Regine Haspeslagh, Sarah Steenbeke, Renee Graveel, Viviane Van Gaver, Marijke Reunes, Christel Malfait, Greet Van de Velde, Tim Lacoere, Jana De Bodt, Mike Taghon, Siska Maertens, Tommy De Ghein, Sandra De Buck, Bart De Waele, Peter Lampaert, Peter Van den Bussche.

My special gratitude are extended to my office-mates João Feiteira, Hugo Eguez Alava, Florent Forest, Adelaide Araujo, Lijie Wang (twice a day), Emma Hernandez-Sanabria,

Giovanni Ganendra, Racha El Hage, Frederiek Maarten Kerckhof, Nicole Hahn, Ralph Lindeboom, Chris Callewaert and to all the colleagues in both Magnel Laboratory and LabMET for their contribution, friendship, motivation, encouragement and joy. Please do not exclude yourself when you are reading this since I did not ignore any of you and any of your contributions to this work.

I would like to thank to Joeri Coppens, Marta Coma, Stephen Andersen, Alberto Scoma, Antonin Prévoteau, Sandra Manso and Kun Guo for the joyful outdoor activities and trips where I could distract myself from the stressful PhD life.

Special thanks to SHeMAT project members and fellows for their effort to keep this project running and for all the memorable training schools where we built strong scientific and personal network. I am specifically thankful to Ann-Sophie Farle and Damian Palin since I had fantastic time in Delft. Thank you guys, you are great hosts.

My comrade, Filipe, thank you for being the friend, the family and the 911 whenever and wherever I needed. I am deeply grateful to you for all the moments we have shared together, for your motivation speeches and for all the endless discussions we had to improve the quality of our PhD student-life.

Special thanks to Prof. Dr. Tuba H. Erguder for virtually guiding me during this PhD period by the fundamental academic skills she has taught to me during my MSc study.

I would like to express my warmest gratitude to my eternal love for her understanding, patience and motivation. Thank you for all the sacrifices you have made to keep us together during this period and sharing all the painful moments I have experienced. Without you and your motivation I wouldn't be able to proceed this far.

I am also thankful to my sister who visited me the most in Belgium and brought a bit of my family life. Thank you very much for being by far the best visitor, helping me to organize my personal life and taking the household burden of a single guy for a while.

Last but not the least, mom and dad, you were my first teachers, without you and your support nothing would be possible. You never let me down and you were always there somehow whenever I needed. I am indebted to you for the every step in my career and life. I hope to update you with further achievements.

For those who are actually intrigued by the scientific work; please proceed to the table of contents page and choose the part you want to read. For those who are not interested in the work; you never know if you are interested in before you read the first page;) I hope the content will be useful for some of you.